ZooKeys 478: 1–26 (2015)
doi: 10.3897/zookeys.478.8512
http://zookeys.pensoft.net

RESEARCH ARTICLE

A peer-reviewed open-access journal
ZooKeys
Launched to accelerate biodiversity research

Descriptions of two azooxanthellate *Palythoa* species (Subclass Hexacorallia, Order Zoantharia) from the Ryukyu Archipelago, southern Japan

Yuka Irei[1], Frederic Sinniger[2,3], James Davis Reimer[1]

1 *Molecular Invertebrate Systematics and Ecology Laboratory, Graduate School of Engineering and Science, University of the Ryukyus, 1 Senbaru, Nishihara, Okinawa 903-0213, Japan* **2** *Environmental Impact Assessment Research Group, R&D Center for Submarine Resources, Global Oceanographic Data Center, Japan Agency for Marine Science and Technology, 224-3 Toyohara, Nago, Okinawa 905-2172, Japan* **3** *Sesoko Station, Tropical Biosphere Research Center, 3422 Sesoko, Motobu, Okinawa 905-0227, Japan*

Corresponding author: *Yuka Irei* (yuka.irei.mugi@gmail.com)

Academic editor: *B.W. Hoeksema* | Received 28 August 2014 | Accepted 2 January 2015 | Published 28 January 2015

http://zoobank.org/ABC6AF6D-8F9C-4017-83EA-ED3A19C3C120

Citation: Irei Y, Sinniger F, Reimer JD (2015) Descriptions of two azooxanthellate *Palythoa* species (Subclass Hexacorallia, Order Zoantharia) from the Ryukyu Archipelago, southern Japan. ZooKeys 478: 1–26. doi: 10.3897/zookeys.478.8512

Abstract

Two new species of zoantharians (Hexacorallia, Zoantharia, Sphenopidae), *Palythoa mizigama* **sp. n.** and *P. umbrosa* **sp. n.**, are described from the Ryukyu Archipelago, southern Japan. Unlike almost all other known *Palythoa* spp., both species are azooxanthellate and inhabit low-light environments such as floors or sides of caves, crevasses, or hollows of shallow coral reefs. The two species were initially considered to be the same species from their similar habitat environments and highly similar morphological features. However, phylogenetic analyses of nuclear internal transcribed spacer (ITS) ribosomal DNA, mitochondrial 16S ribosomal DNA, and cytochrome oxidase subunit I (COI) sequences revealed that these two species have a genetically distant relationship within the genus *Palythoa*. Morphological characteristics, including polyp size, tentacle number, external/internal coloration, and types and sizes of cnidae were examined in this study. As a result, only tentacle coloration was found to be useful for the morphological distinction between the two species. *Palythoa mizigama* possesses white tentacles with black horizontal stripes while *P. umbrosa* possesses white tentacles without any stripe patterns. Considering their distant phylogenetic relationship, it can be assumed that their unique yet similar morphological and ecological characteristics developed independently in each species as an example of parallel evolution.

Keywords

Cave-dwelling, cryptic species, ITS-rDNA, Ryukyu Archipelago, zoantharian

Introduction

Zoantharia are sessile marine cnidarians within the class Anthozoa, subclass Hexacorallia. This taxon is often referred to as intermediate in form between hard corals (Scleractinia) and sea anemones (Actiniaria), as most species lack a skeleton and yet are colonial. Zoantharians are widely distributed and are particularly common in subtropical and tropical regions, where they are one of the major benthic components of coral reefs. Some species contain unique chemicals such as palytoxin or norzoanthamine (Kuramoto et al. 1997, Moore and Scheuer 1971, Vitor and Vitor 2010). Although they are important organisms both ecologically and as a source of bioactive compounds, there is a lack of knowledge on their taxonomy and diversity, with both many synonyms and undescribed species existing (Burnett et al. 1997, Reimer et al. 2004). Zoantharians are usually distinguishable by the combination of two rows of tentacles arranged around the oral disc, colonial life form (although there are some exceptions), and the incrustation of hard particles in their column taken from the surrounding habitat (excepting species of the family Zoanthidae). Within Zoantharia, there are two suborders, Macrocnemina and Brachycnemina, which are distinguished by the state of their fifth mesentery from the dorsal directive, being complete or incomplete, respectively. Macrocnemic zoantharians have a wide habitat range from intertidal to abyssal depths, and polar to tropical waters (Ryland et al. 2000). Additionally, many macrocnemic zoantharians live in association with other organisms such as sponges (Crocker and Reiswig 1981), hydrozoans (Camillo et al. 2010, Sinniger et al. 2010), antipatharians (Sinniger et al. 2010), or they are epizoic on shells inhabited by hermit crabs (Muirhead et al. 1986, Reimer et al. 2010, Schejter et al. 2011). On the other hand, brachycnemic zoantharians inhabit shallow waters in subtropical to tropical waters and most species have symbiotic relationships with *Symbiodinium* spp. (e.g. Trench 1974, Burnett 2002, Reimer et al. 2006b). Brachycnemic zoantharians are abundant on many coral reefs (Sebens 1982, Acosta 2001, Irei et al. 2011) and usually have competitive relationships with other benthic organisms (Suchanek and Green 1981).

The suborder Brachycnemina currently contains three families; Sphenopidae, Zoanthidae, and Neozoanthidae. In the Ryukyu Archipelago in southwestern Japan, one genus of family Sphenopidae (*Palythoa* Lamouroux, 1816), two genera of family Zoanthidae (*Isaurus* Gray, 1828, *Zoanthus* Lamarck, 1801), and one genus in family Neozoanthidae (*Neozoanthus* Herberts, 1972) have been reported (Reimer 2010). Additionally, specimens from the genus *Sphenopus* Steenstrup, 1856 have recently been found in the area (T. Fujii, pers. comm.; J. Reimer, unpubl. obs.). These three families are easily distinguished from each other in the field by external morphological features such as presence or absence of sand incrustation, polyp size, and gross morphology (solitary or colonial) (Reimer 2010).

The two genera in the family Sphenopidae, *Sphenopus* and *Palythoa*, can easily be distinguished from each other by morphological and ecological characteristics. Unusually for a zoantharian, *Sphenopus* is azooxanthellate, has a solitary (=unitary,

not forming colonies) life form and inhabits muddy or sandy bottoms without usually attaching to hard substrates (Gray 1867, Soong et al. 1999). The validity of the genus *Sphenopus* has recently been questioned since molecular analyses have shown that this group is phylogenetically included within the genus *Palythoa* (Reimer et al. 2012b). According to the World Register of Marine Species, three species have been described in this genus (Reimer 2014a). On the other hand, species of the genus *Palythoa* are colonial and zooxanthellate, similar to most other brachycnemic zoantharians. Some *Palythoa* species are known to compete for space and overgrow other organisms in coral reefs (Suchanek and Green 1981).

In this study, we describe two new *Palythoa* species discovered from the Ryukyu Archipelago, southern Japan. These two species were initially considered to be the same species as they were found in similar environments and exhibit highly similar morphological features. However, molecular analyses demonstrated considerable differences between these two groups and subtle morphological differences distinguish the two groups. Uniquely for *Palythoa*, both species are azooxanthellate and are found in caves and cracks in coral reefs. These results lead to a reconsideration of the definition of both *Palythoa* and *Sphenopus*, and provide an example of parallel evolution within Zoantharia.

Methods

Sampling

All specimens were collected between 2008 and 2012 by scuba or snorkeling from depths of 2.6 to 12 m, primarily from the Ryukyu Archipelago, southwestern Japan, with a few additional specimens collected from two locations in Taiwan and one location in New Caledonia (Figure 1, Suppl. material 1: Table 1). Collected specimens were stored in separate vials and fixed in 70–99.5% ethanol for molecular analyses or 4–10% seawater formalin for morphological observations.

Abbreviations of sampling sites:

ADA Ada (Okinawa Island)
IRI Iriomote (Yaeyama Islands)
MIZ Mizugama (Okinawa Island)
NC New Caledonia
ODO Odo (Okinawa Island)
SUN Sunabe (Okinawa Island)
TEN Teniya (Okinawa Island)
TOK Tokashiki (Kerama Islands)
TW Taiwan
YON Yona (Okinawa Island)

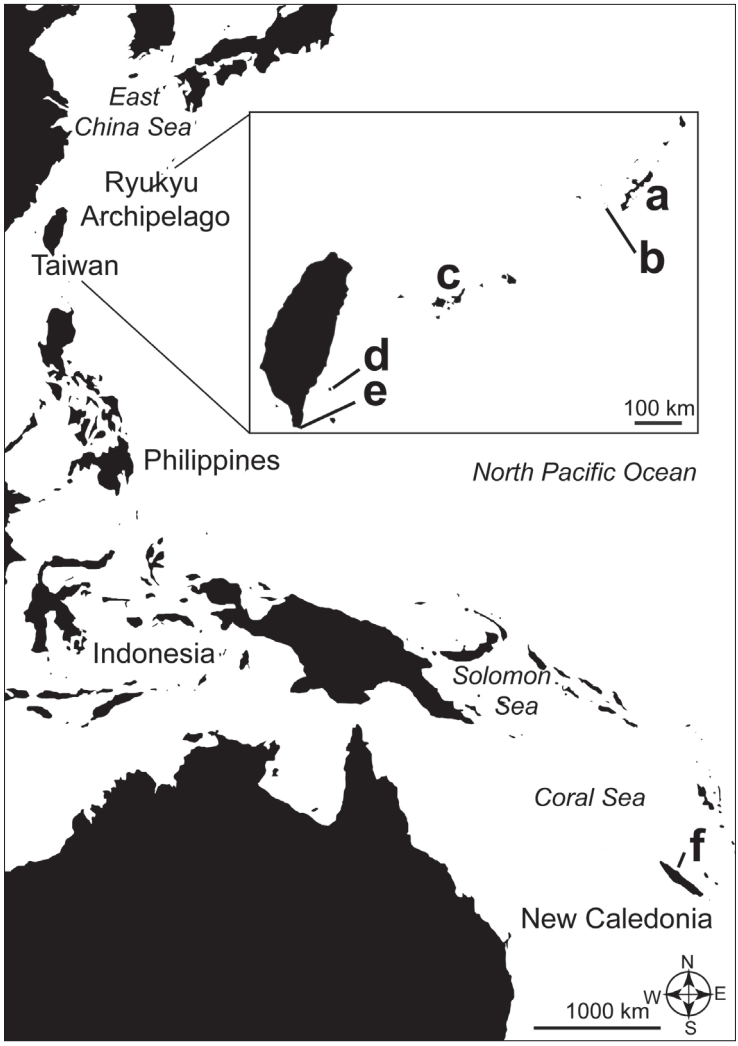

Figure 1. Sampling locations of *Palythoa mizigama* sp. n. and *P. umbrosa* sp. n. specimens. **a** Okinawa Island **b** Tokashiki Island **c** Yaeyama Islands **d** Lyudao (Green Island) **e** Kenting **f** Poindimié. *Palythoa mizigama* was found from Ryukyu Archipelago, Taiwan and New Caledonia (**a, b, c, e, f**), while *P. umbrosa* was found from the Yaeyama Islands and Taiwan (**c, d**).

Molecular analyses

DNA extraction was performed with guanidine following the protocol described in Sinniger et al. (2010). Three DNA markers; mitochondrial cytochrome oxidase subunit I (COI), mitochondrial 16S ribosomal gene (mt 16S rDNA), and the nuclear internal transcribed spacer region of ribosomal DNA (ITS rDNA), were amplified by polymerase chain reaction method with HotStarTaq Master Mix Kit (Qiagen, Tokyo, Japan). The COI region was amplified by using the zoantharian-specific primer

COzoanF (Reimer et al. 2007a) and universal HCO2198 (Folmer et al. 1994). The primers 16Santla and 16SbmoH (Sinniger et al. 2005) were used for mt 16S rDNA, and either the primer pair of ITSfSW and ITSrSW (Swain 2009) or ZoanF and ZoanR (Reimer et al. 2007b) was used to amplify ITS rDNA. PCR products were purified by using shrimp alkaline phosphate (SAP) and Exonuclease I (Takara Bio Inc., Shiga, Japan) and then sequenced either by Macrogen Japan Corp. (Tokyo, Japan) or Fasmac Co., Ltd. (Kanagawa, Japan). Sequences obtained were automatically aligned along with sequences from GenBank (National Center for Biotechnology Information) by MUSCLE (Edgar 2004) and manually inspected by Se-Al v2.0a11 Carbon (Rambaut and Charleston 1997–2001). Phylogenetic trees were constructed by three methods; maximum likelihood (ML), neighbor joining (NJ), and Bayesian posterior probability (Bayes). ML trees were made by PhyML Online (Guindon et al. 2010) under the GTR (general time-reversible model) substitution model. The number of substitution rate categories was set for eight and bootstraps were calculated with 1000 replicates. NJ trees were constructed by using Clustal X 2.1 (Larkin et al. 2007) with 1000 bootstrap replicates. Bayesian trees were constructed in MrBayes 3.1.2 (Ronquist and Huelsenbeck 2003) under the GTR + I + I^{-} model. One cold and three heated Markov chain Monte Carlo (MCMC) chains with default-chain temperatures were run for two million generations, sampling log-likelihoods (InLs), and trees at 100-generation intervals (20,000 InLs and trees were saved during MCMC). The first 2,000 generations were discarded as "burn-in", and Bayesian posterior probabilities and branch-lengths were estimated from the remaining 18,000 generations.

Morphological observations

Color patterns were noted from images taken in situ or observed under stereomicroscope. Relative tentacle length (i.e. ratio of tentacle length to oral disk diameter) was estimated from images taken in situ. Additional in situ images (not shown) were taken with small rulers placed next to colonies and polyps. Height (length) and diameter of polyp column (width) of individual polyps were measured by using calipers after fixation, and numbers of tentacles were counted under stereomicroscope. Additionally, cnidae were observed, characterized and measured from three parts of each polyp; tentacles, pharynx, and mesenterial filaments. Portions of each tissue were removed and put on a separate slide glass and a cover glass was gently placed over tissue after adding a drop of glycerin solution (seawater:glycerin=1:1). The cover glass was slightly pressed to squash and disperse tissue and the edges of the cover glasses were sealed by clear nail polish. Prepared slides were then observed under a differential interference contrast (DIC) microscope (Nikon Eclipse80i, Nikon, Tokyo) and photographs of each type of cnidae were taken with a digital camera (Canon Powershot G11, Canon, Tokyo). Types of cnidae were determined with reference to Ryland and Lancaster (2004) and length and width of each cnida was measured by using ImageJ software (Rasband 1997–2012).

Results

Systematics

Phylum Cnidaria Hatschek, 1888
Class Anthozoa Ehrenberg, 1831
Subclass Hexacorallia Haeckel, 1896
Order Zoantharia Gray, 1832
Suborder Brachycnemina Haddon & Shackleton, 1891
Family Sphenopidae Hertwig, 1882

Genus *Palythoa* Lamouroux, 1816

Type species. *Palythoa mammillosa* (Ellis & Solander, 1786).

Description. Colonial brachycnemic zoantharians with heavily sand-incrusted ectoderm and mesoglea. Occasionally solitary polyps are also seen.

Remarks. Various authors have suggested to include the genus *Protopalythoa* Verrill, 1900 over the past century based on both morphological (Pax 1910, Ryland and Lancaster 2003) and molecular data (Burnett et al. 1997, Reimer et al. 2006a). Polyps of *Palythoa* are embedded in a well-developed coenenchyme (= "immersae", Pax 1910) while those of *Protopalythoa* are more free and clear of the coenenchyme (= "intermediate" or "liberae", Pax 1910). In this study, we consider *Protopalythoa* to be included within *Palythoa*. In general, polyps are firmly attached to stones or reef rocks. Currently, approximately 130 nominal species have been described (*Palythoa* + *Protopalythoa*, Reimer 2014b, c) although some studies have suggested the presence of many synonyms (Burnett et al. 1997, Reimer et al. 2004, Reimer et al. 2012a). All described species are zooxanthellate with the exception of *P. macmurrichi* (Haddon & Shackleton, 1891) (see Remarks below).

Palythoa mizigama sp. n.

http://zoobank.org/097C1C97-02B2-48FA-8E42-25942ECA982D
Figures 1–5, 7–9, Suppl. material 1–2: Table 1–2

Synonymy: "*Palythoa* sp. tokashiki" – Reimer 2010, Reimer et al. 2011b (specimen from Kenting, Taiwan), Reimer et al. 2013 (specimen from Kenting).

Type material. Type-specimens. Holotype. Specimen number NSMT-Co1560 (original number MIZ_33). Fixed in 99.5% ethanol, deposited in National Museum of Nature and Science, Tokyo, Japan. Original label: "HOLOTYPE *Palythoa mizigama*, Japan, Okinawa Island, Kadena, Mizugama, 5 m depth, 13 May 2008, Y. Irei leg. Paratypes: Paratype 1. Specimen number RMNH Coel. 41729 (original number

TOK_2), Japan, Okinawa Prefecture, Kerama Islands, Tokashiki Island, Mutizuni, 26°09'07"N, 127°21'11"E, in a hollow of reef slope at 5 m depth, 5 January 2008, Y. Irei and F. Sinniger leg. Fixed in 99.5% ethanol, deposited in Naturalis Biodiversity Center, Leiden, The Netherlands. Paratype 2. Specimen number USNM 1231375 (original number ODO_25), Japan, Okinawa Prefecture, Okinawa Island, Itoman, Odo, 26°05'06"N, 127°42'32"E, on the wall of reef cave at 11 m depth, 13 January 2008, Y. Irei and F. Sinniger leg. Fixed in 99.5% ethanol, deposited in Smithsonian Institution National Museum of Natural History, Washington, D.C., USA. Paratype 3. Specimen number RUMF-ZG-04375 (original number IRI_JR2829), Japan, Okinawa Prefecture, Yaeyama Islands, Taketomi, Iriomotesuido, 24°21'51"N, 123°57'25"E, at 4.4–5.3 m depth, 1 September 2012, J. Reimer leg. Fixed in 99.5% ethanol, deposited in University Museum, University of the Ryukyus (Fujukan).

Type-locality. Japan, Okinawa Prefecture, Okinawa Island, Kadena, Mizugama, 26°21'35"N, 127°44'18"E, on wall of reef cave at 5 m depth, 13 May 2008, Y. Irei leg.

Description of holotype. Size of colony approximately 2 cm × 3 cm, consisting of six polyps, 3.8–11.2 mm in height and 2.0–3.8 mm in diameter. External color brownish gray to yellowish white with small black blotches on polyp heads and columns. Horizontal wrinkles (1–7 in number) of approximately half the length of column periphery, mostly on inner side of bent polyps. Tentacles approximately 32 in number, color same as column with 7–10 narrow black horizontal lines on tentacles. Columns heavily incrusted with irregularly-sized sand grains.

Habitat and ecological features. This species inhabits low-light environments such as floors or sides of caves, crevasses or under reef overhangs on coral reef flats and reef slopes. In general, polyps are open at night with extended tentacles, and are closed in daytime. Polyps tend to bend parallel to the surrounding substrate when closed although polyps become somewhat erect in a diagonal direction at an acute angle (e.g. not perpendicular to substrate) when open, with oral disks generally facing the opening of the cave or crevasse (Figure 2a–d).

Distribution. Southern Ryukyu Archipelago (Okinawa Island, Tokashiki Island, Yaeyama Islands), Taiwan (Kenting), and New Caledonia (Tibarama, Poindimié) (Figure 1).

Diagnosis. *General.* Azooxanthellate brachycnemic zoantharian with heavily sand-incrusted ectoderm and mesoglea. Colonies usually composed of several to 20 polyps, with each polyp loosely connected to others by a thin stolon (="liberae", Pax 1910). Solitary polyps are also commonly seen. Polyp is cylindrical and upper part of the polyp around pharynx is occasionally constricted when closed (Figure 3a). Expanded polyps are flared, with column becoming wider towards the oral disk and a large oral disk (Figure 2a, c). Columns occasionally have several horizontal wrinkles (1 to up to 10 in number) of one quarter to half the length of column periphery, mostly on inner side of bent polyps (Figure 3a).

Polyp size. Approximately 0.5–1.0 cm in length and 0.2–0.4 cm in width after fixation in 4–10% seawater formalin or 70–99.5% ethanol.

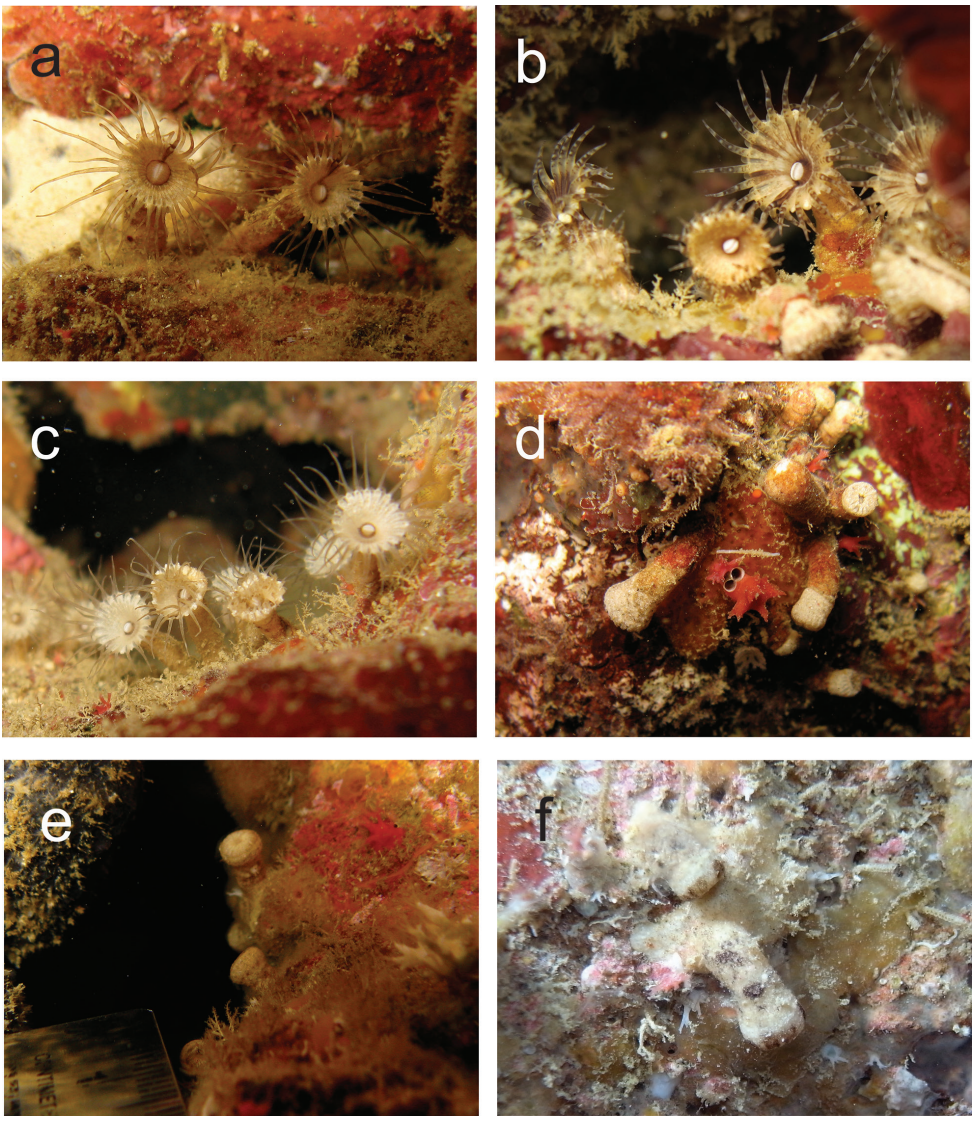

Figure 2. In situ images of *Palythoa mizigama* sp. n. and *P. umbrosa* sp. n. **a** *P. mizigama*; single radial lines visible on oral disks. Image taken by Y. Irei on September 28, 2009, at Mizugama, Okinawa Island, Japan **b** *P. mizigama*; several radial lines visible on oral disks. Image taken by J. Reimer on April 22, 2010, at Mizugama **c** *P. mizigama*; with no radial lines on oral disks. Image taken by Y. Irei on April 12, 2009, at Mizugama **d** *P. mizigama*; closed polyps. Image taken by Y. Irei on June 16, 2009, at Mizugama **e** *P. umbrosa* (TW_18); closed polyps. Image taken by Y. Irei on November 2, 2009, at Lyudao, Taiwan **f** *P. umbrosa* (IRI_TF2); closed polyps. Image taken by T. Fujii on November 9, 2012, at Sotobanari Island, Yaeyama Islands, Japan.

Coloration of polyp column and oral disk. The color of external polyp columns varies from ivory to tan in life, occasionally with irregular black blotches. The color of oral disk is also ivory to tan, often with black radial lines extending outwards from the mouth (Figure 2 a and b, Figure 3 b).

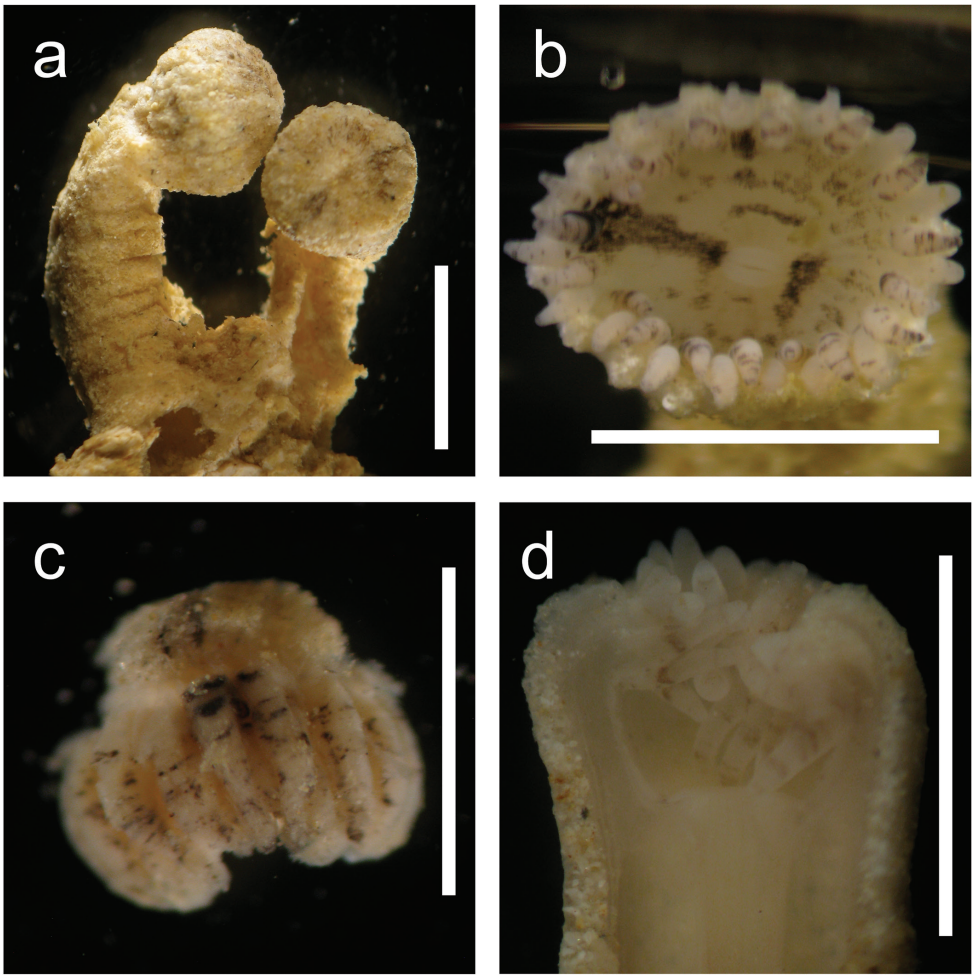

Figure 3. *Palythoa mizigama* sp. n. after fixation in 70–99.5% ethanol (**a, c**) or 4–10% SW formalin (**b, d**). **a** MIZ_33; closed polyps. Scale bar=0.5 cm. Collected by Y. Irei on May 13, 2008 at Mizugama, Okinawa Island, Japan **b** MIZ_071110_2; close up of a partially open polyp. Scale bar=0.5 cm. Collected by Y. Irei on November 7, 2010 at Mizugama **c** MIZ_33; tentacles (isolated). Horizontal black stripes visible. Scale bar=0.25 cm **d** MIZ_260910; close up image of a longitudinal section. Tentacles visible with faint stripes. Note the column wall densely incrusted with sand grains. Scale bar=0.25 cm. Collected by Y. Irei on September 26, 2010 at Mizugama. All images taken through stereomicroscope.

Tentacles. 32–40 in number. Extended tentacles are of the same length or longer than the diameter of oral disks (Figure 2a, c). Tentacle color is white to ivory with 4–10 horizontal black stripes (Figure 3b). The number and density of stripes on the tentacles are variable between different polyps (Figure 3c, d).

Cnidom. Four major cnidae types observed; spirocysts, basitrichs, *p*-mastigophores, and holotrichs. The dominant types of cnidae were spirocysts (length 20.5±3.5 μm, width 3.4±0.7 μm, n=140) in the tentacles, basitrichs (length 23.7±2.3 μm, width 3.6±0.4 μm, n=139) in the pharynx, and *p*-mastigophores (length 15.7±3.6 μm, width 4.7±0.7 μm,

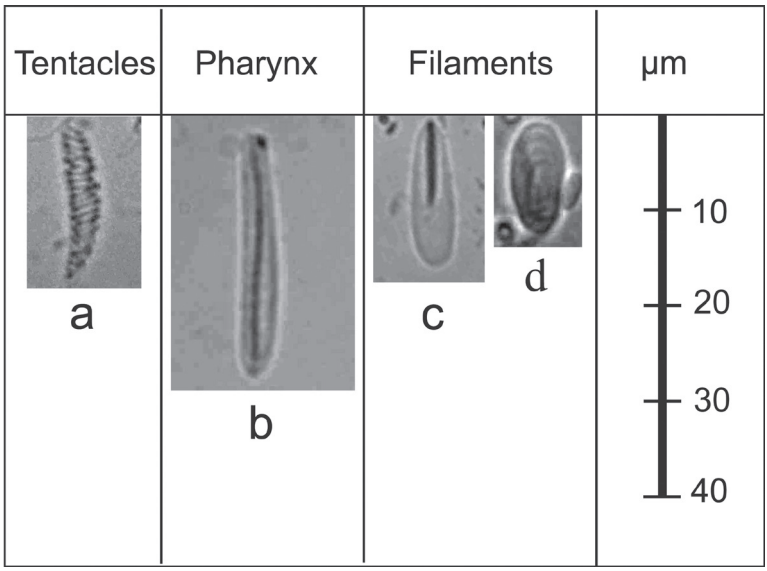

Figure 4. Dominant cnidae types of *Palythoa mizigama* sp. n. and *P. umbrosa* sp. n. tissue. **a** spirocyst **b** basitrich, and **c** *p*-mastigophore **d** holotrich. Scale bar shows 10–40 μm.

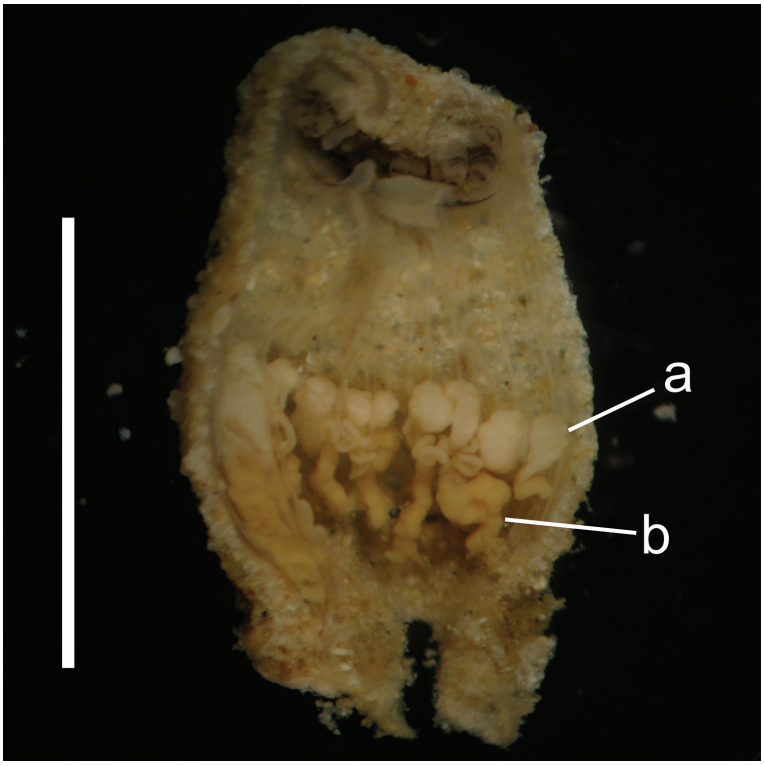

Figure 5. Longitudinal section of a reproductive polyp of *Palythoa mizigama* sp. n. Collected on Aug. 19, 2010 at Mizugama, Okinawa Island, Japan. **a** spermaries **b** ovaries. Scale bar=0.5 cm.

n=140) and holotrichs (length 13.5±1.9 μm, width 4.9±0.7 μm, n=140) in the mesenterial filaments (Figure 4, Suppl. material 2: Table 2). In addition to the four major cnidae types, three large holotrichs were found. Three individual polyps contained one large holotrich each, with two from tentacles (length 28.4 μm, width 13.0 μm; length 25.7 μm, width 11.7 μm) and one from the mesenterial filaments (length 33.4 μm, width 16.9 μm).

Etymology. The specific epithet "mizigama" was named after the type locality of Mizugama. Additionally, "mizi" and "gama" mean "water" and "cave", respectively, in the Okinawan language. Japanese name: Shimate-yami-iwasunaginchaku. "Shimate", "yami", and "iwasunaginchaku" mean "striped hands", "dark", and "*Palythoa*", respectively, in Japanese.

Remarks on reproduction. Simultaneous hermaphrodite. Reproductive polyps containing ovaries and spermaries were found from specimens collected in August - September 2010 at Mizugama, Okinawa Island, Japan (Figure 5).

***Palythoa umbrosa* sp. n.**
http://zoobank.org/6DC531A5-26E6-432F-A726-3A6F15B9D8BF
Figures 1–2, 4, 6–9, Suppl. material 1–2: Table 1–2

Synonymy: "*Palythoa* sp. tokashiki" – Reimer et al. 2011b (specimen from Lyudao (=Green Island), Taiwan), Reimer et al. 2013 (specimen from Lyudao).

Type material. Type-specimens. Holotype. Specimen number NSMT-Co1561 (original number IRI_TF3). Split into two pieces and fixed in 99.5% ethanol and 4-10% formalin, respectively. Deposited in National Museum of Nature and Science, Tokyo, Japan. Original label: "HOLOTYPE *Palythoa umbrosa*, Japan, Yaeyama Islands, Sotobanari Island, 8 m depth, 9 November 2012, J. Reimer leg." Paratypes. Paratype 1. Specimen number RMNH Coel. 41730 (original number IRI_TF1), Japan, Okinawa Prefecture, Yaeyama Islands, Taketomi, Sotobanari Island, 24°22'46"N, 123°43'53"E, at 9 m depth, 9 November 2012, T. Fujii leg. Split into two pieces and fixed in 99.5% ethanol and 4–10% formalin, respectively. Deposited in Naturalis Biodiversity Center, Leiden, The Netherlands. Paratype 2. Specimen number USNM 1231376 (original number IRI_TF2), Japan, Okinawa Prefecture, Yaeyama Islands, Taketomi, Sotobanari Island, 24°22'46"N, 123°43'53"E, at 10 m depth, 9 November 2012, T. Fujii leg. Split into two pieces and fixed in 99.5% ethanol and 4–10% formalin, respectively. Deposited in Smithsonian Institution National Museum of Natural History, Washington, D.C., USA. Paratype 3. Specimen number RUMF-ZG-04376 (original number IRI_31), Japan, Okinawa Prefecture, Yaeyama Islands, Taketomi, Iriomotesuido, 24°21'51"N, 123°57'25"E, at 6 m depth, 7 May 2008, Y. Irei leg. Fixed in 99.5% ethanol, deposited in University Museum, University of the Ryukyus (Fujukan).

Type-locality. Japan, Okinawa Prefecture, Yaeyama Islands, Taketomi, Sotobanari Island, 24°22'46"N, 123°43'53"E, on wall of reef cave at 8 m depth, 9 November 2012, J. Reimer leg.

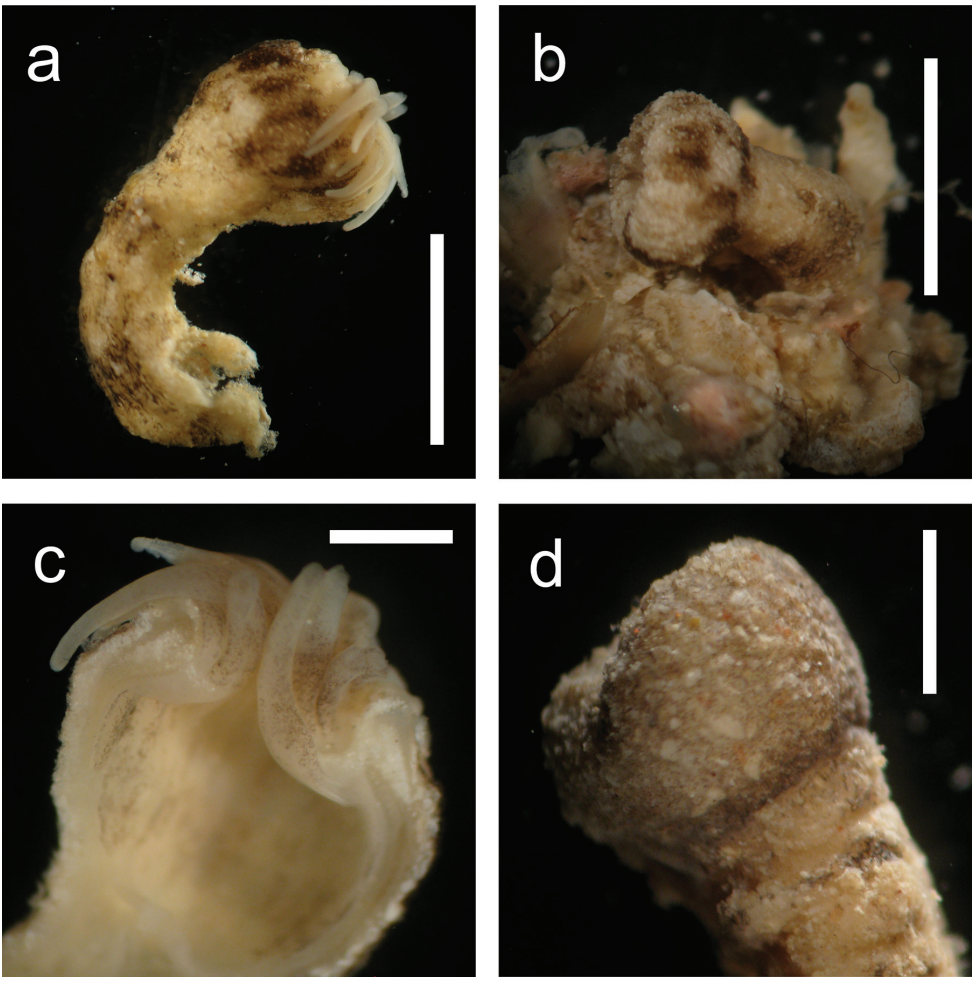

Figure 6. *Palythoa umbrosa* sp. n. after fixation in 4-10% SW formalin. **a** IRI_TF2; slightly expanded polyp. Scale bar=0.5 cm. Collected by T. Fujii on November 9, 2012 at Sotobanari Island, Yaeyama Islands, Japan **b** IRI_TF1; closed polyp. Scale bar=0.5 cm. Collected by T. Fujii on November 9, 2012 at Sotobanari Island **c** IRI_TF2; close up of a longitudinal section. Note the white tentacles with small black dots. Scale bar=0.2 cm **d** IRI_TF2; close up of a polyp capitalum. Column incrusted with irregularly-sized particles. Scale bar=0.25 cm. All images taken through stereomicroscope.

Description of holotype. Size of colony approximately 2 cm × 2 cm, consisting of three polyps, 6.1 mm in height and 2.7–3.0 mm in diameter. Columns yellowish white with irregular black blotches. Dark brown polyp heads. Horizontal wrinkles (3–5 in number) of approximately half the length of column periphery, on mostly inner side of bent polyps. Tentacles approximately 32 in number, white in color. Columns heavily incrusted with irregularly-sized sand grains.

Habitat and behavioral features. This species inhabits low-light environments such as floors or sides of caves, crevasses or under reef overhangs on coral reef flats and

reef slopes. In general, polyps are open at night with extended tentacles, and are closed during the daytime. Polyps tend to bend parallel to the surrounding substrate when closed (Figures 2f, 6b) and become erect in a diagonal direction at an acute angle when open, with oral disks generally facing the opening of the cave or crevasse.

Distribution. Southern Ryukyu Archipelago (Yaeyama Islands) and Taiwan (Lyudao) (Figure 1)

Diagnosis. *General.* Azooxanthellate brachycnemic zoantharian with heavily sand-incrusted ectoderm and mesoglea. Colonies usually composed of several to 20 polyps with each polyp loosely connected to neighbor(s) by a thin stolon (="liberae", Pax 1910). Solitary polyps are also commonly seen. Polyps are cylindrical and upper portion of polyps around pharynx is often but not always constricted when closed (Figure 6b, d). Columns occasionally have several horizontal wrinkles (1 to 10 in number) of one quarter to half the length of column periphery, on mostly inner side of bent polyps (Figure 6d).

Polyp size. 0.5–0.9 cm in length and 0.3–0.5 cm in width after fixation in 4–10% seawater formalin or 70–99.5% ethanol.

Coloration of polyp column and oral disk. Since sampling of *P. umbrosa* was performed only during the daytime, images of expanded polyps in situ were not available and observations were performed under a stereomicroscope. The color of external polyp columns was ivory to tan, occasionally with irregular black/brown blotches (Figures 2f, 6a,b). The color of oral disks was also ivory to tan.

Tentacles. 32–38 in number and white to ivory in color (Figure 6a). Occasionally, very small (<0.01 mm) black dots are present (Figure 6c). No stripes on tentacles, unlike *P. mizigama*.

Cnidom. There were four major cnidae types observed (Figure 4). The dominant types of cnidae were spirocysts (length 21.9±3.1 μm, width 3.5±0.7 μm, n=80) in the tentacles, basitrichs (length 29.5±3.3 μm, width 3.7±0.4 μm, n=80) in the pharynx, and *p*-mastigophores (length 20.5±3.9 μm, width 5.5±0.9 μm, n=80) and holotrichs (length 13.3±1.5 μm, width 5.0±1.1 μm, n=55) in the mesenterial filaments (Suppl. material 2: Table 2). For all cnidae types except holotrichs, the average lengths were significantly longer in *P. umbrosa* than in *P. mizigama* (t-test $p<0.05$). However, there were relatively large overlaps in the range of lengths between these two species (Suppl. material 2: Table 2).

Etymology. Named for habitat environment of this species. The specific epithet "umbrosa" means "shadowy" in latin. Japanese name: Shirote-yami-iwasunaginchaku. "Shirote" means "white hands" in Japanese.

Remarks. The azooxanthellate species *Palythoa macmurrichi* has previously been described from the Torres Strait, northern Australia. It was described based on a single polyp collected from a channel at 20 fathoms (approximately 36.5 m), and the holotype was lost when it was used for histological examination in Haddon and Shackleton (1891). While the few figures of *P. macmurrichi* in the original description could be either of the two new species in this study, they could also be any of many other *Palythoa* species with "liberae" morphology (Pax 1910). Unfortunately, we are unable to

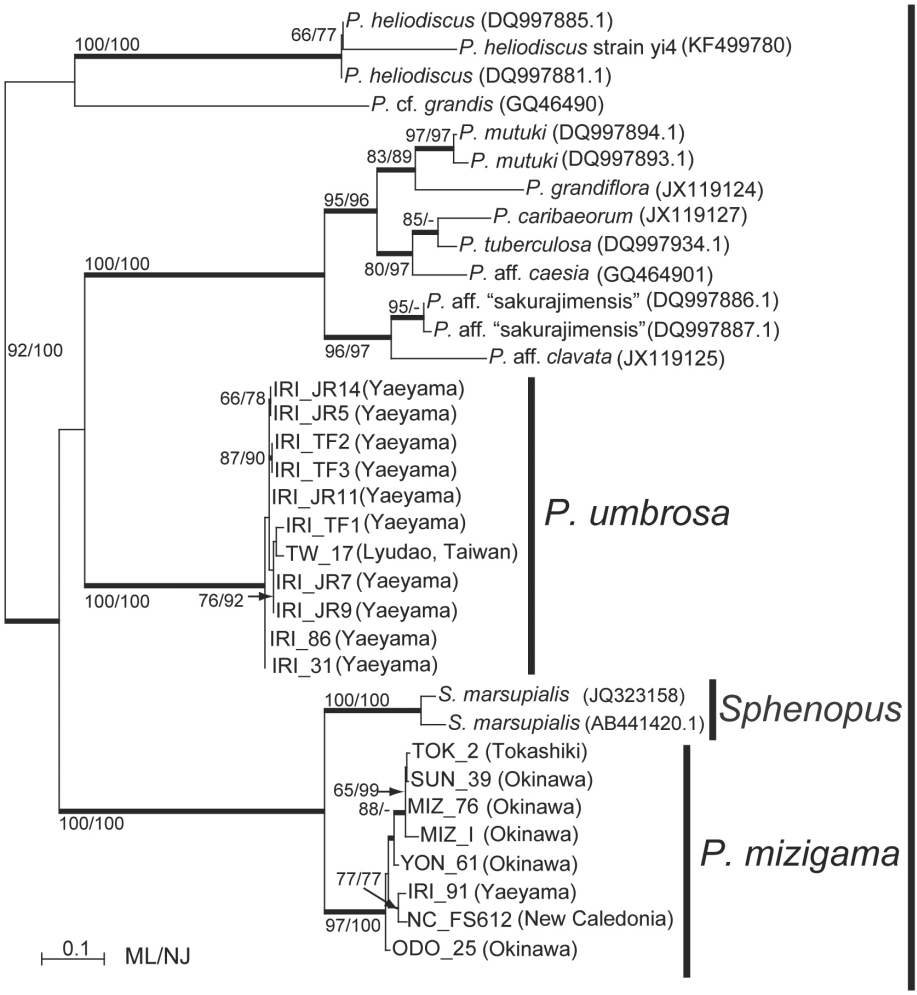

Figure 7. Maximum likelihood tree based on internal transcribed spacer region of ribosomal DNA for family Sphenopidae. Numbers on nodes represent ML and neighbor-joining (NJ) bootstrap values (>65% are shown). Thick branches indicate high supports of Bayesian posterior probabilities (>0.95). Sequences obtained from GenBank are shown with accession numbers.

examine *P. macmurrichi* specimens, as this species has not been mentioned in the literature since Verrill (1900) (asides in nomenclators such as Walsh 1967). The current two new species differ from *P. macmurrichi* in their smaller polyp sizes and external markings. Additionally, the two *Palythoa* species in this study were found only in shallow areas (<12 m depth), different from *P. macmurrichi,* which was collected from ~37 m depth. Our SCUBA surveys in Okinawa and New Caledonia investigated channels of similar depths as the type locality of *P. macmurrichi* but we never came across any similar specimens. Thus, for now, we consider *P. macmurrichi* to be a different species from the two new azooxanthellate species described in this study.

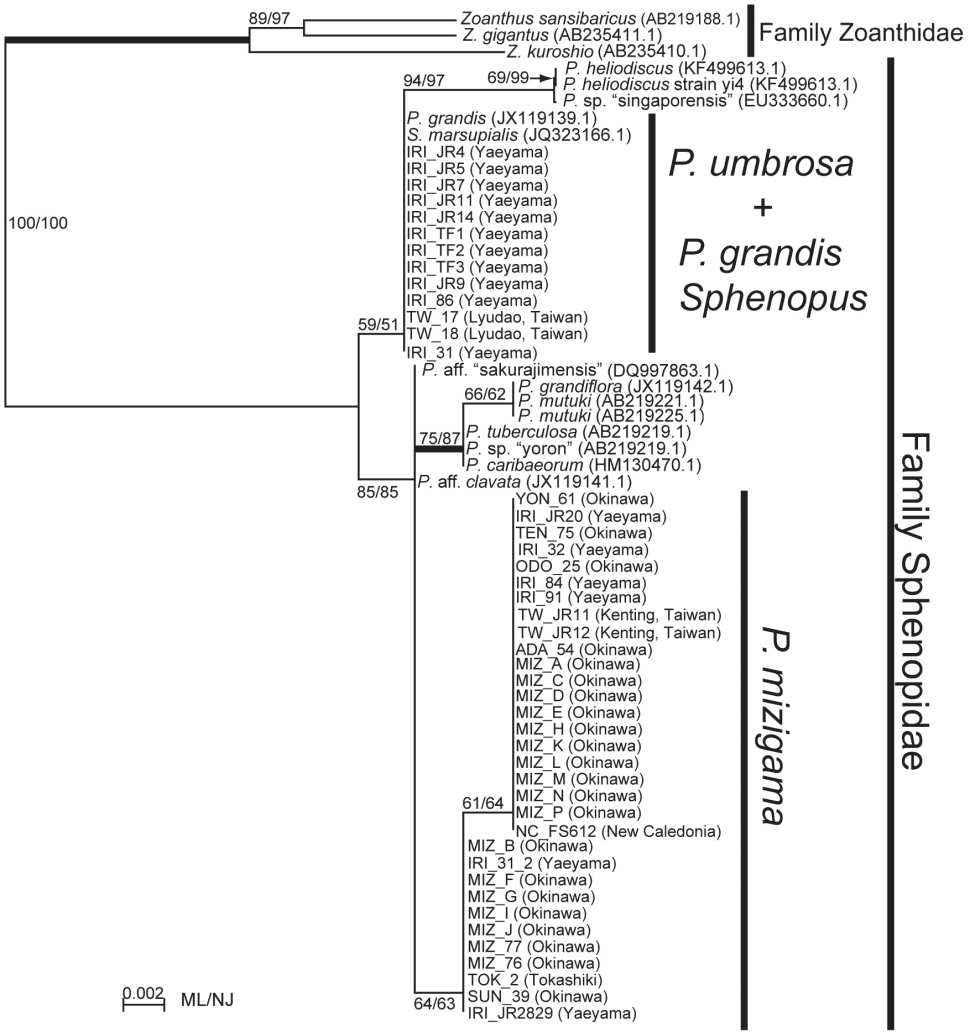

Figure 8. Maximum likelihood tree based on mitochondrial 16S ribosomal DNA for family Sphenopidae. Numbers on nodes represent ML and neighbor-joining (NJ) bootstrap values (>50% are shown). Thick branches indicate high supports of Bayesian posterior probabilities (>0.95). Sequences obtained from GenBank are shown with accession numbers.

Phylogenetic analyses

Palythoa mizigama and *P. umbrosa* were included in a monophyletic clade along with other *Palythoa* spp. in the phylogenetic trees for all three DNA markers (Figures 7–9). Despite the high similarity of the morphological and ecological features of *P. mizigama* and *P. umbrosa*, their sequences consistently formed two separate clades with high support (ML=97%, NJ=100%, Bayes=1.00, and ML=100%, NJ=100%, Bayes=1.00, respectively) in ITS rDNA alignment analyses (Figure 7). The 16S rDNA and COI regions were

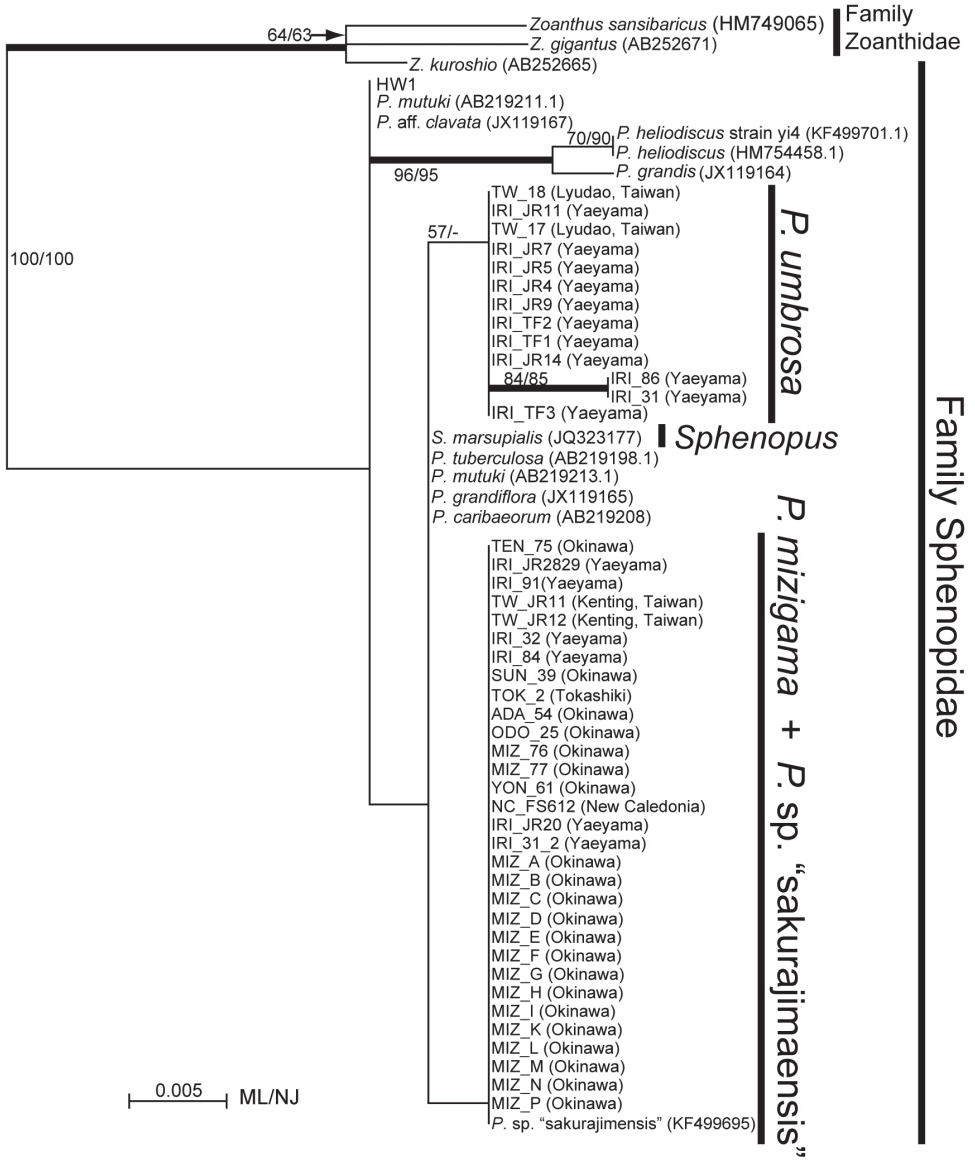

Figure 9. Maximum likelihood tree based on mitochondrial cytochrome oxidase subunit I gene for family Sphenopidae. Numbers on nodes represent ML and neighbor-joining (NJ) bootstrap values (>50% are shown). Thick branches indicate high supports of Bayesian posterior probabilities (>0.95). Sequences obtained from GenBank are shown with accession numbers.

more conservative than the ITS rDNA region (2–4 bp differences between *P. mizigama* and *P. umbrosa*) and bootstrap scores for each species' monophyly were not particularly high, but both trees had similar topologies to the ITS rDNA tree, showing the separation of the specimens collected in this study into different clades (Figures 8 and 9, respectively).

Previously published sequences of *Sphenopus marsupialis* (Fukami et al. 2008, Reimer et al. 2012b) were also included in the monophyletic clade of genus *Palythoa* for all the three DNA markers (Figures 7–9), and the phylogenetic tree of the ITS rDNA region showed a sister relationship between *Sphenopus* and *P. mizigama* with high bootstrap support (ML=100%, NJ=100%, Bayes=1.00) (Figure 7). On the other hand, the 16S rDNA sequence of *S. marsupialis* was identical to the sequences of *P. umbrosa* (Figure 8).

Discussion

Distribution of *Palythoa mizigama* and *P. umbrosa*

This study revealed a wide distribution for *P. mizigama* in the Central Indo-Pacific from the Ryukyu Archipelago in the north to New Caledonia in the south. *Palythoa umbrosa* was found from a more limited region including the Yaeyama Islands (southwest Ryukyu Archipelago) and Lyudao (= Green Island, southeast of Taiwan) (Figure 1). Even after repeated sampling around Okinawa Island, we did not find a single specimen of *P. umbrosa* from this region. Therefore, it is likely that this species is not present around Okinawa Island. On the other hand, *P. umbrosa* was more common than *P. mizigama* around Yaeyama Islands. Remarkably, at the Iriomote-suido site in the Yaeyama Islands, a *P. mizigama* specimen (specimen IRI_31_2) was found occurring directly next to a *P. umbrosa* colony (specimen IRI_31). Thus, it can be concluded that *P. mizigama* and *P. umbrosa* are sympatric in the Yaeyama Islands, although the overall distributions of *P. mizigama* and *P. umbrosa* are different (Figure 1).

Palythoa mizigama and/or *P. umbrosa* may possibly also occur in the Great Barrier Reef, Australia. Burnett et al. (1997) mentioned a *Protopalythoa* (= "liberae" form *Palythoa*) species (*Protopalythoa* sp. 3) with "polyps white or sandy colored, partially buried in coral rock". Burnett et al. (1997) performed allozyme electrophoretic analyses on zoantharians collected from northwestern Australia and included keys for species identification. The results of UPGMA cluster analyses and descriptions of morphological features in the study lead us to conclude that *Protopalythoa* sp. 3 generally matches well with both *P. mizigama* and *P. umbrosa*. However, it is difficult to confirm that *Protopalythoa* sp. 3 is either *P. mizigama* or *P. umbrosa* as the morphological descriptions in Burnett et al. (1997) were not detailed and the molecular methods used in their study are different from those utilized in our study. Sampling in the current study was mainly focused in the Ryukyu Archipelago, and further investigations in other regions are needed to properly ascertain the overall distributions of these two new *Palythoa* species.

Distinction between *Palythoa mizigama* and *P. umbrosa*

Both morphological and molecular characteristics clearly indicate the two new species belong within the genus *Palythoa*. Phylogenetic analyses showed that *P. mizigama* and

P. umbrosa are relatively distantly related to each other within the genus despite their morphological features being almost identical. We detected statistically significant differences in sizes of cnidae between the two species, however, due to large overlaps and relatively high standard deviation values (Suppl. material 2: Table 2), we do not consider cnidae sizes alone as appropriate to distinguish between these species.

The only morphological characteristic that was consistently found to be useful for species identification was tentacle coloration. Specimens of *P. mizigama* and *P. umbrosa* both possessed white tentacles, but black horizontal stripes were always present on the tentacles of *P. mizigama* (Figure 3b–d). On the other hand, *P. umbrosa* specimens had either completely white tentacles or white tentacles with very small black dots that were placed randomly without forming any stripe pattern (Figure 6c). It is recommended to use a stereomicroscope for accurate identification of *P. mizigama* and *P. umbrosa* as *P. mizigama* polyps with sparse stripes on the tentacles (Figure 3d) are hard to distinguish from *P. umbrosa* when observed with the naked eye.

In general, species identification based on coloration has been thought of as not generally reliable for brachycnemic zoantharians as much intraspecific variation is present (Burnett et al. 1995, 1997, Reimer et al. 2004). However, this study suggests that tentacle coloration in *P. mizigama* and *P. umbrosa* reflects their status as separate species, and this character may be useful for rapid field identification of *P. mizigama* and *P. umbrosa*. The utility of coloration has also been mentioned in Sinniger and Häussermann (2009) for macrocnemic zoantharians, which tend to have more uniform coloration. Unlike many zooxanthellate brachycnemic zoantharians, *P. mizigama* and *P. umbrosa* have relatively plain coloration with limited intraspecific variation (e.g. white to tan base color with or without black blotches at random locations on the column). Naturally, polyp columns and oral discs tend to attract more attention than tentacles, as tentacles are generally thin and hard to observe in situ when polyps are closed. Therefore, we recommend that this characteristic not be overlooked, as it is useful for identification in at least these two species.

Causes of morphological and ecological similarities of the two new *Palythoa* species

This study showed a high morphological similarity between *P. mizigama* and *P. umbrosa* in spite of their relatively distant genetic relationship within genus *Palythoa*. Two possibilities can be considered as the potential cause of this situation. One hypothesis is that *P. mizigama* and *P. umbrosa* have recently diverged from each other but their morphological characteristics have not yet diverged. However, our phylogenetic results showed that *P. mizigama* and *P. umbrosa* do not form a monophyletic group with any of three DNA markers used in this study, and even conservative mitochondrial DNA regions (COI and 16S rDNA) differentiated between the two groups. Thus, there is no support for the idea that *P. mizigama* and *P. umbrosa* have recently diverged.

The other hypothesis is that *P. mizigama* and *P. umbrosa* diverged at relatively the same time as many other zooxanthellate *Palythoa* spp. (e.g. *P. mutuki*, *P. heliodiscus*,

P. tuberculosa in Figures 7–9), and their unique yet similar morphological and ecological characteristics developed independently in each species as a case of parallel evolution. *Palythoa mizigama* and *P. umbrosa* are azooxanthellate, and this trait is previously almost completely unknown within *Palythoa*. The phylogenetic trees obtained in this study suggested that the two species lost their zooxanthellae separately (Figs 7–9). It is apparent that their habitat in caves and fissures has had a strong influence on the losses of zooxanthellae. Loss of zooxanthellae in relation to cave dwelling anthozoans has also been reported from a recently described cave-dwelling scleractinian species (Hoeksema 2012). Other brachycnemic zoantharians are all zooxanthellate asides from *Sphenopus* spp. and *P. macmurrichi* (Haddon & Shackleton, 1891) and obtain at least part of their nutritional input from photosynthesis, with the remainder from plankton feeding (Trench 1974). *Palythoa mizigama* and *P. umbrosa* inhabit dim environments where enough sunlight for photosynthesis is not available and thus their source of nutrients appears to be exclusively planktonic. Long tentacles have advantages for plankton feeding (Koehl 1977, Sebens 1981), and are seen in other *Palythoa* species such as *P. variabilis* (Duerden, 1898) (Koehl 1977) and in azooxanthellate, planktonivoric macrocnemic species. White, plain coloration might be due to the lack of zooxanthellae or a lack of host-based pigments that protect animals from UV light (Salih et al. 2000), and a similar lack of coloration has been noted from a wide variety of azooxanthellate Zoantharia species (e.g. *Microzoanthus kagerou* Fujii & Reimer, 2011, *Abyssoanthus nankaiensis* Reimer & Fujiwara, 2007, and many *Epizoanthus* species). There are other characteristics that were observed in the two *Palythoa* species such as non-erect polyps when closed, or black patterning on the external polyps, though advantages or causes of these characteristics are unclear. It is possible that some of the characteristics seen in the two species are symplesiomorphies, inherited from a common ancestor. However, there would also be other factors influencing morphologies of the two species, considering that these characteristics are rare among brachycnemic zoantharians. A combination of relatively similar genomic information and a common habitat may have resulted in large morphological overlaps of the two new species in this study.

Relationship between *Sphenopus* and *Palythoa*

Sphenopus has an unusual morphology and ecology among zoantharians, as it is solitary and buried in sand or soft substrate usually without attaching to the substrate. From these unique characteristics, *Sphenopus* has been considered to be a different genus from *Palythoa*. However, the general morphological characters (e.g. mesenterial arrangement, heavy sand incrustation etc.) of *Sphenopus* asides from the lack of colonial form and lack of attachment are the same as for *Palythoa*. In fact, there are some *Palythoa* species that have somewhat similar ecological features to *Sphenopus*, such as *Palythoa psammophilia* Walsh & Bowers, 1971, which inhabits sandy areas with its polyps partially buried (Walsh and Bowers 1971). Other examples are the two new azooxanthellate species in this study with polyps often found in solitary form. Additionally, the results of current

and previous (Reimer et al. 2012b) phylogenetic analyses indicate that genus *Sphenopus* is genetically positioned within the genus *Palythoa* (Figures 7–9). Arrigoni et al. 2014 also showed that colony form (solitary or colonial) or possession of zooxanthellae does not always reflect the phylogenetic relationship in the family Dendrophylliidae (Scleractinia). These traits probably change quickly by responding to the surrounding environments. Therefore, considering the morphological and ecological overlaps and the phylogenetic results, it may be appropriate to include *Sphenopus* within *Palythoa*. Surprisingly, *Sphenopus marsupialis* showed a sister relationship with *P. mizigama* in the phylogenetic tree of ITS rDNA region (Figure 7), although validity of this result is still somewhat uncertain as it was not supported in the 16S rDNA and COI trees.

Conclusions

Planktonivory (Fabricius and Metzner 2004) combined with an association with *Symbiodinium* spp. is a typical ecological feature of species of genus *Palythoa*. From the discovery of the two new azooxanthellate *Palythoa* species in this study, and considering genus *Sphenopus* should likely be included within genus *Palythoa*, it is clear *Palythoa* encompasses a more ecologically diverse group of species than previously understood. From our phylogenetic results it appears that a loss of *Symbiodinium* symbioses can occur relatively quickly on an evolutionary time scale at the level of individual species. These results further demonstrate how ecological traits in Zoantharia previously considered to be important at higher taxonomic levels (genus, family) may evolve and change more rapidly than has generally been assumed. Similar results have been seen in the losses of sand incrustation (Reimer et al. 2011a) and skeleton secretion (Sinniger et al. 2013). Investigations on the relationships between phylogeny and habitats of *Palythoa* spp. and *Sphenopus* spp. might be helpful to track the evolutionary history of family Sphenopidae.

The two new species have very similar morphological features although their phylogenetic positions are relatively distant and without molecular analyses they could have been misdiagnosed as a single species. To avoid taxonomic confusion of zoantharian identification caused by their morphological plasticity, a combination of molecular and morphological data is recommended (Swain and Swain 2014). As seen in previous studies (Sinniger et al. 2008, Reimer et al. 2012a), the combination of the three DNA markers (mitochondrial COI and 16S rDNA, ITS rDNA) utilized in this study was sufficient to distinguish between species. In this study, conservative mt DNA (Huang et al. 2008) differentiated between the new species, even though a few species share identical sequences with the two new species for some of these regions (e.g. COI sequences of *P. mizigama* and *P.* sp. sakurajimensis are identical, and 16S rDNA sequences of *P. umbrosa*, *P. grandis*, and *S. marsupialis* are identical) (Figures 8 and 9). Although ITS rDNA is useful for species-level identification, development of additional new DNA markers is needed for furthering research and obtaining more robust data, which will help elucidate more detailed intrageneric zoantharian phylogenies.

Acknowledgements

The authors thank Dr T. Fujii (University of the Ryukyus) for his great help providing specimens from Yaeyama Islands, Japan. Drs Y. Nozawa and CA. Chen (Biodiversity Research Center, Academia Sinica; BRCAS) and members of their laboratories for their invaluable assistance in the field in Taiwan. Prof. E. Hirose (University of the Ryukyus), Dr S. Keshavmurthy, CY. Kuo, HJ. Hseih, and AC. Chung (all BRCAS) also greatly assisted with the sample collection in Taiwan. Dr C. Payri, Dr B. Richer-de-Forges and Tiéti diving in Poindimié are thanked for the assistance in the sampling of the New Caledonian specimen. F. Sinniger was partially financed by the Japan Society for Promotion of Science and the senior author was funded by a grant-in-aid from the Japan Society for the Promotion of Science ("Wakate B" #217700896), as well as the Rising Star Program and the International Research Hub Project for Climate Change and Coral Reef/Island Dynamics, both at the University of the Ryukyus. Support was also provided by a Japan Society for the Promotion of Science 'Zuno-Junkan' grant entitled 'Studies on origin and maintenance of marine biodiversity and systematic conservation planning' to the senior author.

References

Acosta A (2001) Disease in zoanthids: dynamics in space and time. Hydrobiologia 460: 113–130. doi: 10.1023/A:1013135702430

Arrigoni R, Kitano YF, Stolarski J, Hoeksema BW, Fukami H, Stefani F, Galli P, Montano S, Castoldi E, Benzoni F (2014) A phylogeny reconstruction of the Dendrophylliidae (Cnidaria, Scleractinia) based on molecular and micromorphological criteria, and its ecological implications. Zoologica Scripta 43: 661–688. doi: 10.1111/zsc.12072

Burnett WJ (2002) Longitudinal variation in algal symbionts (zooxanthellae) from the Indian Ocean zoanthid *Palythoa caesia*. Marine Ecology Progress Series 234: 105–109. doi: 10.3354/meps234105

Burnett WJ, Benzie JAH, Beardmore JA, Ryland JS (1995) Patterns of genetic subdivision in populations of a clonal cnidarian, *Zoanthus coppingeri*, from the Great Barrier Reef. Marine Biology 122(4): 665–673. doi: 10.1007/BF00350688

Burnett WJ, Benzie JAH, Beardmore JA, Ryland JS (1997) Zoanthids (Anthozoa, Hexacorallia) from the Great Barrier Reef and Torres Strait, Australia: systematics, evolution and a key to species. Coral Reefs 16: 55–68. doi: 10.1007/s003380050060

Camillo CG, Bo M, Puce S, Bavestrello G (2010) Association between *Dentitheca habereri* (Cnidaria: Hydrozoa) and two zoanthids. Italian Journal of Zoology 77(1): 81–91. doi: 10.1080/11250000902740962

Crocker LA, Reiswig HM (1981) Host specificity in sponge-encrusting Zoanthidea (Anthozoa: Zoantharia) of Barbados, West Indies. Marine Biology 65: 231–236. doi: 10.1007/BF00397116

Edgar RC (2004) MUSCLE: multiple sequence alignment with high accuracy and high throughput. Nucleic Acids Research 32(5): 1792–1797. doi: 10.1093/nar/gkh340

Fabricius KE, Metzner J (2004) Scleractinian walls of mouths: predation on coral larvae by corals. Coral Reefs 23(2): 245–248. doi: 10.1007/s00338-004-0386-x

Folmer O, Black M, Hoeh W, Lutz R, Vrijenhoek R (1994) DNA primers for amplification of mitochondrial cytochrome c oxidase subunit I from diverse metazoan invertebrates. Molecular Marine Biology and Biotechnology 3(5): 294–299. http://www.mbari.org/staff/vrijen/PDFS/Folmer_94MMBB.pdf

Fukami H, Chen CA, Budd AF, Collins A, Wallace C, Chuang Y, Chen C, Dai C, Iwao K, Sheppard C, Knowlton N (2008) Mitochondrial and nuclear genes suggest that stony corals are monophyletic but most families of stony corals are not (Order Scleractinia, Class Anthozoa, Phylum Cnidaria). PLoS ONE 3(9): e3222. doi:10.1371/journal.pone.0003222

Gray JE (1867) Notes on Zoanthinae, with the descriptions of some new genera. Proceedings of the Zoological Society of London 15: 233–240.

Guindon S, Dufayard JF, Lefort V, Anishmova M, Hordijk W, Gascuel O (2010) New algorithms and methods to estimate Maximum-likelihood phylogenies: Assessing the performance of PhyML 3.0. Systematic Biology 59(3): 307–321. doi: 10.1093/sysbio/syq010

Haddon AC, Shackleton AM (1891) Reports on the zoological collections made in Torres Straits by professor AC Haddon, 1888–1889: Actiniæ. Zoantheæ. Royal Dublin Society, London. doi: 10.5962/bhl.title.46274

Hoeksema BW (2012) Forever in the dark: the cave-dwelling azooxanthellate reef coral *Leptoseris troglodyta* sp. n. (Scleractinia, Agariciidae). ZooKeys 228: 21–37. doi: 10.3897/zookeys.228.3798

Huang D, Meier R, Todd PA, Chou LM (2008) Slow mitochondrial COI sequence evolution at the base of the metazoan tree and its implications for DNA barcoding. Journal of Molecular Evolution 66(2): 167–174. doi: 10.1007/s00239-008-9069-5

Irei Y, Nozawa Y, Reimer JD (2011) Distribution patterns of five zoanthid species at Okinawa Island, Japan. Zoological Studies 50(4): 426–433. doi: 10.1186/1810-522X-52-38

Koehl MAR (1977) Water flow and the morphology of zoanthid colonies. Proceedings of the Third International Coral Reef Symposium, Miami, 1977. 1: 437–444.

Kuramoto M, Hayashi K, Fujitani Y, Yamaguchi K, Tsujii T, Yamada K, Ijuin Y, Uemura D (1997) Absolute configuration of norzoanthamine, a promising candidate for an osteoporotic drug. Tetrahedron Letters 38(32): 5683–5686. doi: 10.1016/S0040-4039(97)01238-0

Larkin MA, Blackshield G, Brown NP, Chenna R, McGettigan PA, McWilliam H, Valentin F, Wallace IM, Wilm A, Lopez R, Gibson TJ, Higgins DG (2007) Clusral W and Clustal X version 2.0. Bioinformatics 23: 2947–2948. doi: 10.1093/bioinformatics/btm404

Moore R, Scheuer PJ (1971) Palytoxin: a new marine toxin from a Coelenterate. Science 172: 495–498. doi: 10.1126/science.172.3982.495

Muirhead A, Tyler PA, Thurston MH (1986) Reproductive biology and growth of the genus *Epizoanthus* (Zoanthidea) from the North-East Atlantic. Journal of the Marine Biological Association of the United Kingdom 66: 131–143. doi: 10.1017/S0025315400039709

Pax F (1910) Studien an westindischen Actinien. In: Spengel JW (Ed.) Ergebnisse einer Zoologischen Forschungreise nach Westindien von Prof. W. Kukenthal und Dr R. Hartmeyer im Jahre, 1907. Zoologische Jahrbucher Supplement 11: 157–330.

Rambaut A, Charleston M (1997–2001) Se-Al: Sequence Alignment Editor. Molecular Evolution Library, University of Oxford, UK. http://evolve.zoo.ox.ac.uk/

Rasband WS (1997–2012) ImageJ. U.S. National Institutes of Health, Bethesda, Maryland, USA. http://imagej.nih.gov/ij/

Reimer JD (2010) Key to field identification of shallow water brachycnemic zoanthids (Order Zoantharia: Suborder Brachycnemina) present in Okinawa. Galaxea 12: 23–29. doi: 10.3755/galaxea.12.23

Reimer JD (2014a) *Sphenopus* Steenstrup, 1856. Accessed through: World Register of Marine Species at http://www.marinespecies.org/aphia.php?p=taxdetails&id=267847 [on 2014-08-29]

Reimer JD (2014b) *Palythoa* Lamouroux, 1816. Accessed through: World Register of Marine Species at http://www.marinespecies.org/aphia.php?p=taxdetails&id=205785 [on 2015-01-01]

Reimer JD (2014c) *Protopalythoa* Verrill, 1900. Accessed through: World Register of Marine Species at http://www.marinespecies.org/aphia.php?p=taxdetails&id=100795 [on 2015-01-01]

Reimer JD, Ono S, Takishita K, Fujiwara Y, Tsukahara J (2004) Reconsidering *Zoanthus* spp. diversity: molecular evidence of conspecificity within four previously presumed species. Zoological Science 21: 517–525. doi: 10.2108/zsj.21.517

Reimer JD, Ono S, Takishita K, Tsukahara J, Maruyama T (2006a) Molecular evidence suggesting species in the zoanthid genera *Palythoa* and *Protopalythoa* (Anthozoa: Hexacorallia) are congeneric. Zoological Science 23(1): 87–94. doi: 10.2108/zsj.23.87

Reimer JD, Takishita K, Maruyama T (2006b) Molecular identification of symbiotic dinoflagellates (*Symbiodinium* spp.) from *Palythoa* spp. (Anthozoa: Hexacorallia) in Japan. Coral Reefs 25: 521–527. doi: 10.1007/s00338-006-0151-4

Reimer JD, Sinniger F, Fujiwara Y, Hirano S, Maruyama T (2007a) Morphological and molecular characterisation of *Abyssoanthus nankaiensis*, a new family, new genus and new species of deep-sea zoanthid (Anthozoa: Hexacorallia: Zoantharia) from a north-west Pacific methane cold seep. Invertebrate Systematics 21: 255–262. doi: 10.1071/IS06008

Reimer JD, Takishita K, Ono S, Tsukahara J, Maruyama T (2007b) Molecular evidence suggesting intraspecific hybridization in *Zoanthus* spp. (Anthozoa: Hexacorallia). Zoological Science 24: 346–359. doi: 10.2108/zsj.24.346

Reimer JD, Hirose M, Nishisaka T, Sinniger F, Itani G (2010) *Epizoanthus* spp. associations revealed using DNA markers: a case study from Kochi, Japan. Zoological Science 27(9): 729–734. doi: 10.2108/zsj.27.729

Reimer JD, Hirose M, Irei Y, Obuchi M, Sinniger F (2011a) The sands of time: rediscovery of the genus *Neozoanthus* (Cnidaria: Hexacorallia) and evolutionary aspects of sand incrustation in brachycnemic zoanthids. Marine Biology 158(5): 983–993. doi: 10.1007/s00227-011-1624-8

Reimer JD, Obuchi M, Irei Y, Fujii T, Nozawa Y (2011b) Shallow-water brachycnemic zoanthids (Cnidaria: Hexacorallia) from Taiwan: A preliminary survey. Zoological Studies 50(3): 363–371. http://zoolstud.sinica.edu.tw/Journals/50.3/363.pdf

Reimer JD, Foord C, Irei Y (2012a) Species diversity of shallow water zoanthids (Cnidaria: Anthozoa: Hexacorallia) in Florida. Journal of Marine Biology vol. 2012, Article ID 856079. doi: 10.1155/2012/856079

Reimer JD, Lin M, Fujii T, Lane DJW, Hoeksema BW (2012b) The phylogenetic position of the solitary zoanthid genus *Sphenopus* (Cnidaria: Hexacorallia). Contributions to Zoology 81(1): 43–54. http://dpc.uba.uva.nl/ctz/vol81/nr01/art03

Reimer JD, Irei Y, Fujii T, Yang S (2013) Molecular analyses of shallow-water zooxanthellate zoanthids (Cnidaria: Hexacorallia) from Taiwan and their *Symbiodinium* spp. Zoological Studies 52(38). doi: 10.1186/1810-522X-52-38

Ronquist F, Huelsenbeck JP (2003) MrBayes 3: Bayesian phylogenetic inference under mixed models. Bioinformatics 19: 1572–1574. doi: 10.1093/bioinformatics/btg180

Ryland JS, Lancaster JE (2003) Revision of methods for separating species of *Protopalythoa* (Hexacorallia: Zoanthidea) in the tropical West Pacific. Invertebrate Systematics 17: 407–428. doi:10.1071/IS02008

Ryland JS, Lancaster JE (2004) A review of zoanthid nematocyst types and their population structure. Hydrobiologia 530(531): 179–187. doi: 10.1007/s10750-004-2685-1

Ryland JS, Putron S, Scheltema RS, Chimonides PJ, Zhadan DG (2000) Semper's (zoanthid) larvae: pelagic life, parentage and other problems. Hydrobiologia 440: 191–198. doi: 10.1007/978-94-017-1982-7_18

Salih A, Larkum A, Cox G, Kühl M, Hoegh-Guldberg O (2000) Fluorescent pigments in corals are photoprotective. Nature 408: 850–853. doi: 10.1038/35048564

Schejter L, Mantelatto FL (2011) Shelter association between the hermit crab *Sympagurus dimorphus* and the zoanthid *Epizoanthus paguricola* in the southwestern Atlantic Ocean. Acta Zoologica 92(2): 141–149. doi: 10.1111/j.1463-6395.2009.00440.x

Sebens KP (1981) The allometry of feeding, energetics, and body size in three sea anemone species. Biological Bulletin 161(1): 152–171. doi: 10.2307/1541115, http://www.biolbull.org/content/161/1/152.short

Sebens KP (1982) Intertidal distribution of zoanthids on the Caribbean coast of Panama: effects of predation and desiccation. Bulletin of Marine Science 32: 316–335. http://www.ingentaconnect.com/content/umrsmas/bullmar/1982/00000032/00000001/art00023#expand/collapse

Sinniger F, Häussermann V (2009) Zoanthids (Cnidaria: Hexacorallia: Zoantharia) from shallow waters of the southern Chilean fjord region, with descriptions of a new genus and two new species. Organisms Diversity & Evolution 9(1): 23–36. doi: 10.1016/j.ode.2008.10.003

Sinniger F, Montoya-Burgos JI, Chevaldonné P, Pawlowski J (2005) Phylogeny of the order Zoantharia (Anthozoa, Hexacorallia) based on the mitochondrial ribosomal genes. Marine Biology 147: 1121–1128. doi: 10.1007/s00227-005-0016-3

Sinniger F, Reimer JD, Pawlowski J (2008) Potential of DNA sequences to identify zoanthids (Cnidaria: Zoantharia). Zoological Science 25(12): 1253–1260. doi: 10.2108/zsj.25.1253

Sinniger F, Reimer JD, Pawlowski J (2010) The Parazoanthidae (Hexacorallia: Zoantharia) DNA taxonomy: description of two new genera. Marine Biodiversity 40(1): 57–70. doi: 10.1007/s12526-009-0034-3

Sinniger F, Ocana OV, Baco AR (2013) Diversity of zoanthids (Anthozoa: Hexacorallia) on Hawaiian seamounts: description of the Hawaiian gold coral and additional zoanthids. PLoS ONE 8(1): e52607. doi: 10.1371/journal.pone.0052607

Soong K, Shiau YS, Chen CP (1999) Morphological and life history divergence of the zoanthid, *Sphenopus marsupialis* off the Taiwanese Coast. Zoological Studies 38(3): 333–343.

Suchanek TH, Green DJ (1981) Interspecific competition between *Palythoa caribaeorum* and other sessile invertebrates on St. Croix reefs, U.S. Virgin Islands. Proceedings of the Fourth International Coral Reef Symposium, Manila, 1981. 2: 679–684.

Swain TD (2009) Phylogeny-based species delimitations and the evolution of host associations in symbiotic zoanthids (Anthozoa, Zoanthidea) of the wider Caribbean region. Zoological Journal of the Linnean Society 156: 223–238. doi: 10.1111/j.1096-3642.2008.00513.x

Swain TD, Swain LM (2014) Molecular parataxonomy as taxon description: examples from recently named Zoanthidea (Cnidaria: Anthozoa) with revision based on serial histology of microanatomy. Zootaxa 3796 (1): 81–107. doi: 10.11646/zootaxa.3796.1.4

Trench RK (1974) Nutritional potentials in *Zoanthus sociathus* (Coelenterata, Anthozoa). Helgoländer Wissenschaftliche Meeresuntersuchungen 26(2): 174–216. doi: 10.1007/BF01611382

Verrill AE (1900) Additions to the Anthozoa and Hydrozoa of the Bermudas. In: Verrill AE (Ed.) Zoology of Bermuda, New Haven, 551–572.

Vitor R, Vitor V (2010) Palytoxin and analogs: Biological and Ecological effects. Marine Drugs 8(7): 2021–2037. doi: 10.3390/md8072021

Walsh GE (1967) An annotated bibliography of the families Zoanthidae, Epizoanthidae, and Parazoanthidae (Coelenterata, Zoantharia). No. 13. Hawaii Institute of Marine Biology, Hawaii.

Walsh GE, Bowers RL (1971) A review of Hawaiian zoanthids with descriptions of three new species. Zoological Journal of the Linnean Society 50(2): 161–180. doi: 10.1111/j.1096-3642.1971.tb00757.x

Supplementary material 1

Table 1

Authors: Yuka Irei, Frederic Sinniger, James Davis Reimer

Data type: Microsoft Excel File (xlsx)

Explanation note: List of *Palythoa mizigama* sp. n. and *P. umbrosa* sp. n. specimens used in molecular analyses.

Supplementary material 2

Table 2

Authors: Yuka Irei, Frederic Sinniger, James Davis Reimer

Data type: Microsoft Excel File (xlsx)

Explanation note: Length and widths of four major cnidae types found in *Palythoa mizigama* sp. n. and *P. umbrosa* sp. n.

ZooKeys 478: 27–43 (2015)
doi: 10.3897/zookeys.478.8037
http://zookeys.pensoft.net

RESEARCH ARTICLE

A peer-reviewed open-access journal
ZooKeys
Launched to accelerate biodiversity research

Molecular identification of blood meal sources of ticks (Acari, Ixodidae) using cytochrome b gene as a genetic marker

Ernieenor Faraliana Che Lah[1,2], Salmah Yaakop[2], Mariana Ahamad[1], Shukor Md Nor[2]

1 *Acarology Unit, Infectious Diseases Research Centre, Institute for Medical Research, Jalan Pahang, 50588, Kuala Lumpur, Malaysia* **2** *School of Environmental and Natural Resource Sciences, Faculty of Sciences and Technology, University Kebangsaan Malaysia, 43600 Bangi, Selangor, Malaysia*

Corresponding author: *Ernieenor Faraliana Che Lah* (erniee@imr.gov.my)

Academic editor: *D. Apanaskevich* | Received 5 June 2014 | Accepted 30 December 2014 | Published 28 January 2015

http://zoobank.org/A6589F9C-293D-4EBF-B419-6FF2E3677922

Citation: Che Lah EF, Yaakop S, Ahamad M, Md Nor S (2015) Molecular identification of blood meal sources of ticks (Acari, Ixodidae) using cytochrome b gene as a genetic marker. ZooKeys 478: 27–43. doi: 10.3897/zookeys.478.8037

Abstract

Blood meal analysis (BMA) from ticks allows for the identification of natural hosts of ticks (Acari: Ixodidae). The aim of this study is to identify the blood meal sources of field collected on-host ticks using PCR analysis. DNA of four genera of ticks was isolated and their cytochrome b (Cyt *b*) gene was amplified to identify host blood meals. A phylogenetic tree was constructed based on data of Cyt *b* sequences using Neighbor Joining (NJ) and Maximum Parsimony (MP) analysis using MEGA 5.05 for the clustering of hosts of tick species. Twenty out of 27 samples showed maximum similarity (99%) with GenBank sequences through a Basic Local Alignment Search Tool (BLAST) while 7 samples only showed a similarity range of between 91–98%. The phylogenetic trees showed that the blood meal samples were derived from small rodents (*Leopoldamys sabanus*, *Rattus tiomanicus* and *Sundamys muelleri*), shrews (*Tupaia glis*) and mammals (*Tapirus indicus* and *Prionailurus bengalensis*), supported by 82–88% bootstrap values. In this study, Cyt *b* gene as a molecular target produced reliable results and was very significant for the effective identification of ticks' blood meal. The assay can be used as a tool for identifying unknown blood meals of field collected on-host ticks.

Keywords

Ticks, Blood meal, Vector control, hosts, Cytochrome b

Introduction

The tick is a member of the class Arachnida that belongs to the sub-class Acari. It relies heavily on other animals as hosts to complete their life cycle (Mihalca et al. 2012). The tick is the second important vector after mosquitoes and is able to transmit disease in both man and livestock (Dalgic et al. 2010, Smith et al. 2010). Ticks may transmit a range of disease agents that are of medical and veterinary importance when taking a blood meal. Ticks that live in close proximity to humans, especially those on rodents, play a significant role in the transmission of several diseases (Chul-Min et al. 2006). Besides their role as hosts, rodents also serve as reservoirs of tick-borne pathogens (Paulauskas et al. 2009, Harrison et al. 2010, Paziewska et al. 2010). The close association between rodents and human is a risk factor for the transmission of diseases such as rickettsiosis, babesiosis and Lyme borreliosis (Killilea et al. 2008, Kia et al. 2009, Mihalca et al. 2012).

Research on the identification of a natural host for ticks is valuable and is the main goal of a blood meal analysis (BMA). The analysis is a tool used to identify the hosts of blood feeding arthropods (Gariepy et al. 2012). Research into the composition of blood meals of arthropod vectors has been shown to provide evidence of link vector species with their specific hosts that can be used to determine possible disease reservoirs (Scott et al. 2012, Onder et al. 2013). Knowledge of vector host identification of ticks is critical in understanding the transmission cycle of vector-borne diseases (Christine 2011) and thus can provide important information to public health stakeholders for the development of more effective control strategies. Initially, attempts to identify blood meals of arthropods were made using serological techniques such as precipitin and latex agglutination tests (Walker and Davies 1971, Nevil and Anderson 1972). An improvement on the sensitivity of blood meal origin analysis was later studied using enzyme-linked immunosorbent assays (ELISA) (Elias et al. 2010, Maria Stella et al. 2012). While those techniques continue to provide valuable and insightful data, the identification of many blood meal sources is limited to just the order or family level and species could only be identified when antibodies were available. The advert of the polymerase chain reaction (PCR) and the availability of DNA sequence data of various vertebrates quickly led to a shift towards DNA-based identification (Mukabana et al. 2002, Humair et al. 2007, Kent 2009, Garros et al. 2011).

The progressive development of molecular analysis has resulted in the use of markers that were originally designed to study phylogenetic relationships among vertebrates being applied to determine the blood meal origin of haematophagous arthropods (Boakye et al. 1999, Ninio et al. 2011). Tobolewski et al. (1992) reported that DNA techniques are much faster and more reliable to determine host species compared to other techniques that depend on antibodies. Humair et al. (2007) used 12S rDNA as a genetic marker for identification of blood meal sources in *Ixodes ricinus* ticks while Pichon et al. (2003) used a set of universal primers to amplify part of the vertebrate 18S rRNA gene followed by reverse line blot hybridization for host identification of *Ixodes ricinus*. Understanding the origin of blood meals will give

some information on the species involved in disease transmission cycles, as well as the disease risk posed to human.

Analysis of blood meals of local ticks to determine their natural hosts is still poorly understood. There is a critical necessity to document information of potential hosts for local ticks as part of the nation's preparedness for emerging and re-emerging infections. Thus, the aim of this study was to identify the blood meal sources of ticks in Peninsular Malaysia based on the cytochrome b (Cyt *b*) gene. The obtained Cyt *b* genes were then used to construct a phylogenetic tree for the clustering of hosts of tick species.

Materials and methods

Study area and ticks sampling

On-host ticks were collected from four different states of Peninsular Malaysia (Figure 1). The study sites were in Janda Baik, Pahang; Labu, Negeri Sembilan; Hulu Langat, Selangor; and Gunung Tebu, Terengganu. The collections were conducted from March to July 2012. The localities were chosen based on the records from available previous data of high numbers of tick infestation on small animals. The ecology for all localities was similar; consisting of mainly pristine tropical lowland rainforest, secondary growths, scrubs and riverine vegetation. One hundred wire traps were used to capture wild rodents and tree-shrews in each study site. Traps were placed on the ground and on tree branches along existing trails at approximately five meter intervals. Traps were baited with bananas, oil palm fruits, tapioca or potatoes and checked once daily for 5 consecutive days of trapping. Caught animals were placed in cloth bags and brought back to the Institute for Medical Research (IMR). The animals were anesthetized with chloroform before screening and the ticks were collected in the laboratory. The epidemiology data such as locality and ecology were recorded.

Tick Morphological identification

The species of animals were identified by their morphological traits following Medway (1983), Francis (2008) and Payne et al. (2005). A total of 27 on-host ticks were collected either using sterile soft forceps or sharpened wooden applicator sticks. The ticks were then kept individually in vials containing 70% ethanol prior to identification using specific illustrated morphological taxonomic keys (Kohl 1957, Walker et al. 2003).

DNA extraction of blood meals in ticks

Prior to DNA extraction, each engorged tick was individually washed 3 times with sterile distilled water. Extraction of DNA using QIAamp Mini Kit (Qiagen, Germany) was per-

Figure 1. Map of the study sites in Peninsular Malaysia: **1** Hulu Langat, Selangor **2** Labu, Negeri Sembilan **3** Janda Baik, Pahang **4** Gunung Tebu, Terengganu.

formed according to the manufacturer's protocols. DNA of ticks was extracted by adding 80 µl of PBS buffer and 100 µl of ATL buffer into the sample. The ticks were then macerated using sterile tips for 5 minutes before adding of 20 µl of proteinase K. The samples were incubated at 56 °C (6 hours) for complete lyses. The following steps were the same as those in the manufacture's protocols. The DNA was then used for subsequent PCR.

PCR amplification of the mtDNA Cyt *b* gene

A portion of mitochondrial DNA, Cyt *b* gene was amplified by Polymerase Chain Reaction (PCR) with a set of vertebrate-universal primers and reaction conditions as described by Kent and Norris (2005). The primers used were UNFOR403 and UNREV1025 (Table 1) that preferentially amplified a 623-bp region of the Cyt *b* gene from the mitochondrial DNA of vertebrates. The PCR reactions were conducted in 50 µl reaction tubes with the following reagents: 25 µl Taq PCR master 2X, 2.5 µl of

Table 1. List of primers used for PCR amplification

Gene	Primer name	Sequences (5'–3')
Cyt *b*	UNFOR403	5'-TGA GGA CAA ATA TCA TTC TGA GG-3'
	UNREV1025	5'-GGT TGT CCT CCA ATT CAT GTT A-3'

0.5 µM of each primer, 10 µl of nuclease free water and 10 µl of DNA template. The amplification program consists of a total of 35 cycles, denaturing at 94 °C for 3 min, annealing at 52 °C for 1 min, and extension at 72 °C for 1 min, with an initial denaturation at 94 °C for 1 min. PCR was carried out using an Eppendorf Master Cycler Personal machine (Eppendorf, Germany). For each PCR reaction, a negative control containing the DNA of unfed ticks and a positive control containing vertebrate DNA was included. The amplicons were visualized in 1.5% agarose gels stained with ethidium bromide and viewed under an ultraviolet trans-illuminator (wavelength 254 nm).

Sequencing analysis and Alignment

The PCR product was excised with a sterile gel cutter and purified using 5 Prime PCR Agarose Gel Extract Mini Kit (Hamburg, Germany) according to the manufacturer's protocols. The purified product was then sent to the sequencing service company, Medigene Sdn. Bhd. in Petaling Jaya, Selangor. The sequencing was bi-directional for all specimens and the primer combination for this step was the same as that used in the PCR amplification. Sequencing results were exported as FASTA sequence files. The Cyt *b* gene sequences of samples were aligned using ClustalW multiple alignment of BioEdit (Thompson et al. 1994, Hall 2005).

BLAST analysis

The obtained sequences were then compared with available sequences in the GenBank database using the Basic Local Alignment Search Tool search (NCBI website, http://www.ncbi.nlm.nih.gov/BLAST/) for the identification of the host species. This approach was reported to be simple and robust for rapid comparison of query sequences to database sequences leading to species identification (Altschul et al. 1990, Mitler et al. 2010). The approach enabled the similarity of sequences to be measured depending on several criterias such as expected value, maximum identical, query coverage and maximum score.

Clustering analysis

The clustering analysis for all sequences of hosts was carried out by performing phylogenetic analysis using MEGA software (version 5.05). For distance analysis, a neigh-

bor-joining (NJ) tree was generated from a Kimura two-parameter distance matrix. Maximum-parsimony (MP) analysis was performed with Tree-Bisection-Reconnection (TBR) heuristic algorithm to reconstruct a character based phylogenetic tree. Internal branches of both trees were statistically supported by bootstrapping with 1,000 replications. In this study, *Apodemus sylvaticus* (GenBank Accession no. AJ298599.1) was selected as an outgroup for Cyt *b* gene.

Results

A total of 27 engorged ticks collected from four different localities (Table 2) were amplified from Cyt *b* using PCR analysis. Six species of hosts comprising three rodents (*Leopoldamys sabanus*, *Sundamys muelleri* and *Rattus tiomanicus*); a shrew, *Tupaia glis* and two mammals identified as *Tapirus indicus* and *Prionailurus bengalensis*, were identified. Mixed stages of on-host ticks were collected from the animals and identified into four genera: *Ixodes*, *Amblyomma*, *Haemaphysalis* and *Dermacentor*.

Table 2. Details of ticks samples used in analysis.

Code samples	Tick species	Locality	Ecology
K1a	*Amblyomma testudinarium*	Krau Wildlife Reserved, Pahang	Pristine tropical rainforest
K2a	*Dermacentor* sp.	Krau Wildlife Reserved, Pahang	Pristine tropical rainforest
K3c	*Dermacentor* sp.	Krau Wildlife Reserved, Pahang	Pristine tropical rainforest
K4b	*Amblyomma* sp.	Krau Wildlife Reserved, Pahang	Pristine tropical rainforest
K5b	*Amblyomma* sp.	Krau Wildlife Reserved, Pahang	Pristine tropical rainforest
SBN 01	*Ixodes granulatus*	Labu, Negeri Sembilan	Scrubs
SBN12_1	*Dermacentor* sp.	Labu, Negeri Sembilan	Scrubs
SBN23_1	*Ixodes granulatus*	Labu, Negeri Sembilan	Scrubs
SBN 14	*Ixodes* sp.	Labu, Negeri Sembilan	Scrubs
JBB01_1	*Dermacentor* sp.	Janda Baik, Pahang	Riverine vegetation
JBB03_1	*Haemaphysalis* sp.	Janda Baik, Pahang	Riverine vegetation
JBB03_2	*Haemaphysalis* sp.	Janda Baik, Pahang	Riverine vegetation
JBB03_3	*Haemaphysalis* sp.	Janda Baik, Pahang	Riverine vegetation
JBB03_4	*Haemaphysalis* sp.	Janda Baik, Pahang	Riverine vegetation
HL01	*Ixodes granulatus*	Hulu Langat, Selangor	Pristine tropical rainforest
HL02	*Ixodes granulatus*	Hulu Langat, Selangor	Pristine tropical rainforest
HL03_2	*Ixodes granulatus*	Hulu Langat, Selangor	Pristine tropical rainforest
HL03	*Ixodes granulatus*	Hulu Langat, Selangor	Pristine tropical rainforest
HL04_15	*Ixodes granulatus*	Hulu Langat, Selangor	Pristine tropical rainforest
HL02_4	*Ixodes granulatus*	Hulu Langat, Selangor	Pristine tropical rainforest
HL02_5	*Ixodes granulatus*	Hulu Langat, Selangor	Pristine tropical rainforest
HL02_3	*Ixodes granulatus*	Hulu Langat, Selangor	Pristine tropical rainforest
HL07	*Ixodes granulatus*	Hulu Langat, Selangor	Pristine tropical rainforest
HL02_1	*Ixodes granulatus*	Hulu Langat, Selangor	Pristine tropical rainforest
GT23_2	*Ixodes granulatus*	Gunung Tebu, Terengganu	Secondary growth
GT23_3	*Ixodes granulatus*	Gunung Tebu, Terengganu	Secondary growth
GT23_5	*Ixodes granulatus*	Gunung Tebu, Terengganu	Secondary growth

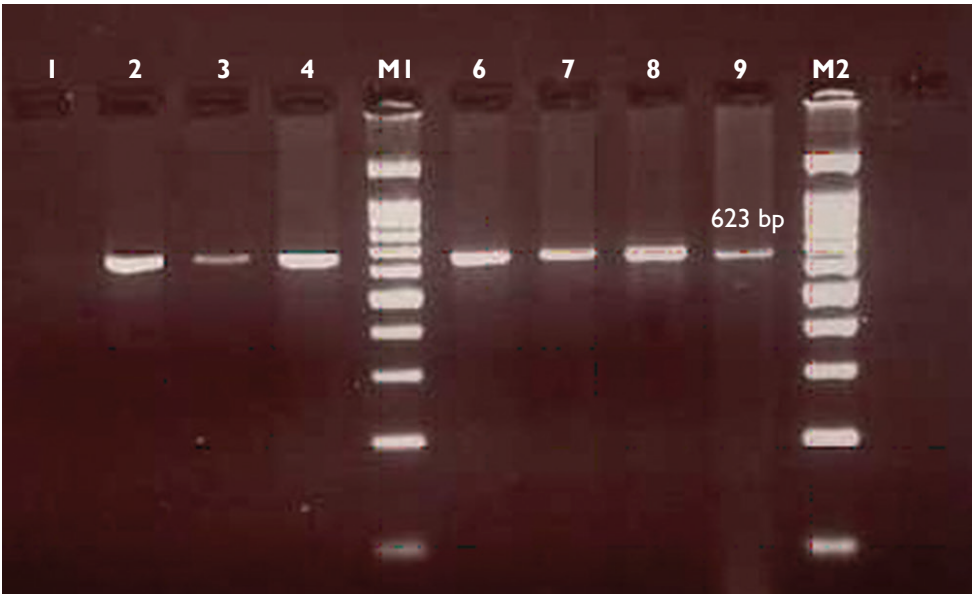

Figure 2. Amplification of Cyt *b* gene produced 623 bp of PCR products from ticks species. *Lane 1*: unfed ticks (negative control); *Lane 2*: vertebrate DNA (positive control); *Lanes 3–8*: DNA of field-collected ticks (*Ixodes* sp., *Dermacentor* sp., *Amblyomma* sp., *Amblyomma testudinarium*, *Haemaphysalis* sp., *Haemaphysalis* sp.,) and *Lanes* M1, M2: 100 bp DNA ladder (Bioron, Germany).

PCR products and BLAST analysis

Vertebrate DNA was successfully amplified from 27 engorged ticks. The amplification of a single fragment encoding a 623 bp sequence of the Cyt *b* gene yielded the expected amplification products (Figure 2). Negative control (unfed ticks) yielded no PCR product implying that only host DNA patterns were detected in the amplifying specimens. All blood meals were identified down to species level. In general, the percent similarity between queried (unknown) sequences and the closest match in GenBank was between 91–100% (Table 3). Twenty out of 27 sequences (74.1%) showed maximum homology (99%) while 2 sequences (HL04_15 and SBN23_1) displayed 98% similarity with the online database. One sequence (HL03) showed maximum homology to *L. sabanus* with a 97% similarity while four sequences from Janda Baik matched to *S. muelleri* with a 91%. Some of the differences were probably due to intraspecific variation and in some cases, it could be due to poor sequence quality, particularly when unassigned nucleotides (n's) were present in the sequence.

Clustering inferens

From the 27 aligned DNA sequences, a total of 575-bp portion of the Cyt *b* gene was used for analysis. Out of 575 characters from Cyt *b* fragments, 252 variable sites were

Table 3. Blasting results against available sequences in GenBank.

Code samples	Tick species	Host species (morphological)	% similarity with GenBank (species)
K1a	*Amblyomma testudinarium*	*Tapirus indicus*	99 (*Tapirus indicus*)
K2a	*Dermacentor* sp.	*Tapirus indicus*	99 (*Tapirus indicus*)
K3c	*Dermacentor* sp.	*Tapirus indicus*	99 (*Tapirus indicus*)
K4b	*Amblyomma* sp.	*Tapirus indicus*	99 (*Tapirus indicus*)
K5b	*Amblyomma* sp.	*Tapirus indicus*	99 (*Tapirus indicus*)
SBN 01	*Ixodes granulatus*	*Rattus tiomanicus*	99 (*Rattus tiomanicus*)
SBN12_1	*Dermacentor* sp	*Rattus tiomanicus*	99 (*Rattus tiomanicus*)
SBN23_1	*Ixodes granulatus*	*Rattus tiomanicus*	98 (*Rattus tiomanicus*)
SBN 14	*Ixodes* sp.	*Rattus tiomanicus*	99 (*Prionailurus bengalensis*)
JBB01_1	*Dermacentor* sp.	*Tupaia glis*	99 (*Tupaia glis*)
JBB03_1	*Haemaphysalis* sp.	*Sundamys muelleri*	91 (*Sundamys muelleri*)
JBB03_2	*Haemaphysalis* sp.	*Sundamys muelleri*	91 (*Sundamys muelleri*)
JBB03_3	*Haemaphysalis* sp.	*Sundamys muelleri*	91 (*Sundamys muelleri*)
JBB03_4	*Haemaphysalis* sp.	*Sundamys muelleri*	91 (*Sundamys muelleri*)
HL01	*Ixodes granulatus*	*Leopoldamys sabanus*	99 (*Leopoldamys sabanus*)
HL02	*Ixodes granulatus*	*Leopoldamys sabanus*	99 (*Leopoldamys sabanus*)
HL03_2	*Ixodes granulatus*	*Leopoldamys sabanus*	99 (*Leopoldamys sabanus*)
HL03	*Ixodes granulatus*	*Leopoldamys sabanus*	97 (*Leopoldamys sabanus*)
HL04_15	*Ixodes granulatus*	*Sundamys muelleri*	98 (*Sundamys muelleri*)
HL02_4	*Ixodes granulatus*	*Leopoldamys sabanus*	99 (*Leopoldamys sabanus*)
HL02_5	*Ixodes granulatus*	*Leopoldamys sabanus*	99 (*Leopoldamys sabanus*)
HL02_3	*Ixodes granulatus*	*Leopoldamys sabanus*	99 (*Leopoldamys sabanus*)
HL07	*Ixodes granulatus*	*Leopoldamys sabanus*	99 (*Leopoldamys sabanus*)
HL02_1	*Ixodes granulatus*	*Leopoldamys sabanus*	99 (*Leopoldamys sabanus*)
GT23_2	*Ixodes granulatus*	*Leopoldamys sabanus*	99 (*Leopoldamys sabanus*)
GT23_3	*Ixodes granulatus*	*Leopoldamys sabanus*	99 (*Leopoldamys sabanus*)
GT23_5	*Ixodes granulatus*	*Leopoldamys sabanus*	99 (*Leopoldamys sabanus*)

detected, among which 203 (35.3%) variable characters were parsimony-informative while 49 (8.5%) characters were parsimony-uninformative. Additionally, the conserved sites were constituted by 323 (56.1%) characters showing that Cyt *b* gene is a very conserved gene in the mtDNA.

The mitochondrial Cyt *b* gene sequences of host species were grouped into 2 major clades by NJ and MP analysis; one group of small rodents and another consisting of shrews and large mammals. The tree topology showed that all 27 host sequences examined fell into two distinct genetic lineages: Clade A (consists of *L. sabanus*, *R. tiomanicus* and *S. muelleri*) and Clade B (consists of *T. glis*, *P. bengalensis* and *T. indicus*). NJ tree topology revealed a distinction with 95% bootstrap value for Clade A but a lower bootstrap value of 85% for Clade B (Figure 3). Significant grouping of *L. sabanus*, *R. tiomanicus* and *S. muelleri* in each independent monophyletic subclade was obtained with a 100% bootstrap value. The NJ tree also showed the infestation of *Ixodes* ticks

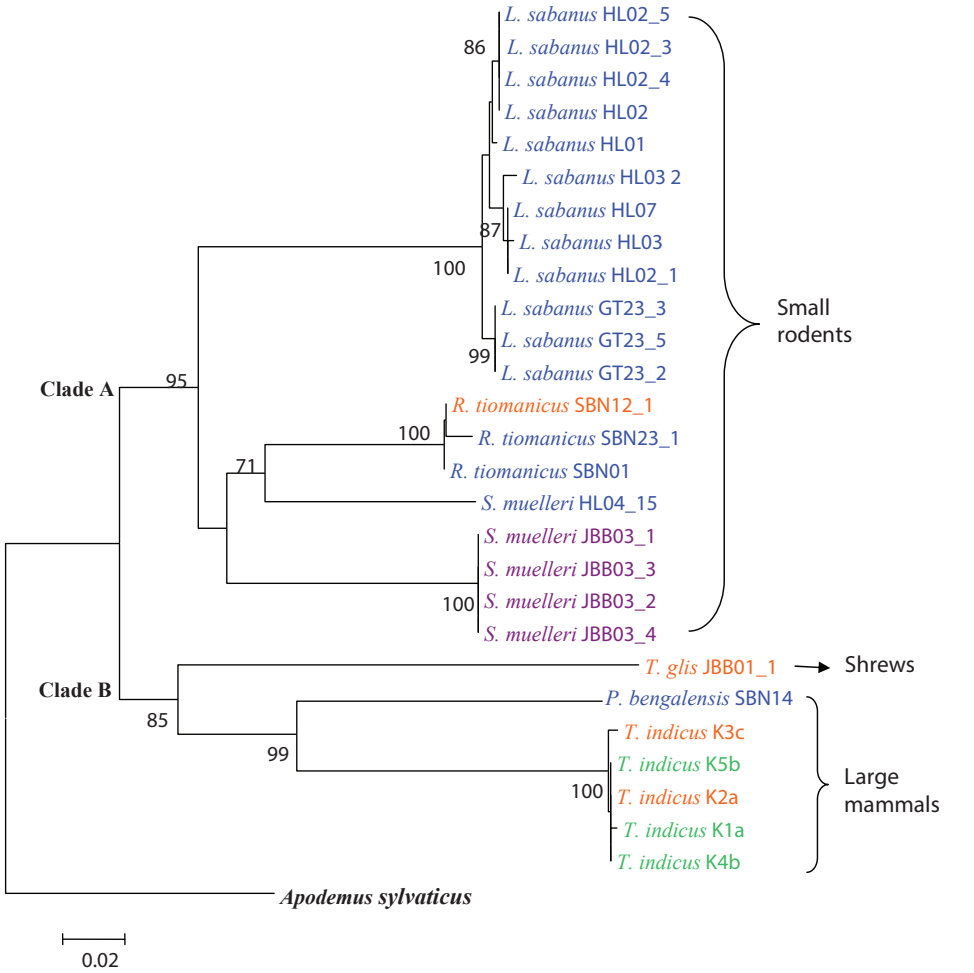

Figure 3. Neighbor-joining tree constructed from 28 sequences (including one outgroup sequence) of the Cyt *b* gene. The numbers at the branches stand for bootstrap values 70% and above of 1000 replications. Genera of ticks represented by blue for *Ixodes* sp., orange for *Dermacentor* sp., violet for *Haemaphysalis* sp. and green for *Amblyomma* sp.

on 3 species of different hosts that is *L. sabanus*, *R. tiomanicus* and *P. bengalensis* while the *Haemaphysalis* ticks infested only on a single host, *S. muelleri*.

Seven parsimonious trees were produced by the MP analysis using equally weighted TBR. The best tree had 497 steps (Figure 4) with a consistency index of 0.67114, a homoplasy index of 0.70422 and a retention index of 0.88804. The MP tree is concordant with the NJ tree as it shares a relatively similar tree topology of phylogenetic relationships. Two distinct monophyletic clades are clearly shown on the phylogenetic tree of potential hosts of ticks. These small rodents and large mammals were fully supported by high bootstrap values of 82% and 88%, respectively.

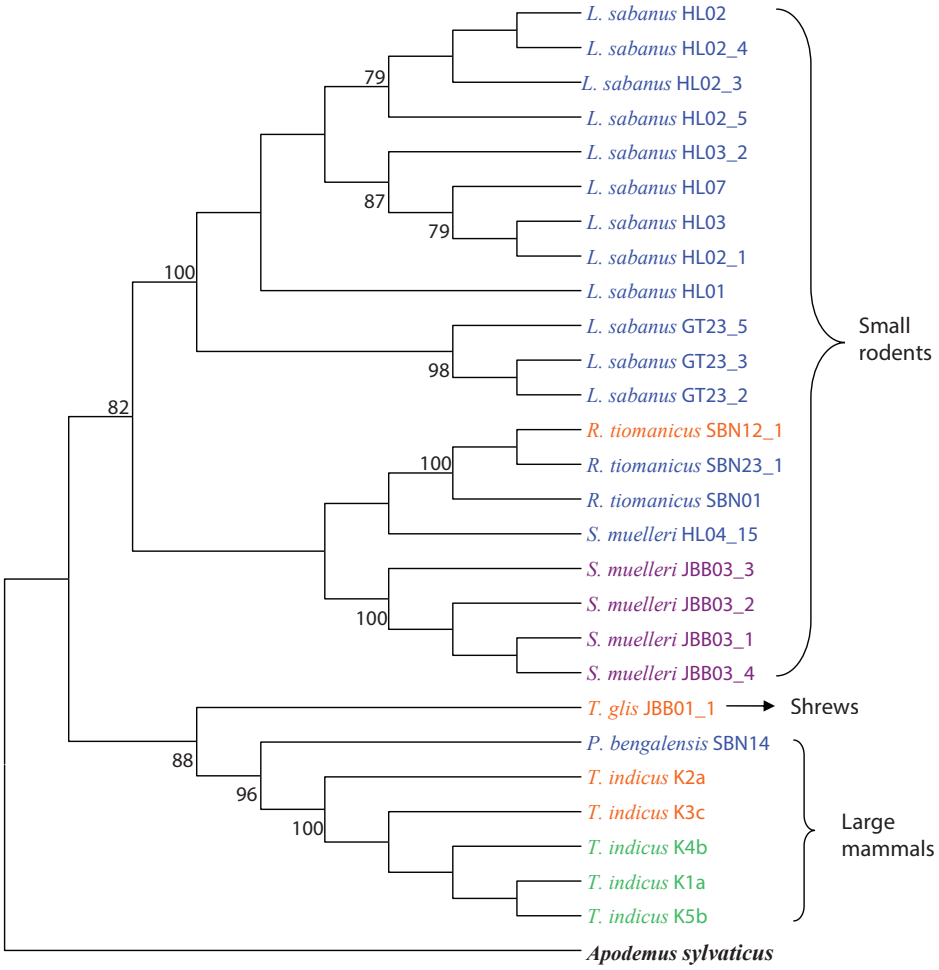

Figure 4. Maximum parsimony tree constructed from 28 sequences (including one outgroup sequence) of the Cyt *b* gene. The numbers at the branches stand for bootstrap values 70% and above of 1000 replications. Genera of ticks represented by blue for *Ixodes* sp., orange for *Dermacentor* sp., violet for *Haemaphysalis* sp. and green for *Amblyomma* sp.

Discussion

The study produced the first analysis of host identification for local ticks that identifies animals to the species level by detecting their Cyt *b* gene in engorged on-host ticks. The usefulness of blood meal analysis in determining the identity of the host species by PCR has been demonstrated by a recent study (Ernieenor et al. 2012). The identification of the vertebrate hosts using molecular detection of the Cyt *b* gene displayed an exact match and this adds more confidence to the use of this analysis. In the present case, all the samples were conclusively identified to species level. The results of this

study also indicated that local ticks are not host specific because they have a wide host range from small rodents to mammals.

In this study, the Cyt *b* gene was successfully proven as a discriminatory molecular marker for the identification of host DNA in ticks. Cyt *b* was selected as the target gene because of its track record in blood meal identification assays and its utilization in developing mammalian phylogeny (Kirstein and Gray 1996, Pierce et al. 2009). Moreover, the Cyt *b* gene has been widely used to make reliable blood meal identification of arthropods inclusive ticks due to its high copy numbers as mitochondrial genes and sufficient genetic variations at the primary sequence level among vertebrate taxa (Ngo and Kramer 2003, Maleki-Ravasan et al. 2009).

The most significant aspect of the method is its sensitivity to detect minuscule amounts of host DNA. In this study, host DNA could be detected in the 27 engorged ticks as determined by electrophoresis on agarose gel. The successful identification presumably because ticks sample was in the freshly engorged state, sufficient intact host DNA was present in the midgut. Adult stage of the ticks was used in this analysis may also eventually give positive identification of host. Cadenas et al. (2007) had similar complications, reporting that the ability to detect host DNA in adult ticks was significantly higher than in nymphs, probably due to the higher quantity of blood ingested by ticks during their previous bloodmeals as nymphs and larvae.

This study shows that *Ixodes granulatus* may probably pose greater problems than most other ticks because of its capability to infest various hosts such as rodents and larger animals. This finding is in accordance with studies that reported *I. granulatus* as the most notable tick infesting rodents (Mariana et al. 2008, Nadchatram 2008, Paulauskas et al. 2011, Mihalca et al. 2012, Mihalca and Sandor 2013). The species is a common acarine ectoparasite of rodents in Malaysia with wide distribution extends from Southeast Asia to eastern India and China (Nadchatram 2008). *Ixodes* are the most common genus of ticks that feed on humans (Briciu et al. 2011) may also infest rodents that can serve as reservoir hosts for human diseases (Marchette 1966, Schorn et al. 2011). Several genera of ticks found feeding on one individual of host is a common feeding behavior in wild rodents (Mariana et al. 2005). The sharing of host by different genera or species of ticks is important mainly for the bridging of microbial pathogens through reservoir hosts (Bursali et al. 2010). The ecological importance of reservoir hosts is greater if the animals are also common hosts for competent ticks (Mihalca et al. 2012).

An interesting finding was observed in this study where *Ixodes* ticks (SBN 14) collected from *R. tiomanicus* gave a high similarity (99%) of blood meal to *P. bengalensis*. It was probably due to incomplete or an interruption of feeding that occurred before the tick attached itself to another host (Allan et al. 2010). Another possible reason is the short duration of feeding on the first host before the partially fed ticks dropped off-host and attached to a new host (*P. bengalensis*) for a blood meal. A similar finding known as co-feeding transmission was also reported by Gern and Rais (1996) and Shih and Spielman (1993).

The finding of *T. indicus* as one of the hosts for *Amblyomma* ticks (K1a, K4b and K5b) was rare because the ticks were generally host specific on wild reptiles and am-

phibians (Pandit et al. 2011). That appears to indicate that the population of reptiles and amphibians surrounding the locality are scarcely found and the ticks have no choice to feed on any other animals available in the area. Rodents such as *Leopoldamys sabanus*, *Rattus diardii* and *Niviventer rapit* were also reported as alternative hosts for *Amblyomma* ticks (Nadchatram et al. 1966, Paramasvaran et al. 2009).

Partial Cyt *b* mtDNA gene sequences used in this study seems to be effective in identifying the phylogenetic relationships between ticks and their hosts. This is because both NJ and MP tree topology showed very clear distinction between groups of small rodents, shrews and large mammals with a highly supported monophyletic clade. In small rodents, the node is solved in the NJ and MP tree as two monophyletic clades, representing the species of *L. sabanus*, *R. tiomanicus* and *S. muelleri*. The tree topologies also show that *T. glis* formed their own distinct monophyletic clade separated from other larger mammals which consists of *P. bengalensis* and *T. indicus*. The information obtained has further corroborated the morphological identification and classification of *T. glis* which comes under the group of shrews. Such knowledge gained through host preference studies is essential to understanding the relationship of host and vector and their roles in the enzootic transmission cycle (Ngo and Kramer 2003). Therefore, analyses of ticks bloodmeals will create a better understanding of epidemiologically important vectors-their hosts that can be lead to the design of more effective control strategies (Kirstein and Gray 1996).

Of particular interest was the high numbers of ticks infesting small rodents compared to larger mammals. This finding is in agreeable with a previous study which reported that the abundance of small rodents compensate even if the intensity of tick parasitism on them is smaller than the larger hosts (Randolph 2004). The capability of rodents as host for ticks has been extensively investigated until to date mainly because they can be easily captured in large numbers and are easier to handle or maintain in the laboratory (Gern and Humair 2002). This is in line with our catch which was represented mainly by rodents as they were abundantly found in all localities.

For further studies, it is recommended that ticks are collected from sites frequently visited by animals including the wallows, wildlife main trails and river banks to include a more diverse group of animals in order to generate better results (Pichon et al. 2005, Pierce et al 2009). A bigger sample size with heterogeneous host species collection needs to be examined in parallel with different molecular markers to enable researchers to draw reliable conclusions and provide alternative views on the relationship between ticks and their natural hosts in Malaysia.

Conclusion

The PCR direct sequencing system using vertebrate Cyt *b* gene is a potential screening tool for the identification of ticks' blood meal. The Cyt *b* gene was selected for this study based on their higher nucleotide variations for the effective identification of hosts. Blood meal identification of field collected ticks by molecular methods offer a

direct and efficient approach for understanding the contributions of both competent and incompetent hosts for the transmission dynamics of tick-borne diseases. Furthermore, this valuable information can confirm a strong association between hard ticks and hosts (especially rodents) and this will assist public health officials with efforts to outline an effective tick-borne diseases control program.

Acknowledgements

The authors wish to thank the Director-General of Health, Malaysia, for permission to publish this paper. We wish to thank staff of the Acarology Unit, IMR for their assistance in the field. For the revision of English of the manuscript, we thank Serina Abdul Rahman. The study was supported by National Institute of Health grant (Code: JPP-IMR 11-010) from the Ministry of Health, Malaysia and ERGS/1/2011/STWN/UKM/03/9.

References

Allan BF, Goessling LS, Storch GA, Thach RE (2010) Blood meal analysis to identify reservoir hosts for *Amblyomma americanum* ticks. Emerging Infectious Diseases 16(3): 433–440. doi: 10.3201/eid1603.090911

Altschul SF, Gish W, Miller W, Myers EW, Lipman DJ (1990) Basic local alignment search tool. Journal of Molecular Biology 215(3): 403–410. doi: 10.1016/S0022-2836(05)80360-2

Boakye DA, Tang J, Truc P, Merriweather A, Unnasch TR (1999) Identification of blood meals in haematophagous Diptera by cytochrome B heteroduplex analysis. Medical and Veterinary Entomology 13: 282–287. doi: 10.1046/j.1365-2915.1999.00193.x

Briciu VT, Titilincu A, Tatulescu DF, Carstina D, Lefkaditis M, Mihalca AD (2011) First survey on hard ticks (Ixodidae) collected from humans in Romania: possible risks for tick-borne diseases. Experimental and Applied Acarology 54(2): 199–204. doi: 10.1007/s10493-010-9418-0

Bursali A, Tekin S, Orhan M, Keskin A, Ozkan M (2010) Ixodid ticks (Acari: Ixodidae) infesting human in Tokat Province of Turkey: species diversity and seasonal activity. Journal Vector Ecology 35: 180–186. doi: 10.1111/j.1948-7134.2010.00075.x

Cadenas FM, Rais O, Humair PF, Douet V, Moret J, Gern L (2007) Identification of host bloodmeal source and *Borrelia burgdorferi* sensu-lato in field-collected *Ixodes ricinus* ticks in Chaumont (Switzerland). Journal of Medical Entomology 44(6): 1109–1117. doi: 10.1603/0022-2585(2007)44[1109:IOHBSA]2.0.CO;2

Christine Z (2011) Development of genetic barcodes for hosts of the blacklegged tick (*Ixodes scapularis*) in Southern New York. Dissertation, New York, United State: Fordham University.

Chul-Min K, Ying-Hua Y, Do-Hyeon Y et al. (2006) Tick-borne rickettsial pathogens in ticks and small mammals in Korea. Applied & Environmental Microbiology 72: 5766–76. doi: 10.1128/AEM.00431-06

Dalgic A, Kandogan T, Kavak H, Ari A, Erkan N, Ozuer MZ (2010) Ticks in the external auditory canal. Hong Kong Journal of Emergency Medicine 17(2): 190–192.

Elias SL, Mariana SF, Luiz Claudio MDO, Jeronimo A, Carlos BM (2010) Blood meal identification of selected mosquitoes in Rio De Janeiro, Brazil. Journal of the American Mosquito Control Association 26(1): 18–23. doi: 10.2987/09-5914.1

Ernieenor FCL, Mariana A, Mohd Subail H, Ho TM (2012) Establishment of a molecular tool for blood meal identification in Malaysia. Asian Pacific Journal of Tropical Biomedicine 2(3): 223–227. doi: 10.1016/S2221-1691(12)60046-X

Francis CM (2008) Field guide to the mammals of South-east Asia. Princeton Press, London, 392 pp.

Gariepy TD, Lindsay R, Ogden N, Gregory TR (2012) Identifying the last supper utility of the DNA barcode library for blood meal identification in ticks. Molecular Resources Ecology 12: 646–652. doi: 10.1111/j.1755-0998.2012.03140.x

Garros C, Gardes L, Allene X, Rakotoarivony I, Viennet E, Rossi S, Balenghien T (2011) Development of an allele-specific multiplex PCR assay for the identification of blood meal source in *Culicoides* (Ceratopogonidae: Diptera). Applications on Palaeartic bitting midges species. Infection Genetic & Evolution 11: 1103–1110. doi: 10.1016/j.meegid.2011.04.002

Gern L, Humair PF (2002) Ecology of *Borrelia burgdorferi* sensu lato in Europe. In: Gray JS, Kahl O, Lane RS, Stanek G (Eds) Lyme Borreliosis: Biology, Epidemiology and Control. CABI, 149–174. doi: 10.1079/9780851996325.0149

Gern L, Rais O (1996) Efficient transmission of *Borrelia burgdorferi* between cofeeding *Ixodes ricinus* ticks (Acari: Ixodidae). Journal of Medical Entomology 33: 189–192.

Hall T (2005) Bioedit version 7.0.4. Department of Microbiology, North Carolina State University.

Harrison A, Scantlebury M, Montgomery WI (2010) Body mass and sex-biased parasitism in wood mice *Apodemus sylvaticus*. Oikos 119(7): 1099–1104. doi: 10.1111/j.1600-0706.2009.18072.x

Humair PF, Douet V, Cadenas FM, Schouls LM, Van De Pol I, Gem L (2007) Molecular identification of blood meal source in *Ixodes ricinus* ticks using 12S rDNA as a genetic marker. Journal of Medical Entomology 44: 869–880. doi: 10.1603/0022-2585(2007)44[869:MIOBSI]2.0.CO;2

Kent RJ (2009) Molecular methods for arthropod bloodmeal identification and applications to ecological and vector-borne disease studies. Molecular Ecology Resources 9: 4–18. doi: 10.1111/j.1755-0998.2008.02469.x

Kent RJ, Norris D (2005) Identification of mammalian blood meals in mosquito by a multiplexed Polymerase Chain Reaction targeting cytochrome b. American Journal of Tropical Medicine Hygience 73(2): 336–342.

Kia EB, Moghddas-Sani H, Hassanpoor H et al. (2009) Ectoparasites of rodents captured in Bandar Abbas, Southern Iran. Iranian Journal of Arthropod-Borne Diseases 3: 44–9.

Killilea ME, Swei A, Lane RS, Briggs CJ, Ostfeld RS (2008) Spatial dynamics of Lyme disease: A review. Ecohealth 5(2): 167–195. doi: 10.1007/s10393-008-0171-3

Kirstein F, Gray JS (1996) A molecular marker for the identification of the zoonotic reservoirs of *Lyme borreliosis* by analysis of the blood meal in its European vector *Ixodes ricinus*. Appllied of Environmental Microbiology 62: 4060–4065.

Kohls GM (1957) Ticks (Ixodidae) of Borneo and Malaya. Study, Institute for Medical Research Malaya 28: 65–94.

Maleki Ravasan N, Oshaghi MA, Javadian E, Rassi Y, Sadraei J, Mohtarami F (2009) Blood meal identification in field-captured sand flies: Comparison of PCR-RFLP and ELISA assays. Iranian Journal of Arthropod-Borne Diseases 3(1): 8–18.

Marchette NJ (1966) Rickettsiosis (Tick typhus, Q-fever, Urban-typhus) in Malaya. Journal of Medical Entomology 4: 393–71.

Maria Stella BB, Andrea de Barros PV, Natalia Goes B (2012) Standardization of Enzyme Linked Immunosorbent Assay (ELISA) for the identification of blood meal in black flies (Diptera: Simuliidae). Revista Panamericana Infectologia 14(1): 12–16.

Mariana A, Zuraidawati Z, Ho TM, Mohd Kulaimi B, Saleh I, Shukor MN, Shahrul-Anuar MS (2005) A survey of ectoparasites in Gunung Stong Forest Reserve, Kelantan, Malaysia. Southeast Asian Journal of Tropical Medicine of Public Health 36(5): 1125–1131.

Mariana A, Zuraidawati Z, Ho Tm et al. (2008) Ticks (Ixodidae) and other ectoparasites in Ulu Muda Forest Reserve, Kedah, Malaysia. Southeast Asian Journal of Tropical Medicine of Public Health 39: 496–506.

Medway L (1983) The wild mammals of Malaya (Peninsular Malaysia and Singapore). Oxford University Press, Kuala Lumpur.

Mihalca AD, Sandor AD (2013) The role of rodents in the ecology of *Ixodes ricinus* and associated pathogens in Central and Eastern Europe. Frontiers in Cellular and Infections Microbiology 3(56): 1–3.

Mihalca AD, Dumitrache MO, Sandor AD, Magdas C, Oltean M et al (2012) Tick parasites of rodents in Romania: host preferences, community structure and geographical distribution. Parasites & Vector 5(266): 1–7.

Mittler T, Levy M, Chad F, Karen S (2010) MULTBLAST: A web application for multiple BLAST searches. Bioinformation 5(5): 224–226. doi: 10.6026/97320630005224

Mukabana WR, Takken W, Seda P, Killen GF, Hawley WA, Knols BGJ (2002) Analysis of arthropod blood meals using molecular genetic markers. Trends in Parasitology 18(11): 505–509. doi: 10.1016/S1471-4922(02)02364-4

Nadchatram M (2008) The beneficial rain forest ecosystem with environmental effects on zoonoses involving ticks and mites (acari), a Malaysian perspective and review. Tropical Biomedicine 25: 1–92.

Nadchatram M, Damrow R, Ng CK (1966) Parasitic acarina of the mammals. Bulletin of National Musuem of Singapore 31: 129–140.

Nevil EM, Anderson D (1972) Host preference of *Culicoides* midges (Diptera: Ceratopogonidae) in South Africa as determined by precipitin test and light trap catches. Onderstepoort Journal Veterinary Research 39: 147–152.

Ngo KA, Kramer LD (2003) Identification of mosquito blood meals using polymerase chain reaction (PCR) with order-specific primers. Journal of Medical Entomology 40: 215–222. doi: 10.1603/0022-2585-40.2.215

Ninio CD, Augot JC, Delecolle B, Dufour B, Depaquit J (2011) Contribution to the knowledge of *Culicoides* (Diptera: Ceratopogonidae) host preference in France. Parasitology Research 108: 657–663. doi: 10.1007/s00436-010-2110-9

Onder O, Shao W, Kemps BD, Lam H, Brisson D (2013) Identifying sources of blood meals using unidentified tandem mass spectral libraries. Nature Communication 4: 1746. doi: 10.1038/ncomms2730

Pandit P, Bandivdekar R, Geevarghese G, Pande S, Mandka O (2011) Tick infestation on wild snakes in Northern part of Western Ghats of India. Journal of Medical Entomology 48(3): 504–507. doi: 10.1603/ME10164

Paramasvaran S, Sani RA, Hassan L, Krishnasamy M, Jeffery J, Oothuman P et al. (2009) Ectoparasite fauna of rodents and shrews from four habitats in Kuala Lumpur and the states of Selangor and Negeri Sembilan, Malaysia and its public health significance. Tropical Biomedicine 26(3): 303–311.

Paulauskas A, Radzijevskaja J, Rosef O, Turcinaviciene J, Ambrasiene D (2009) Infestation of mice and voles with *Ixodes ricinus* ticks in Lithuania and Norway. Estonian Journal of Ecology 58(2): 112–125. doi: 10.3176/eco.2009.2.05

Paulauskas A, Radzijevskaja J, Rosef O (2011) Rodents as carriers of tick-borne zoonotic diseases and their eological impact. 8th European Vertebrate Pest Management Conference Julius-Kuhn-Archiv 432: 182–183.

Payne J, Francis CM, Phillips K (2005) A field guide to the mammals of Borneo. Sabah Society, Kota Kinabalu, 332 pp.

Paziewska A, Zwolinska L, Harris PD, Bajer A, Sinski E (2010) Utilisation of rodent species by larvae and nymphs of hard ticks (Ixodidae) in two habitats in NE Poland. Experimental and Applied Acarology 50(1): 79–91. doi: 10.1007/s10493-009-9269-8

Pichon B, Egan D, Rogers M, Gray J (2003) Detection and identification of pathogens and host DNA in unfed host-seeking *Ixodes ricinus* L. (Acari: Ixodidae). Journal of Medical Entomology 40: 723–731. doi: 10.1603/0022-2585-40.5.723

Pichon B, Roger M, Egan D, Gray J (2005) Blood meal analysis for the identification of reservoir hosts of tick-borne pathogen in Ireland. Vector-Borne & Zoonotic Diseases 5(2): 172–180. doi: 10.1089/vbz.2005.5.172

Pierce KA, Paddock CD, Sumner JW, Nicholson WL (2009) Pathogen prevalence and blood meal identification in *Amblyomma* ticks as a mean of reservoir host determination for ehrlichial pathogens. Clinical Microbiology and Infectious Diseases 15 (Suppl. 2): 37–38. doi: 10.1111/j.1469-0691.2008.02166.x

Randolph SE (2004) Tick ecology: processes and patterns behind the epidemiological risk posed by ixodid ticks as vectors. Parasitology 129: S37–S65. doi: 10.1017/S0031182004004925

Schorn S, Pfister K, Reulen H, Mahling M, Silaghi C (2011) Occurrence of *Babesia* spp., *Rickettsia* spp., and *Bartonella* spp. In: *Ixodes ricinus* in Bavarian public parks, Germany. Parasitology Vectors 4: 135. doi: 10.1186/1756-3305-4-135

Scott MC, Harmon Jr, Tsao JI, Jones CJ, Hickling G (2012) Reverse line blot probe design and polymerase chain reaction optimization for blood meal analysis of ticks from the eastern United States. Journal of Medical Entomology 49(3): 697–709. doi: 10.1603/ME11162

Shih CM, Spielman A (1993) Accelerated transmission of Lyme disease spirochetes by partially fed vector ticks. Journal of Clinical Microbiology 31: 2878–2881.

Thompson JD, Higgins DG, Gibson TJ (1994) CLUSTAL W: Improving the sensitivity of progressive multiple sequence alignment through sequence weighting, position-specific

gap penalties and weight matrix choice. Nucleic Acid Research 22(22): 4673–4680. doi: 10.1093/nar/22.22.4673

Tobolewski J, Kaliszewski MJ, Colwell RK, Oliver JH (1992) Detection and identification of mammalian DNA from the gut of museum specimens of ticks. Journal of Medical Entomology 29: 1049–1051.

Walker AR, Davies FG (1971) A preliminary survey of the epidemiology of bluetongue in Kenya. Journal of Hygience 69(1): 47–60. doi: 10.1017/S0022172400021239

Walker AR, Bouattour A, Camicas JL, Estrada-Pena A, Horak IG, Latif A, Pegram RG, Preston PM (2003) Ticks of domestic animals in Africa, A guide to identification of species. Biosciences Reports, United Kingdom, 157 pp.

ZooKeys 478: 45–128 (2015)
doi: 10.3897/zookeys.478.8057
http://zookeys.pensoft.net

RESEARCH ARTICLE

A peer-reviewed open-access journal
ZooKeys
Launched to accelerate biodiversity research

Phylogeny and biogeography of Asthenopodinae with a revision of *Asthenopus*, reinstatement of *Asthenopodes*, and the description of the new genera *Hubbardipes* and *Priasthenopus* (Ephemeroptera, Polymitarcyidae)

Carlos Molineri[1], Frederico F. Salles[2], Janice G. Peters[3]

1 *Instituto de Biodiversidad Neotropical, CONICET (Argentine Council of Science & Technology), Universidad Nacional de Tucumán, M. Lillo 205, San Miguel de Tucumán, 4000, Tucumán, Argentina, UNASUR* **2** *Laboratório de Sistemática e Ecologia de Insetos, Depto. de Ciências Agrárias e Biológicas, Universidade Federal do Espírito Santo, CEP 29.933-415, São Mateus, ES, Brazil* **3** *Florida A&M University, Tallahassee, Florida, USA*

Corresponding author: *Carlos Molineri* (carlosmolineri@gmail.com)

Academic editor: *E. Dominguez* | Received 6 June 2014 | Accepted 15 December 2014 | Published 28 January 2015

http://zoobank.org/EC360FAF-6BF9-4FEF-96DA-F336302D1789

Citation: Molineri C, Salles FF, Peters JG (2015) Phylogeny and biogeography of Asthenopodinae with a revision of *Asthenopus*, reinstatement of *Asthenopodes*, and the description of the new genera *Hubbardipes* and *Priasthenopus* (Ephemeroptera, Polymitarcyidae). ZooKeys 478: 45–128. doi: 10.3897/zookeys.478.8057

Abstract

The Neotropical species of Asthenopodinae are revised in a formal phylogenetic context. The five known species of *Asthenopus* Eaton, 1871, together with other five new species were included in a cladistic analysis using morphological characters (continuous and discretes). Representatives of the Afro-Oriental group of the subfamily (*Povilla* Navás, 1912 and *Languidipes* Hubbard, 1984) were also included to test the monophyletic hypothesis traditionally accepted for the group. Additional taxa representing the other subfamilies of Polymitarcyidae were incorparated: *Ephoron* Williamson, 1802 (Polymitarcyinae) and *Campsurus* Eaton, 1868, *Tortopus* Needham & Murphy, 1924 and *Tortopsis* Molineri, 2010 (Campsurinae). A matrix of 17 taxa and 72 characters was analyzed under parsimony resulting in a single tree supporting the monophyly of the subfamily Asthenopodinae. Other results include the monophyly of the Afro-Oriental taxa (*Povilla* and *Languidipes*), the paraphyletic nature of Neotropical Asthenopodinae, and the recognition of four South American genera: *Asthenopus* (including *A. curtus* (Hagen), 1861, *A. angelae* de Souza & Molineri, 2012, *A. magnus* **sp. n.**, *A. hubbardi* **sp. n.**, *A. guarani* **sp. n.**), *Asthenopodes* Ulmer, 1924, **stat. n.** (including *A. picteti* Hubbard, 1975, **stat. n.**, *A. traverae* **sp. n.**, *A. chumuco* **sp. n.**), *Priasthenopus* **gen. n.** (including *P. gilliesi* (Domínguez), 1988, **comb. n.**), and *Hubbardipes* **gen. n.** (including *H. crenulatus* (Molineri et al.), 2011, **comb. n.**). Descriptions, diagnoses, illustrations and keys are presented

for all Neotropical taxa of Asthenopodinae (adults of both sexes, eggs and nymphs). Additionally a key to the subfamilies and genera of Polymitarcyidae is included. A quantitative biogeographic analysis of vicariance is presented and discussed through the study of the "taxon history" of the group.

Resumen

Se revisan las especies neotropicales de Asthenopodinae en un contexto filogenético. Las cinco especies de *Asthenopus* Eaton, 1871, junto con otras cinco nuevas especies, son analizadas cladísticamente a partir de caracteres morfológicos externos (continuos y discretos). También se incluyen representantes del grupo Afro-Oriental de la subfamilia (*Povilla* Navás, 1912 y *Languidipes* Hubbard, 1984) para comprobar la hipótesis de monofilia tradicionalmente aceptada para el grupo. Se incorporaron taxones adicionales representando las otras subfamilias de Polymitarcyidae: *Ephoron* Williamson, 1802 (Polymitarcyinae) y *Campsurus* Eaton, 1868, *Tortopus* Needham & Murphy, 1924 y *Tortopsis* Molineri, 2010 (Campsurinae). Se analizó bajo parsimonia una matriz de 17 taxa y 72 caracteres resultando un sólo árbol que apoya la monofilia de Asthenopodinae. Otros resultados incluyen la monofilia del grupo Afro-Oriental (*Povilla* y *Languidipes*), la naturaleza parafilética de los Asthenopodinae neotropicales, y el reconocimiento de cuatro géneros sudamericanos: *Asthenopus* (incluyendo a *A. curtus* (Hagen), 1861, *A. angelae* de Souza & Molineri, 2012, *A. magnus* **sp. n.**, *A. hubbardi* **sp. n.**, *A. guarani* **sp. n.**), *Asthenopodes* Ulmer, 1924, **stat. n.** (*A. picteti* Hubbard, 1975, **stat. n.**, *A. traverae* **sp. n.**, *A. chumuco* **sp. n.**), *Priasthenopus* **gen. n.** (*P. gilliesi* (Domínguez), 1988, **comb. n.**), y *Hubbardipes* **gen. n.** (*H. crenulatus* (Molineri et al.), 2011, **comb. n.**). Se presentan descripciones, diagnosis, ilustraciones y claves para todos los taxones neotropicales de Asthenopodinae (adultos de ambos sexos, huevos y ninfas). Adicionalmente se incluye una clave para subfamilias y géneros de Polymitarcyidae. Se presenta un análisis biogeográfico cuantitativo de vicarianza y se discute la historia particular del grupo.

Keywords

Ephemeroptera, Ephemeroidea, Fossoriae, vicariance, evolution, Neotropics, Campsurinae, *Campsurus*, *Tortopus*, *Tortopsis*, *Povilla*, *Languidipes*

Introduction

Polymitarcyidae Banks (Ephemeroptera) have long attracted the attention of freshwater biologist because their nymphs burrow tunnels in submersed wood, live in aquatic plants and sponges, and some inorganic sediment as clay, mud or sand (Arndt 1938, Hartland-Rowe 1958, Sattler 1967). Vejhabongse (1937) reported the damage caused by larvae of *Povilla* Navás, 1912 (Asthenopodinae) in woody structures. Leal et al. (2003) studied the capacity of *Campsurus* Eaton, 1868, larvae as bioturbators in soft mud bottom of Amazonian lakes; and *Tortopsis* Molineri, 2010, nymphs play an important role in the erosion of river clay banks (Molineri, unpubl.).

The family Polymitarcyidae is composed of three subfamilies (Polymitarcyinae, Asthenopodinae, and Campsurinae, Edmunds and Traver 1954, Bae and McCafferty 1995), and shows a broad distribution in the Holartic, Paleartic, Oriental and Neotropical regions (McCafferty 2004). Ogden et al. (2009) included one representative of each of these subfamilies in a combined molecular and morphological study of the entire order Ephemeroptera – in their work the traditionally known relationships were recovered with Polymitarcyinae spliting first and then Campsurinae as sister to Asthe-

nopodinae. The monophyly of the submafilies and the relationships inside Asthenopodinae were not formally tested yet, except for some groups in Campsurinae (*Tortopus* and *Tortopsis*, Molineri 2010; *Campsurus*, Molineri and Salles 2013). The Neotropical genera of the family include *Asthenopus* Eaton, 1871 (Asthenopodinae), *Campsurus*, *Tortopus* Needham & Murphy, 1924, and *Tortopsis* (Campsurinae). All Campsurinae genera are represented in the Nearctic by at least one species, but the majority of them are known from tropical and subtropical South America, as is the case with all the species of *Asthenopus* (Domínguez et al. 2006).

Asthenopus is presently classified in Asthenopodinae, together with the Afro-Oriental *Povilla* Navás and *Languidipes* Hubbard, 1984 (Edmunds and Traver 1954, Baumgardner et al. 2012) but a formal phylogenetic analysis supporting this subfamily as monophyletic is wanting. Some of their shared features (e.g., ring-like prothorax, parallel ICu veins in forewings) may prove to be plesiomorphies, others (e.g., straight CuA, median remnant of styliger plate) are absent in *Languidipes* (Baumgardner et al. 2012), and at least one putative synapomorphic state, the loss of basal segment of the forceps in *Asthenopus* and Campsurinae indicate a probable sister relation among all the South American genera (Kluge 2004). Additionally, Kluge (2004) treated *Povilla* and *Asthenopus* as synonyms.

Asthenopus is presently known from five South American species: *A. curtus* (Hagen), 1861, *A. crenulatus* Molineri, Cruz & Emmerich, 2011, *A. gilliesi* Domínguez, 1988, *A. picteti* (Hubbard), 1975, and *A. angelae* de Souza & Molineri, 2012. All of them are known at least from male adults, but only two (*A. curtus* and *A. angelae*) are known also from the nymphs. Nevertheless, the nymphal stage of *A. curtus* is redescribed here because it has been described from missidentified specimens (Sattler 1967, Berner 1978, Domínguez 1989). *Asthenopodes* Ulmer, was described from males of a single species (Ulmer 1924), presently *Asthenopus picteti* (Hubbard). *Asthenopodes* was proposed as a junior subjective synonym of *Asthenopus* by Hubbard and Domínguez (1988) based on the discovery of *Asthenopus gilliesi* Domínguez (1988) that showed intermediate characters between both genera.

The main objective of the present paper is to evaluate in a phylogenetic context the validity of the generic groups of Asthenopodinae (e.g., *Asthenopus*, *Asthenopodes*, *Povilla* and *Languidipes*). As a result we propose two new genera, revalidate *Asthenopodes* at the generic rank, and describe five new Neotropical species.

Additionally we describe and illustrate some unknown stages of previously known species, propose a key to the subfamilies and genera of Polymitarcyidae, and to the species of Neotropical Asthenopodinae. New country records are given and biogeographical aspects of the group are discussed.

Material and methods

Material deposition

Material is deposited in the following Institutions: CUIC (Cornell University Insect Collection, Ithaca, NY), FAMU (Florida A&M University, Tallahassee, FL), IFML

(Instituto-Fundación Miguel Lillo, Tucumán), IBN (Instituto de Biodiversidad Neotropical, Tucumán), MACN (Museo Argentino de Ciencias Naturales, Buenos Aires), MECN (Museo Ecuatoriano de Ciencias Naturales, Quito), MUSENUV (Museo de la Universidad del Valle, Cali), RBINS (Royal Belgian Institute of Natural Sciences, Brussels), FCE-Ep (Facultad de Ciencias, Entomología, Montevideo, Uruguay), CZNC (Coleçao Zoológica Norte Capixaba, São Mateus, Espírito Santo), INPA (Instituto Nacional de Pesquisas da Amazônia, Manaus), and ZMH (Zoologisches Museum Hamburg).

Morphological characters

Characters are scored from external morphological features of adults (male imago unless otherwise indicated), nymphs and eggs. Dissected parts of the nymphs and adults were mounted on microscope slides using Canada Balsam, except wings that were mounted dried. All the material is preserved in ethyl alcohol 96%. Photographs were taken using a NIKON SMZ-10 stereomicroscope or a microscope, with a Nikon D5000 digital camera; some pictures were modified with Combine ZP (Hadley 2010). Line drawings were done using a camera lucida attached to a microscope. Structures used for SEM study were dehydrated in a graded ethanol series, dried by the critical point method, sputter coated with gold and observed with a JEOL 35 CF scanning electron microscope.

The measures and ratios used in some characters are explained and illustrated to permit repeatability. To score variation in shape of genitalic structures (chars. 12–17) some measures were defined (see Appendix 1). Ratios between some of them were used instead of the original data to avoid the spurious differences occasioned by the great variation in size common in the group. Characters 0 to 11 also are ratios or counts to represent characteristics commonly used in the taxonomy of the group, for example the length of forelegs of male and its relation to other structures. Fore and hind wings are abbreviated FW and HW respectively throughout the text. A complete list of the characters, their definitions and character states is given in Appendix 1.

Taxa

A matrix of 17 taxa and 72 characters was constructed (Appendix 3). Trees were rooted in *Ephoron* Williamson, 1802 (Polymitarcyinae). Four representatives of Campsurinae were also included as additional outgroups (*Campsurus violaceus* Needham & Murphy, 1924, *C. vulturorum* Emmerich & Molineri, 2011, *Tortopus harrisi* Traver, 1950, and *Tortopsis sarae* Domínguez, 1985). The African and Oriental Asthenopodinae were represented in the analysis by *Povilla adusta* Navás, 1912 and *Languidipes corporaali* (Lestage), 1922. All species of Neotropical Asthenopodinae were scored, including the five species of *Asthenopus* and five new species described here. The formerly described species include: *A. curtus* (Hagen), *A. picteti* (Hubbard), *A. gilliesi* Domínguez,

A. crenulatus Molineri et al., and *A. angelae* de Souza & Molineri. The material studied includes type and fresh material of all species, detailed under each specific section.

Outgroups were scored either from fresh material (*Ephoron album* Say, 1823: 2 nymphs and 1 male imago from USA, Alabama, Perry County, Cahaba River, 27-vi-1968, Peters et al. cols.; *Povilla adusta*: 1 nymph from Afrique, Mali, Bas. Sénégal, Riv. Falémé, 13-xi-1984, ORSTOM col., 16 male imagos from Afrique, Mali, Bas. Niger, Riv. Niger, Gao, 7-ix-1987, ORSTOM col.; 3 male and 2 female imagos from Afrique, Guinée, Bas Senegal, Riv. Bafing Loc., Timbo-Dabola (route), 31.01.1987, ORSTOM col.) or from figures and descriptions (*Ephoron* spp from Ishiwata 1996; *Languidipes corporaali*, Hubbard 1984, Baumgardner et al. 2012). *Campsurus paraquarius* Navás (1920) , treated here as nomen nudum in Asthenopodinae, was not included in the matrix because of lack of data (only a figure of the Cu field of male is known, figure 1 in Navás 1920).

Cladistic analysis

Searches were conducted in TNT (Goloboff et al. 2008) under implied weights (k = 3), and using the "implicit enumeration" command (under "Analyse"). Implied weighting was suggested to ameliorate the problems of scaling in continuous characters (Goloboff et al. 2006). By the implicit enumeration, the complete universe of possible trees for the matrix is calculated, then picking the shortest ones. All characters were treated as non-additive except for continuous characters (chars. 0 to 26). Absolute and relative Bremer supports were calculated with 2000 suboptimal trees (up to 8 steps longer than shortest tree), with the commands "suboptimal" (under "Analyse") and "Bremer Supports" (under "Trees"). Frequency difference (GC, Goloboff et al. 2003), using 400 replications of symmetric jacknifing, was also calculated as a measure of group support. The optimizations of individual continuous characters given in Figs 21 and 22 were obtained in TNT using the commands "Optimize: Characters: Character Mapping".

Biogeographical methods

All the available geographic records (448 records for 17 taxa) of the species or genera included in the phylogeny were compiled. Concerning *Asthenopus* species, only records from specimens (or photographs) revised by us were included, since much confusion exists in the literature in relation to *A. curtus* and similar species. All records are exact points of occurrence except some for *Ephoron* species from North America and Europe, which were only roughly approximated from the maps in McCafferty (1975) and de Jong (2012), respectively. Some of the records (ca. 100) for *Tortopsis*, *Ephoron* and *Povilla* were downloaded from Global Biodiversity Information Facilities (http://www.gbif.org/, last accesed February 10th 2014).

The biogeographical analysis was performed through spatial analysis of vicariance (Arias et al. 2011), a method that reconstructs taxon biogeographic history by looking

at disjoint sister pairs in a given phylogeny. Besides a cladogram, it uses as input the distributional records of the terminals; and is implemented in the software VIP (Vicariance Inference Program) available at http://www.zmuc.dk/public/phylogeny/vip (Arias 2010). A grid of 1° × 1° was used (maximum fill = 0) in a world vegetation map (obtained in http://neo.sci.gsfc.nasa.gov) to represent distributions as absence/presence data in each cell. The "OR reconstruction" was used under the default settings except that cost of distribution removal was set to 1.5, and cost of partial removal to 0.75. Reconstructions using different grid size (5° × 5°) and costs were also conducted for comparative purposes, but results were similar.

Results

Phylogeny and taxonomic status of genera and species

Parsimony under implied weights (IW) resulted in a single tree (Figs 1–2), with an adjusted homoplasy of 14.64 and a total fit of 54.36. Neotropical Asthenopodinae was not recovered as a monophyletic group: *Asthenopus* s.s. is sister to the Afro-Oriental clade (*Povilla-Languidipes*). *Asthenopodes* is revalidated as a distinct genus since its type species (*A. picteti* Hubbard) was recovered in a group with other two new species. *Asthenopodes* stat. n. presents defining characters in all stages (see below). The species described from adults by Molineri et al. (2011) as *Asthenopus crenulatus* is now known in all the stages (see below) and a new genus *Hubbardipes* is proposed for it. *Hubbardipes* gen. n. is supported as sister to the remaining Asthenopodinae (i.e., excluding *Asthenopodes*). Another new monotypic genus, *Priasthenopus* gen. n. is proposed for *A. gilliesi*, only known from adults and eggs. *Priasthenopus* is sister to the clade *Povilla* + *Asthenopus*.

The type species of *Asthenopus* (*A. curtus*) forms a clade with *A. angelae* and three new species. Synapomorphies of each clade are numerous; changes on continuous and discrete characters are presented separately in Figs 1 and 2, respectively. For details on changes see generic diagnosis and Appendix 2. Group support is strong for most clades (Fig. 3).

Summarizing, the taxonomic changes needed to adjust formal classification with the phylogeny include: 1) revalidation of *Asthenopodes* as a distinct genus and the corresponding new combination for its type species (*Asthenopodes picteti*), 2) the erection of *Hubbardipes* gen. n. and the new combination *Hubbardipes crenulatus* (Molineri et al.) for its single species, and 3) the erection of *Priasthenopus* gen. n. and the new combination *P. gilliesi* (Domínguez). This phylogeny also was the framework used to describe the five new species in the corresponding genus (see "Descriptions"): *Asthenopodes traverae*, *Asthenopodes chumuco*, *Asthenopus hubbardi*, *Asthenopus magnus*, and *Asthenopus guarani*.

An additional taxonomic change is proposed for *Campsurus paraquarius* Navás (1920) that undoubtedly pertains to Asthenopodinae as recognized by Lestage (1923) and Kluge (2004), most likely it is related with *P. gilliesi* (Domínguez). *C. paraquarius* is here considered a nomen nudum (see discussion under *Priasthenopus* below).

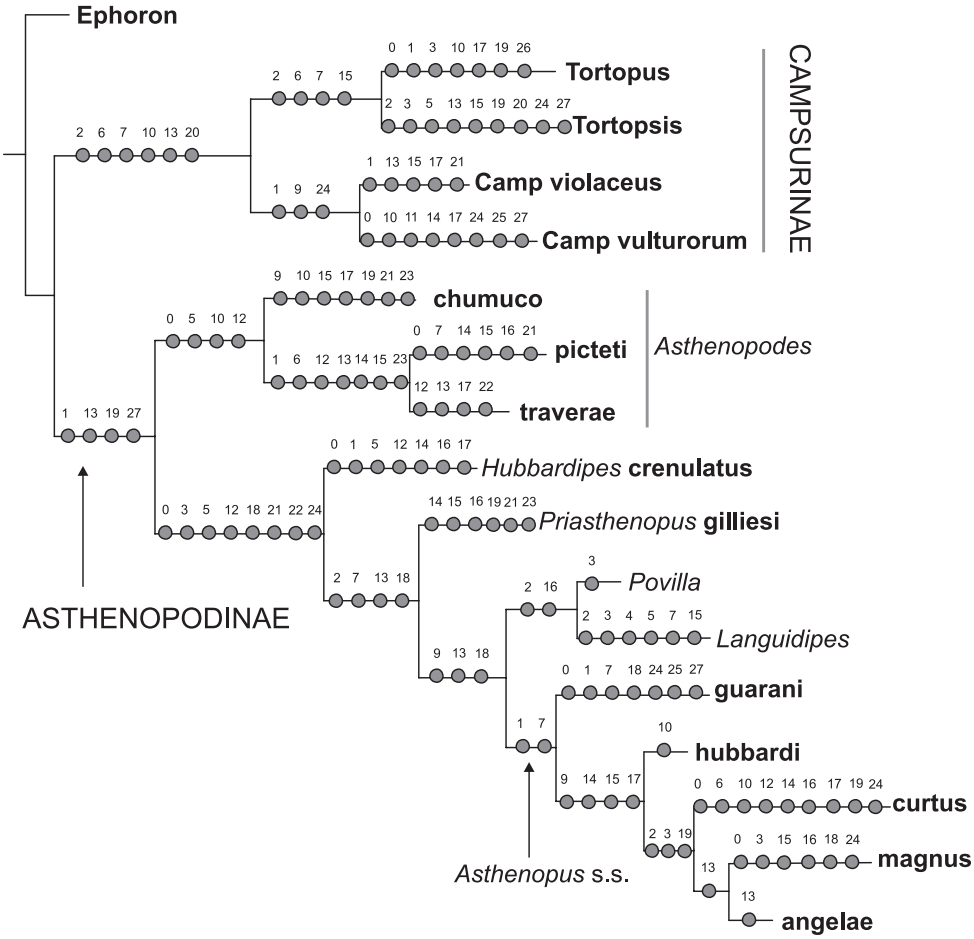

Figure 1. Most parsimonious tree with changes on continuous characters (number above circles are character numbers, see Appendix 1).

Asthenopodinae

The subfamily Asthenopodinae is composed in our analysis by four main groups, three Neotropical (*Asthenopodes*, *Hubbardipes*, and *Priasthenopus*) and one vicariant (Neotropical *Asthenopus* vs Ethiopic-Oriental *Povilla* + *Lanquidipes*) (Fig. 3). *Asthenopodes* is sister to the remaining groups, then *Hubbardipes* and *Priasthenopus* splits consecutively and finally *Asthenopus* is sister to *Povilla* + *Languidipes*.

Asthenopodinae is defined by numerous derived character states (see Appendix 2 for details) including: shorter male foretibia, wider forceps, shorter female cerci, female sternum VIII with anteromedian keel; eggs with large and small disk-like chorionic structures; nymphs with wider mandibular tusks, tusk with two or three apical denticles (right and left tusks respectively) and with a small basal tubercle on outer dorsal surface, occipital region strongly expanded and convex, and foretarsal claws with marginal row of denticles.

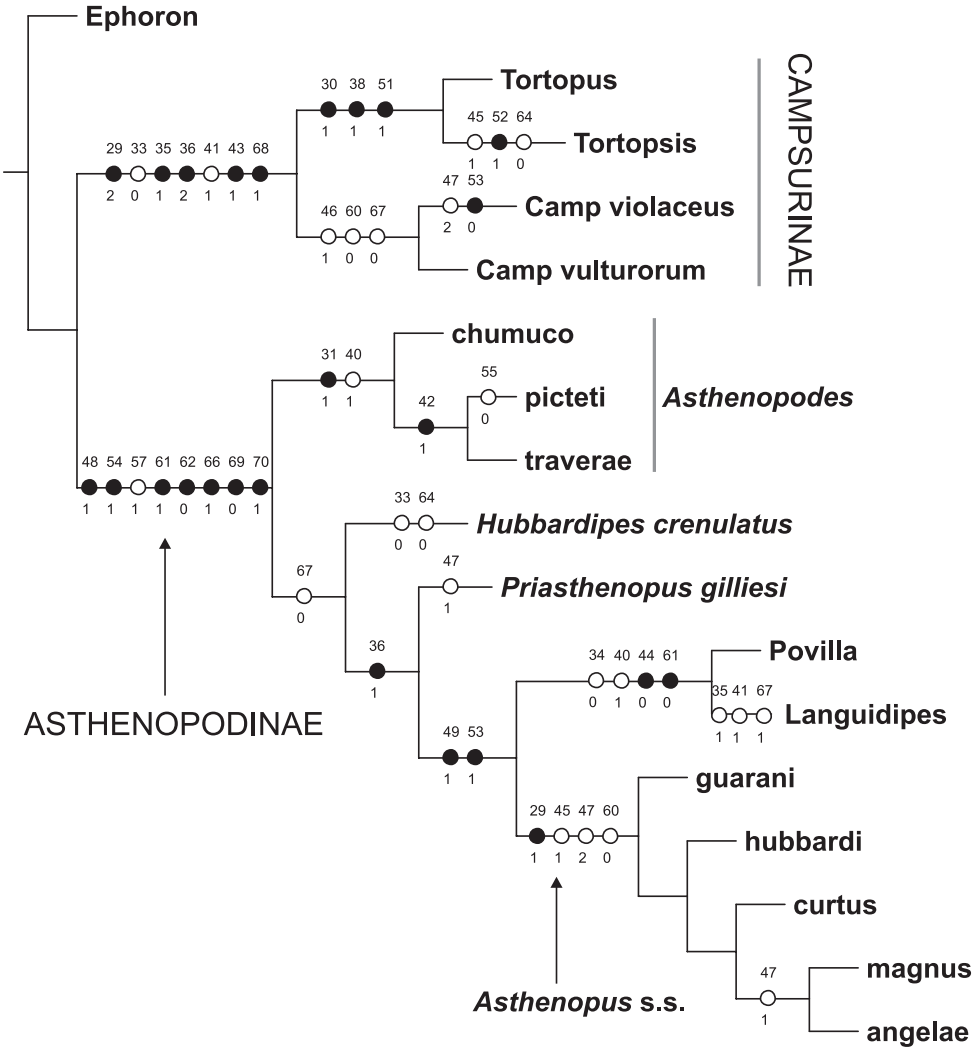

Figure 2. Most parsimonious tree (same for Fig. 1) showing changes on discrete characters (number above and below circles are character and state number, respectively, see Appendix 1). Black circles indicate unique apomorphies.

It is interesting to note some characters that simultaneously change in opposite "directions", showing a certain tendency in *Asthenopodes* but the contrary in it sister group (remaining Asthenopodinae). For example the following features define *Asthenopodes* and its sister group: the male foretibia is thinner distally (vs wider in the remaining Asthenopodinae, Figs 20, 22A), median remnant of styliger plate shorter (vs longer), larger HW (vs smaller, Fig. 22B). Other synapomorphic changes associated to Asthenopodinae excluding *Asthenopodes* are given in Appendix 2.

The sister relation between *Priasthenopus* and the clade *Povilla* + *Languidipes* + *Asthenopus* is supported by (see Appendix 2, node 23): additional shortening of foreleg,

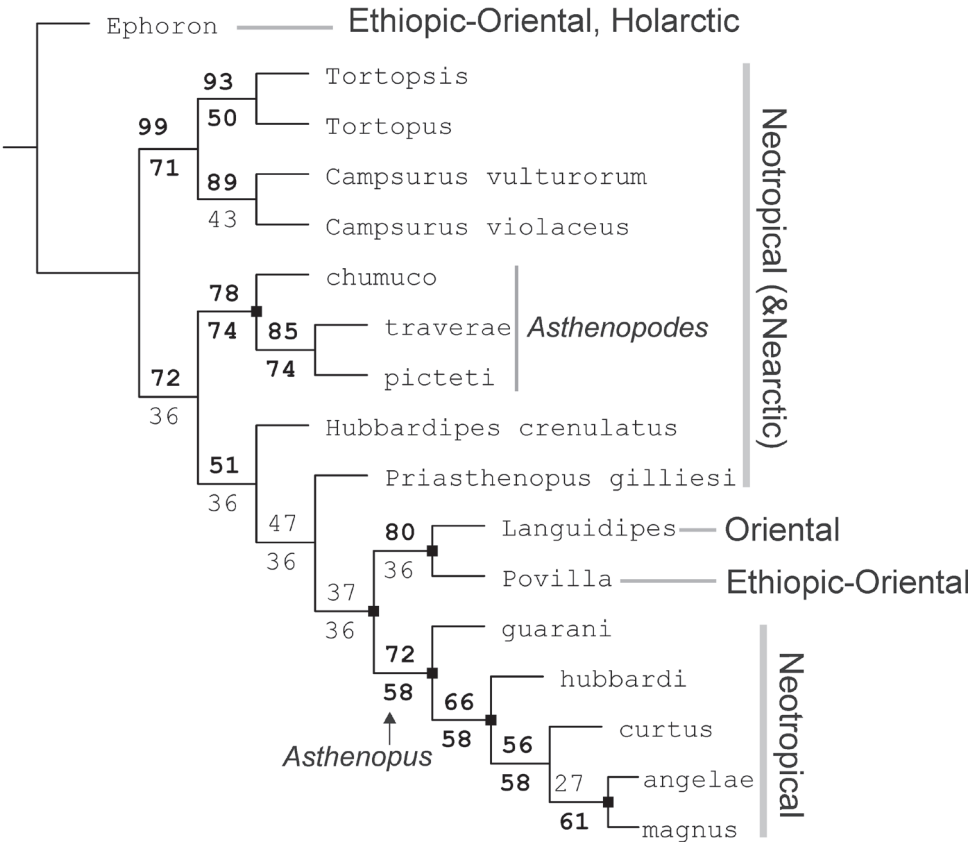

Figure 3. Group support and vicariant nodes. Numbers above branches indicate GC values (400 replicates, Symmetric Resampling), below branches Relative Bremer supports (from 2000 trees, up to 8 steps longer) are indicated. Support values higher than 50 are bolded. Black squares indicate nodes with allopatric descendants (see text for explanation).

shorter and less anastomosed cross veins in the margin of FW, additional increase in forceps width, even wider and shorter female prothorax.

The clade formed by *Asthenopus* together with the Afro-Oriental genera share (Appendix 2): even wider forceps, shorter and less anastomosed intercalary veins in both wings, slightly shorter female pronotum, female sternum VIII with long and slender anteromedian keel, sockets small, and nymphal mandibular tusks with large basal tubercle in inner margin (this last state may be present also in *Priasthenopus gilliesi*, but nymphs remain unknown).

Povilla and *Languidipes* form a monophyletic group because both show shorter forelegs in male, blade-like penes relatively straight not curved inward, MP_2 shorter than IMP in FW (non-unique, also in Campsurinae), IMP connected to MP_1, forceps two-segmented, pedestals much narrower basally, and nymphal left mandibular tusk with an additional apical denticle.

Campsurinae

In spite of Campsurinae being only marginally represented in the matrix, we consider useful to note the derived character states defining the subfamily and genera (see Appendix 2 for details): much shorter forelegs in male, slender forceps, ICu_1 joins hind margin of FW close to tornus while ICu_2 joins it on basitornal margin, intercalary marginal veins absent or if present not anastomosed, median remnant of styliger plate absent, double penial arm articulation (sternum IX and base of pedestal), nymph with dorsum of head with dense patches of short setae on frons. *Campsurus* is very sparsely represented in the matrix (only 2 spp from more than 40 known) so only the character states defining *Tortopus* + *Tortopsis* may have some interest: slender penes, male foreleg slightly shorter, foretarsal segment 5 apically trilobed, intercalary marginal veins rarely present in male FW, HW anal area with many crossveins forming a network, forceps two-segmented.

Evolution of selected features

Variation in the relative length of male foreleg segments has been repeatedly used by different authors in the taxonomy of the family. One of our characters concerning this variation (char. 1, ratio length tarsal segment 2/tibia) presented many changes: most important are those defining the genus *Asthenopus* and the pair *Asthenopodes traverae* – *A. picteti*, indicating opposite changes in these nodes (encircled arrows in Fig. 21A).

In the nymphs, the robustness of the mandibular tusks is an important feature distinguishing different subfamilies. The optimization of character 27 (ratio length/width of tusk, Fig. 21B) shows an apomorphic change in the base of Asthenopodinae, indicating that the slender tusks of Campsurinae are plesiomorphic.

Trends in some charecteristics are markedly manifested, for example the width of male foretibia (char. 0 ratio width tibia/tarsal segment 2, Fig. 22A) decreases at the base of *Asthenopodes* and become thinner again later in *Asthenopodes picteti*. On the contrary, it becomes more robust in the base of the sister clade to *Asthenopodes* (the remainning Asthenopodinae) and wider again in *Hubbardipes crenulatus* (Fig. 22A).

The length of male foreleg is another character commonly used to define groups (here represented as the ratio length of FW/foreleg, Fig. 22C): a paulatine shortening of male foreleg in two lineages (Fig. 22C) and female pronotum (in just one of them, Fig. 22D) were obtained in the phylogeny. Both trends are only coupled (i.e., show simultaneous variation in the same node) in the clade including *Priasthenopus gilliesi*, *Povilla* and *Asthenopus* s.s. It is interesting to note that a character commonly used to define the subfamily Asthenopodinae (ring-like prothorax in the male) did not present changes in our phylogeny because of large intraspecific variation. Another character used as defining the subfamily (parallel ICu veins in forewings) is a plesiomorphy (the apomorphic state is present in Campsurinae).

General shape of the forceps in male adults shows opposing tendencies, becoming slender in Campsurinae but stouter in Asthenopodinae (Fig. 21C). The reduction in

the number of segments from three in *Ephoron*, to one in the base of Campsurinae + Asthenopodinae is independently reversed twice (in the ancesters of *Tortopus* + *Tortopsis*, and *Povilla* + *Languidipes*). Independent losses involve also to *Languidipes* and Campsurinae in relation to median remnant of styliger plate. A reduction in the length and anastomosis of marginal intercalary veins (reduction of a marginal archedictyon) is present independently in both subfamilies (Campsurinae and Asthenopodinae).

Geographical comments

Polymitarcyidae is widely distributed (Fig. 23), including tropical and temperate areas, with the exception of Australia and New Zealand (Kluge 2004, McCafferty 2004). Polymitarcyinae (*Ephoron* and *Eopolymitarcys*) is widely distributed in the Holarctic, Ethiopian and Oriental regions, sharing southern portions of its range with selected species of the other subfamilies (Asthenopodinae in Africa, and Campsurinae in North America, Fig. 23). Neotropical Asthenopodinae is not a monophyletic group, because *Asthenopus* s.s. is sister to the Ethiopian-Oriental clade (*Povilla* and *Languidipes*). Campsurinae is mainly a Neotropical group, with only 6% of its species reaching the Nearctic (squares in Fig. 23).

The spatial analysis of vicariance found 6 disjoint sister pairs (Fig. 3): 1) the Neotropical *Asthenopus* (Amazonas and Paraná basins) vs *Povilla* + *Languidipes* (Ethiopian-Oriental) (Fig. 23, barrier 1); 2) *Povilla* in Africa and SE Asia vs *Languidipes* in the Malayan peninsula and the Island of Java (Fig. 23, barrier 2); 3) *Asthenopus guarani* known only from the Parana Basin vs its sister clade (*A. hubbardi*(*A. curtus* (*A. magnus* + *A. angelae*))) known from the Amazonas and Parana basins (Fig. 24, barrier 3); 4) *A. hubbardi* in Colombian Amazonas vs (*A. curtus* (*A. magnus* + *A. angelae*)) more widely distributed (Fig. 24, barrier 4); 5) *A. magnus* in the Ecuadorean Napo vs *A. angelae* more to the East in the Amazonas and Parana basins (Fig. 24, barrier 5); and 6) *Asthenopodes chumuco* known from three localities in Amazonas lowlands, Guyana and Eastern-Central Brazil (Espirito Santo) vs *Asthenopodes picteti* + *A. traverae* known from the Parana basin (Fig. 25, barrier 6).

Key to the subfamilies and genera of Polymitarcyidae

A key to the subfamilies of Polymitarcyidae is presented because new species described here show some of the characteristics (e.g., many crossveins, numerous anastomosed marginal intercalaries, etc.) previously used to diagnose other subfamilies. A key to the genera is proposed to include new or recently described genera (*Tortopsis*, *Hubbardipes* and *Priasthenopus*) or those raised to generic status (*Languidipes*, in Baumgardner et al. 2012, and *Asthenopodes*, here). The triangullar cell in Cu sector mentioned by Baumgardner et al. (2012) as diagnostic for *Languidipes* is not used in the key because it is also present in some *Asthenopus* females.

Key to the species of *Asthenopodes* and *Asthenopus* are given after each generic section (see below). Please note that in male genitalia, the pedestals are considered part of the styliger plate (Kluge 2004), thus number of forceps segments does not include them.

Key to adults (imagos and subimagos, except measures and ratios aplicabble only to imagos) and eggs of Polymitarcyidae

1 FW with vein Sc ending before the tip of the wing, its apical portion not curved posteriorly; cubital area of FW broadly expanded, usually with 3–5 intercalaries and many cross veins and marginal intercalaries; FW with MA fork 1/3 or more distance from wing base (i.e., a long MA stem is present); HW with convex intercalary between R_1 and Rs field (x.i. in Fig. 16 L); forceps with long basal and 2 slender apical segments; eggs with polar cap of type II (formed by tubular-shaped accumulations of attachment threads)..... .....**Polymitarcyinae (Holarctic, Ethiopian, Oriental)**

– FW (e.g., Figs 11, 16) with vein Sc ending at the tip of the wing or beyond, its apical portion strongly curved posteriorly; cubital field narrow with two ICus present, MA fork near base of the wing (i.e., MA stem very short); HW of male without convex intercalary between R_1 and Rs; forceps without short apical segments (e.g., Figs 12, 17); eggs with polar cap absent, single or double, of type III when present (formed by loosely coiled threads).....**2**

2 Pronotum ring-like (ratio width/length ca. 1/3); FW with CuA relatively straight, ICus subparallel (e.g., Figs 11, 16); median remnant of styliger plate present (e.g., Fig. 12E–F), except in *Languidipes*; all female legs present and complete but reduced in size; eggs ovoid, without a concave side, polar cap present at both poles (e.g., Fig. 13A–C) or dettached from the egg (Fig. 18I–K), chorion smooth or with disk-like structures .....Asthenopodinae...**3**

– Pronotum longer (width similar to length), in male with triangular anterior portion; CuA sigmoid, ICus apically diverging; median remnant of styliger plate absent; female forelegs generally absent in imago (may be present in subimago), if complete much reduced in size and twisted; eggs C-shaped, resembling a sphere with one side pushed in, polar cap single if present, chorion punctuated at least in the concave face ..... Campsurinae (Neotropical, Nearctic)...**8**

3 Eyes of male enlarged, separated on meson of head by a distance subequal to width of lateral ocellus ..... ***Languidipes* Hubbard (Oriental)**

– Eyes of male normal, similar to female, separated on meson of head by a distance greater than 2 times the width of lateral ocellus **4**

4 Penes blade-like (Fig. 19D, G); female sternum 8 with anteromedian keel basally swollen (Fig. 19C, E–F); egg without polar caps, chorion mainly smooth but few disk like structures may be present (Fig. 19K) .... ***Povilla* Navás (6 spp, Ethiopean, Oriental)**

– Penes variable but commonly cylindrical (Figs 7A, 8A, 12, 17); if an anterior keel is present in female sternum 8, it is not swollen basally (Figs 18F–H); eggs with two polar caps, chorion covered with disk-like structures (Figs 7D, 8K, 13A–C, 18A–E) ..... Neotropical Asthenopodinae...**5**

5 Penes with many spines on outer subapical margin (Fig. 7A); male foretarsal segment 1 partially fused to tarsal segment 2 (Fig. 20D); female sternum VIII with a protruding subcircular anteromedian structure (figures 12–13 in Molineri et al. 2011); eggs with the space between large plates completely covered by smaller plates (Fig. 7D–E).....***Hubbardipes* gen. n.**

– Penes with smooth outer margin (Figs 8A–C, 12, 17); male foretarsal segment 1 distinct (Fig. 20E–J) or completely fused with tibia (Fig. 20A–C); female sternum VIII with an anteromedian keel (Figs 13D, 18F–H) or a flat oval structure (Fig. 8J); eggs with the space between plates smooth, if small plates are present, also smooth chorion is present around them (Figs 8K–L, 13A–C, 18A–E).....**6**

6 Foreleg (FL) much shorter in length than FW (ratio FW/FL length = 1.4–2.0), foretarsal segment 1 distinct (Fig. 20E–J), apex of claws not strongly expanded; 0–2 (rarely with a third, weak) crossveins between R and M, basal to R fork (Figs 8D–E, 16); female sternum VIII with a long anteromedian keel (Fig. 18F–H) or with a pair of medium sized sockets (Fig. 8J); polar caps about as wide or wider than egg (Figs 8K, 18C, 18H) **7**

– FL subequal in length to FW (ratio FW/FL length: 1.0–1.2); 3–5 crossveins between R and M, basal to R fork; foretarsal segment completely fused with tibia (Fig. 20A–C), apex of claws strongly expanded (Figs 13E–F); female sternum VIII with a short anteromedian keel (Fig. 13D); polar caps usually smaller, not as wide as egg (Fig. 13B–C), except in *picteti*, with a cap subequal in width to egg (Fig. 13A).....***Asthenopodes*** (3 spp, Neotropical)

7 Penes with a short apical spine-like projection (arrow in Fig. 17C, D, F); female sternum VIII with a long and thin anteromedian keel (Fig. 18F–H) and very reduced sockets; eggs with polar caps formed by 3–8 tightly twisted threads (Fig. 18A–E)..... ***Asthenopus*** (5 spp, Neotropical)

– Penes apically rounded or slightly pointed but never with a spine (Fig. 8A–C); female sternum VIII with a short blunt keel with larger sockets (Fig. 8J); eggs with polar caps formed by 14–16 tightly twisted threads (Fig. 8K)..... .....***Priasthenopus*** (only *P. gilliesi*, Neotropical)

8 Legs II and III flap-like without tibia and tarsi, in both sexes; forceps 1-segmented; eggs with one polar cap (some species show the cap on the convex face)..... ***Campsurus* Eaton** (45 spp, Neotropical, except 1 Nearctic species)

– Legs II and III weak and twisted, but complete; forceps 2-segmented (a weak line separates a short basal segment); eggs without polar caps (a long thread coiled around the egg is present in one species, Molineri 2010) **9**

9 Male sternum IX not divided medially along its length; penes fused basally; pedestal with relatively short parastylus; female FW with IRs complete;

sockets on sternum VIII small and submedian ..... ***Tortopus*** **Needham & Murphy** (7 spp, Neotropical, 1 reaches southern Texas)

– Male sternum IX divided medially along its length; penes completely separated; pedestal with long and curved parastylus; female FW with IRs incomplete (2 IR veins are wanting); sockets on sternum VIII larger and sublateral .... ***Tortopsis*** **Molineri** (8 Neotropical and 2 Nearctic species)

Nymphs (modified from Molineri 2010)

1 Outer edge of mandibular tusks with many large tubercles; tarsus and tibia of foreleg separated ..... **Polymitarcyinae**

– Outer edge of tusks without large tubercles (Figs 5B, 9C–F, 14A–C) (*Povilla* presents a median indentation, Fig. 14D, H) but small blunt tubercles may be present; tarsus and tibia of foreleg fused (a fusion line with a row of setae may be distinguishable or not, Figs 6A, 10A, 15A) **2**

2 Dorsum of head mostly glabrous, without large tufts of tightly grouped short setae (Figs 5A, 9A–B, 14I–J); occiput roundly convex; apex of left mandibular tusk with 3–4 pointed processes (Figs 5B, 9C–F, 14A–C)... Asthenopodinae...**3**

– Dorsum of head with dense patches of short setae, mainly anteriorly to lateral ocelli; occiput flat, subquadrate in dorsal view; apex of left mandibular tusk with 1 pointed process ..... Campsurinae...**7**

3 Mandibular tusks relatively long and slender, without tubercles or large spines on inner margin (Figs 5B, D) ..... ***Hubbardipes***

– Mandibular tusks robust, stout (Figs 9C–F, 14A–C), with one or more tubercles on inner margin (arrow in Figs 9D and 14F) **4**

4 Mandibular tusks without large subbasal tubercle on inner margin; foretarsal claw with double row of denticles (Fig. 10B) ..... ***Asthenopodes***

– Mandibular tusks with a large subbasal tubercle on inner margin (arrows in Fig. 14G); foretarsal claw with single row of denticles (Fig. 15G) **5**

5 Apex of left mandibular tusk with 4 pointed processes (Ethiopian and Oriental) **6**

– Apex of left mandibular tusk with 3 pointed processes (Fig. 14A–C) (Neotropical) ..... ***Asthenopus*** (3 spp known as nymphs)

6 Outer margin of mandible with a tooth-like indentation (Fig. 14H); abdominal gill I bifid ..... ***Povilla***

– Outer margin of mandible smooth; abdominal gill I uniramous.... ***Languidipes***

7 Mandibular tusks with prominent basal or sub-basal tubercle on median margin (rarely tubercle absent), from some to many apical crenulations, numerous setae on outer margin of mandibles; abdominal gill I bifurcated..... ..... ***Campsurus***

– Mandibular tusks with 1 or 2 prominent tubercles on distal third of median margin, few long setae on outer margin of mandibles; abdominal gill I single ...**8**

8 Mandibular tusks with 2 tubercles (submedian and subapical) on median margin; distal projection of foretibia-tarsus 2/5 the length of claw ..... ***Tortopus***

– Mandibular tusks with a single subapical tubercle on median margin; distal projection of foretibia-tarsus 2/3 the length of claw ..... ***Tortopsis***

Discussion

Taxonomy and phylogeny

Lestage (1922) reported a concise summary of the meandering story of the early taxonomic stages of *Asthenopus*: *Asthenopus* was erected by Eaton (1871) for the species *Asthenopus curtus* (Hagen) and also for *A. dorsalis* (Burmeister). Later Eaton (1883), without mentioning *Asthenopus*, treated these species at *Campsurus*. *Asthenopus* is not mentioned in the systematic literature until Ulmer (1921) reinstated it as a valid name for *Asthenopus albicans* Pictet (nec Percheron), *A. curtus* (Hagen) and *A. amazonicus* (Hagen 1888), but treating *A. dorsalis* as a *Campsurus*.

Shortly after, Ulmer (1924) erected *Asthenopodes* for *A. albicans*. Ulmer's consideration of *A. albicans* as a species authored by Pictet was an error (Hubbard 1975), and it was renamed by this last author as *Asthenopodes picteti* Hubbard. In 1978 Berner synonymyzed *A. curtus* with *A. amazonicus*. Thus, Neotropical Asthenopodinae was at that moment known by two species: *Asthenopus curtus* (Hagen) and *Asthenopodes picteti* Hubbard. Domínguez (1988) described *Asthenopus gilliesi*, a species showing some characters shared by *Asthenopus* and *Asthenopodes* and based on this Hubbard and Domínguez (1988) combined both genera. More recently, two species were added to *Asthenopus*: *A. crenulatus* Molineri, Cruz & Emmerich (2011) and *A. angelae* de Souza & Molineri (2012).

Ulmer (1942) discussed many characters to differentiate *Asthenopus* from *Campsurus*, most of them measures and ratios of different structures (prothorax, forewing veins, legs, forceps). In contrast, Ulmer (1942) found only two characters to distinguish *Asthenopus* from *Povilla*, an African Asthenopodinae described by Navás (1912): 1) ICu_2 free at base or joined by crossveins to nearby veins in *Asthenopus*, but ICu_2 springing from CuP in *Povilla*; and 2) penis lobes curved and cylindrical in *Asthenopus* but straight and rod-shaped in *Povilla*. The first character is present in *P. adusta* but not in the other species of *Povilla* (including *Languidipes corporaali*), so it is not useful at the generic level. The second, may still be used to distinguish both genera, but it is not useful to separate *Hubbardipes* gen. n. from *Povilla* (both showing blade-like penes).

Domínguez (1988) presented a more detailed description concerning these genera, and reported that *Povilla* differs from *Asthenopus* because the former shows: 1) forceps 2-segmented (1-segmented in *Asthenopus*, note that here the genitalia was reinterpreted following Kluge 2004 and the basal segment or pedestal is considered part of the styliger plate), 2) penes bladelike (cylindrical in *Asthenopus*), 3) bifurcation Rs from base to margin: 1/10 (2–2.5/10 in *Asthenopus*), and 4) MP_2 shorter than IMP (subequal in *Asthenopus*).

Kluge (2004) did not differentiate both genera, apparently treating them as synonyms. But he summarized the features traditionally associated with the subfamily Asthenopodinae (at that time = *Asthenopus* + *Povilla*), distinguishing two "synapomorphies" in the nymph: mandibular tusks specialized in biting (not long, very thick and stout, with serrate inner margin), and foretarsal claw with a row of denticles. Kluge (2004) also listed the following "plesiomorphies" shared by this group: 1) FW with CuA not so strongly curved as in Campsurinae, thus both ICu veins go nearly parallel to basitornal margin and terminate near or anteriad to tornus; 2) genitals retain small median remnant of styliger which is articulated to posterior margin of sternite IX and bears immobile pedestals (narrow basally, and with muscles that move forceps); 3) penial arms retain lateral articulations with postero-lateral angles of tergite IX; 4) imaginal moult is present in both sexes (not in female Polymitarcyinae); 5) egg ellipsoid as usual, two polar caps or none; 6) nymphal gill I bilamellate. Note that a formal quantitative phylogeny was not presented by Kluge (2004), so his use of "synapomorphy" and "plesiomorphy" are *ad hoc* hypotheses.

The inclusion of many of these characters in a formal cladistic analysis permitted us to recognize apomorphic from plesiomorphic states, showing that some of the hypothesized synapomorphies for Asthenopodinae (or particular genera) were not homogeneous in the corresponding clade (e.g., some members of Asthenopodinae may show Campsurinae features, etc.). For this reason, a list of the synapomorphies for each genus is given either in the descriptions and taxon discussion (for *Hubbardipes*, *Priasthenopus*, *Asthenopus* and *Asthenopodes*) or in Appendix 2 (for Asthenopodinae, and the other genera).

The revalidation of *Asthenopodes* is in general coincident with the observations of previous authors (i.e., the character changes defining the group are those previously reported by Ulmer 1924, Traver 1956 and Hubbard 1975), and new characters are added to its diagnosis due to the knowledge of the egg and nymph. The generic status of *Hubbardipes* and *Priasthenopus* are supported by many autapomorphic character states and its position in the phylogeny is intermediate between *Asthenopodes* and *Asthenopus*. That the Neotropical species do not form a monophyletic group is a novel hypothesis obtained in our study.

Biogeography

Polymitarcyidae probably originated in Pangea and with the break up of the supercontinent in Laurasia and Gondwana, the first division of the family occurred. The subfamily Polymitarcyinae diferentiated as a Laurasian group (but this would require the ad hoc hypothesis of a later expansion to Africa) (triangles in Fig. 23), indicating a vicariant pattern with the ancestor of Asthenopodinae + Campsurinae, a Gondwanic group. This Gondwanic group probably was always restricted to temperate or warm climates because it is absent from Southern South America, Australia and New Zealand. Asthenopodinae still shows this pattern but Campsurinae extended its range

(originally Neotropical) to the Nearctic region but marginally (only 4 of the 62 species, Fig. 23). The ancestor of Campsurinae and Asthenopodinae was most probably distributed in tropical-subtropical Gondwana, where it originated at least five groups: 1) Campsurinae, 2) *Asthenopodes*, 3) *Hubbardipes*, 4) *Priasthenopus*, and 5) the ancestor of *Asthenopus* + *Povilla* + *Languidipes*. Subsequently, the formation of the Atlantic Ocean separated the South American *Asthenopus* from the Ethiopean-Oriental group (ancestor of *Povilla* + *Languidipes*).

Two fossils may falsify these hypotheses. *Mesopalingea* Whalley & Jarzembowski (a Campsurinae sensu McCafferty 2004) is known in the nymphal stage from the late Jurasic-early Cretaceus of Spain. Kluge (2004) classifies it as Fossoria insertae sedis (a group including almost all the burrowing families), thus not recognizing this genus as a Polymitarcyidae. The tusks of *Mesopalingea* strongly resemble those of *Campsurus*, but we suspect that this similarity is only superficial because at least two features would place the fossil outside Campsurinae: a somewhat prominent frontal projection and a very short ring-like prothorax.

The second fossil with contradictory information, *Asthenopodichnium* Thenius (1979) is known from 2 trace species (tubular marks in wood and bones) from the Miocene of Vienna. These tubular marks were atributed to Polymitarcyinae by Thenius (1979, 1988) or Asthenopodinae by McCafferty (2004). There is no evidence that they were produced by a mayfly; actually other animal taxa produce similar traces, so we agree with Kluge's (2004) treatment of *Asthenopodichnium* as Animalia insertae sedis.

Five groups (Campsurinae, *Asthenopodes*, *Hubbardipes*, *Priasthenopus* and *Asthenopus*) constitute independent sources to study biogeographic patterns inside the Neotropical region. Vicariant patterns in Campsurinae are only known for *Campsurus* (Molineri & Salles, 2013), which can be compared to those here indicated by *Asthenopodes* and *Asthenopus* (*Hubbardipes* and *Priasthenopus* are monotipic). *Asthenopodes* shows a single disjoint sister pair (*A. chumuco* in the Amazonas subregion vs *A. traverae* + *A. picteti* in the Parana subregion, barrier 6 in Fig. 25), coincident with the disjunction between *Asthenopus guarani* vs the remaining species of *Asthenopus* (barrier 3 in Fig. 24). This pattern resembles that of *Campsurus amapaensis* vs *C. argentinus* + *C.major* (Molineri & Salles, 2013) and was probably initiated by the appearance of drier areas (Chacoan biogeographic subregion) separating Amazonas subregion to the North from the Paranaense subregion in the SE (Morrone 2001). The two more recent vicariant events involve species in *Asthenopus*: barrier 4 separating *A. hubbardi* from *A. curtus* + *A. angelae* + *A. magnus* (detail in Fig. 24) and barrier 5 with *A. magnus* in the Napo Region vs *A. angelae* more to the East, Fig. 24). Without a molecular dating of these clades we can only speculate possible explanations related with pleistocene refugia (Hooghiemstra and van der Hammen 1998).

But perhaps the most interesting biogeographic pattern found in the present work is the paralogy in tropical South American areas caused by the paraphyletic nature of the Neotropical Asthenopodinae. The accepted hypothesis of vicariance between South American and Afro-Oriental Asthenopodinae was the formation of the Atlantic Ocean during the breakup of Gondwana (Lomolino et al. 2006). But as this event

was found here to be more recent than those involving the more basal clades (*Asthenopodes*, *Hubbardipes* and *Priasthenopus*), a more complex taxon history of the group is suggested. As these events (generic and suprageneric divergences) are deeper than the divergence of sister species in *Asthenopus* mentioned above, marine transgressions (>10 millions years, Ortiz-Jaureguizar and Cladera 2006) become possible scenarios.

Descriptions

***Hubbardipes* gen. n.**
http://zoobank.org/7A588525-40FB-41B1-976F-1E915BAF813F
Figs 4A, 5–7, 20D

Asthenopus (partim) Molineri et al. 2011: 34.

Type species. *Asthenopus crenulatus* Molineri, Cruz & Emmerich, 2011 (original designation).

Species included. *Hubbardipes crenulatus* (Molineri, Cruz & Emmerich) comb. n.

Diagnosis. Eight autapomorphies define the genus *Hubbardipes* in our cladistic analysis (Appendix 2), some of them are: 1) male foretibia very wide apically (Fig. 20D), first tarsal segment partially fused with second tarsal segment (Fig. 7B); 2) thumb (inner basal projection) of penes reduced, indistinguishable (Fig. 7A); 3) apex of penis lobe wider than base and with many marginal spines (Fig. 7A); and 4) nymphal mandibular tusk with smooth to slightly crenulated inner margin, without submedian tubercles (Figs 5B, D). Additionally, the following combination of characters is useful to distinguish *Hubbardipes* from other genera in Polymitarcyidae: 1) ratio length male FW/foreleg = 1.1; 2) male foreleg with large and apically widening tibia, tarsal segment 1 small and partially fused to tarsal segment 2, tarsal claws slender slightly wider at apex; 3) pronotum width/length ratio: 1.5 (male), 2.2 (female); 4) marginal intercalary veins present on the entire margin of fore and hind wings, generally shorter than distance between longitudinal veins in male, but longer and anastomosed in female; 5) in both sexes FW with 3–4 crossveins between R and M, basally to R fork; 6) basal relation of FW veins IMP-MP_1 variable (IMP joined to MP_1, or basally free), MP_2 curved toward CuA and fused to CuA and MP_1 by cross veins (forming a characteristic oblique Y) ; 7) median remnant of styliger plate subquadrate and small, pedestals short also subquadrate and relatively small; 8) forceps slender, ratio length/basal width = 8.5–9.0 (Fig. 7A); 9) penes relatively thin, with many spines near the apex on outer edge, slightly curved inward (Fig. 7A); 10) female abdominal sternum VIII with anteromedian paired sockets on a protruding subcircular structure; 11) eggs with relatively large polar caps (almost as wide as egg, ratio width egg/cap 1.2–1.4), each cap formed by 4–7 threads, chorion completely covered by large disk-like plates and smaller irregular plates (Figs 7D–E); 12) nymphal head with a small median projection on the frons (arrow in Fig. 5C); 13) nymphs with long robust tusks, without

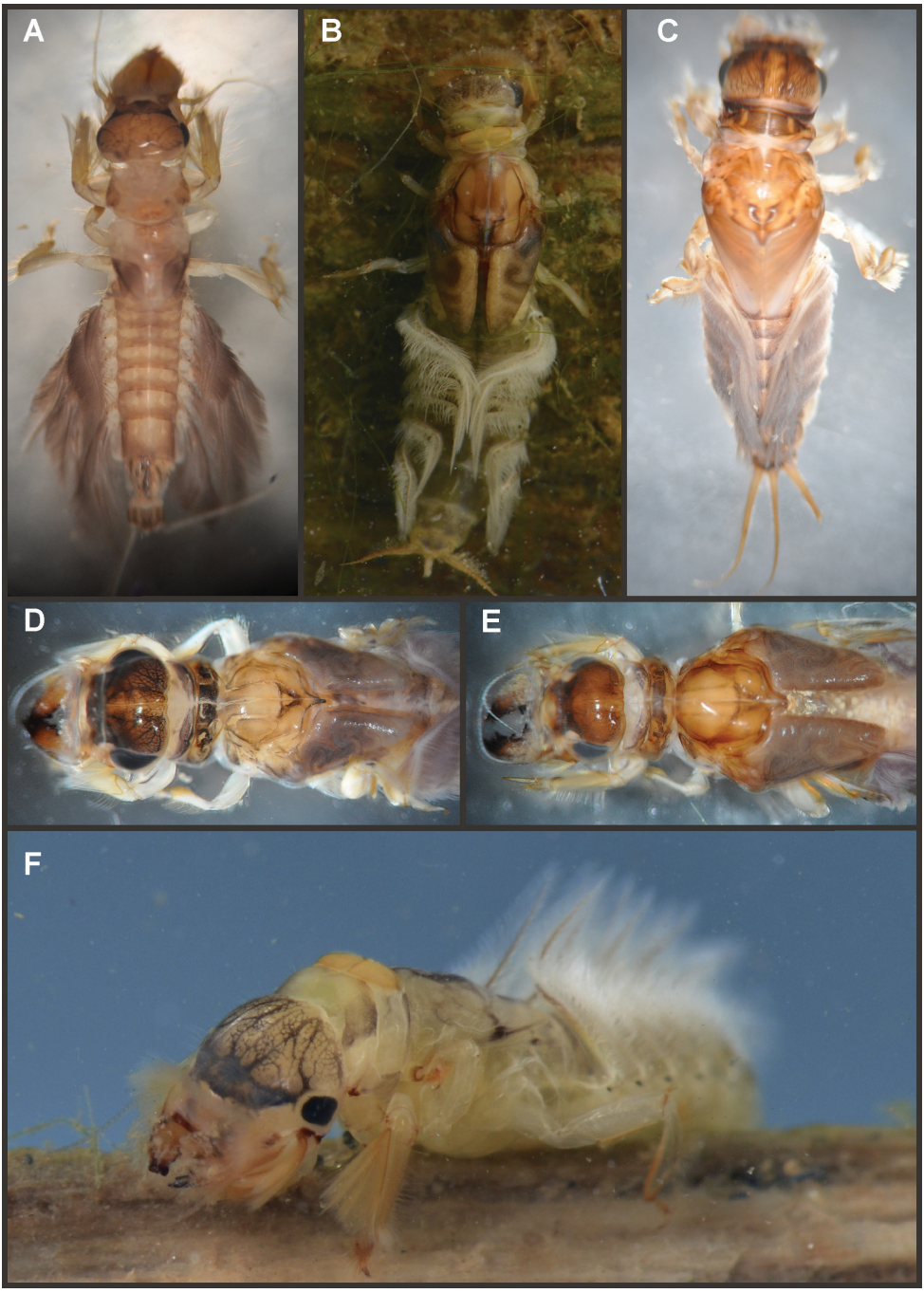

Figure 4. Asthenopodinae nymphs: **A** *Hubbardipes crenulatus* **B** *Asthenopodes chumuco* **C** *Asthenopus magnus* **D** *Asthenopus angelae* **E** *Asthenopus curtus* **F** *Asthenopodes chumuco*.

inner tubercles, with 2 or 3-pointed apex (right and left mandible respectively) (Figs 5A–B, D); 14) nymphal foretarsal claw with single row of about 14 denticles, denticles are small basally, and larger medially, 3 denticles are closer together near the apex, and the last one is much smaller (Fig. 6D); 15) nymphal dorsal apex of hind femur with ca. 20 stout spines (Fig. 6E).

Male imago. Length (mm): body, 7.0–7.8; FW, 7.5–8.6; HW, 3.1–3.7; foreleg, 6.2–6.9; cerci, 21.6. Antennae: scape slightly longer than pedicel; flagellum bristle-like. Thorax. Pronotum width/length: 1.5–2.5. Legs. Forelegs relatively long, ratio length FW/foreleg = 1.1; tarsal segment 1 fused to tarsal segment 2 (Fig. 20D), longest segment is tibia, ratio length tarsal segment 2/tibia = 0.8; tarsal segments long decreasing in length from 2>3>4>5 (Fig. 7B); claws different in size, one long the other short, not strongly widened distally (Fig. 7C). Wings. FW with 14 marginal intercalaries along hind margin, also present along entire hind margin of HW; these intercalaries present relatively numerous connections with other cross and longitudinal veins but they are not very anastomosed; 3–4 crossveins between R and M sectors basally to R fork; Rs stem length/Rs from fork to margin = 0.24; ratio MA from fork to margin/stem length = 9–12; IMP fused basally to MP_1; MP_2 fused to CuA. Genitalia (Fig. 7A): median remnant of styliger plate present, and with pedestals short and subquadrate with inner apical corner slightly protruding distally; forceps relatively long and slender, ratio length/basal-width = 9. Terminal filament reduced, cerci long (ratio length FW/cercus = 0.35).

Female adult. Length (mm): body, 10.2–10.8; FW, 11.1; HW, 4.3. Thorax. Pronotum width/length = 1.5–2.3. Wings with more crossveins and intercalaries than male. Abdominal sternum VIII with paired anteromedian sockets on an oval and ventrally protruding structure, sockets small, shallow and contiguous. Terminal filament reduced, shorter than tergum VIII, with few thin annuli; cercus 0.5–0.6 times the length of abdomen.

Eggs (Fig. 7D–E). Length, 221–266 μ; width, 143–152 μ. Oval (ratio maximum length / maximum width = 1.5–1.7), with two medium sized polar caps on apices (ratio maximum with of egg/maximum width of coiled polar cap = 1.2–1.4), each cap formed by 4–7 very long filaments. Chorionic surface completely covered by plates: large disk-like structures frequently 3-partited with a fine microsculpture forming a dashed pattern, and many small (and irregular in shape) plates covering completely the spaces between the large plates.

Nymphs (Fig. 4A). Length (mm): body, 11.0–14.5; cerci, 4.5–5.5; terminal filament, 6.0. Head (Figs 5A, C) subquadrate in dorsal view, smooth (without pilose area), antennae 1.7–2.0 times length of head. Occipital region well developed, convex (Fig. 5A). Head capsule dorsally projected at bases of antennae. Frontal ridge marked only by a dense transversal row of setae; frons acutely projected medially (Fig. 5C); clypeus and labrum membranous and small, labrum densely covered with long setae on dorsum. Mandibular tusks (Figs 5A, B, D) relatively long and slender, similar in length to head capsule, dorso-ventrally flattened, left tusk apically with 3 tubercles (the median is reduced in length), right tusk with 2 tubercles; dorsal

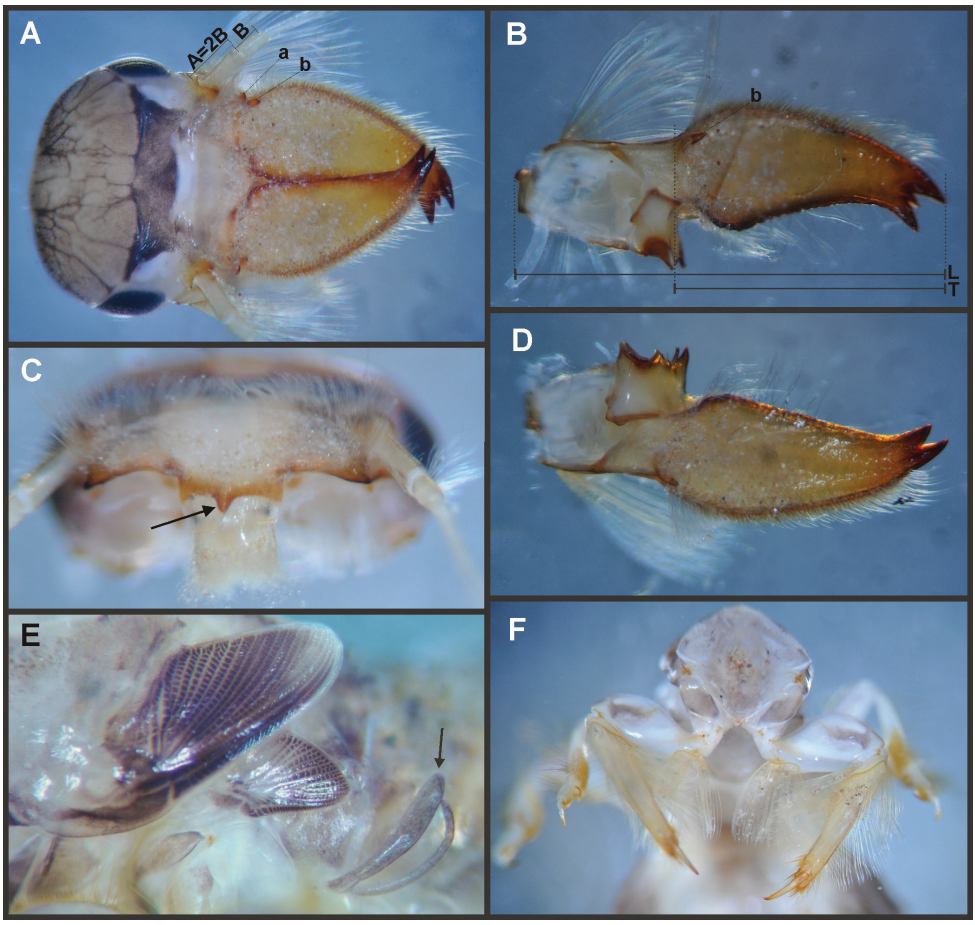

Figure 5. *Hubbardipes crenulatus*, nymph. **A** head, d.v. **B** left mandible, d.v. **C** head, frontal view (arrow indicates frontal anteromedian projection) **D** right mandible, d.v. **E** wingbuds and gill I **F** frontal view of thorax (head removed).

surface of tusks wide, with crenulated inner margin bearing long setae; outer margin with a small dorsal tubercle near base ("b" in Figs 5A–B) and densely covered with stout setae along entire margin; the small basal tubercle ("b") forms an additional articulation between mandible and head capsule ("a" in Fig. 5A). Body of mandible: molae and canines present but small, margin between them sharp-edged (acutely protruding in right mandible, Fig. 5D); with basal U-row of long filtering setae in both mandibles. Thorax. Pronotum with short anterior ring (collar), 1/3 the length of posterior ring (length taken at the medio-longitudinal line), anterolateral corners projected, spine-like. Legs (Fig. 6). Leg I (Fig. 6A): femora very wide, well developed, with a double ventro-basal row of long filtering setae; tibio-tarsus (fused) with 3 rows of filtering setae (2 on anterior face and 1 on inner margin), roundly projected apically; tarsal claw long and slender with a row of marginal denticles (Fig.

6D). Leg II (Fig. 6B): smaller, with thinner femora, with scattered long setae, mostly basally and along hind margin; tibia and tarsi with row of long setae on outer (dorsal) margin, ventrally with many stout spines on apical half, with a distal brush of thick setae; tarsal claw weaker, without denticles. Leg III (Fig. 6C): as leg II except larger and with anterior margin of femur densely covered with thick setae, femur distally with a group of acute stout spines (Fig. 6E), tibia without distal brush. Coxae I and II directed ventrally, coxae III directed laterally. Abdomen. Sternite I stronger and partially fused with metasternum. Gill I reduced in size, dark gray, double, both portions of a similar length, but the dorsal is wider (arrow in Fig. 5E). Gills II–VII well developed, ventral portion smaller than dorsal portion. Tergum X with short and blunt, poorly developed posterolateral spine. Cerci slightly shorter than terminal filament, with long setae at joinings.

Etymology. *Hubbardipes* from "Hubbard" and "pes", Latin, masculine, meaning "foot". We dedicate the genus to Mike Hubbard, mayfly specialist, who devoted many of his works to the Polymitarcyids.

Distribution. Amazonas subregion (Amazonas river in Colombia and Brazil).

Discussion. *Hubbardipes* was recovered as sister to a larger clade containing *Priasthenopus*, *Asthenopus*, *Povilla* and *Languidipes* (see synapomorphies in Appendix 2), not related with *Asthenopodes*, as previously thought (Molineri et al. 2011). *Hubbardipes* shows many differences in the adult stage and, more markedly in the nymph and egg here described for the first time. Male genitalia is unique in form and structure (Molineri et al. 2011), nymphal tusks and microsculpture on disk-like structures of the egg are exceptional as well.

Hubbardipes crenulatus (Molineri, Cruz & Emmerich), comb. n.

Asthenopus crenulatus Molineri, Cruz & Emmerich, 2011: 34.

Material. Listed in Molineri et al. (2011), from Brazil (Amazonas, Presidente Figueiredo) and Colombia (Amazonas, Leticia, Reserva Natural Palmarí). Additional material: 2 male subimagos and 3 nymphs from BRAZIL: Amazonas, Tefé, São João do Catuaí, Igarapé Jutaí (A07), S 3°41'52.8" - W 64°9'18", 12.ix.2003, luz UV1, 067 FCM (CZNC); 7 nymphs from COLOMBIA, Dpto. Amazonas, rio Yavari junction Orejon, S 4°7'12" - W 69°55'43", E. Domínguez & N. Torres col. (IBN).

Diagnosis. *Hubbardipes crenulatus* (Molineri et al., 2011) comb. n. is known from adults of both sexes, eggs and nymphs, and for the moment it is the only known species in the genus. The characters useful to distinguish it from other Asthenopodinae are listed in the generic diagnosis.

Nymphs (Fig. 4A). Length (mm): body, 11.0–14.5; cerci, 4.5–5.5; terminal filament, 6.0. General coloration whitish light brown. Head with a gray band between lateral ocelli and fine netting pattern on occiput (Fig. 5A). Antennae: scape bare, long and slender, pedicel shorter with many dorsal setae, flagellum bare with numerous

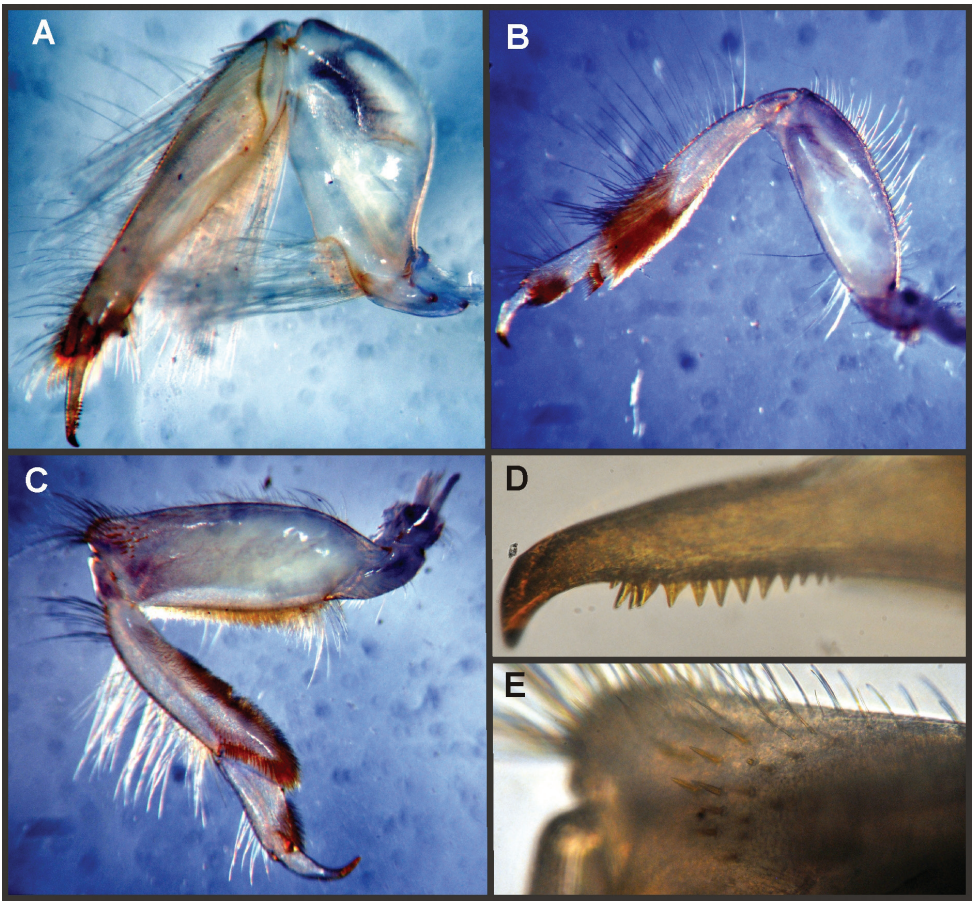

Figure 6. *Hubbardipes crenulatus*, nymph. **A** foreleg, d.v. (functionally frontal) **B** middle leg, d.v. **C** hind leg, v.v. (functionally dorsal) **D** foretarsal claw, detail **E** detail of apical spines on hind femur.

annuli increasing in length distally. Thorax. Pronotum shaded black on anterior ring and more slightly shaded witn brownish-gray on posterior ring except on a pair of submedian longitudinal pale lines. Meso- and metanotum shaded widely with gray, with dark gray wingbuds, developing veins paler (Fig. 5E). Legs (Fig. 6). All coxae and trochanters shaded with gray, femur I shaded with gray, remaining segments and legs II and III whitish-yellow; foretarsal claw with ca. 20 denticles increasing in size distally. Abdomen. Terga more or less uniformly shaded brownish-gray, except on pale transverse dashes laterally, and pale subcircular submedian marks; tergum X with two submedian pale bands; sterna paler than terga, shaded with gray very slightly, somewhat darker on sterna IX–X. Gill I dark gray, gills II–VII brownish gray, ventral portion paler than dorsal portion. Caudal filaments whitish.

Distribution. Amazonas river, from Leticia (Colombia) to Manaus (Brazil).

Discussion. *Hubbardipes crenulatus* (Molineri et al., 2011) comb. n. was recently described from male and female adults in the genus *Asthenopus*, with the knowledge

of the nymphs and based on the results of the phylogenetic analysis, it became evident that this species pertain to a distinct group, that we propose here as a new genus.

***Priasthenopus* gen. n.**
http://zoobank.org/6EDB4C4E-8A74-47F6-9B8A-E7955DFADA2E
Figs 8, 20E

Asthenopus (partim) Domínguez 1988: 21; Hubbard and Domínguez 1988: 207.

Type species. *Asthenopus gilliesi* Dominguez, 1988 (original designation).

Species included. *Priasthenopus gilliesi* (Dominguez), 1988 comb. n.

Diagnosis. *Priasthenopus* gen. n. presents seven autapomorphies in our cladistic analysis (Appendix 2), six are variations in continuous characters (e.g., stoutter penis lobe and larger thumb) and the seventh is the presence of a short closed cleft between the aforementioned structures. This genus can be distinguished from the other by the following combination of characters: 1) ratio length male FW/foreleg = 1.6–2.0; 2) first tarsal segment subquadrate not fused with tibia (Fig. 20E); 3) pronotum width/length ratio: 2.1–2.5 (male), 2.6 (female); 4) 5–10 marginal intercalary veins present on the margin of FW (Figs 8F, H), about as long as the distance between longitudinal veins in male, slightly longer in female, HW without marginal intercalaries; 5) male FW with 1 cross vein between Rs and MA basal to Rs fork (2 in female); 6) vein MP_1 basally free (types from Uruguay and specimens from Colombia, Fig. 8D) or tending to fuse, although not completely, with MP_2 (in specimens from Bolivia, Fig. 8E), IMP basally free; 7) median remnant of styliger plate rectangular thin and convex posteriorly, pedestals rectangular (Fig. 8A); 8) ratio total length/basal width of forceps 6.3–7.3 (Fig. 8A); 9) penes relatively short with a similar width along their length, strongly curved, without apical spine or spine very slightly marked as a subapical indentation, thumb rounded (Figs 8A–C); 10) female sternum VIII with well distinguishable anteromedian sockets (Figs 8J); 11) eggs with relatively large polar caps formed by 14–16 long threads (Fig. 8K), chorion loosely covered by medium-sized and small circular plates (Fig. 8L).

Male imago. Length (mm): body, 5.0–8.0; forewing, 5.7–8.4; hind wing, 2.6–3.9; foreleg, 3.1–4.5; cerci, 19.0–25.0. Pronotum width/length: 2.1–2.5. Wings (Figs 8D–G). FW with 5–10 marginal intercalary veins (Fig. 8F), each imv is about as long as the distance between corresponding longitudinal veins; vein MP2 basally free (Fig. 8D) or base directed towards MP1 (but not completely fused with it, Fig. 8E); IMP basally free; 1 cross vein present between Rs and MA basal to Rs fork. HW without marginal intercalaries (Fig. 8G). Legs. Forelegs about half the length of FW, middle and hind legs reduced in length and poorly sclerotized but with all the segments present and distinguishable. Genitalia (Figs 8A–C): median remnant of styliger plate rectangular, thin and convex posteriorly, pedestals rectangular and relatively small (Fig. 8A); 1-segmented forceps, ratio total length/basal width 6.3–7.3 (Fig. 8A); penes (Figs 8A–C) relatively short with a similar width along their length, strongly curved medially, and

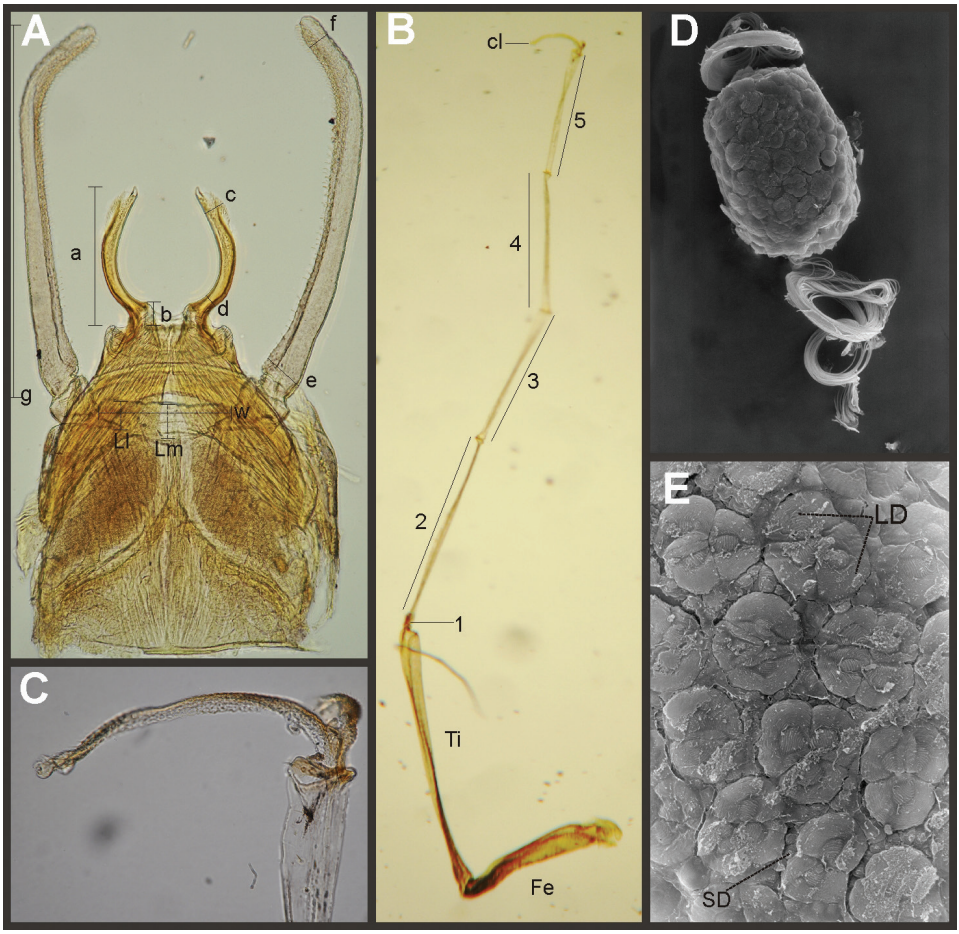

Figure 7. *Hubbardipes crenulatus*, male imago and egg: **A** male genitalia, v.v. **B** male foreleg **C** detail of foretarsal claw **D** egg, general view **E** detail of chorion (LD = large disks).

without apical spine. Cerci long and well developed, terminal filament extremely reduced as common in the family.

Female adult. Length (mm): body, 6.5; FW, 8.9; HW, 3.3; cerci, 1.5. Pronotum ring-like. Wing venation (Figs 8H–I) similar to male except FW with 2 cross vein between Rs and MA basal to Rs fork (arrows in Fig. 8H). Abdominal sternum 8 with anteromedian pair of small sockets (Fig. 8J). Cerci short, about 0.2 the length of FW.

Eggs (Figs 8K–L). Length, 240–275 μ; width, 150–165 μ. Two large polar caps (maximum width, 140–185 μ), formed by 14–16 very long coiled threads. The caps are as wide as or wider than the egg. Chorionic surface with medium sized and small subcircular disks.

Etymology. Arbitrary combination of letters.

Discussion. Treating this sole species in a new genus, distinct from *Asthenopus* is justified by its phylogenetic position (sister to the clade *Povilla-Asthenopus*). The other

possibility to fit taxonomy to phylogeny would be to synonymize the entire clade (including *Povilla* and *Languidipes* besides *gilliesi*) in *Asthenopus*. This is the scheme apparently presented by Kluge (2004) but this seems inadequate to us because of relatively large morphological gaps between the groups (including characters from eggs, nymphs and adults of both sexes). Furthermore, we tested *P. gilliesi* position considering the hypotethical situation that its nymphs (still unknown) be identical to *Asthenopus* s.s., since male genitalia of both groups are similar. Even so, there were no changes in the resulting tree. The description of female adults and eggs is an original contribution of this work that gives additional diagnostic characters to genus level.

Priasthenopus gilliesi (Domínguez), comb. n.

Asthenopus gilliesi Domínguez 1988: 21; Hubbard and Domínguez 1988: 207; Domínguez et al. 2006: 562

Material. Paratype male (IFML TEPH095, slide 041) from URUGUAY, Artigas, San Gregorio, orillas río Uruguay, 29.xi.1959, light trap, C.S. Carbonell col.; 5 male imagos (slide IBN141CM) and 1 male and 1 female (slide IBN471CM) subimagos (IBN) from COLOMBIA, Amazonas, P. N. Amacayacu, río Amacayacu, 93 m, S 3°48'28" – W 70°15'21", 3.ii.1999, light trap 18–20 h PM, E. Domínguez, M.C. Zúñiga & C. Molineri cols.; 5 male imagos and 1 female subimago (IBN) from BOLIVIA, Santa Cruz, near Once Por Ciento, río Blanco, 250 m, S 15°21'39.7" – W 63°17'28.8", 14.vi.2000, light trap, E. Domínguez col.; 1 female adult (CZNC) from BRAZIL, Rio N. Aripuanã, Rio Juma, Ig. Campineiro Gde., 8–9.ix.2004, Pennsylvãnia light trap; and 2 male imagos (CZNC) from Amazonas, Barcelos, rio Demene, ´boca´barco, 8–9.viii.2009, Pennsylvania light trap.

Diagnosis. *Priasthenopus gilliesi* is known from adults of both sexes and eggs, and is the only species known in the genus. The characters useful to distinguish it from other Asthenopodinae are listed in the generic diagnosis.

Male imago. See generic section above and original description in Domínguez (1988).

Female subimago. Length (mm): body, 6.5; FW, 8.9; HW, 3.3; cerci, 1.5. General coloration yellowish white with gray markings. Head cream extensively shaded gray dorsally, the shading is uniform anteriorly but in the form of a fine netted pattern posteriorly to lateral ocelli, occiput with a pair of submedian pale anterior spots and a pair of submedian dark posterior spots; venter of head whitish. Antennae yellowish white shaded with gray on scape and pedicel. Thorax cream. Anterior ring of prothorax very thin, less than 1/4 the dorsal length of posterior ring; ratio width/length: 2.6; pronotum shaded blackish on median area except pale medial line, presternum paler, shaded gray before coxa. Mesonotum shaded very diffusely with gray, darker on longitudinal carinae and between posteroscutal protuberances; mesosternum and pleurae paler, shaded gray on anterior corner of katepisternum. Metanotum shaded gray on posterior half, except on a pale median triangular mark, shaded darker posteriorly to this pale mark; metasternum whitish. Legs whitish except coxae yellowish shaded gray and apex

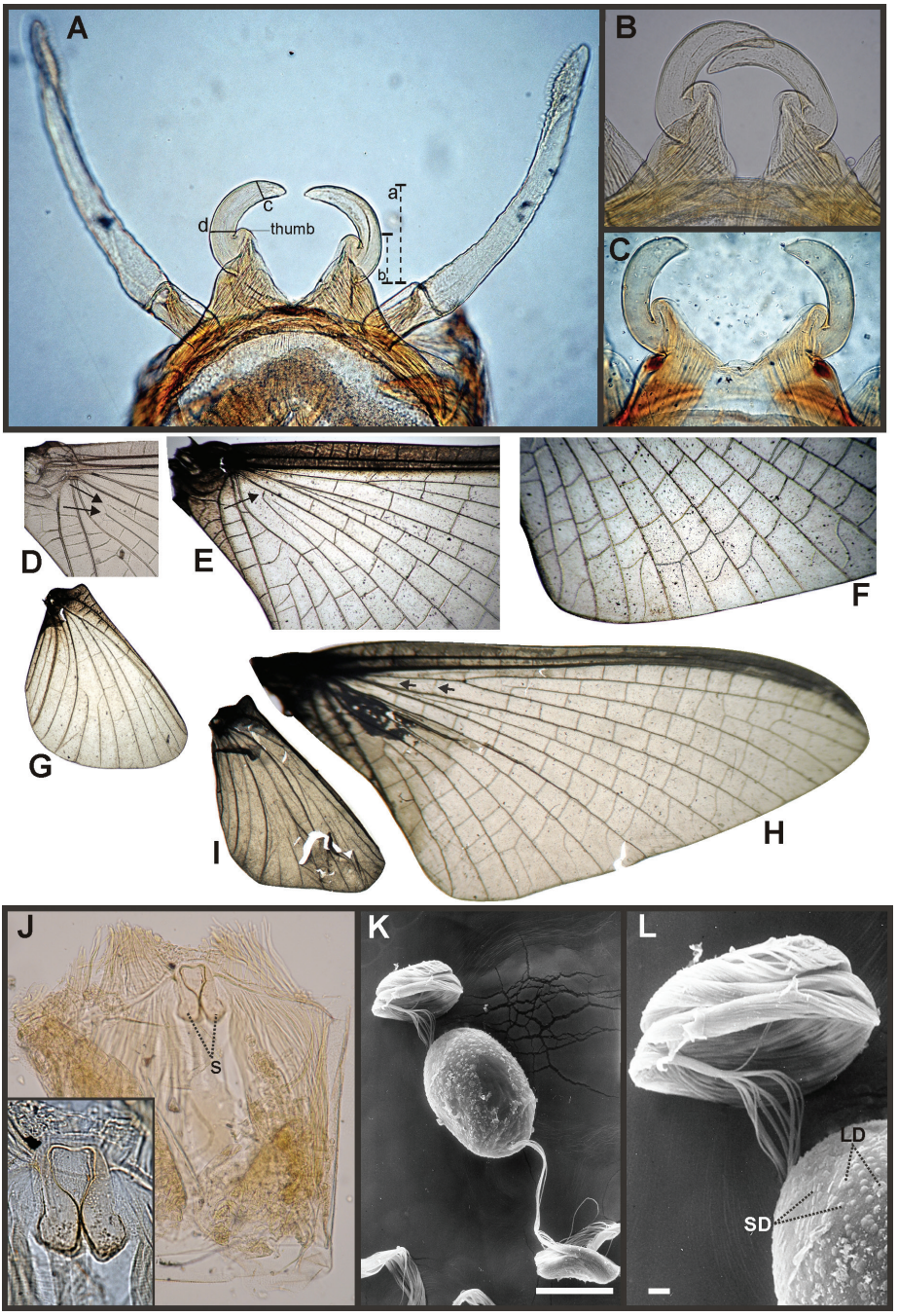

Figure 8. *Priasthenopus gilliesi*, adults and egg. Male imago: **A** genitalia, v.v. (Colombian specimen) **B** penes (Bolivian specimen) **C** penes (Uruguayan paratype) **D–E** FW detail of base (arrows indicate veins IMP and MP2) **F** detail of FW, posterior margin **G** hind wing. Female subimago: **H** forewing **I** hind wing **J** sternum VIII and detail of sockets (s). Egg (SEM): **K** general view **L** detail of cap and chorion, LD = large disks, SD = small disks.

of hind trochanter pointed and yellowish orange. Wings (Figs 8H–I). Membrane of fore and hind wings slightly shaded with light brown, veins translucent shaded with light brown, markedly on larger veins (C, Sc, Rs); marginal intercalaries relatively long (Fig. 8H), MP_1 fused with MP_2 at base; 2 crossveins present between M and R stems basally to Rs fork. Abdomen whitish, shaded with gray dorsally and darkening posteriorly, shading on terga interrupted on medial paler line, this line is wide on terga 1–4, narrows posteriorly on 5–7, thin on 8, and widens posteriorly on 9–10; sterna whitish translucent except gill sclerites yellowish white; sternum 8 with anteromedian pair of relatively large sockets (Fig. 8J). Cerci whitish, about 0.2 the length of FW.

Eggs. See generic description.

Distribution. This species presents a wide geographic range that spans from the Amazon River in the North to the Uruguay River in the South, also extending towards the West in Bolivian Chiquitania.

Discussion. *Priasthenopus gilliesi* male imagos were adequately described by Domínguez (1988), females and eggs are described here for the first time. There are no morphological differences between the male imagos examined from the different localities, except for the penes of the Colombian males are slightly stouter, and those from the Bolivian males are slightly slender than the penes of the Uruguayan types. In the forewings, vein MP_1 is basally free except on Bolivian males where this vein tends to fuse with MP_2, although not completely.

Campsurus paraquarius Navás, nom. n.

Campsurus paraguarius [lapsus] Navás 1920: 53; Lestage 1923: 122; Traver 1947b: 371; Hubbard 1982a: 271; Kluge 2004: 267.
Campsurus paraquarius; Navás 1924a: 359.

Material examined. None.

Discussion. In the forewings of *Priasthenopus gilliesi*, vein MP_1 is basally free except on Bolivian males where this vein tends to fuse with MP_2, although not completely. This last arrangement of the MP sector is also present in *Campsurus paraquarius* Navas (1920) and, also coincident, are the length and arrangement of the two imv (intercalary marginal veinlets) figured by Navás, the relatively short ICu veins and the vein AA basally curved to CuP; also the small size of the male described by Navás coincide with *Priasthenopus* size range. Navás described the color of legs without saying that middle and hind legs are reduced (as *Campsurus*), so probably they were present and complete as in all Asthenopodinae. Finally Navás stated that the pronotum is wider than long (transverse), feature also present in *Priasthenopus* and related genera (*Asthenopus*, *Povilla*) but not in *Campsurus* males. Other species of Neotropical Asthenopodinae show shorter intercalary marginal veins (*Asthenopus* s.s.) or longer ICu veins (*Asthenopodes*). Lestage (1923) noted the similiraty of Navás species with the genus *Asthenopus* and Kluge (2004) treated this species in *Asthenopus* because of the arrangement of veins

in the Cu sector of FW. We here coincide with these authors and because of the bad original description by Navás, and the apparent loss of type material, we treat the name *paraquarius* (Navás 1920) as a NOMEN NUDUM.

***Asthenopodes* stat. n.**
Figs 4B, 4F, 9–13, 20A–C

Asthenopodes Ulmer 1924: 26; Traver 1950: 611; Traver 1956: 1; Hubbard 1975: 111; Hubbard and Domínguez 1988: 209; Domínguez 1988: 24.

Type species. *Palingenia albicans* Pictet, original designation (= *Asthenopodes picteti* Hubbard)

Species included. *Asthenopodes picteti* Hubbard, *A. traverae* sp. n., *A. chumuco* sp. n.

Diagnosis. Seven autapomorphies define the genus *Asthenopodes* in our cladistic analysis (Appendix 2), some of them include: 1) Male foretarsal segment 1 fused with tibia (Figs 20A–C); 2) apex of male foretarsal claw strongly expanded (apex 3 times wider than stalk, Fig. 13E–F); and 3) pedestal relatively large, elongated, narrow at the base (Fig. 12). The following combination of characters representing the entire range of variation of the three included species, is useful to distinguish *Asthenopodes* from other genera in Polymitarcyidae: 1) ratio length male FW/foreleg = 1.0–1.6; 2) tarsal segment 1 indistinct (fused to tibia), tibia distally subequal in width to base of tarsal segment 2 (Figs 20A–C); 3) pronotum width/length ratio: 1.2–1.9 (male), 1.5–2.3 (female); 4) in both sexes FW marginal intercalary veins relatively long and anastomosed (from 9 to 22 in male FW, Fig. 11); 5) in both sexes FW with 3–6 (most commonly 4, but variable depending in size of specimen) crossveins between R and M, basally to R fork; 6) FW vein IMP slightly longer than MP_1, both frequently free at base but may be joined to one another and to MP_2 by crossveins (Fig. 11); 7) median remnant of styliger plate present in *A. chumuco* (subrectangular as other Asthenopodinae) but medially very short and with a strongly marked lateral lobe in the sister pair *A. picteti- A. traverae*; pedestals relatively large and thinner at the base; 8) forceps relatively slender, ratio length/basal-width = 4.7–9.5; 9) penes variable in form but curved medially rather than ventrally, basal thumb well separated from penial lobe, penial lobe apically acute (Fig. 12); 10) female abdominal sternum VIII with anteromedian paired sockets reduced in size (Fig. 13D); 11) eggs (Fig. 13A–C) with relatively small polar caps subequal to much thinner than egg, formed by 5–16 threads, chorion covered with medium-sized circular plates, surrounded by many smaller plates; 12) nymphal head dorsally strongly convex on occiput, frons not projecting medially (Figs 9A–B); 13) nymphs with very short and robust tusks (Figs. 9C–H), without large submedian inner tubercle, with 2 or 3-pointed apex (asymmetric); 14) nymphal foretarsal claw with 2 rows of marginal denticles, a long row of 15 denticle and one shorter row of 12 denticles (Fig. 10B); 15) apex of femur dorsally with ca. 30 strong and rounded spines (Fig. 10D).

Male imago. Length (mm): body, 7.3–13.5; FW, 7.0–14.5; HW, 3.7–7.3; foreleg, 5.0–14; cerci, 20.0–38.5. Antennae: scape subequal to pedicel; flagellum bristle-like.

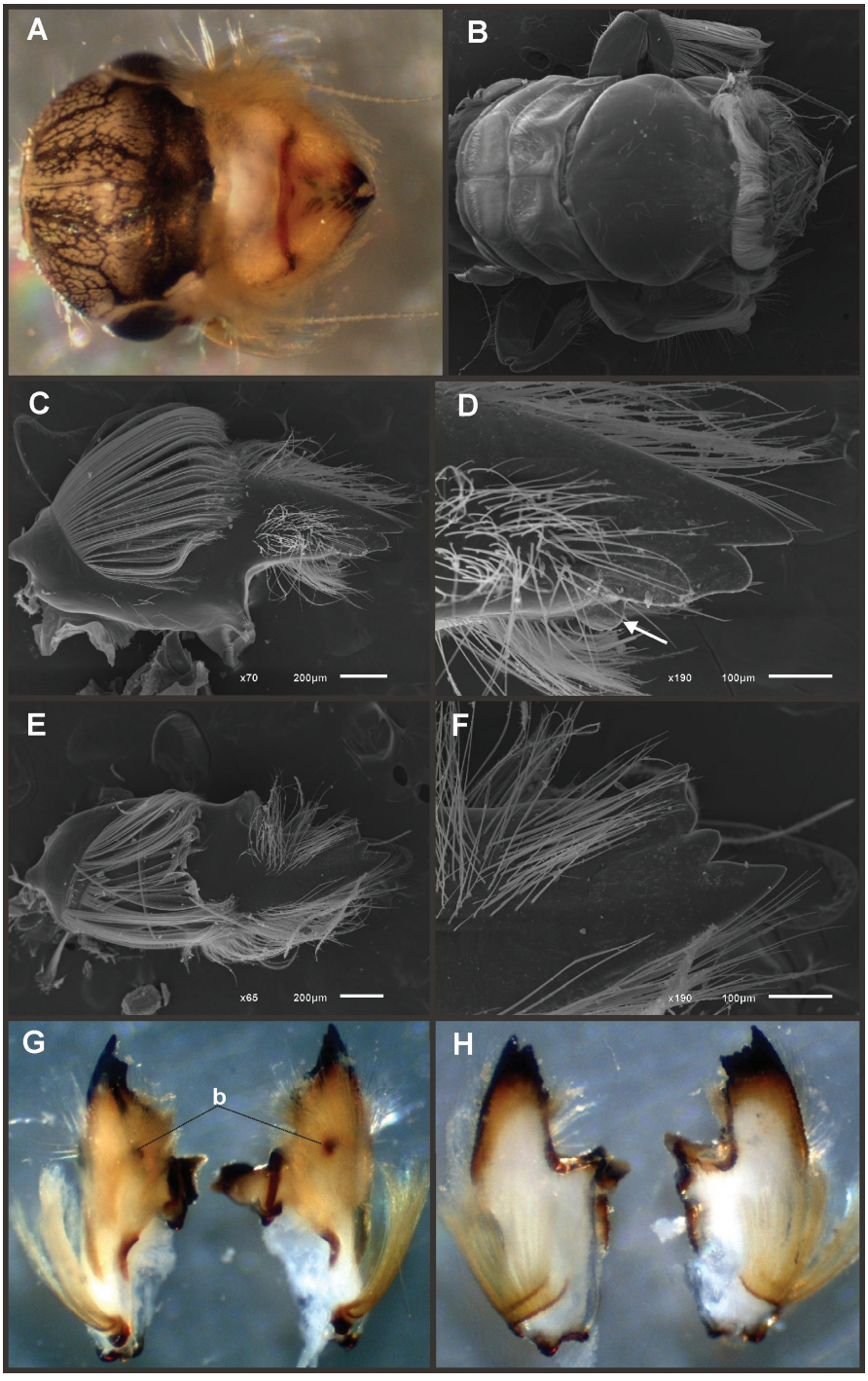

Figure 9. *Asthenopodes* nymph. *A. chumuco*: **A** head, dorsal view **B** head and pronotum, d.v. **C–D** right mandible and detail of apex, v.v. (arrow = subdistal tubercle) **E–F** left mandible and detail of apex, v.v. **G** mandibles, d.v. (b = dorsal tubercle) **H** same, v.v. **A, G, H** stereomicroscope photographs **B–F** SEM.

Thorax. Pronotum width/length: 1.2–1.9. Legs. Forelegs relatively long, ratio length FW/foreleg = 1.0–1.6; tarsal segment 1 fused to tibiae (Fig. 20A–C); longest segment is tarsal segment 2 or tibia (variable), ratio length tarsal segment 2/tibia = 0.6–1.5; tarsal segments long decreasing in length from 2>3>4>5; claws different in size, one long the other short, strongly widened distally (Fig. 13E–F). Wings (Fig. 11). FW with 9–22 marginal intercalaries along hind margin, also present along entire hind margin of HW; these intercalaries present numerous connections with other cross and longitudinal veins (i.e., very anastomosed); 3–6 crossveins between R and M sectors basally to R fork; Rs stem length/Rs from fork to margin = 0.2–0.4; ratio MA from fork to margin/stem length = 9–15; IMP fused basally to MP_1 or free; MP_2 fused to IMP. Genitalia (Fig. 12): median remnant of styliger plate with posterolateral corners roundly projecting, pedestal long to very long; forceps relatively long and slender, ratio length/basal-width = 4.7–6.7. Terminal filament reduced, cerci long (ratio length FW/cercus = 0.32–0.44).

Female length (mm): body, 7.2–19.0; FW, 12.2–22.5; HW, 5.3–11.5; cerci 1.2–4.0. Thorax. Pronotum width/length = 1.5–2.3. Wings with crossveins and intercalaries more numerous than in male. Abdominal sternum VIII (Fig. 13D) with reduced paired anteromedian sockets, sockets small, shallow and contiguous located at the base of a blunt subquadrate projection. Terminal filament reduced, shorter than tergum VIII, with few thin annuli; cercus very short, 0.1–0.2 times the length of FW.

Eggs (Fig. 13A–C). Length, 221–355 μ; width, 143–240 μ. Oval (ratio maximum length / maximum width = 1.3–1.7), with two relatively small polar caps on apices (ratio maximum with of egg/maximum width of uncoiled polar cap = 1.2–3.1), each formed by 5–16 long coiled filaments. Chorionic surface with fine granulated aspect or regularly spaced plates.

Nymphs, nearly mature (Fig. 4B, F). Length (mm): body, 7.8; cerci, 2.0–2.3; terminal filament, 3.1. Head subquadrate in dorsal view, smooth (without pilose areas), antennae subequal in length to head. Occipital region well developed, convex (Figs 9A–B). Head capsule dorsally projecting at bases of antennae. Frontal ridge marked only by a dense transversal row of setae; frons not projecting medially; clypeus and labrum membranous and small, labrum densely covered with long setae on dorsum. Mandibular tusks very short and robust, the part visible in dorsal view ca. 1/3 the length of head capsule; left tusk (Fig. 9E–H) apically with 3 teeth, the median reduced in length, and the innermost is strongly widened appearing as a ridge with two points (Fig. 9F); right tusk (Fig. 9C–D, G–H) with 2 distal teeth; inner surface with a small tubercles located distally (in relation to other Asthenopodinae), dorsal surface with a small tubercle ("b" in Fig. 9G) that forms an additional articulation between mandible and head capsule; tusk densely covered with long setae, except at apex. Body of mandible: molae strongly protruded medially, canines present but small, margin between them sharp-edged (acutely protruding in right mandible); with basal U-row of long filtering setae in both mandibles. Thorax. Pronotum with anterior ring (collar) subequal in length to posterior ring (length taken at the medio-longitudinal line), anterolateral corners projecting, spine-like, posterior ring with dense patches of short setae medially (Figs 4F, 9B). Legs (Fig. 10A–D). Leg I (Fig. 10A): femora robust, relatively slender,

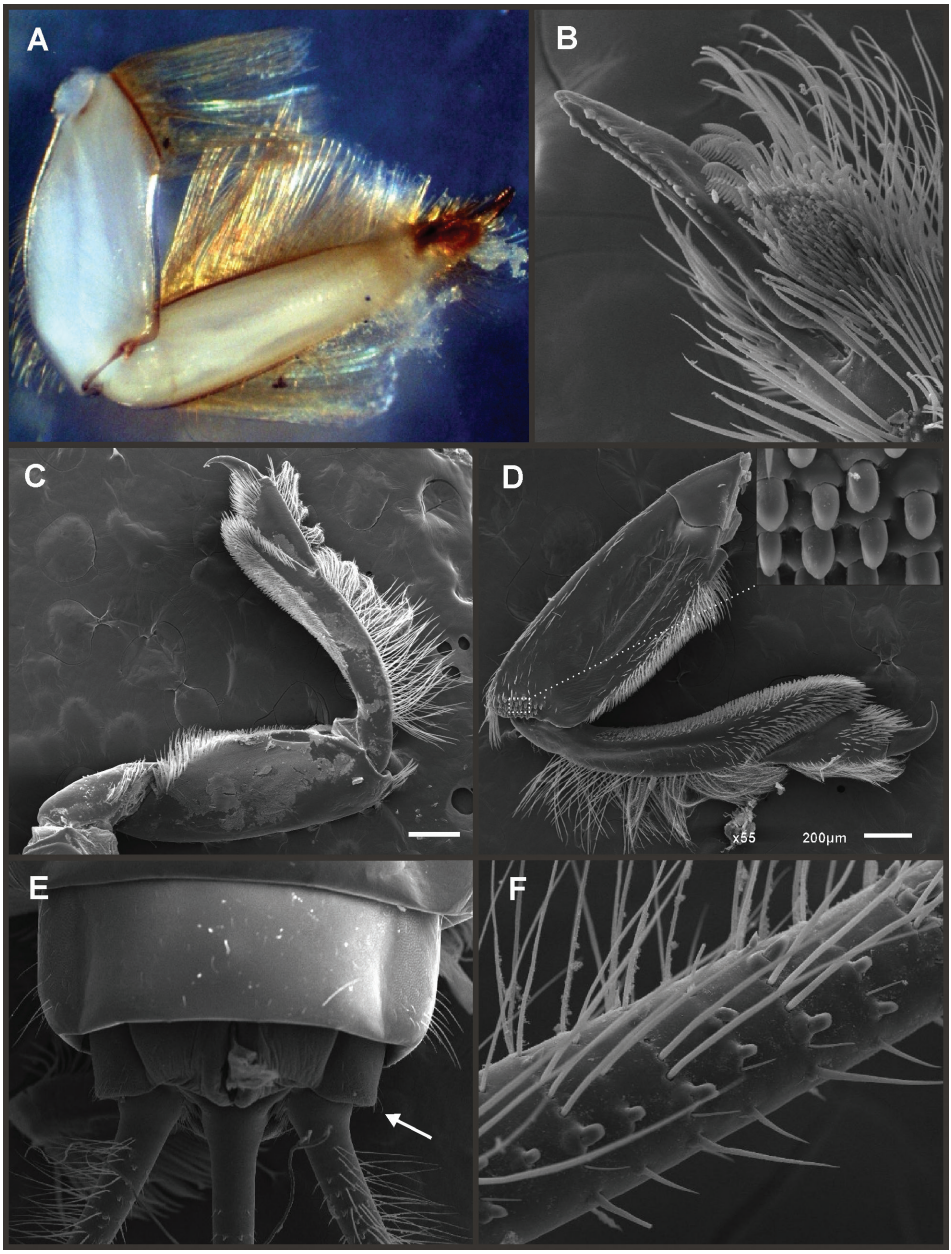

Figure 10. *Asthenopodes* nymph. *A. chumuco*: **A** foreleg, v.v. **B** detail of foretarsal claw **C** middle leg, d.v. **D** hind leg, d.v. with detail of femoral apex **E** abdominal sterna IX–X (arrow indicate absence of spine on paraproct) **F** detail of cercus. All figs from SEM except A from stereomicroscope.

with a U-shaped ventro-basal row of long filtering setae, distal points of the U almost touching each other; tibio-tarsus (fused) with 2 U-rows of filtering setae: 1 on anterior face (each branch well separated in the base) and 1 on inner margin, with the branches

near each other, apex of tibio-tarsus relatively pointed; tarsal claw with 2 rows of marginal denticles (Fig. 10B). Leg II (Fig. 10C): smaller, with thinner femora, with scattered long setae basally and a row of long and short setae along outer margin; tibia and tarsi with row of long setae on outer (dorsal) margin, ventrally with many stout spines on apical half, anterior face of tibia with a distal row of thick setae (at base of tarsus) and with a crown of thick setae at apex; tarsal claw weaker, without denticles. Leg III (Fig. 10D): intermediate in size, outer margin of femur with row of short setae, longer at apex, distal corner of femur densely covered with thick, blunt setae; inner margin of femur, tibia and tarsus densely covered with short setae; margin between tibia and tarsus with row of thick setae; outer margin of tibia and tarsus with row of long pectinated setae. Coxae I and II directed ventrally, coxa III directed postero-laterally. Abdomen. Sternite I longer than the others and partially fused with metasternum. Gill I reduced in size, whitish, single and lanceolate. Gills II–VII well developed, ventral portion smaller than dorsal portion. Tergum X without posterolateral spine (Fig. 10E). Cerci slightly shorter than terminal filament, with long setae at joinings, basal 1/4 with thick blunt setae ventraly (Fig. 10F).

Distribution. Amazonas and Parana subregions (Argentina, Brazil, Colombia, Guyana, Uruguay).

Discussion. *Asthenopodes* and *Asthenopus* have been treated as synonyms (Hubbard and Domínguez 1988) after the discovery of *Priasthenopus gilliesi* (Domínguez, 1988), that somewhat blurred the distinction between both genera. Additionally, Hubbard and Domínguez (1988) based their synonymic proposal in the fact that all known nymphs of Asthenopodinae from South America where indistinguishable and could be classified in a single genus. As the knowledge of this group had largely improved in last years we are proposing here a new rearrengement of supraspecific taxa.

The characteristics traditionally associated with *Asthenopodes* (summarized in Domínguez 1988) are: 1) ratio foreleg/forewing of male: 7/8; 2) male foretarsus 3.5 times longer than foretibia; 3) foretarsal segment 2 very long (almost as long as tarsal segments 3 and 4 combined, and 1.5 times the length of tibia); 4) Rs fork base to margin: 2.5/10; 5) cubital intercalaries parallel, ICu_2 arising basally from ICu_1, or basally free but connected to ICu_1 and CuP by cross veins, 6) ICu_2 ending at hind margin, 7) long marginal intercalary veins present; 8) forceps ratio width/length: 1/10; 9) penes thin from the base; 10) MA fork base to margin 7/100; 11) IMP–MP_1 fused; 12) MP_2-IMP similar in length, fused; 13) foretarsal claws of male greatly expanded apically. The discovery of *P. gilliesi* (Domínguez) put in doubt the value of characters 5, 7, 8, 9 and 10, for generic diagnoses, because this species showed some intermediary states between *Asthenopodes* and *Asthenopus* (Domínguez 1988, Hubbard and Domínguez 1988). In our phylogenetic analysis the intermediate position of *P. gilliesi* is mantained, but it is clearly located outside both genera.

The revalidation of the genus *Asthenopodes* Ulmer is based not only in the clade that its type species (*Asthenopodes picteti*) forms with other two new species, but also on the fact that the nymph shows characters considered important at the generic level in the family, mainly the shape of nymphal mandibular tusks, legs and gill I.

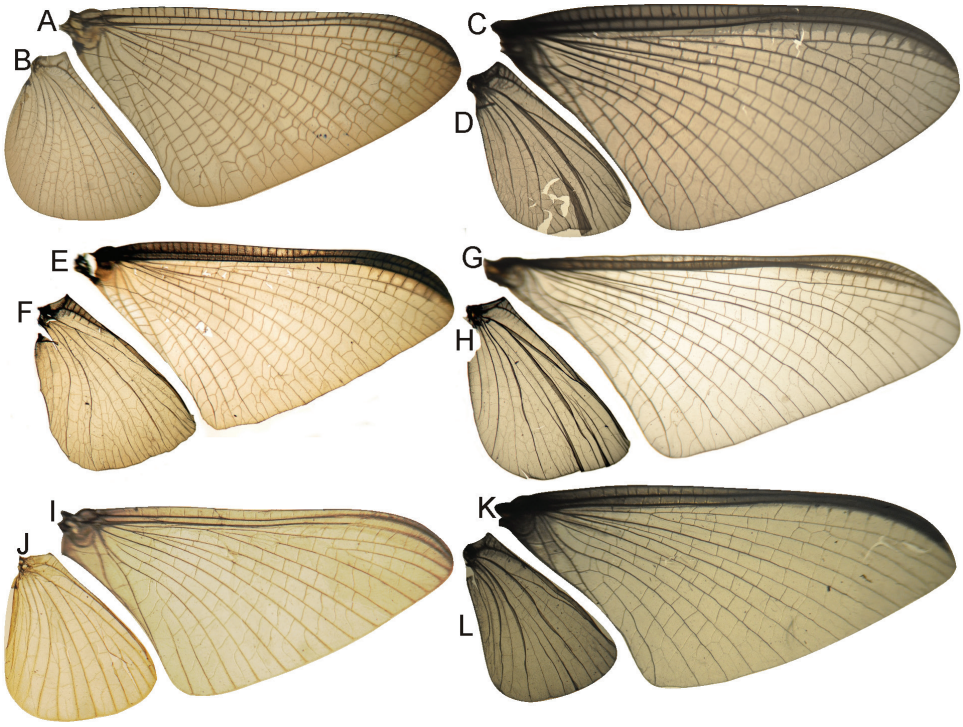

Figure 11. *Asthenopodes* wings, steromicroscope photographs. Males to the left, females to the right: **A–D** *A. picteti* **E–H** *A. traverae* **I–L** *A. chumuco*. Not to scale.

Key to the species of *Asthenopodes*

Male imagos

1 Large species (FW > 14 mm); wings smoky yellowish (Fig. 11E–F); penes markedly twisted and curved inwards (Fig. 12C–D)..... ***A. traverae* sp. n.**

– Smaller species (FW < 12 mm); wings hyaline, yellowish areas sometimes present along hind margin; penes much less curved and not twisted (Figs 12A–B, E–F) **2**

2 FW 11.4–11.9 mm; genitalia as in Fig. 12A–B..... ***A. picteti* Hubbard**

– Smaller species, FW 7.0–8.8 mm; genitalia as in Fig. 12E–F.... ***A. chumuco* sp. n.**

Female and eggs

1 FW with single imv in most spaces (Figs 11G,K); body blackish brown; eggs with small polar caps, ratio maximum width of egg/maximum width of PC = 2.3–3.1 (Figs 13B–C) **2**

– FW with double or triple imv (Fig. 11C); body yellowish light brown; polar caps wider, ratio maximum width of egg/maximum width of PC = 1.2–1.5 (Fig. 13A) ..... ***Asthenopodes picteti***

2 Wings (Fig. 11G–H) translucent yellowish (transmitted light), large size (FW 15.5–22.5 mm); polar cap of eggs formed by 5–6 long coiled threads (Fig. 13B) ..... ***A. traverae***

– Wings hyaline (Fig. 11K–L), smaller size (FW 12.2–14.8 mm); polar cap of eggs formed by 14–16 long coiled threads (Fig. 13C) ..... ***A. chumuco***

***Asthenopodes picteti* Hubbard, stat. n.**
Figs 11A–D, 12A–B, 13A, 20A

Palingenia albicans Pictet 1843: 149 (misidentification)
Campsurus albicans, Eaton 1871: 58.
Asthenopus albicans, Ulmer 1920c: 107, Ulmer 1921: 239, Lestage 1924c: 39.
Asthenopodes albicans, Ulmer 1924: 26, Traver 1956: 2.
Asthenopodes picteti, Hubbard 1975: 111, Domínguez 1988a: 24.
Asthenopus picteti, Hubbard and Domínguez 1988: 207, Domínguez et al. 2006: 562.

Type material. Type material was not studied; it consists of the holotype male imago, damaged, with many parts missing including the genitalia. It is a pinned specimen deposited at Naturistorisches Museum Wien, Hubbard and Domínguez (1988) presented a figure of the holotype forewing.

Additional material. 3 male subimagos from ARGENTINA, Misiones, Parque Provincial Urugua-í, Arroyo Yacutinga, S 25°44'51" – W 54°03'37", 355 m, 30.xi.2001, Domínguez et al. cols.; 8 female and 2 male imagos same data except Arroyo Uruzú, S 25°51'29" – W 54°10'10", 322 m, 25.xi–2.xii.2001; 1 female and 1 male imagos (slides IBN3–93 and 3–96) from URUGUAY, Maldonado, Arroyo de la Quinta, 4.i.1984, M. T. Gillies col. All the material deposited in IBN.

Diagnosis. *Asthenopodes picteti*, type species of the genus *Asthenopodes* (Ulmer 1924, Traver 1956, Hubbard 1975) presents 7 autapomorphies (Appendix 2) including: thinner male foretibia and slender penes. This species can be distinguished from the other species of the genus by the following combination of characters: 1) general coloration yellowish white (male), darker in female (yellowish light brown); 2) male FW 11.4–11.9 mm, female FW 14.5–19.0 mm, membrane whitish hyaline tinged with yellowish near hind margin; 3) foreleg length 0.9 times the length of FW; 4) pronotum width/length ratio: 1.6–1.9 (male), 1.5–2.3 (female); 5) 14–17 marginal intercalary veins present on the entire margin of FW (Fig. 11A) and HW (Fig. 11B), miv generally longer than distance between longitudinal veins; 6) male FW with 4 to 6 cross veins between Rs and MA basal to Rs fork; 7) ratio total length/basal width of forceps 6.7 (Fig. 12A); 8) penes long and slender (Fig. 12A–B), male median remnant of styliger plate posterolaterally expanded forming a pair of rounded projections ("Ll"

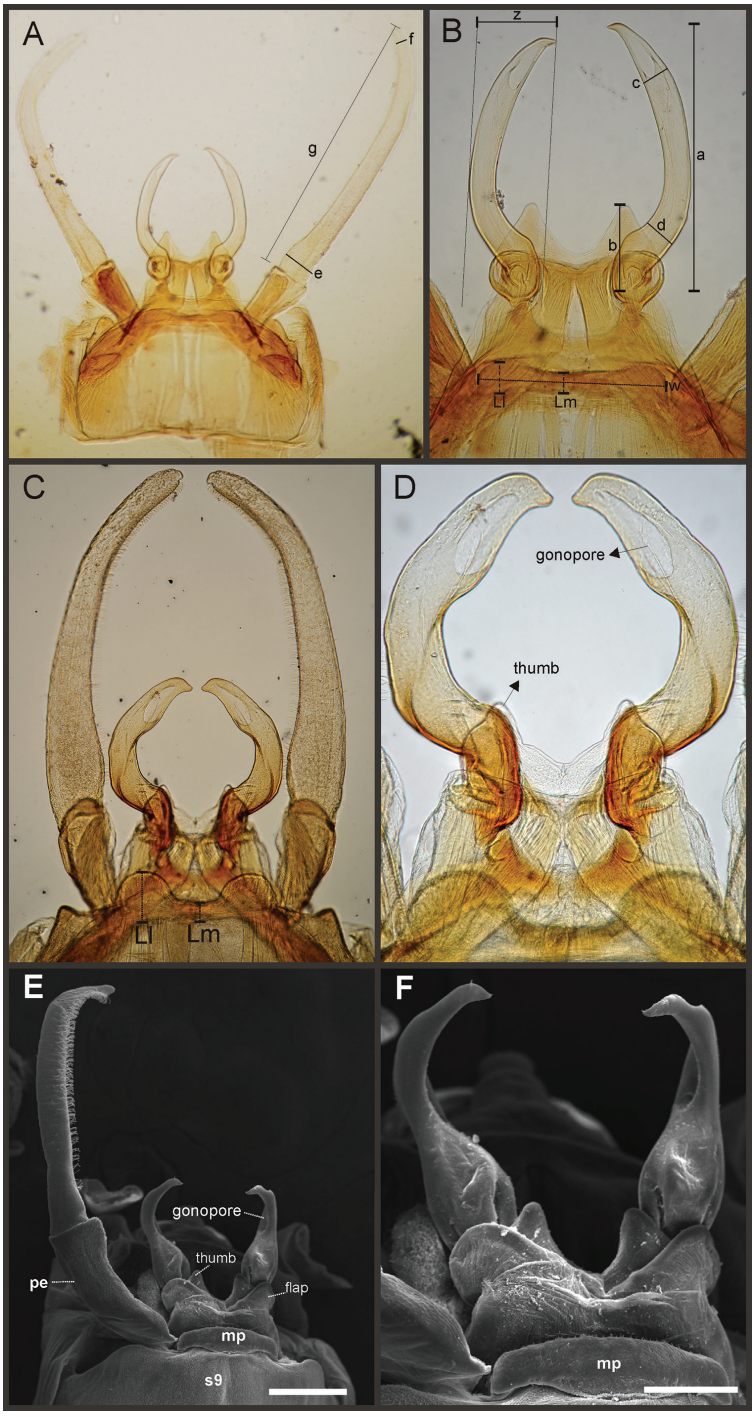

Figure 12. *Asthenopodes*, male genitalia: general view to the left, detail of penes to the right. **A–B** *A. picteti* **C–D** *A. traverae* **E–F** *A. chumuco*. Scale bar = 200 μ in **E** 100 μ in **F**. Abbreviations: mp = median plate of stryliger; pe = pedestal; s9 = ninth sternum; see Appendix 2 for explanation of measures (letters a to g, and z).

in Fig. 12B); 9) female sternum VIII, anteromedian sockets present but concolorous with sternum, not evident; 10) egg polar caps only slightly thinner than maximum width of the egg, formed by 6 filaments; medium-sized and small chorionic disks-like structures present (Fig. 13A).

Male imago. Length (mm): body, 9.3–11.2; FW, 11.4–11.9; HW, 5.8–6.2; foreleg, 10.0–10.3; cerci, 30.1. Described in Traver (1956) and Domínguez (1988a). Additions to these descriptions follow: Prothorax width/length: 1.6–1.9. Wings. Hind margin of FW (Fig. 11A) with 14–17 marginal intercalary veins, relatively long; 4–6 cross veins between R and M, basal to R stem; IMP basally free or fused to MP_1 by a cross veins, MP_2 fused to IMP. HW as in Fig. 11B. Genitalia (Fig. 12A–B): forceps length/width ratio: 6.7; median remnant of styliger plate with posterolateral corners roundly projecting.

Female adult. Length (mm): body, 11.5–12.6; FW, 14.5–19.0; HW, 6.3–9.4. General coloration yellowish light brown. Head dorsally blackish except on median zone, paler; venter of head yellowish white. Antennae light brown, shaded gray on scape. Thorax yellowish brown with blackish membranes, shaded with brownish gray on pronotum and with black on posteromedian marks on meso- and metanotum. Pronotum width/length: 1.5–2.3. Legs whitish yellow shaded brownish on dorsum of leg I and on apex of femur III. Wings (Fig. 11C–D), membrane tinged with light brown, veins yellowish brown. Abdomen. Terga brownish with a pale mediolongitudinal line and paler areas on lateral margins on terga I–VII; sterna whitish yellow; female sternum VIII with anteromedian sockets, small and almost not distinguishable. Terminal filament whitish, shorter than tergum VIII; cerci yellowish brown paler apically, 0.5–0.6 times the length of the abdomen (0.2 the length of FW).

Eggs (Fig. 13A). Length, 325–355 μ; width, 215–235 μ. Two large and flat polar caps (maximum width, 155–180 μ), formed by 6 very long coiled threads. Chorionic surface with a fine granulated aspect, with small disk like structures.

Distribution. Uruguay, Argentina. *A. picteti* is here newly recorded from Argentina. The record from Guyana given by Domínguez et al. (2006, p.562) is no longer valid since this material is now considered a different species (*A. chumuco* see below).

Discussion. *Asthenopodes picteti* Hubbard was only partially known from the damaged holotype male from Brazil until Traver (1956) redescribed it (at that time as *Asthenopodes albicans*) based on a complete male from Uruguay. Later Hubbard (1975) gave a new name to this species (*A. picteti*). Domínguez (1988) and Hubbard and Domínguez (1988) presented additional discussion and illustrations of the male imago, from type and non-type material (also collected in Uruguay). The description of Traver (1956) coincides with the new material studied, except for the relation of the male foretibia and forefemur. Traver reported that tibia is 1.33 times the length of femur but we found that it is 1.7 times that length.

Domínguez (1988) reported 2 female imagos collected at the same time than the males he redescribed, but did not presented a formal description of them. Both females and additional ones from Argentina (see list of material) are here shortly described and figured. It is difficult from the material available to determine if the

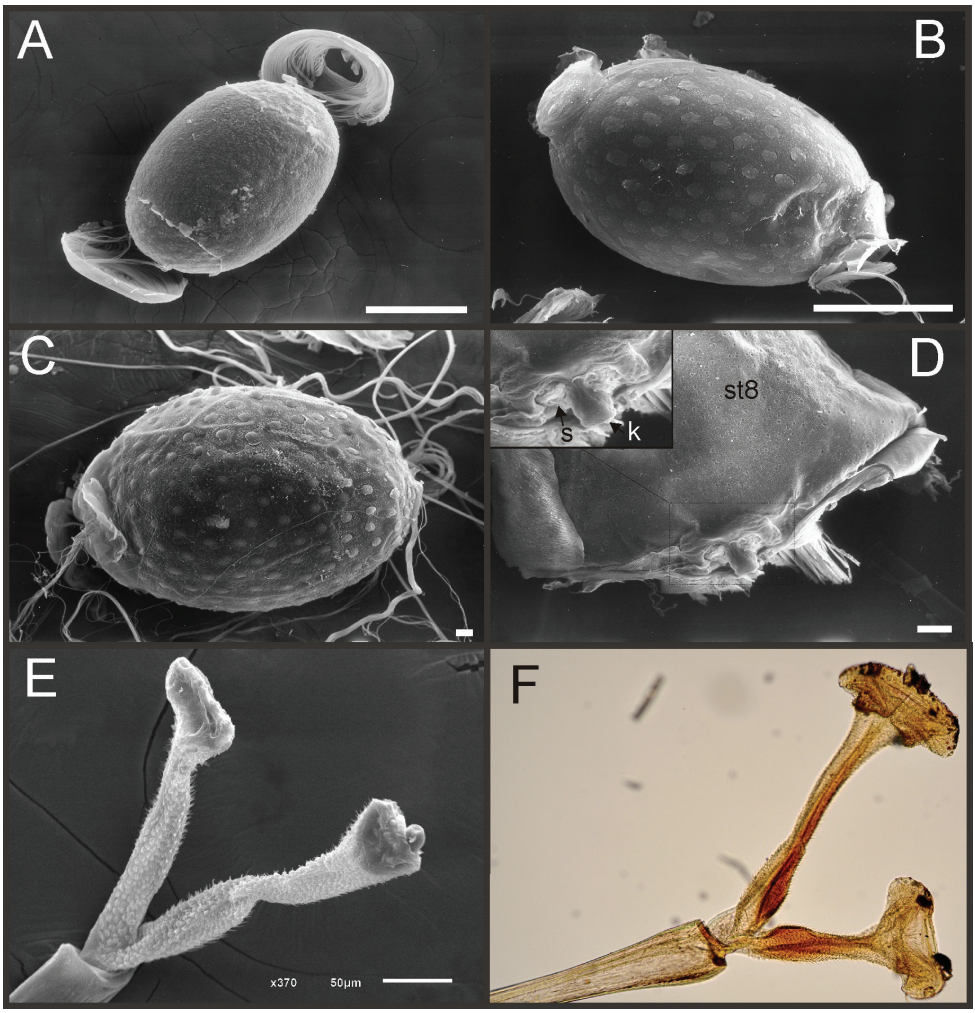

Figure 13. *Asthenopodes*, egg and adults. Eggs: **A** *A. picteti* **B** *A. traverae* **C** *A. chumuco*. Female imago: **D** *A. traverae*, abdominal sternum VIII, and detail of keel (k) and sockets (s). Male imago foretarsal claw: **E** *A. chumuco* **F** *A. traverae*.

females are in subimaginal or imaginal stage, so they are here referred as "adults". The females are similar to the sympatric *A. traverae* but can be separated from this species because *A. picteti* females are lighter in color, hind femora only shaded black on apex, paired female sockets present but small and hard to distinguish, cerci light colored, abdominal gill sclerites smaller, FW wider with shorter marginal intercalaries joined to main veins and partially anastomosed. The eggs present wider polar caps, only slightly thinner than the egg. Males can be separated from those of *A. traverae* because the hind femora are only shaded black on apex and the penes are much slender.

***Asthenopodes traverae* sp. n.**
http://zoobank.org/D3A80802-232F-4930-99FC-D7C0EDC862D1
Figs 11E–H, 12C–D, 13B, D, F, 20C

Asthenopodes sp. "females from Uruguay", Traver 1956: 5.

Material. Holotype (IBN) male and paratypes (IBN) 4 males and 22 females (slides IBN468–469CM) from ARGENTINA, Misiones, Parque Provincial Urugua-í, Arroyo Uruzú, 7–11.xii.1999, C. Molineri col.; 1 female imago ("*Asthenopodes* sp." Traver det.) from URUGUAY, Artigas (Uruguay 19), 9.i.1952; and 27 female adults from URUGUAY, Artigas, Sepulturas (D-3), 18.xii.1952, Carbonell col. Paratypes from Uruguay deposited in FCE-Ep.

Non-type material: 1 female (wings on slide) from BRAZIL, Sao Paulo, Jacareí, rio Paraiba do Sul, 21.xi.1987, CG Froehlich et al. cols (deposited at MZSP).

Diagnosis. Four autapomorphies characterize this species, all are small changes in continuous characters, except the marked shortening of the median remnant of styliger plate (at the middle, since laterally a tong-like projection is present, Fig. 12C). *Asthenopodes traverae* sp. n. is known in the alate and egg stages, all females are subimagos even those that apparently have laid the eggs (empty females). This species can be distinguished from the other species of the genus by the following combination of characters: 1) males yellowish white, females blackish; 2) FW length male 14.0–14.5 mm, female 15.5–22.5 mm, membrane yellowish hyaline; 3) male foreleg length 0.9–1.0 times the length of FW; 4) pronotum width/length ratio: 1.3–1.9 (male), 2.0 (female); 5) 16–22 marginal intercalary veins present on the entire margin of FW (also present in HW) generally longer than distance between longitudinal veins, fused to main veins, poorly anastomosed (Fig. 11E–H); 6) male FW with 4 to 5 cross veins between Rs and MA basal to Rs fork; 7) ratio total length/basal width of forceps 4.7–4.9 (Fig. 12C–D); 8) median remnant of styliger plate posterolaterally expanded forming a pair of rounded projections, penes large and robust, sclerotized, curved and twisted (Fig. 12C–D); 9) female sternum VIII with anteromedian sockets well developed, whitish surrounded by a large brownish area (Fig. 13D); 10) egg caps small, much thinner than maximum width of the egg, formed by 5–6 filaments; medium-sized and small chorionic plates present (Fig. 13B).

Male imago. Length (mm): body, 12.2–13.5; FW, 14.0–14.5; HW, 6.8–7.3; foreleg, 12.3–14.0; cerci, 35.5–38.5. General coloration yellowish white. Head shaded black dorsally almost entirely, with a pair of distinct submedian black marks anteriorly to median ocellus; occipital hind margin with pale median zone; head ventrally pale without markings. Antennae: scape and pedicel short, yellowish on venter of pedicel, both slightly shaded with gray; flagellum very thin, hyaline, similar in length to forefemur. Thorax. Pronotum translucent, shaded slightly with gray except on membranes separating anterior and posterior rings, darker laterally; pronotum width/length: 1.3–1.9. Meso- and metanotum yellowish white with gray markings mainly posteriorly but also on sutures. Thoracic pleurae and sterna yellowish white shaded gray only at base of coxae and wings. Legs. Forelegs: coxa dorsally whitish with a gray mark, ventrally

yellowish; femur dorsally yellowish shaded gray on apical third, ventrally whitish; tibia whitish translucent shaded gray mainly on dorsum; tarsi translucent shaded slightly with gray; large claws, stalk with brown inner margin, rest whitish; articulations between femur-tibia and tibia-tarsus very sclerotized, brownish. Middle and hind legs yellowish, shaded with gray from half of femur to apex of leg. Wings (Fig. 11E–H). Membrane hyaline slightly tinged with gray on costal and subcostal sectors (membrane yellowish under transmitted light); all veins light gray, lighter toward hind margin; 5 cross veins between R stem and M sector; long marginal intercalaries on hind margin of both wings. Abdomen yellowish white widely shaded with gray, some darker marks as follows: submedian short anterior dashes and sublateral oblique stripes on terga III–VIII, lateral margins of terga VIII–IX, and median line of IX–X (thinner on X). Abdominal sterna whitish except gill sclerites yellowish white. Genitalia (Fig. 12C–D): lateral margins of sternum IX and pedestals yellowish; median remnant of styliger plate whitish with a gray strip on hind margin between the tongue-like projections ("Ll"Fig. in Fig. 12D); pedestals well separated from each other, relatively long and becoming wider distally; forceps whitish, long and wide; base of penes well developed, subquadrate, whitish; penes strongly sclerotized, orangeish basally but yellowish distally. Cerci whitish, terminal filament reduced to 7–8 thin annuli, straight, whitish.

Female subimago. Length (mm): body, 9.5–19.0; forewing, 15.5–22.5; hind wing, 7.5–11.5; cerci 3.5–4.0. General coloration dark brown shaded widely with black. Head black dorsally, yellowish white ventrally except on remnants of tusks, brownish. Antennae dark brownish except apical half of flagellum whitish. Thorax. Sclerites dark brown, membranes shaded black. Pronotum width/length: 2. Legs brownish except membranous portions, whitish. Wings (Fig. 11G–H) with yellowish brown membranes and veins, veins C and Sc darker. Abdomen. Terga dark brown completely shaded black; sterna paler, brownish laterally, yellowish medially, with two or more pairs of small pale dots; sternum VIII with two small anteromedian sockets (Fig. 13D). Caudal filaments brownish, terminal filament shorter than tergum VIII, cerci 0.3–0.4 times the length of the abdomen (0.2 the length of FW).

Eggs (Fig. 13B). Length, 305–355 μ; width, 195–225 μ. Two small polar caps (maximum width, 70–82.5 μ) formed by 5–6 long coiled threads. Chorionic surface smooth with regularly spaced chorionic plates. Chorionic plates ("disk-like" structures) relatively small and rounded, with irregular margins. Smaller plates, irregular in form scattered between the larger ones.

Etymology. The species is dedicated to the great mayfly specialist Jay R Traver, who visited Uruguay and worked with Mr. C. S. Carbonell's collections at the "Museo de la República" recognizing the females of this species as distinct from *A. picteti* (also unknown at that time).

Distribution. Parana biogeographic subregion in Argentina, Uruguay and Brazil.

Biological remarks. Females subimagos were collected (in Misiones Province) while swarming in compact groups at about 3 m above water in pool areas around sunset. The same behavior was reported by Traver (1956) for the Uruguayan females. Males were caught at light traps during the first hours of dark, so the male flight is unknown.

Discussion. Traver (1956) described females of *A. traverae* as distinct from *A. picteti* in spite of the fact that the female of that species was also unknown at that time. Nevertheless Traver realized that they differ from *A. picteti* males in color and size, and left them unnamed. With the collection of new material from both species (and sexes) in Misiones (Argentina), it became evident that they constitute a new species. *Asthenopodes traverae* females can be distinguished from *A. picteti* females by their black general coloration, somewhat slender forewings, femora and cerci widely shaded with black, and enlarged abdominal gill sclerites (remnants of nymphal gill muscles insertions), for other differences see discussion under *A. picteti*. Very similar in aspect but much smaller are the females of *A. chumuco*, the allopatric sister species of *A. traverae*.

***Asthenopodes chumuco* sp. n.**
http://zoobank.org/DEC97104-1A64-4492-B34A-719E784CE531
Figs 4B, F, 9, 10, 11I–L, 12E–F, 13C, E, 20B

Asthenopodes sp? Traver 1950: 611.
Asthenopus picteti Domínguez et al. 2006: 562.

Type material. Holotype and 3 paratypes male imagos from Brazil, Amazonas, Barcelos, rio Demene, ´boca´barco, S 0°25'28.7" - W 62°54'20", 8–9.viii.2009, Pennsylvania. Holotype and 1 paratype in INPA, 2 paratypes in IBN.

Additional material. 3 male slides (CUIC) from British Guiana, Bartica District, Kartabo, 20.iv.1919, C.U. Expedition col. Five female imagos (1 in CZNC, 2 in IBN, IBN533CM, 2 in MUSENUV) from Colombia, Amazonas, Puerto Nariño, Loreto Yacu, S 3°44'26" – W 70°27'19", 5.ii.1999, luz 18–20 h, M. C. Zúñiga, E. Domínguez and C. Molineri cols.

Diagnosis. *Asthenopodes chumuco* known from all the stages presents seven autapomorphies, all of them are changes in continuous characters (Appendix 2). This species can be distinguished from the other species of the genus by the following combination of characters: 1) general coloration yellowish white in male, dark brown in female; 2) male FW 7.0–9.0 mm, female FW 12.2–14.8 mm; 3) male, ratio FW/foreleg length 1.4–1.6; 4) pronotum width/length male 1.3–1.4, female 2.0–2.1; 5) 7–14 marginal intercalary veins present on the entire margin of FW (Fig. 11I, K), HW (Fig. 11J, L) with 3–7 marginal intercalary veins, generally longer than distance between longitudinal veins, fused to main veins, poorly to heavily anastomosed; 6) male FW (Fig. 11I) with 3–4 cross veins between Rs and MA basal to Rs fork; 7) ratio total length/basal width of forceps 7.8–9.5 (twisted CUIC slide 6.3–6.7) (Fig. 12E); 8) male median remnant of styliger plate subrectangular, slightly convex (not expanded forming a pair of rounded lateral projections), penes long and slender, acute distally (Fig. 12E–F), rectangular pedestals strongly enlarged, ½ the length of forceps; 9) female sternum VIII, with small reduced anteromedian female sockets at the base of a median keel;

10) egg caps small, much thinner than maximum width of the egg, formed by 14–16 filaments; large and small chorionic plates present (Fig. 13C).

Male imago. Length (mm): body, 7.3–8.0; forewing, 7.0–8.8; hind wing, 3.7–4.3; foreleg, 5.0–5.8; cerci, 20.0–23.0. General coloration yellowish white. Head shaded gray dorsally almost entirely, frons with black dot at base of antenna, with medial line and irregular black marks; occipital region with pale median zone; head ventrally pale without markings. Antennae: scape and pedicel short, subequal in length, whitish shaded with purplish; flagellum very thin, hyaline. Thorax. Pronotum whitish with anterior and posterior portion subequal in size, shaded gray in a transverse band between both portions, posterior portion black along hind and lateral margins; pronotum width/length: 1.2–1.3. Mesonotum yellowish white shaded with gray on posterior half of medial line, on area between posterolateral protuberances and on anterior margin of these structures. Metanotum yellowish slighlty shaded with gray medially. Thoracic pleurae and sterna yellowish white shaded gray dorsally and anteriorly to mid coxa. Legs. Forelegs: whitish completely shaded with gray; large claws, apically expanded (Fig. 13E). Middle and hind legs yellowish white, shaded with gray on coxae. Wings (Fig. 11I–J). Membrane hyaline shaded with gray on basal 1/3 of costal and subcostal sectors; all veins translucent, except costal cross veins grayish; 3–4 cross veins between R stem and M sector; long marginal intercalaries on hind margin of both wings. Abdomen whitish shaded with gray on terga, mainly on lateral margin, submedian black dot on terga III–VIII. Abdominal sterna pale. Genitalia (Fig. 12E–F): yellowish white, except for penis apically yellowish; pedestals well separated from each other, very long, ½ length of forceps; median remnant of styliger plate with slightly convex hind margin; base of penis rounded, projecting posterolaterally, lobe of penis long and sclerotized, curved ventromedially, constricted on median length, gonopore well developed. Cerci whitish; terminal filament reduced to 5–7 thin annuli, straight, whitish.

Note: Cornell male (slides, male imago). Length (mm): body missing; FW, 9.0; HW, 4.5. FW with 11 long marginal intercalary veins; 3 cross veins between R and M basad to R stem; IMP fused basally to MP_1 or free; MP_2 fused to IMP. HW with 6 long intercalary veins on hind margin. Genitalia: penes robust, twisted; median remnant of styliger plate without posterolateral projections; forceps long and slender, ratio length/basal width: 6.3–6.7.

Female imago. Length: body, 7.2 (shrunken, empty)–12.3; FW, 12.2–14.8; HW, 5.3–6.0; cerci, 1.2–1.3. General coloration dark brown. Head dorsally black except on clypeus, whitish with a pair of lateral brownish bands, ventraly much paler brownish white. Thorax brownish with blackish membranes and carinae. Pronotum with a pair of distinct black marks submedially; width/length ratio: 2. Legs pale, brownish white. Wings (Fig. 11K–L) with hyaline membrane, slightly whitish translucent; veins whitish tinged with brownish basally; 2 to 4 crossveins between M and R, basally to R stem; MP_2 joined basally to IMP; marginal intercalaries relatively numerous and long, anastomosed. Abdomen. Terga brownish slightly paler on median band and pleural folds,

sterna much paler brownish white. Cerci basally brownish turning whitish distally; very reduced in size, less than 0.1 the length of FW.

Eggs. Length 210–240 μ, width 180–200 μ. Subovate, yellowish, with two small whitish polar caps (maximum width, 75–85 μ), polar caps much thinner than the egg and formed by 14–16 threads. Under SEM the larger disk-like chorionic structures are surrounded by many smaller ones, which at their time are surrounded by smooth chorion (Fig. 13C).

Nymphs. Length (mm): body, 7.8; cerci, 2.0–2.3; terminal filament, 3.1. General coloration yellowish light gray (Fig. 4B, F). Head with a black band between lateral ocelli and fine netting pattern on occiput (Fig. 4F). Antennae: scape bare, slightly longer than pedicel, pedicel with many dorsal setae, flagellum bare with numerous annuli increasing in length distally. Thorax. Pronotum shaded black on sublateral area of anterior ring and laterally on posterior ring. Meso- and metanotum shaded widely with gray, with dark gray wingbuds, developing veins paler. Legs (Fig. 10A–D). Coxae and trochanters of mid and hind legs slightly shaded with gray, remainder of legs yellowish-white; foretarsal claw with double parallel rows of 15 and 12 denticles each (Fig. 10B). Abdomen. Terga more or less uniformly shaded brownish-gray, except on pale transverse dashes laterally, thin medial line on tergum I–IX becoming wider posteriorly and pale with subcircular submedian sigilla; sterna yellowish. Gill I whitish, gills II–VII purplish gray, ventral portion paler than dorsal portion. Caudal filaments yellowish.

Etymology. "Chumuco" is one of the common names applied to river cormorans in some South American countries. The penis lobe of this new species resembles the neck and head of that bird.

Distribution. Brazil (Amazonas, Espírito Santo), Colombia (Amazonas), Guyana.

Discussion. The male imago of this species has been known since Traver (1950) found a group of slides containing some body parts of a missing specimen. She stated that it was surely not the type species of *Asthenopodes* mainly because its smaller size. Domínguez et al. 2006 (p. 562) treated this specimen in *Asthenopus picteti*, extending the distribution of this last species to British Guiana. With the discovery of new specimens (male and female adults) we gathered more morphological information and realized that a new species must be described. One of the results is that *A. picteti* is no longer considered to be in British Guiana. The Colombian females described here as *Asthenopodes chumuco* are associated with the males, because of the egg morphology, compared with those extracted from a pharate female from São Mateus. Adults show the smallest size of the genus, further differing from the other two species in many morphological aspects. The females are similar to *A. picteti* in coloration of hind femur and abdomen but wing venation and sockets on sternum VIII are different, also the female cerci of *A. chumuco* are much less developed. The eggs are similar to those of *A. traverae*, because of the small polar caps, nevertheless *A. chumuco* presents much more threads forming each cap (between 14 and 16, but each thread is relatively very thin).

***Asthenopus* Eaton**
Figs 4C–D, 14–18, 20F–J

Asthenopus Eaton 1871: 59; Lestage 1922: 142; Traver 1950: 605; Traver 1956b: 7; Hubbard and Domínguez 1988: 209; Domínguez 1988a: 24.

Type-species. *Palingenia curta* Hagen, original designation.

Species included. *A. curtus*, *A. angelae*, *A. magnus* sp. n., *A. hubbardi* sp. n., *A. guarani* sp. n.

Diagnosis. Five autapomorphies were recovered for *Asthenopus*: 1) character 1 (ratio length second foretarsal segment/foretibia) decreases from 0.645–0.652 to 0.584–0.587; 2) char. 7 (marginal connectivity = n°of connections among imv/n°of imv) decreases from 0.700–1.167 to 0.222–0.300; 3) male foretarsal segment 1 subrectangular; 4) penes with an apical spine; and 5) long and open cleft present between penial lobe and thumb. The following combination of characters is useful to distinguish *Asthenopus* from other genera in Polymitarcyidae: 1) ratio length male FW/foreleg = 1.4–1.8; 2) tarsal segment 1 distinct and subrectangular in form (not fused to tibia), ratio subapical width of foretibia/subbasal width of second tarsal segment 1.5–2.3 (Fig. 20F–J) ; 3) pronotum width/length ratio 1.7–2.4 (male, but frequently around 2.0), 2.0–3.0 (female); 4) in both sexes FW marginal intercalary veins short and not anastomosed (4–25 in number, Fig. 16); 5) in both sexes FW with 0–4 (most commonly 2, but variable depending on size of specimen) crossveins between R and M, basally to R fork; 6) FW vein IMP basally free, subequal in length to MP_2, forming a characteristic oblique "Y" with associated cross veins (arrow Fig. 16A, E); 7) median remnant of styliger plate present, pedestals well developed (Fig. 17); 8) forceps relatively stout, ratio length/basal-width = 4.7–7.0; 9) penes relatively short and stout, curved ventrally (and medially), with a thumb attached at the base, and with the apex of penial lobe distinctly shaped as a spine; 10) female abdominal sternum VIII with anteromedian paired sockets, much reduced in size, and with a keel as in Figs 18F–H; 11) eggs with relatively large polar caps formed by 3–8 (commonly 5) long coiled threads, chorion covered with disk-like structures (Fig. 18A–E); 12) head dorsally strongly convex on occiput, frons not projecting medially (Fig. 14I–J); 13) nymphs with very short and robust tusks (Fig. 14A–C, E–G), with large submedian inner tubercle, with 2 or 3-pointed apex (asymmetric); 14) nymphal foretarsal claw with a single row of denticles (Fig. 15G); 15) apex of femur 3 with a group of ca. 50 stout pointed spines (Fig. 15F).

Male imago. Length: body, 6.5–10.5; FW, 7.0–10.1; HW, 2.9–4.8; foreleg, 5.1–7.5; cerci, 22.0–37.0. Antennae: scape slightly longer than pedicel, flagellum bristle-like. Thorax. Pronotum width/length: 1.7–2.4. Legs. Forelegs subequal to shorter than body, ratio length FW/foreleg 1.4–1.8; longest segment is tibia (ratio length tarsal segment 2/tibia = 0.4–0.7); tarsal segment 1 distinct, not fused, very short (Fig. 20F–J); remaining tarsal segments relatively short subequal in length except tarsal segment 2 slightly longer; claws differing in length, one long the other short, very slightly widened distally. Wings (Fig. 16). FW with 4–25 marginal intercalaries, sometimes present

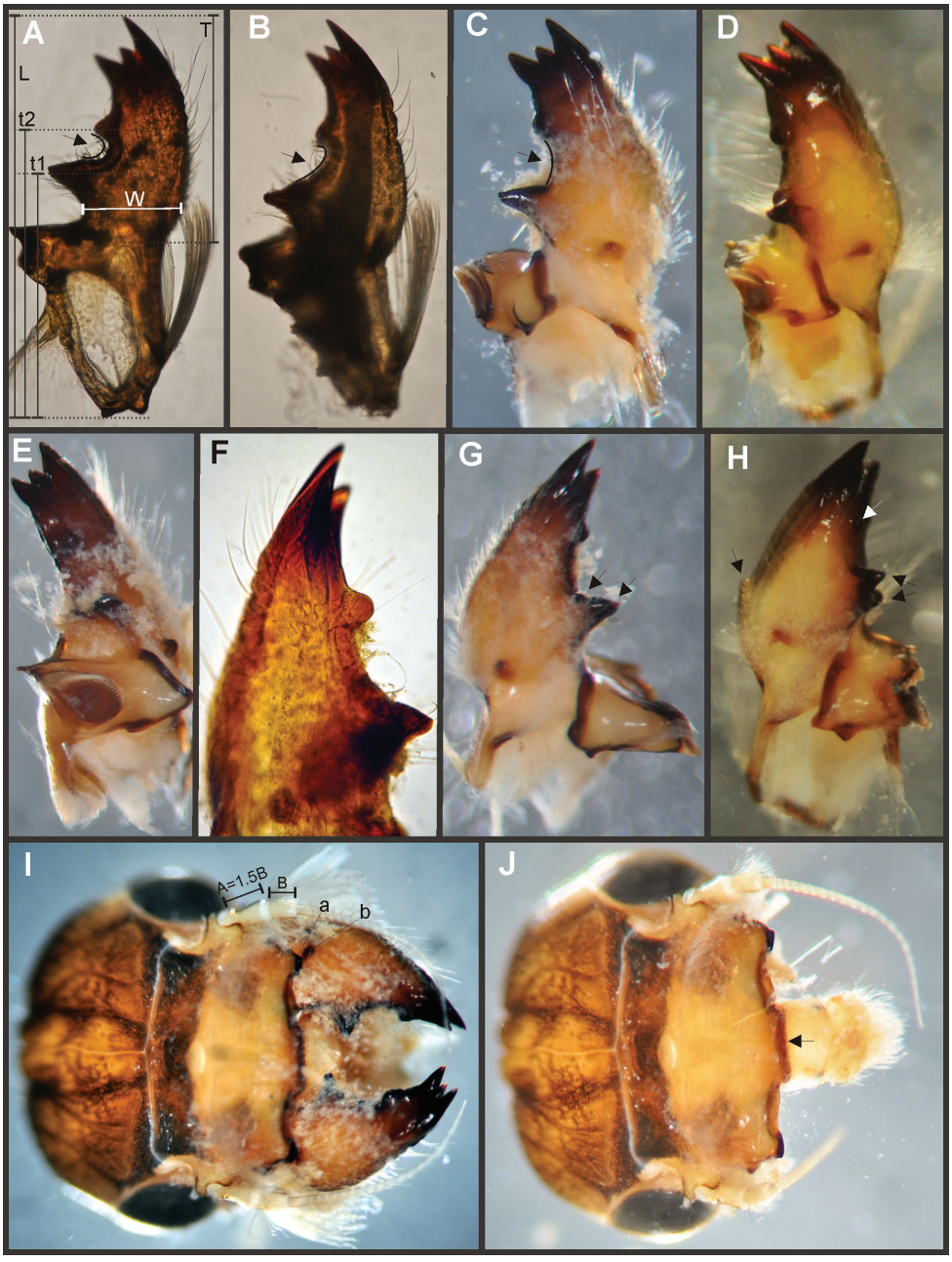

Figure 14. *Asthenopus* (and *Povilla*) nymphs, head and mandibles. **A–D** left mandibles, d.v.: **A** *A. curtus* **B** *A. angelae* **C** *A. magnus* **D** *Povilla adusta*. **E** left mandible dorso-oclusal view, *A. magnus*. Right mandibles, d.v.: **F** *A. angelae*, **G** *A. magnus* **H** *P. adusta*. **I–J**, *A. magnus* head capsule, d. v., with and without mandibles.

in HW but not in all spaces; intercalaries not strongly anastomosed; 0–4 cross veins between MA and R, basad to R stem; R stem length/Rs from fork to margin = 0.17–0.31. Ratio MA length from fork to margin/stem length = 7–15; IMP fused basally to MP_1 or free; MP_2 fused to IMP. Genitalia (Fig. 17): median remnant of styliger plate subrectangular to subovate; pedestals subrectangular to subovate, relatively small; forceps relatively wide to very wide, ratio length/basal width 4.7–7.0; penes tubular and robust, curved ventro-medially, and with well-developed basal thumb. Terminal filament reduced, cerci long (ratio length FW/cercus = 0.25–0.36).

Female adult. Length: body, 8.0–19.5; FW, 12.0–18.5; HW, 4.6–7.8; cerci, 3.0–7.0. Thorax. Pronotum width/length = 2–3. Wings with more crossveins and intercalaries than in male. Abdominal sternum VIII with anteromedian keel (Fig. 18F–H), at each side of keel´s base a very small "socket" is present ("s" in Fig. 18F). Terminal filament reduced, shorter than tergum VIII, with few thin annuli. Cercus short, 0.25–0.50 times length of FW.

Eggs (Fig. 18A–E). Length, 210–285 µ; width, 135–163 µ. Oval (ratio maximum length / maximum width = 1.4–1.8), with two relatively large polar caps (ratio maximum with of egg/maximum width of uncoiled polar cap = 1.1–1.5), formed by 3–8 very long coiled threads. Chorionic surface with large subcircular chorionic plates, sometimes each plate is divided in 2–3 portions.

Nymphs. Length (mm): body, 9.7–15.0 mm; cerci, 4.0–7.0; terminal filament, 5.0–5.1. Head suboval in dorsal view, smooth (without pilose area); occipital region well developed, strongly convex (Figs 4C–D, 14I–J). Head capsule with a dorsal spine-like projection at bases of antennae. Antennae 1.1–1.5 times length of head (length of head taken from hind margin to the apex of clypeus); pedicel with tuft of setae on dorsum, flagellum with minute scattered setae; length (mm): scape (0.5), pedicel (0.28), flagellum (2.0). Frons with anterior margin more or less straight (arrow in Fig. 14J), with a small blunt lateral projection ("a" in Fig. 14I), without median projection. Clypeus and labrum small, membranous, with many setae on dorsum of labrum. Mandibular tusks robust, relatively stout, left tusk (Fig. 14A–C, E) with 3 apical teeth, increasing in size from the median (smallest), inner and outer; inner tooth slightly directed medially, others directed distally; right tusk (Fig. 14F–G) with 2 teeth, the inner shorter. Inner margin of both tusks with a rounded small tubercle near subapex and a larger and pointed subbasal tubercle (associated with a tuft of rigid setae), this large basal tubercle shows a small basal protuberance (giving the impression of a bifid tubercle but with one of the sides aborted); ventral surface and outer margin of tusks with small rounded protuberances on the extremely hard cuticle; dorsal surface of tusks with numerous setae and with a small basal tubercle; this small dorsal tubercle is easily seen without dissecting the mandible and gives an additional point of articulation between the mandible and the head capsule ("a" and "b" in Fig. 14I). Incisors and prostheca of both mandibles very reduced in size, molae relatively well developed. Maxillae with a small subtriangular basal membranous "gill" (membranous outgrouth). Thorax. Anterior ring of pronotum (or collar sensu Kluge 2004) short (ca. 1/4 the length of posterior ring), anteriorly projecting as spines on lateral corners; posterior ring longer, ring-like. Legs (Fig. 15A–D, F–G). Leg I (Fig. 15A–B): femora very wide, well developed,

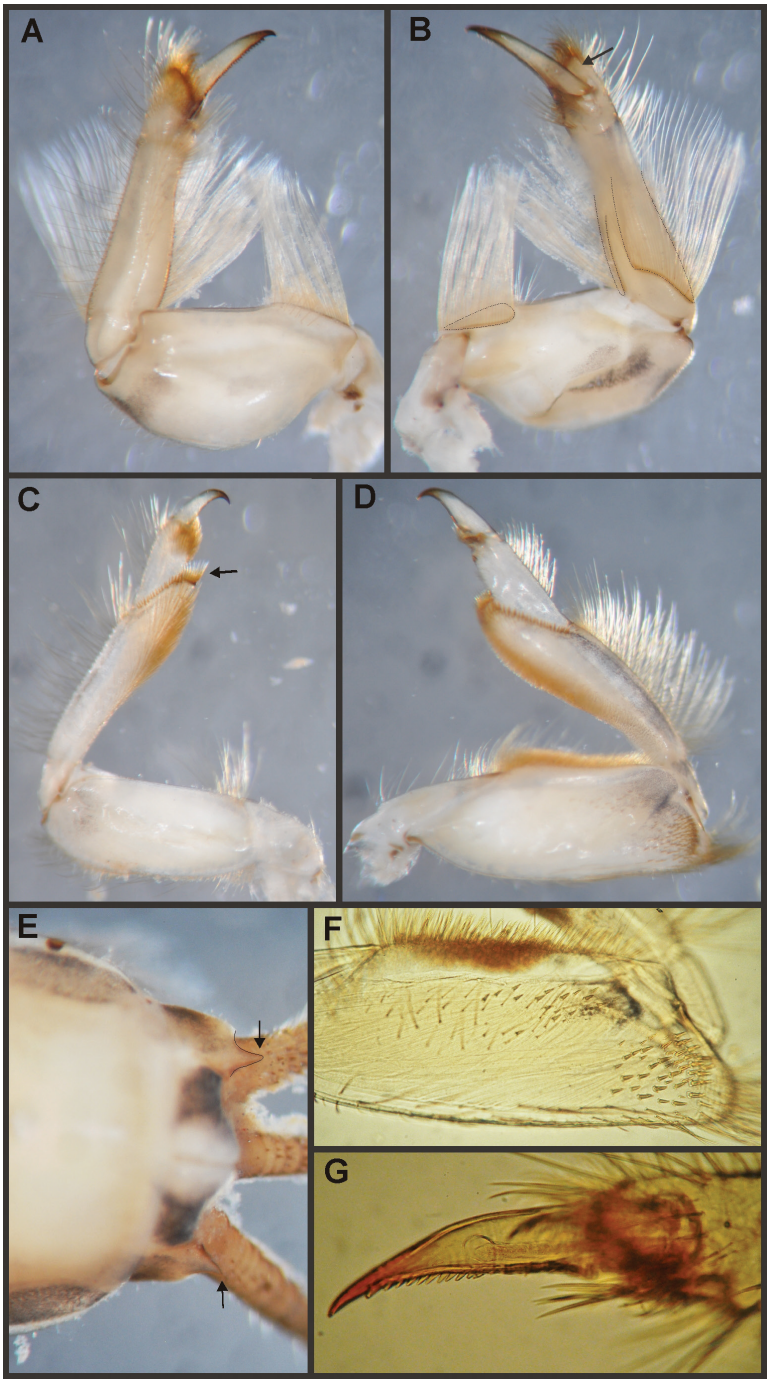

Figure 15. *Asthenopus* nymphs. *A. magnus*: **A** foreleg, d.v. **B** same, v.v. (arrow indicates apical projection of tibiotarsus) **C** middle leg, d.v. (arrow indicates distal brush on tibia) **D** hind leg **E** abdominal sterna **IX–X** (arrow indicates spine on paraproct). *A. angelae*: **F** hind femur, d.v. **G** foretarsal claw. **A–G** stereomicroscope photographs **F–G** light microscope photographs.

with a double ventro-basal row of long filtering setae; tibio-tarsus (fused, but fusion line distinguishable) with 3 rows of filtering setae (2 on dorsal "face" and 1 on inner margin), tarsus slightly and bluntly projecting apically (arrow in Fig. 15B); tarsal claw relatively large and stout with a row of marginal denticles (Fig. 15G). Leg II (Fig. 15C): smaller, with thinner femora, with scattered long setae, mostly basally and along hind margin; tibia and tarsi with row of long setae on outer (dorsal) margin, ventrally with many stout spines on apical half, with a distal brush of thick setae (arrow in Fig. 15C); tarsal claw relatively small, without denticles. Leg III (Fig. 15D, F): as leg II except larger and with anterior margin of femur densely covered with thick setae, and posterior margin roundly expanded at apex bearing a group of stout acute spines (Fig. 15F); tibia without distal brush. Coxae I and II directed ventrally, coxae III directed laterally. Abdomen. Gill I reduced in size, double, both portions subequal in length and width. Gills II–VII well developed, ventral portion smaller than dorsal portion; tergum X with well developed ventral spine on posterior margin (not visible dorsally, Fig. 15E). Caudal filaments short (curved in mature nymphs) with whorls of stout spines and simple setae at joinings.

Distribution. Amazonas and Parana biogeographic subregions (Argentina, Bolivia, Brazil, Colombia, Ecuador, Peru).

Discussion. The genus *Asthenopus* has been distinguished by means of the following characters (Domínguez 1988): 1) ratio foreleg/FW male: 3/5–4/5; 2) male foretarsus 2.5 times longer than foretibia; 3) foretarsal segment 2 similar to the others, and 2/3 the length of tibia); 4) ratio length of Rs stem/fork to margin 1/4 (or fork Rs at 2/10 from base to margin) ; 5) cubital intercalaries slightly diverging toward hind margin, ICu_2 and ICu_1 basally fused to CuA by cross veins; 6) ICu_2 ending at anal margin or in the tornus, 7) marginal intercalary veins absent; 8) forceps ratio width/length: 1/7; 8) penes robust on basal 2/3; 9) MA fork base to margin 10/100; 11) IMP–MP_1 not fused basally; 12) MP_2-IMP similar in length, not fused; 13) foretarsal claws of male not so expanded distally (as in *Asthenopodes*). Our phylogenetic analyses only recovered some of these character states as synapomorphies of this genus (see diagnosis and Appendix 2). The proposal of Domínguez (1988) and Hubbard & Domínguez (1988) concerning the intermediacy of *Priasthenopus gilliesi* with respect to *Asthenopus curtus* and *Asthenopodes picteti* is in concordance with our results. *Priasthenopus gilliesi* resulted sister to the *Povilla-Asthenopus* clade, presenting some plesiomorphic character states shared with *Asthenopodes*.

Key to the species of *Asthenopus*

Male

1 Penile lobe (distad to basal thumb) with a similar width along its length, basal thumb separated by a wide furrow (Figs 17A–C, E–F); forceps very stout (ratio length/ basal width = 4.7–6.0) **2**

– Penile lobe (distad to basal thumb) wider basally, basal thumb fused to penile lobe (Fig. 17D,G); forceps relatively slender (ratio length/ basal width = 6.2–7.0) **4**

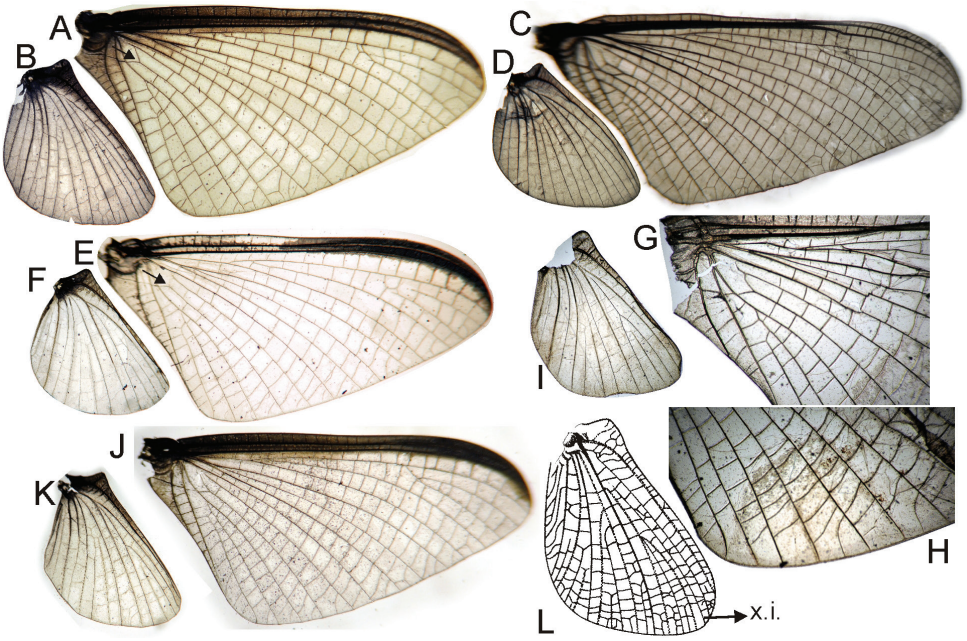

Figure 16. *Asthenopus* fore (FW) and hind wings (HW) of male imago. **A–B** *A. curtus* FW & HW **C–D** *A. magnus* FW & HW **E–F** *A. hubbardi* FW & HW **G–I** *A. guarani*, FW (details) & HW **J–K** *A. angelae* (from Argentina) FW & HW. *Ephoron* sp.: **L** male HW (x.i. = extra intercalary). Stereomicroscope photographs (except **L** line drawing).

2 Apical spine of penes long and acute (Fig. 17A–B) ..... ***A. curtus***
– Apical spine of penes short (Fig. 17C, E–F) **3**
3 Penes long, apical spine slightly marked, median remnant of styliger plate projecting laterally (Fig. 17E–F) ..... ***A. guarani***
– Penes short, apical spine well marked, median remnant of styliger plate normal (Fig. 17C) ..... ***A. hubbardi***
4 FW 9.5–10.1; penile lobe strongly widened basally (ratio length / basal width = 2.9, Fig. 17G) and with a small distal indentation near apical spine (arrow in Fig. 17G) ..... ***A. magnus***
– FW 7.0–9.5 mm; penile lobe not so wide at the base (ratio length / basal width = 4.0–5.0, Fig. 17D); without apical indentation as above ..... ***A. angelae***

Female and eggs of *Asthenopus* species are strongly similar. They may be identified by comparison with co-occurring males. Nevertheless the eggs extracted from female adults or mature nymphs may be keyed as follows:

1 Disk like structures on the equatorial area relatively well separated from each other, separation about 0.6 or more of maximum width of a disk (Fig. 18B, C, E) **2**

– Disk like structures on the equatorial area almost touching each other, maximum separation about 0.3 or less of maximum width of a disk (Fig. 18A, D).... ..... ***A. curtus / A. hubbardi***

2 With a group of 2–3 very small disks beneath each disk like structure (Fig. 18C) ..... ***A. guarani***

– Only smooth chorion below the disk like structures (Fig. 18B, E) .... ***A. angelae / A. magnus***

Nymphs (only 3 species known, almost undistinguishable, the characters below should be confirmed with the study of more material)

1 On the inner margin of left mandibular tusk, the space between the subbasal and the submedian tubercles is short and strongly concave (Fig. 14A); right mandible with distal corner of mola strongly protruding ..... ***A. curtus***

– On the inner margin of left mandibular tusk, the space between the subbasal and the submedian tubercles is longer and straighter (Figs 14B–C); right mandible with distal corner of mola not strongly protruding **2**

2 Ratio total length of mandible/mandibular tusk length: 1.59–1.62 (Fig. 14B, F) ..... ***A. angelae***

– Ratio total length of mandible/mandibular tusk length < 1.5 (Fig. 14C, E, G) ..... ***A. magnus*** (only known from Napo, Ecuador) / ***A. guarani*** (Paraná and Uruguay basins)

***Asthenopus curtus* (Hagen)**
Figs 4E, 14A, 16A–B, 17A–B, 18A, G, 20G

Palingenia albifilum var.; Walker 1853: 554.
Palingenia curta Hagen 1861: 304.
Campsurus curtus; Eaton 1868: 84; Eaton 1883: 40; Ulmer 1921: 240.
Asthenopus curtus; Eaton 1871: 59; Ulmer 1920c: 107; Ulmer 1921: 240; Lestage 1922b: 142; Ulmer 1942: 105; Traver 1956b: 7; Kimmins 1960: 312; Sattler 1967: 104; Berner 1978: 103; Hubbard 1982a: 270; Domínguez 1988a: 24; Hubbard and Domínguez 1988: 207; Domínguez 1989a: 173 (described as *A. magnus* sp. n. below); Domínguez et al. 2006: 561.
Campsurus amazonicus Hagen 1888: 230.
Asthenopus amazonicus; Ulmer 1920c: 107; Lestage 1923: 124; Ulmer 1942: 106; Traver 1950: 606; Traver 1956b: 7; Sattler 1967: 104; Berner 1978: 103.

Type material. Photographs of the type at the British Museum were studied.

Additional material. Two male imagos (IBN, slide 480) from COLOMBIA, Amazonas, Leticia, caño km 15, S 4°5'41" – W 69°59'1", 93 m, 11.ii.1999, light trap 4–6

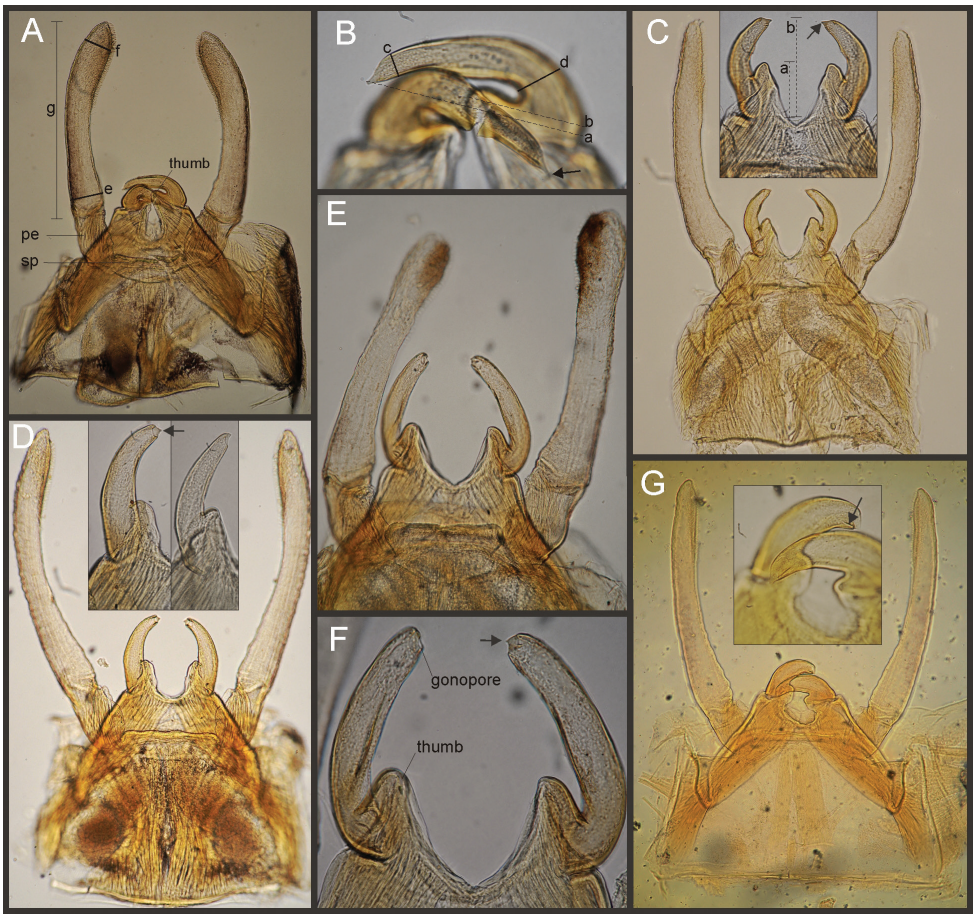

Figure 17. *Asthenopus*, general ventral view of male genitalia and detail of penes. **A–B** *A. curtus* **C** *A. hubbardi* **D** *A. angelae* **E–F** *A. guarani* **G** *A. magnus*. Light microscope photographs.

h, E. Domínguez, M.C. Zúñiga & C. Molineri cols.; male imaginal slides (FAMU) from BRAZIL, Amazonas, Careiro Island, Divinopolis, SE of Manaus, 29.vii.1961, E.J. Fittkau; 2 male and 1 female pharate subimagos (IBN642CM-eggs, 643-female, 644-male) from BRAZIL, Amazonas, São Paulo de Olivença, Bom Sucesso, 4.ix.2003, (aprox. S 3°28' – W 68°59').

Diagnosis. *Asthenopus curtus* is the type species of the genus, and is known from adults of both sexes, nymphs and eggs. Nine autapomorphies were recovered in the cladistic analysis, and are useful to diagnose the species (see Appendix 2). The following combination of characters is useful to distinguish *A. curtus* from the other species of the genus: 1) male FW 10.0, female FW 14.0–18.5; 2) male foreleg length 0.69–0.74 times the length of FW; 3) pronotum width/length ratio: 2.0–2.3 (male), 2.7–3.0 (female); 4) 18–25 marginal intercalary veins present on the entire margin of

forewings (Fig. 16A–B), 2–3 times shorter than distance between longitudinal veins in male (not anastomosed), hind wings with marginal intercalaries in at least 4 spaces between main veins; 5) male FW with 0 to 1 crossveins between Rs and MA basal to Rs fork; 6) ratio total length/basal width of forceps 5.4 (Fig. 17A–B); 7) penes very sclerotized, contrasting strongly with the remaining genital parts, apex projecting acutely; a deep furrow separates penis lobe from thumb, median remnant of styliger plate subrectangular without marked projections, pedestals subrectangular and large, outer margin projecting posteriorly on outer margin along forceps base; 8) female sternum VIII with anteromedian keel and reduced sockets as in Fig. 18G; 9) egg ratio maximum width of egg/maximum width of PC 1.1–1.3, cap formed by 3–5 filaments, chorionic plates separated by smooth chorion (Fig. 18A); 10) nymphal mandible: ratio total length of mandible/mandibular tusk length 1.6–1.7; 11) space between the subbasal and the submedian tubercles in inner margin of left mandibular tusks is short and concave (Fig. 14A).

Male imago. Length: body, 8.0–8.7; FW, 10.0; HW, 4.4; foreleg, 7.5; cerci, 33.0–35.0. General coloration yellowish light brown. Head whitish, heavily shaded black dorsally, paler on posteromedian zone of occiput, black shading extending anteriorly on frons as two parallel lines surrounding median ocellus. Antennae pale, slightly shaded gray on dorsum. Thorax. Pronotum yellowish translucent completely shaded gray, darker on anterior ring; paler on two transverse lines, one separating anterior and posterior rings and another more posterior and obliquely transverse; pleurae shaded with black, sternum with a median gray macula. Pronotum width/length ratio: 2.0–2.3. Mesonotum whitish yellow (or brownish in some males) with a black median triangle between posteroscutal protuberances, metanotum similar in color, also shaded black posteromedially; mesopleurae and sterna paler, shaded with black along anterior margin of katepisternum. Legs yellowish white shaded with gray dorsally on all coxae, femora and tibiae; foretarsal segment 1 blackish (Fig. 20G), remaining tarsal segments paler shaded with gray distally, claws grayish thin troughout. Wings (Fig. 16A–B). Membrane hyaline shaded very slightly with brownish near anterior margin and turning whitish translucent towards apical zone of C–Sc areas; veins translucent shaded with brown. Abdomen yellowish white shaded extensively with grayish brown dorsally, darkening very slightly towards rear segments. Sterna pale very slightly shaded gray, shaded stronger on mediolongitudinal line near anterior margin of sterna VIII–IX, this line is blurred posteriorly; a grayish black triangular mark is present at each side of this line, on anterior margin of sterna VIII–IX; sternum X shaded black except medially. Genitalia (Fig. 17A–B): median remnant of styliger plate and pedestals yellowish, forceps whitish translucent shaded gray along outer margin, penes dark orange with whitish base. Caudal filaments whitish, shaded gray at base of terminal filament.

Female adult. Length: body, 10.5–13.2; FW, 14.0–18.5; HW, 5.7; cerci, 5.8–7.0. Morphologically very similar to female adults of *A. angelae* described in detail in de Souza and Molineri (2012). Here only those characters that differ from the cited description are mentioned. Pronotum almost 3 times wider than long, width/length ratio = 2.7–3.0 (see continuous characters in phylogenetic matrix, Appendix 3).

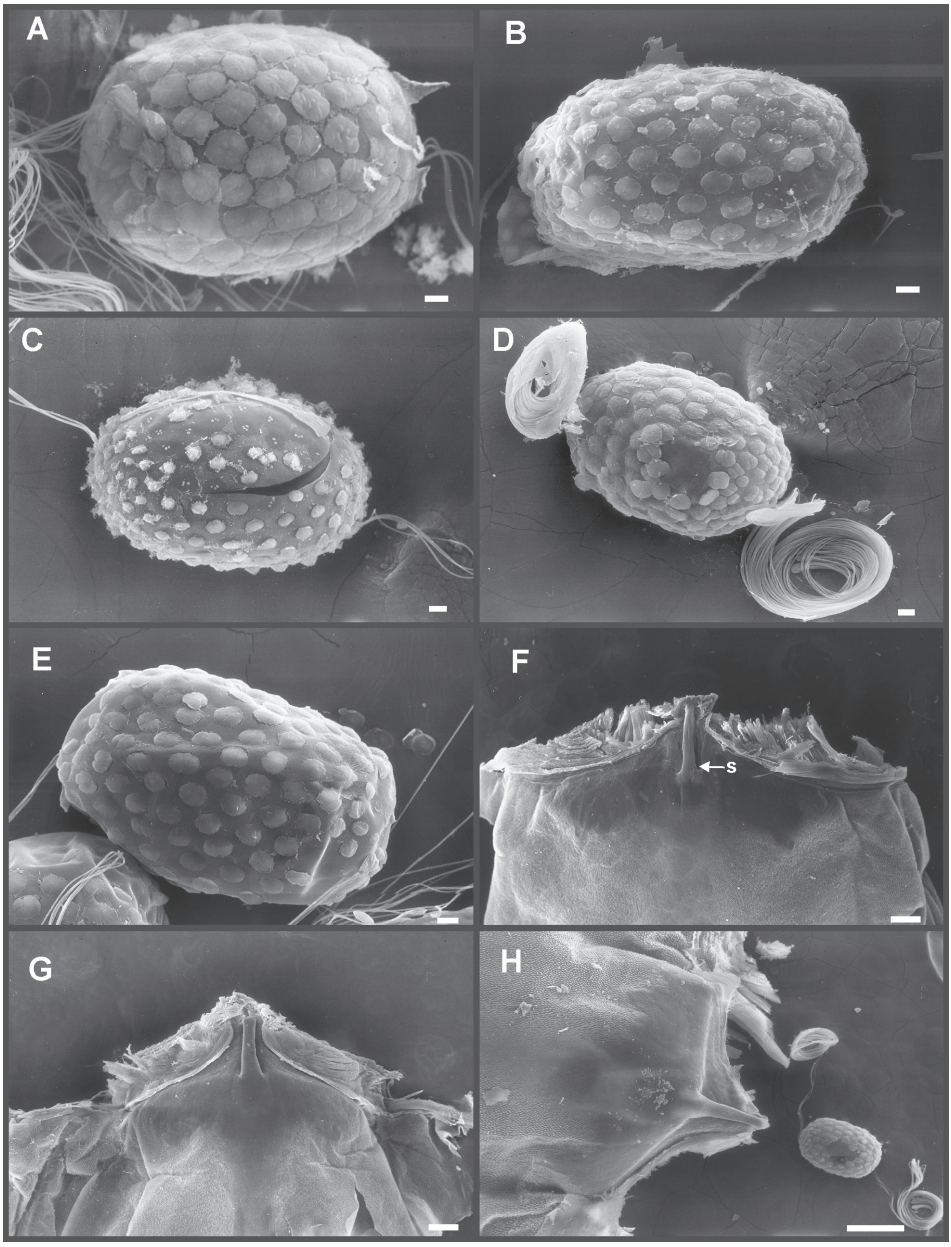

Figure 18. *Asthenopus*, SEM photographs. Eggs: **A** *A. curtus* (egg extracted from mature nymph), **B** *A. angelae* (egg extracted from mature nymph) **C** *A.* cf. *guarani* **D** *A. hubbardi*, **E** *A. magnus*. Female abdominal sternum VIII: **F** *A. magnus* **G** *A. curtus* **H** *A. hubbardi*.

Mesonotum uniformely brownish (cuticular pigmentation), almost without gray markings (dermic pigments). Female sternum VIII with anteromedian keel and reduced sockets as in Fig. 18G. Cercus about half the length of FW, cercus length/FW length: 0.4–0.5.

Eggs (Fig. 18A). Length, 200–220 μ; width, 130–155 μ. Two polar caps (maximum width, 110–120 μ), formed by 3–5 very long coiled threads. Chorionic surface smooth with relatively large subcircular chorionic plates, the plates are regularly spaced and some of them are divided in two or three subequal parts.

Mature nymph. Length of male: body, 9.5–9.7; cercus, 7.0; terminal filament, 5.0. Length of female: body, 17.0; cercus, 8.0; terminal filament, 7.0. Only characters that differ from *A. angelae* are given here, refer to that description for more detailed information. Head (occipital area) dorsally brownish uniformly shaded with gray. Mouthparts. Left mandibular tusks with a relatively shorter space between the large subbasal tubercle and the smaller subdmedian one, this space is somewhat C-shaped (Fig. 14A). Right mandible with distal corner of mola strongly protruding. Thorax. Mesonotum uniformly brownish (cuticular) without strongly gray-shading on carinae (Fig. 4E). Legs and paraprocts identical to those on Fig. 15.

Distribution. Amazonas River from Leticia (Colombia) to Manaus (Brazil).

Discussion. Much confusion exists in the literature concerning this species. Many authors mention *A. curtus* but from missidentified material. For example Ulmer (1942) described and illustrated (as *A. curtus*) a pair of males of *Asthenopus angelae*. The material from Ecuador studied by Domínguez (1988) proved to be a different but related species (*A. magnus* sp. n.). Berner (1978) synonymized *A. curtus* with *A. amazonicus*, showing that the differences between both species were only attributable to sexual dimorphism, but he was working with *A. angelae* males (de Souza and Molineri 2012). Nevertheless, Berner conclusions were correct given that sexual dimorphism in FW venation is present in both species. As it is impossible to assign any specimen to *A. amazonicus*, we prefer to treat it as synonym of *A. curtus*, as Berner proposed. Actually, only one specimen from previous works is positively determined as *A. curtus*: the type, studied by Eaton (1883) and illustrated by Kimmins (1966). We add here some other records from the Amazonas River: a pair of males from Colombia, some reared nymphs from Brazil and Fittkau's slides at FAMU. These male imagos show the characteristic genitalia of the holotype of *A. curtus*, with extremely wide forceps, long penis lobes and slender and very acute apical spines, and the more or less uniform brownish mesothoracic coloration (an exception of this last character are the males from Colombia-Leticia, much paler). The egg of *A. curtus* (Fig. 18A) is similar to that of *A. hubbardi* (Fig. 18D), in the shape and relative large size of the disk-like structures that leaves exposed only a reduced surface of smooth chorion. On the contrary the egg of *A. angelae* presents smaller disk-like structures with a larger surface of smooth chorion among them (Fig. 18B).

As the result of the present study, the female adult, egg, and nymphal stages are described here for the first time. Previous descriptions of female and nymphs in the literature were done from specimens of *A. angelae* or other species but are not useful to clearly distinguish the species.

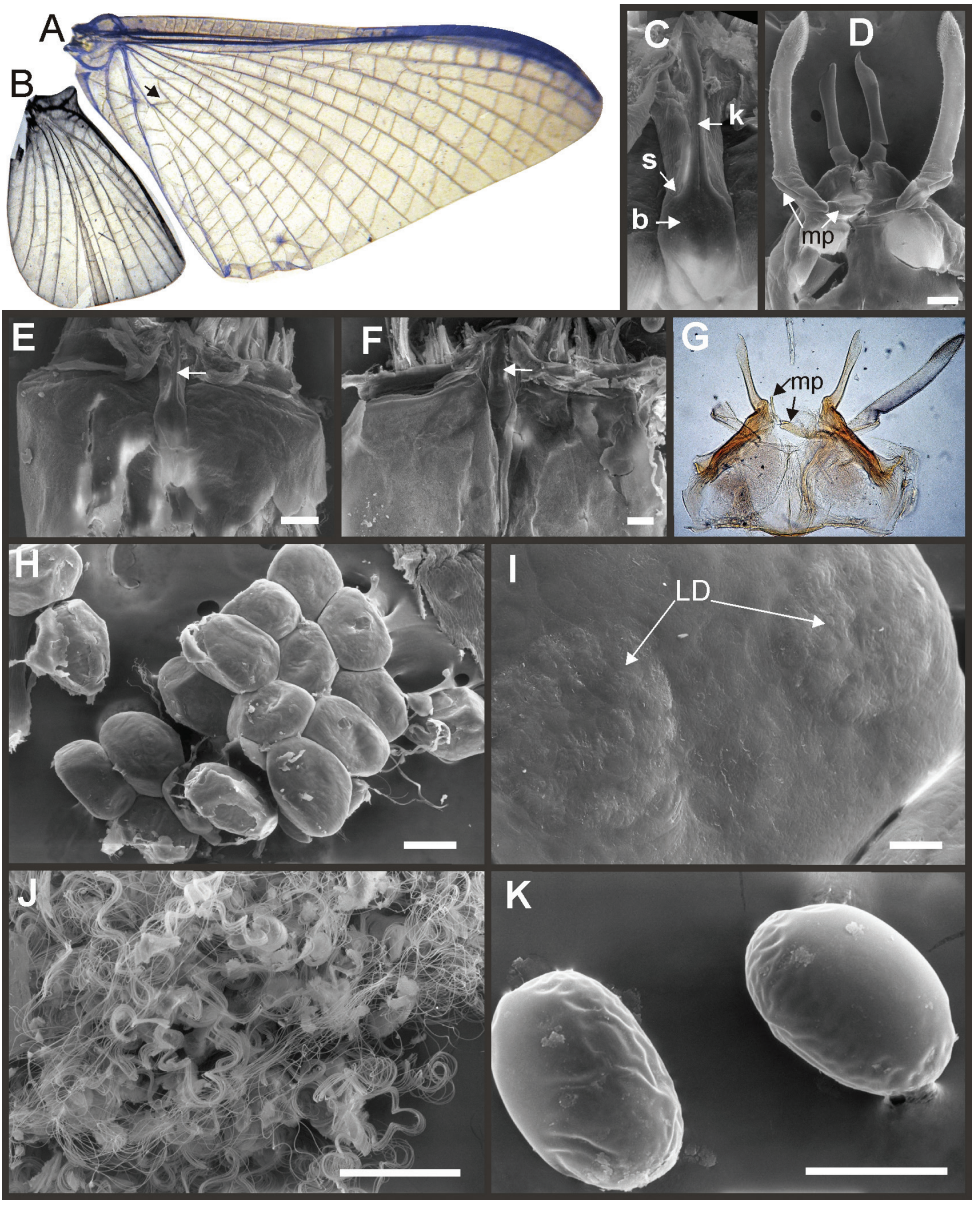

Figure 19. *Povilla* spp, SEM and light microscope photographs. *P. adusta*: **A** male forewing **B** male hind wing **C** detail of keel on female abdominal sternum 8 (b = base, k = keel, s = socket) **D** male genitalia (mp = median remnant of styliger plate) **E–F** female abdominal sternum 8 (general view) **G** male genitalia (median remnant of styliger plate partially broken and detached from right pedestal) **H–I** eggs and detail of chorion (LD = large disks). *P.* cf. *heardi*: **F** female abdominal sternum VIII **J** filaments surrounding the eggs inside female abdomen **K** eggs. Scale bar = 100 μ, except Figure 1 (10 μ).

***Asthenopus magnus* sp. n.**
http://zoobank.org/70A79C87-DD63-4371-8085-7BD7B5E55C26
Figs 4C, 14C, E, G, I–J, 15A–D, 16C–D, 17G, 18E–F

Asthenopus curtus, Domínguez 1989: 173; Domínguez et al. 2006: 561 (missidentification).

Material. Holotype (IBN) male imago from Ecuador, Napo Province, Laguna Limon Cocha, 250 m, 6.iv.1984, E. Domínguez col.(aprox. S 0°24' – W 76°38'). Paratypes, same data as holotype, separated in 16 vials including: 1 nymph dissected (parts in alcohol), 2 male imagos (parts on slides: IBN-2–64ED, IBN-2–70ED), 1 male imago (IBN-2–67ED), 2 nymphs/3 exuviae/1 pharate male, 1 pharate male subimago and nymphal cuticle (IBN483CM), 1 male imago (IBN481CM), 3 nymphal exuviae (IBN640CM, IBN641CM), 7 nymphal exuviae (1 at FAMU, 1 at CZNC), 5 female adults (used for SEM); 7 male imagos (used for the description; 1 at FAMU, 1 at CZNC), 20 male subimagos, 10 female adults, 1 male and 8 female subimagos, 10 female adults, 9 female adults (1 at FAMU, 1 at CZNC), 1 female adult (IBN-2–71ED). All the material is deposited in IBN except otherwise indicated.

Diagnosis. *Asthenopus magnus*, known from all the stages, can be distinguished from other species in the genus by the following combination of characters (also see the six autapomorphies in Appendix 2): 1) male FW 9.0–10.1, female FW 16.0–17.5; 2) forelegs of male 0.69–0.73 × the length of FW; 3) pronotum width/length ratio: 1.7–2.4 (male), 2.0–2.2 (female); 4) FW (Fig. 16C) with 6–14 relatively short marginal intercalaries (21–28 in female), hind wings with 2–4 (5–7 in female) marginal intercalaries; 5) male FW with 0 to 2 (2–3 in female) cross veins between Rs and MA basal to Rs fork; 6) forceps relatively slender, ratio length/basal width 6.1–6.2 (Fig. 17G); 7) penes tubular and robust, with well developed thumb, curved ventro-medially, with apex projecting medially as a distal spine, furrow separating penis lobe from thumb reduced; median remnant of styliger plate subrectangular, pedestals subrectangular to subovate, relatively large (Fig. 17G); 8) female sternum VIII with reduced, not distinguishable female sockets, but with a long anteromedian keel (Fig. 18F); 9) eggs (Fig. 18E) ratio maximum width of egg/maximum width of PC 1.2–1.3, cap formed by 4–5 filaments, chorionic plates separated by smooth chorion; 10) nymph, ratio total length of mandible/mandibular tusk length 1.4–1.5; 11) inner margin of left mandibular tusk with subbasal and submedian tubercles well separated (Fig. 14C, E).

Male imago. Length (mm): body, 9.0–10.5; FW, 9.0–10.1; HW, 4.0–4.8; leg I, 6.5–7.4; cerci, 37.0. General coloration yellowish light brown. Head whitish shaded black dorsally on pale median mark on hind margin and along inner margin of eyes; frons pale except paired submedian black lines. Antennae: whitish shaded diffusely with gray on scape and apex of pedicel; length (mm): scape 2.25, pedicel 1.5, flagellum 7.25. Thorax. Pronotum yellowish translucent shaded with black dorsally except at pale median membrane between both pronotal rings, on mediolongitudinal line and along margins; the black shading presents many scattered and small pale spots. Pronotum width/length: 1.7–2.4. Meso- and metanotum yellowish shaded with grayish on carinae, pos-

Figure 20. Foreleg of male imago, detail of articulation between tibia and tarsus: **A** *Asthenopodes picteti* **B** *Asthenopodes chumuco* **C** *Asthenopodes traverae* **D** *Hubbardipes crenulatus* **E** *Priasthenopus gilliesi* **F** *Asthenopus angelae* **G** *Asthenopus curtus* **H** *Asthenopus guarani* **I** *Asthenopus hubbardi* **J** *Asthenopus magnus*;**K** *Povilla adusta* **L** *Ephoron* sp. Abbreviations: Ti = tibia; Ta1 = tarsal segment 1; Ta2 = tarsal segment 2.

teromedian triangular mark (on mesonotum), and scutellum (both). Thoracic pleurae and sterna paler, shaded gray on pleural sclerites. Legs yellowish white, shaded gray on all coxae. Leg I shaded gray almost completely, stronger on femur and tibia, paler on tarsal segments (Fig. 20J). Legs II–III shaded with black dorsally on apex of femora and entire dorsum of tibiae, rest pale. Wings (Fig. 16C–D). Membrane hyaline shaded grayish

near costal margin on basal half, more whitish apically; all veins translucent completely shaded gray; 1–3 cross veins between MA and R, basad to R stem. Abdomen yellowish white shaded with gray and black dorsally except on median and lateral zones and intersegmental membranes. Median pale areas on terga II–IX are oval and are surrounded by darker pigments, a delicate mediolongitudinal black line is present but sometimes is only visible on tergum IX. Sterna whitish turning yellowish laterally and on sternum IX, shaded gray on paraproct and basally to terminal filament. Genitalia (Fig. 17G): forceps whitish, penes yellowish white. Cerci whitish very slightly shaded with gray.

Female imago. Length (mm): body, 15.5–19.5; FW, 16.0–17.5; HW, 5.2–7.8; cerci, 3.5–5.0. Pronotum width/length: 2. Morphologically very similar to *A. curtus* and *A. angelae*, the last is described elsewhere (de Souza and Molineri 2012). Color pattern similar to male but more strongly marked, exceptions follows: pale median mark on occiput longer, reaching median ocellus; wing membrane tinged with yellowish near costal margin and base, all veins shaded brown; shading on abdominal terga more extended, shaded widely gray except medially, tergum VIII–IX (sometimes also II–VII) with a black line in the pale median zone; medial margins of gill sclerites on abdominal sterna II-VII and lateral margins of sterna VIII–IX grayish; Sternum VIII with keel as in Fig. 18F. Cerci yellowish, 0.3–0.4 the length of FW.

Eggs (Fig. 18E). Length, 250–285 μ; width, 145–160 μ. Two polar caps (maximum width, 115–135 μ), formed by 4–5 very long coiled threads. Chorionic surface smooth with relatively large subcircular chorionic plates, the plates are regularly spaced and some of them are divided in two or three subequal parts.

Nymphs. Length of male (mm): body, 10.0–11.0 mm; cerci, 7.0–8.0; terminal filament, 5.0–5.5. Length of female (mm): body, 17.0–20.0 mm; cerci, 4.0–5.0; terminal filament, 5.0. General coloration brownish. Head (Fig. 14I–J) yellowish brown extensively shaded with grayish brown, darker on a band between ocelli, occiput with a profuse netted grayish pattern, except on paler median zone and along inner margin of eyes; paler areas also present basally to antennae and around median ocellus. Antennae yellowish white, length (mm): scape (0.5), pedicel (0.28), flagellum (2.0). Mandibular tusks with relatively large space between large basal tubercle and smaller subdistal tubercle, not C-shaped as in *A. curtus* but in the form of broad "C" or bracket-shaped (Fig. 14C, E, G). Thorax. Anterior ring of pronotum (collar) blackish; posterior ring shaded gray except on mediolonitudinal line and a pair of sublateral pale marks; pronotal membranes whitish. Mesonotum brownish, lighter toward apex of wingpads. Thorax ventrally whitish. Legs (Fig. 15A–D) whitish yellow shaded with gray on coxae, apex of femora and along tibiae; foretarsal claw with 20 (male) to 31 (female) denticles in a marginal row, increasing in size distally; distal region of hind femur with a group of ca. 60 (male) to ca. 100 (female) stout spines. Abdomen. Terga shaded gray dorsally, except on paler median band, a thin black median line is present inside this pale area on tergum IX–X; lateral zones of terga below gills, pale. Gills whitish almost completely shaded with gray, darker on outer (exposed) zones. Sterna whitish shaded with gray on lateral margins of sterna VIII–IX, and with grayish black on paraprocts (Fig. 15E). Caudal filaments yellowish.

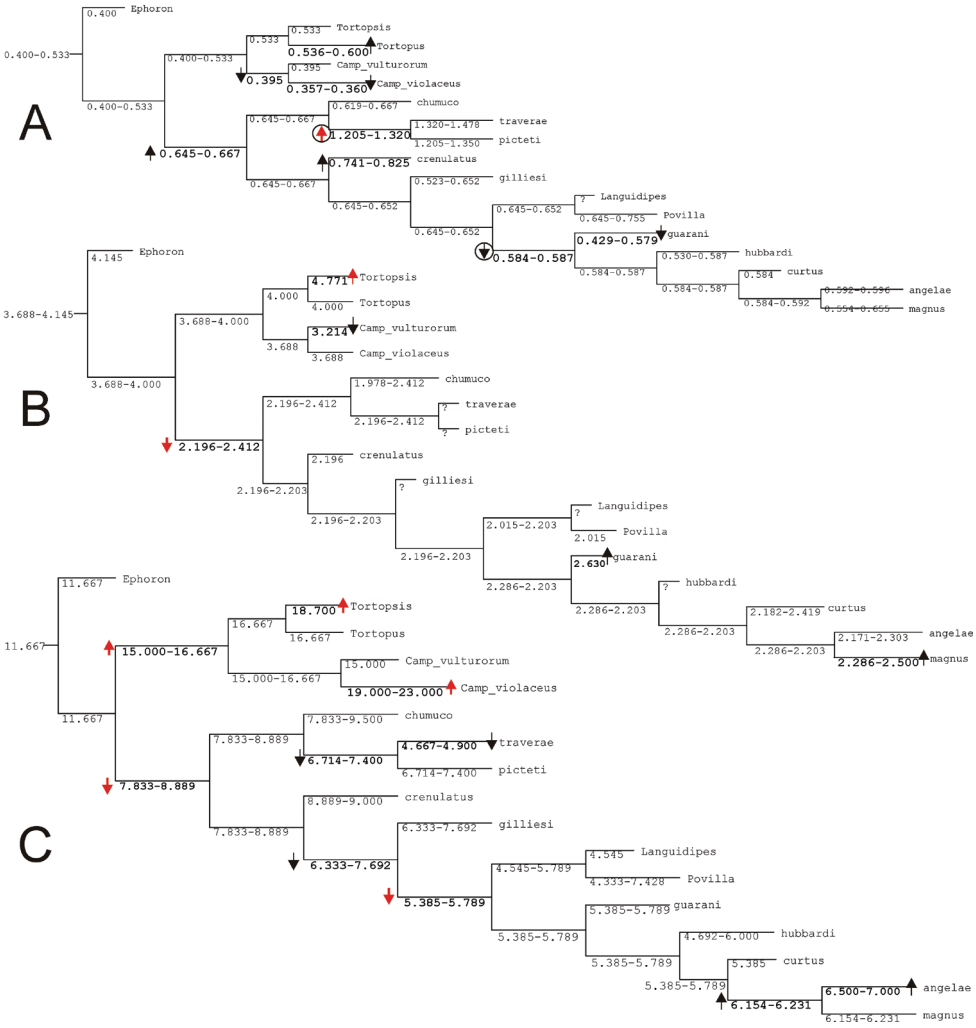

Figure 21. Optimization of selected continuous characters. **A** Char. 1 (1.416 steps) Ratio length second foretarsal segment/foretibia **B** Char. 27 (3.791 steps) Nymph, width of tusk as ratio between length of tusk (T) / width of tusk at the base (W) **C** Char. 13 (23.811 steps) Ratio A(total length forceps)/E(basal width). Arrows indicate increments or decrease in the characters (up and bottom directed arrows, respectively); red arrows indicate a marked change for the node.

Etymology. From Latin "magnus" meaning "large", noun in apposition. The name alludes to the general size of the individuals, mainly the female adults.

Distribution. Only known from the type locality in Napo (Ecuador).

Discussion. The type series described here as *A. magnus* were previously treated as *A. curtus* (Domínguez 1989: 173; Domínguez et al. 2006: 561), and used to record the latter species in Ecuador. As a result of our study we found some characters distinguishing these specimens as a new species, and thus *A. curtus* is no more considered to be present in that country. Nymphs and adults of both sexes were associated by nymphal exuviae and adults caught at the moment of emergence.

***Asthenopus hubbardi* sp. n.**
http://zoobank.org/1904C509-C6F5-45F3-9623-F7256CA7D022
Figs 16E–F, 17C, 18D, 18H, 20I

Material. holotype male imago (slide IBN479CM) from Colombia, Amazonas, Puerto Nariño, Loreto Yacu, S 3°44'26" – W 70°27'19", 5.ii.1999, luz 6–8 h, M.C. Zúñiga, E. Domínguez and C. Molineri cols.; and paratypes: 1 female imago (slide IBN574CM) same data as holotype; and 1 male imago (slide IBN605CM) from Colombia, Amazonas, Puerto Nariño, Lago Tarapoto, S 3°47'47" – W 70°25'17", 4.ii.1999, light trap 18–20 hs, M.C. Zúñiga, E. Domínguez and C. Molineri cols. Holotype deposited in MUSENUV, paratypes in IBN.

Diagnosis. *Asthenopus hubbardi*, known from adults of both sexes, can be distinguished from the other species in the genus by the following combination of characters (one autapomorphy is listed in Appendix 2): 1) male FW 7.8–9.2 (Fig. 16E–F), female FW 13.0; 2) forelegs of male 0.57–0.65 × the length of FW, apex of foretibia with stout spines (Fig. 20I); 3) pronotum width/length ratio: 2.1 (male), 2.7 (female); 4) FW with 4–14 relatively short marginal intercalaries (ca. 20 in female), hind wings without marginal intercalaries (present in all spaces in female); 5) FW with 2–3 cross veins between Rs and MA basal to Rs fork, in both sexes; 6) forceps relatively slender, ratio length/basal width 4.7–6.0 (Fig. 17C); 7) penes tubular and robust, furrow separating penis lobe from thumb well marked, median remnant of styliger plate subrectangular, pedestals subrectangular to subovate, relatively large (Fig. 17C); 8) female sternum VIII with reduced female sockets, anteromedian keel present (Fig. 18H); 9) eggs ratio maximum width of egg/maximum width of PC 1.1–1.3, cap formed by 3–8 filaments, chorionic plates almost contiguous (Fig. 18D).

Male imago. Length (mm): body, 7.0–7.1; FW, 7.8–9.2; HW, 3.3–4.0; leg I, 5.1–5.2; cerci, 22.0–23.0. General color whitish brown. Head whitish shaded black dorsally except thin line along hind margin, with a pair of blackish short lines anteriorly to median ocellus. Antennae whitish shaded gray at margins of scape. Thorax. Pronotum ratio width/length: 2.1. Pronotum yellowish translucent widely shaded black, except on pale transversal line between anterior and posterior rings, and on mediolongitudinal line of posterior ring, and posterolateral oblique dashes. Meso- and metanotum whitish yellow shaded black on carinae and margins, also shaded on black on posteromedian triangular zone. Legs whitish shaded gray on dorsum of foreleg, all coxae, and on legs II–III on apex of tibiae and dorsum of tarsi; foretarsal segment 1 is shown in Fig. 20I. Wings (Fig. 16E–F) membrane hyaline except apically whitish on C and Sc areas, veins translucent yellow turning hyaline distally, except basal 2/3 of veins Sc and R_1 yellowish; 2 cross veins between R and M basally to R stem. Abdomen whitish shaded almost completely with brownish gray except at pale intersegmental membranes, oblique dashes on lateral zones of terga I–VIII, submedian pale spots on anterior margin of terga II–IX, and single posteromedian pale spot on terga III–IX. Genitalia (Fig. 17C) whitish except penes yellowish. Caudal filaments whitish, slightly shaded gray on basal segments of cerci.

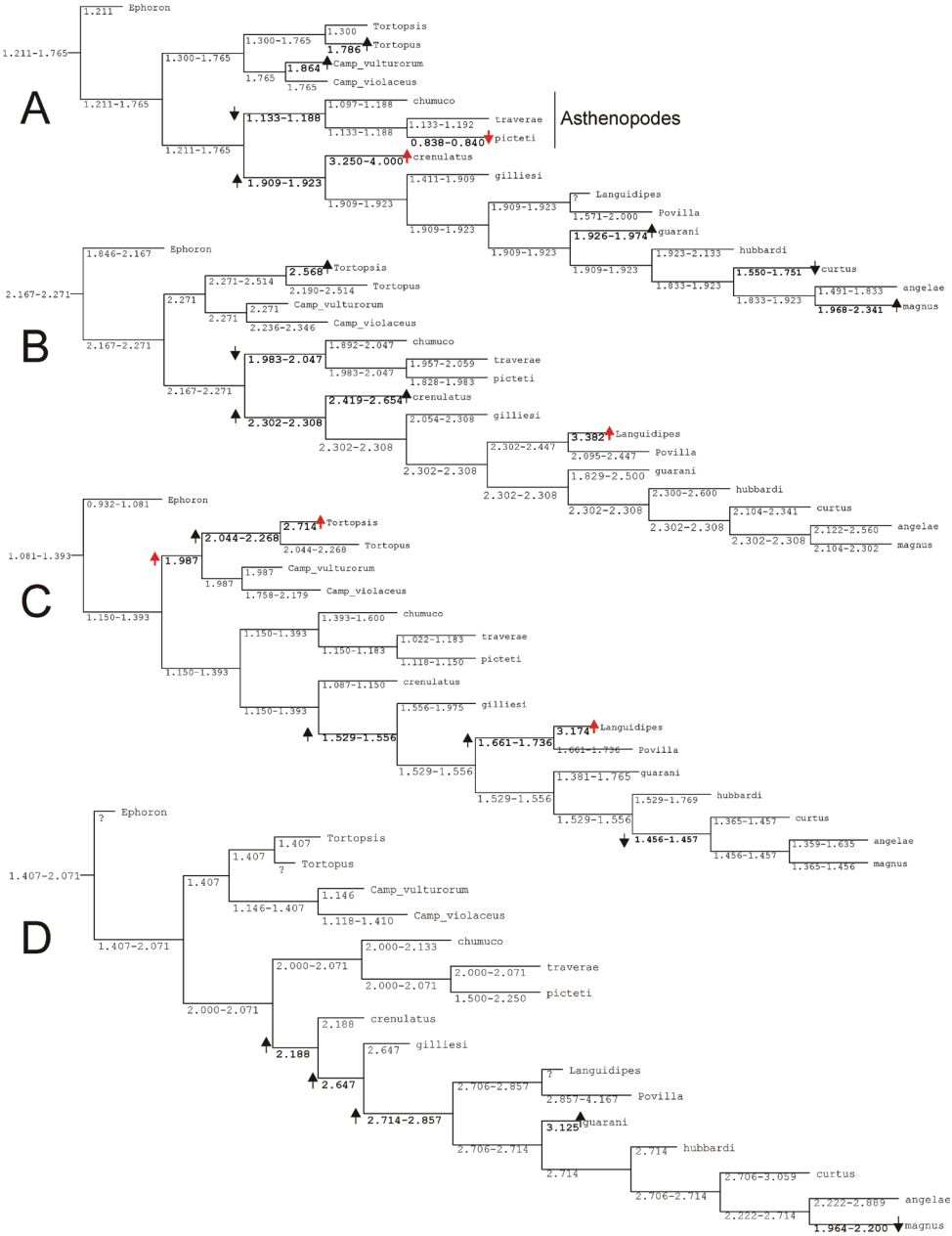

Figure 22. Optimization of selected continuous characters. **A** Char. 0 (3.873 steps) Ratio subapical width of foretibia/subbasal width of tarsal segment 2 **B** Char. 5 (2.344 steps) Ratio length FW/HW **C** Char. 2 (4.148 steps) Ratio FW/foreleg length **D** Char. 18 (2.225 steps) female prothorax, width/length. Arrows indicate increments or decrease in the characters (up and bottom directed arrows, respectively); red arrows indicate a marked change for the node.

Female imago. Length (mm): body, 10.5; FW 13.0; HW, 5.0, cerci 3.8. Similar to male, shaded dorsally more uniformly and markedly. Pronotum ratio width/length: 2.7. FW with 4 cross veins between R and M basal to R stem (none of them just below fork). Abdominal sternum VIII with keel as in Fig. 18H. Cerci yellowish turning whitish apically; ratio length cercus /FW = 0.3.

Eggs (Fig. 18D). Length, 210–245 μ; width, 135–150 μ. Polar caps (maximum width, 110–135 μ) formed by 3–8 long coiled threads. The chorionic plates are almost contiguous, leaving a reduced smooth chorionic surface among them (Fig. 18D).

Etymology. The species is named for Mike Hubbard who has contributed significantly to the understanding of mayflies throughout the world.

Distribution. Two near localities in the Amazonas River from Colombia.

Discussion. This species is very similar to *A. angelae*, and both were collected in the same lightraps in Colombia, nevertheless they can be separated because *A. hubbardi* shows translucent veins in the wings (brownish in *A. angelae*); in most specimens a cross vein is present just below R fork in *A. angelae* (more basal or distal in *A. hubbardi*), and the penes are shorter and well separated from the basal thumb in *A. hubbardi* (similar to *A. curtus*). *Asthenopus hubbardi* is further characterized because foretibia (Fig. 20I) presents strong marginal spines (weak or absent in *A. curtus*).

***Asthenopus guarani* sp. n.**
http://zoobank.org/E2D5EC68-E2C3-4894-B4FC-452D3320F105
Fig. 16G–I, 17E–F, 18C

Type material. Holotype male imago (slide IBN473CM) from Argentina, Corrientes, Parque Nacional Mburucuya, Selva Misionera (sector 6), luz, 29.iii.2001, F. Navarro col.

Additional, non-type material. One reared female subimago (IBN524CM) and nymphal cuticle (IBN639CM) from Argentina, Corrientes, Laguna Brava, 27.i.1977, Poi de Neiff col. (egg in Fig. 18C extracted from this female); and 1 male imago (IBN638CM) from Uruguay, Salto, near Salto Grande, frente a Isla del Paredón, 20–21.I.1975, luz 22hs; 4 male and 10 female imagos from Brazil, São Paulo, Luiz Antonio, 10.iv.1991, C.G. Froelich col. (MZSP); 1 male and 4 female imagos from Brazil, São Paulo, Luiz Antonio, Reserva Jatai, 9.iv.1990, C.G. Froelich col. (MZSP).

Diagnosis. *Asthenopus guarani*, known from all stages, can be distinguished from the other species in the genus by the following combination of characters (seven autapomorphies are detailed in Appendix 2): 1) male FW 8.0–9.0 mm (Fig. 16G–H), female FW 16.0 mm; 2) Ratio FW/foreleg length 1.4–1.8; 3) pronotum width/length ratio: 2.15 (male), 3.1 (female); 4) male FW with 4–6 marginal intercalaries (24–26 in female), slightly shorter than the separation of main veins, HW (Fig. 16I) with 2–4 marginal intercalaries (8–9 in female); 5) male FW with 0–2 cross veins between Rs and MA basal to Rs fork (3 in female); 6) forceps relatively slender, ratio length/basal width 4.8–5.8 (Fig. 17E–F); 7) penes tubular and slender, furrow separating penis lobe from thumb well marked; median remnant of styliger plate with lateral rounded lobes as in Fig. 17E). 8)

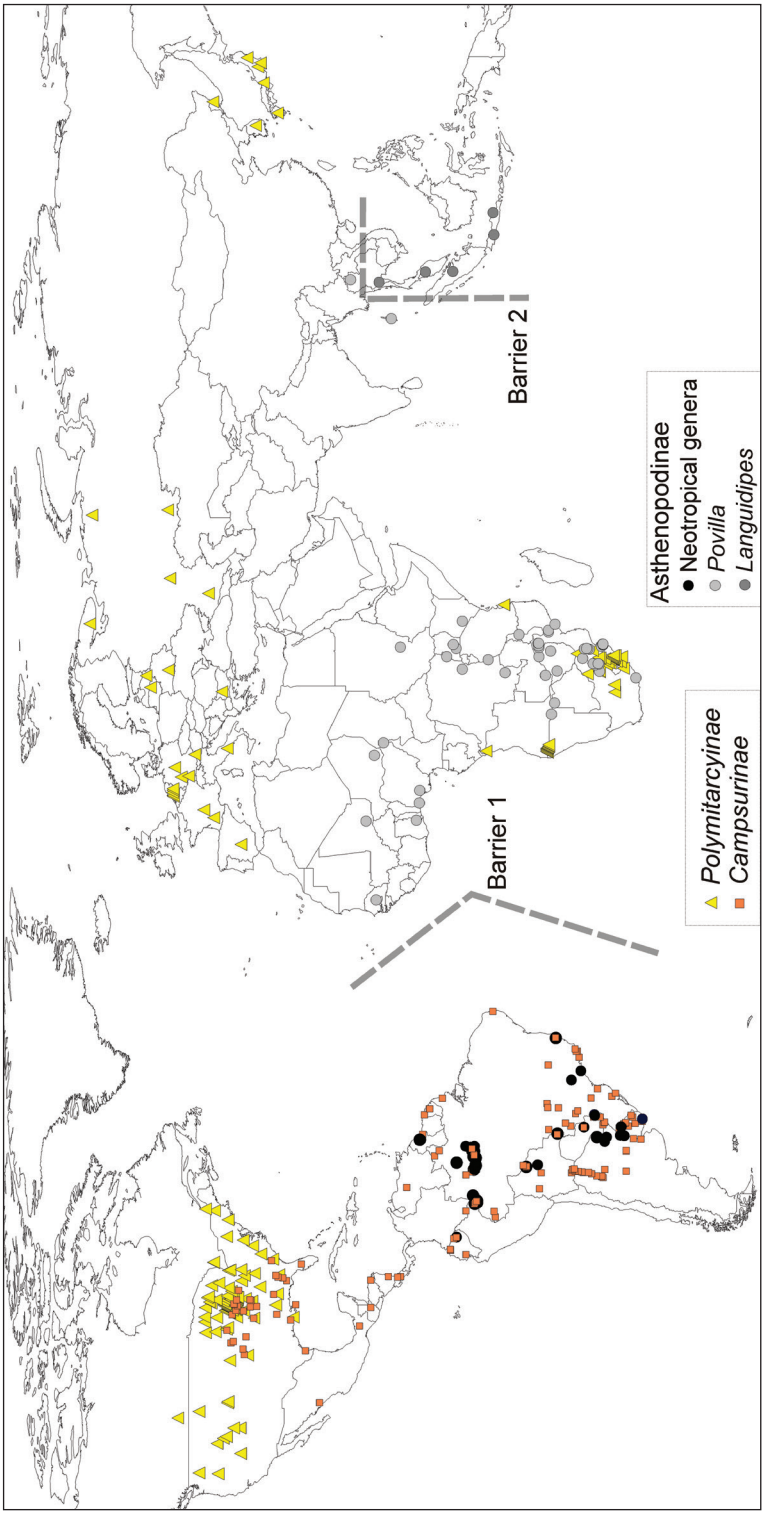

Figure 23. World map indicating the distribution of the three subfamilies in Polymitarcyidae. Additionally, barriers 1 (separating the genus *Asthenopus* vs *Povilla* + *Languidipes*) and 2 (separating *Povilla* from *Languidipes*) found in the biogeographical analysis are marked.

female sternum VIII with reduced, not distinguishable female sockets, but with a long anteromedian keel; 9) eggs (Fig. 18C) ratio maximum width of egg/maximum width of PC 1.2, cap formed by 3–8 filaments, disk-like structures well separated by smooth chorion, with 2–3 small disks beneath each larger disk (Fig. 18C); 10) nymph, ratio total length of mandible/mandibular tusk length 1.4; 11) inner margin of left mandibular tusk with subbasal and submedian tubercles well separated (similar to Fig. 14C, E).

Male imago. Length (mm): body, 6.5–9.0; FW, 8.0–9.0; HW, 3.6–4.0; foreleg, 5.1–5.4; cerci, 25.4–28.0. General coloration yellowish white. Head whitish shaded with black dorsally except on hind margin and posteromedian pale mark; frons pale shaded with a pair of black submedian longitudinal lines; venter of head pale. Antennae whitish shaded with gray on scape; length (mm): scape 1.75, pedicel 1.25, flagellum 7.5. Thorax. Pronotum whitish translucent, shaded black on anterior ring and lateral margins; posterior rings shaded gray, with darker mediolongitudinal line. Meso- and metanotum yellowish white, shaded gray on scutellum; sterna pale shaded gray only on mesokatepisternum. Legs whitish shaded gray on coxae. Foreleg completely shaded gray, paler on base of tarsal segments 2–5 (Fig. 20H). Middle and hind legs shaded gray on apical half of femora and apical 2/3 of tibiae, tarsi and claws translucent. Wings (Fig. 16G–I). Membrane of both wings hyaline, except shaded with light gray at base of costal margin in both wings and whitish on the apex of costal margin of FW; veins translucent, except Sc and R_1 whitish, all veins shaded slightly gray but more diffusely toward apex. Abdomen whitish, terga uniformly shaded gray, paler laterally and anteriorly to each tergum; sterna whitish. Genitalia (Fig. 17E–F) whitish, penes yellowish white. Cerci whitish translucent.

Female subimago. Length (mm): body, 12.5; FW, 16.0; HW, 6.5; cerci broken off and lost. General coloration orangish yellow shaded widely black. Head dorsally blackish except medial line on occiput, and anteriorly to median ocellus. Thorax. Pronotum width 2.5 mm, total length 0.8 mm; cream shaded black on thin anterior ring, with gray on posterior ring, membranes whitish. Mesothorax orangish yellow with gray markings. Wings translucent whitish, veins whitish except basal half of C, Sc and R yellowish. Abdomen uniformely shaded gray dorsally, except on pale medial line. Sternum VIII with long and thin anteromedian keel. Base of caudal filaments whitish (rest broken off and lost).

Eggs (Figs 18C). Length, 160–200 μ; width, 100–160 μ. Polar caps (max. width 130 μ) formed by 3–8 long coiled threads. The disk-like structures are circular and entire (not partitioned as other species), very well separated by smooth chorion, and when removed, a group of 2–3 very small disks are visible beneath (Fig. 18C).

Nymph (cuticle from reared female described above). Length (mm): body, 16.5 mm; cerci and terminal filament, 7.0 (both broken at apex). Antennae broken off and lost. Mouthparts. Mandibular tusks with relatively large space between the large basal tubercle and smaller subdistal tubercle, not C-shaped (similar to Fig. 14C, E, G). Legs. Foretarsal claw with a row of 26–29 denticles. Apex of hind femur with a group of 90–100 stout acute spines.

Etymology. The name refers to one of the etnic groups inhabiting the area where the specimens were collected.

Distribution. Argentina (Corrientes), Brazil (Sao Paulo), Uruguay (Salto).

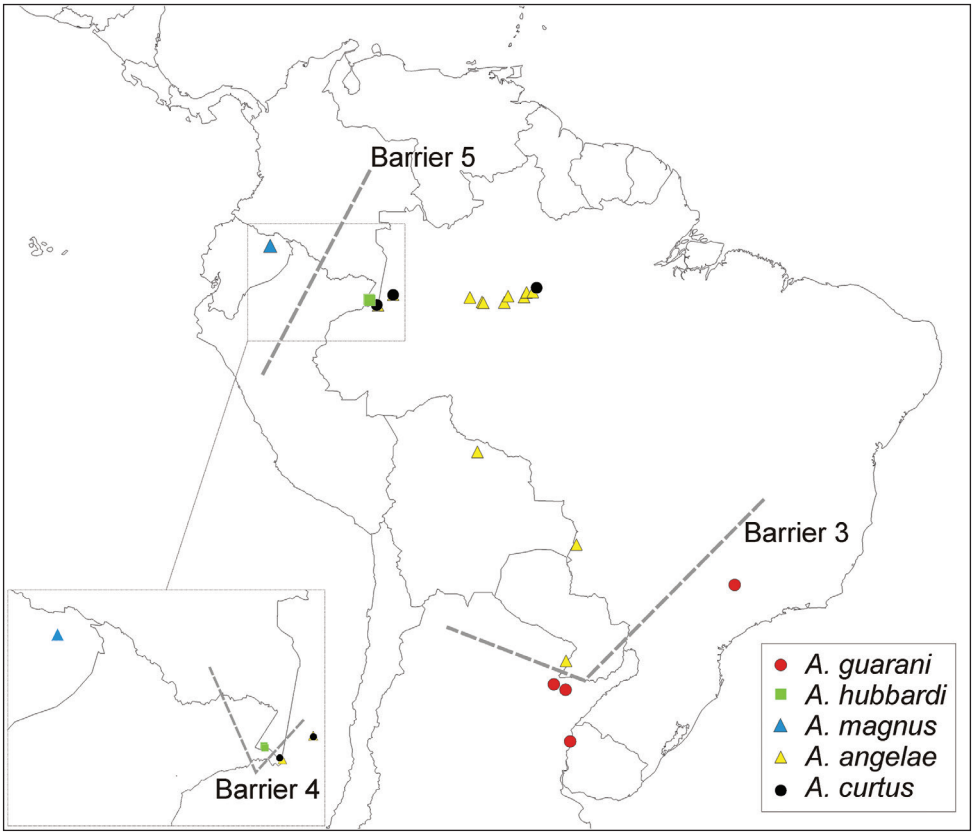

Figure 24. Map of South America (in part) showing the distribution of *Asthenopus* species. Barrier 3 found in the biogeographical analysis separates *A. guarani* from the remaining species in the genus. Barrier 4 (see detail at left bottom) separates *A. hubbardi* from the rest; and Barrier 5 separates *A. magnus* from its sister *A. angelae*.

Discussion. This species is very distinctive, not only by the long and slender penis lobe, but also because of the presence of relatively long marginal intercalary veins (in male FW and HW). The reared female subimago is tentatively associated with the male, because of similarity in coloration and shared distributional range. Eggs extracted from this female show also some differences from the other known in the genus, mainly the larger extent of smooth chorion around the plates and the presence of small disks below the larger ones (Fig. 18C).

Asthenopus angelae de Souza & Molineri

Figs 4D, 14B, F, 15F–G, 16J–K, 17D, 18B

Material (see de Souza and Molineri 2012). Additional records: 13 nymphs (including 3 male and 1 female pharate subimago) from BRAZIL, Amazonas, Codajás, Urucurizinho,

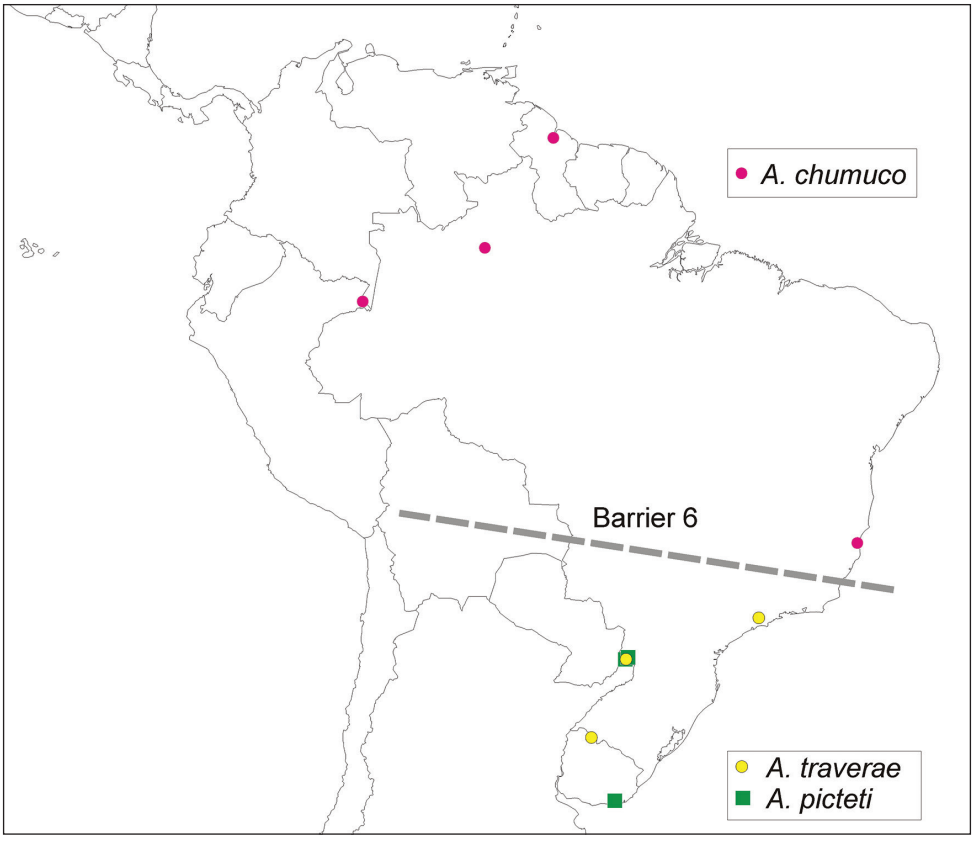

Figure 25. Map of South America (in part) showing the distribution of *Asthenopodes* species. Barrier 6 found in the biogeographical analysis separates *A. chumuco* from the remaining species in the genus.

Lago Cuxuará (A10-lago Aquapi 14), 15.ix.2003 (slides IBN645CM and IBN646CM) (aprox. S 3°55' – W 62°3'); and 1 pharate male subimago from BRAZIL, Amazonas, São Paulo de Olivença, Bom Sucesso (A02-agapito), 9.iv.2003 (slide IBN606CM) (aprox. S 3°28' – W 68°59'). Deposited in INPA (4 nymphs), CZNC (6 nymphs), IBN (3 nymphs).

Diagnosis. Only one autapomorphy was recovered in our analysis for *A. angelae*, a change in the ratio A (total length forceps)/E(basal width) from 6.2 to 6.5–7.1 (i.e., forceps become slightly slender). This species can be recognized by the following combination of characters: 1) FW size male 7.0–10.0 mm (Fig. 16J–K), female 12.0–17.0 mm; 2) ratio FW/foreleg length 1.4–1.6; 3) pronotum width/length ratio: 2.0–2.2 (male), 2.2–2.9 (female); 4) 5–11 imv present in male FW, relatively short and poorly anastomosed; 5) male FW with 1–4 cross veins between Rs and MA basal to Rs fork; 6) ratio total length/basal width of forceps 6.5–7.1 (Fig. 17D); 7) penes tubular, with well developed thumb, curved ventro-medially, with apex projecting acutely, furrow separating penial lobe from thumb reduced or absent (Fig. 17D), pedestals subrectangular to subovate, relatively large; 8) female sternum VIII with anteromedian keel and reduced sockets similar to

other species; 9) eggs (Fig. 18B) with 3–5 threads on polar caps, ratio maximum width of egg/maximum width of PC 1.1–1.3, chorion with smooth area around rounded disks; 10) nymph, ratio total length of mandible / mandibular tusk length 1.6; 11) space between the subbasal and the submedian tubercles relatively long and straight (Fig. 14B).

Distribution. Argentina, Bolivia, Brazil, Colombia and Peru.

Discussion. This species was recently described from all the stages (de Souza and Molineri 2012), and in our analysis it appears as sister to *A. magnus*, but with relatively low support. In the original description, nymphs and female adults were not distinguished from *A. curtus*, because of lack of characters. We proposed (above in diagnosis) some characters that should be checked and confirmed with the study of more material. We suggest that specific identification of this and the other species of the genus should be confirmed when possible with the study of male genitalia. Peru was mentioned by de Souza and Molineri (2012) in the list of material but not in the distribution, so here it is added in that section.

Acknowledgements

We acknowledge Dr. Marco Guimarães and Jairo Oliveira from the Laboratório de Ultraestrutura Celular Carlos Alberto Redins (LUCCAR), CCS/UFES, as well as edital MCT/FINEP/CT–INFRA - PROINFRA 01/2006, and to Centro Integral de Microscopía Electrónica (CIME), CONICET, Tucumán, Argentina for the SEM images. Special thanks to Michel Sartori for loan of out-group material, Paula Souto for photographs of *A. guarani* males and Eduardo Dominguez for most of the material, including the new species *A. magnus*. Wills Flowers and David Baumgardner made useful comments and suggestions. We acknowledge Willi Hennig Society for the TNT software. Some of the geographic records used in this article were downloaded from GBIF website and produced by the U.S. Environmental Protection Agency through its Environmental Monitoring and Assessment Program (EMAP), University of Alberta Museums-Freshwater Invertebrate Collection, South African National Biodiversity Institute-Albany Museum, Dutch Foundation for Applied Water Research (STOWA), Illinois Natural History Survey, and Gunma Museum of Natural History (Japan). Partial support for this research was provided by FAPES (Fundação de Amparo à Pesquisa do Espírito Santo, process number 54689627/2011). FFS also thanks CNPq (Conselho Nacional de Desenvolvimento Cientifico e Tecnológico) for a research fellowship. CM acknowledges CONICET (National Council for Scientific Reasearch, Argentina) for external fellowship to Brazil, and reasearch grants PIP0330 and PICT1067.

References

Arias JS (2010) VIP: Vicariance Inference Program. Program, Code, and Documentation. www.zmuc.dk/public/phylogeny/vip [accessed on 28 October 2011]

Arias JS, Szumik CA, Goloboff PA (2011) Spatial analysis of vicariance: a method for using direct geographical information in historical biogeography. Cladistics 27: 1–12. doi: 10.1111/j.1096-0031.2011.00353.x

Arndt W (1938) Spongilliden. Exploration du Parc National Albert (Mission H. Damas, 1935–1936), Fase 2: 1–26.

Bae YJ, McCafferty WP (1995) Ephemeroptera tusks and their evolution. In: Corkum LD, Ciborowski JJH (Eds) Current directions in research on Ephemeroptera. Canadian Scholars' Press Inc., Toronto, 377–406.

Banks N (1913) The Stanford expedition to Brazil, 1911. Neuropteroid insects from Brazil. Psyche 20: 83–89. doi: 10.1155/1913/39865

Baumgardner DE, Peters JG, Idris IA, Hubbard MD (2012) The adult stage of Languidipes corporaali (Lestage, 1922), new status and the validity of Povilla (Navas) (Ephemeroptera: Polymitarcyidae: Asthenopodinae). Aquatic Insects 34: 107–113. doi: 10.1080/01650424.2012.713487

Berner L (1978) The status of *Asthenopus curtus* (Hagen) (Ephemeroptera: Polymitarcyidae). Acta Amazonica 8: 103–105.

de Jong YSDM (2012) Fauna Europaea version 2.5. www.faunaeur.org

De-Souza MR, Molineri C (2012) The adults and nymphs of Asthenopus angelae new species (Ephemeroptera: Polymitarcyidae) from Argentina, Bolivia, Brazil and Colombia. Zootaxa 3399: 45–52.

Domínguez E (1988) *Asthenopus gilliesi* sp. n. y su importancia en la taxonomía de la subfamilia Asthenopodinae (Ephemeroptera: Polymitarcyidae). Anales del Museo de Historia Natural de Valparaíso 19: 21–26.

Domínguez E (1989) Primera cita de Asthenopus curtus (Hagen) (Ephemeroptera : Polymitarcyidae) para la Republica de Ecuador. Revista de la Societad Entomologica Argentina 45: 173–174.

Domínguez E, Molineri C, Pescador ML, Hubbard MD, Nieto C (2006) Ephemeroptera of South America. Aquatic Biodiversity in Latin America. Pensoft, 650 pp.

Eaton AE (1868) An outline of re-arrangement of the genera of Ephemeridae. Entomologist Monthly Magazine 5: 82–91.

Eaton AE (1871) A Monograph of the Ephemeridae. Transactions of the Entomological Society of London 1871: 1–164.

Eaton AE (1883–1888) A revisional monograph of recent Ephemeridae or mayflies. Transactions of the Linnean Society of London, 2nd Ser Zoology 2: 1–352.

Edmunds GF, Traver JR (1954) An outline of a reclassification of the Ephemeroptera. Proceedings of the Entomological Society of Washington 56: 236–240.

Emmerich D, Molineri C (2011) A new species of *Campsurus* (Ephemeroptera: Polymitarcyidae: Campsurinae) from Argentina and Uruguay and redescription of *C. evanidus* and *C. jorgenseni* with new synonymies. Zootaxa 2965: 51–60.

Goloboff PA, Farris JS, Kallersjo M, Oxelman B, Ramırez MJ, Szumik CA (2003) Improvements to resampling measures of group support. Cladistics 19: 324–332. doi: 10.1111/j.1096-0031.2003.tb00376.x

Goloboff PA, Farris JS, Nixon K (2008) TNT, a free program for phylogenetic analysis. Cladistics 24: 774–786. doi: 10.1111/j.1096-0031.2008.00217.x

Goloboff PA, Matoni C, Quinteros S (2006) Continuous characters analyzed as such. Cladistics 22: 589–601. doi: 10.1111/j.1096-0031.2006.00122.x

Hadley A (2010) CombineZP software. http://www.hadleyweb.pwp.blueyonder.co.uk/CZP/Installation.htm

Hagen H (1888) Unsere gegenwärtige Kenntniss der Ephemeren. Entomologische Zeitung Stettin 49: 221–232.

Hagen HA (1861) Synopsis of the Neuroptera of North America with a list of the South American species. Smithsonian Miscellaneous collections, 1–347.

Hartland-Rowe R (1958) The biology of a tropical mayfly Povilla adusta Navàs (Ephemeroptera, Polymitarcidae) with special reference to the lunar rhythm of emergence. Revue de Zoologie et de Botanique Africaines 58: 185–202.

Hooghiemstra H, van der Hammen T (1998) Neogene and Quaternary development of the neotropical rain forest: the forest refugia hypothesis, and a literature overview. Earth-Science Reviews 44: 147–183. doi: 10.1016/S0012-8252(98)00027-0

Hovenkamp P (1997) Vicariance events, not areas, should be used in biogeographical analysis. Cladistics 13: 67–79. doi: 10.1111/j.1096-0031.1997.tb00241.x

Hovenkamp P (2001) A direct method for the analysis of vicariance patterns. Cladistics 17: 260–265. doi: 10.1006/clad.2001.0176

Hubbard MD (1975) The genus Asthenopodes Ulmer and its type species (Ephemeroptera: Polymitarcidae). The Florida Entomologist 58: 111–112. doi: 10.2307/3493392

Hubbard MD (1982) Catalogo abreviado de Ephemeroptera da America do sul. Papeis Avulsos de Zoologia, Sao Paulo 34: 257–282.

Hubbard MD (1984) A revision of the genus Povilla (Ephemeroptera: Polymitarcyidae). Aquatic Insects 6: 17–35. doi: 10.1080/01650428409361158

Hubbard MD (1995) Towards a Standard Methodology for the Description of Mayflies (Ephemeroptera). In: Corkum LD, Ciborowski JJH (Eds) Current directions in research on Ephemeroptera. Canadian Scholars' Press Inc., Toronto, 361–370.

Hubbard MD, Dominguez E (1988) Synonymy of the neotropical mayfly genera Asthenopus and Asthenopodes (Ephemeroptera : Polymitarcyidae : Asthenopodinae). The Florida Entomologist 71: 207–210. doi: 10.2307/3495369

Kimmins DE (1960) The Ephemeroptera types of species described by A.E. Eaton, R. McLachlan and F. Walker, with particular reference to those in the British Museum (Natural History). Bulletin of the British Museum (Natural History) Entomology 9: 269–318.

Kluge NJ (2004) The phylogenetic system of Ephemeroptera. Kluwer, 442 pp.

Koss RW, Edmunds GF (1974) Ephemeroptera eggs and their contribution to phylogenetic studies of the order. Zoological Journal of the Linnaean Society 55: 267–349. doi: 10.1111/j.1096-3642.1974.tb01648.x

Leal JJF, Esteves FA, Farjalla VF, Enricht-Prast A (2003) Effect of *Campsurus notatus* on NH+4, DOC fluxes, O2 uptake and bacterioplankton production in experimental microcosms with sediment-water interface of an Amazonian lake impacted by bauxite tailings. International Revue Hydrobiologia 88: 167–178. doi: 10.1002/iroh.200390012

Lestage J-A (1922) Notes sur les genres Asthenopus-Povilla (Ephemeroptera) et description d'une espèce javanaise nouvelle (Asthenopus corporaali sp. n.). Annales de la Société entomologique de Belgique 62: 142–148.

Lestage J-A (1923) L'imbroglio campsurien. Notes critiques sur les Campsurus (Ephemeroptera). Annales de la Société entomologique de Belgique 63: 113–124.

Lestage J-A (1924) Notes sur les Ephémères de la Monographical Revision de Eaton. Annales de la Société entomologique de Belgique 65: 33–60.

Lomolino MV, Riddle BR, Brown JH (2006) Biogeography, third edition. Sinauer Associates, Inc., Sunderland, Massachusetts, 845 pp.

McCafferty WP (1975) The burrowing mayflies of the United States (Ephemeroptera: Ephemeroidea). Transactions of the American Entomological Society 101: 447–504.

McCafferty WP (2004) Higher classification of the burrowing mayflies (Ephemeroptera : Scapphodonta). Entomological News 115: 84–92.

McCafferty WP, Bloodgood DW (1989) The female and male coupling apparatus in *Tortopus* mayflies. Aquatic Insects 11: 141–146. doi: 10.1080/01650428909361361

Molineri C (2010) A cladistic revision of *Tortopus* Needham & Murphy with description of the new genus *Tortopsis* (Ephemeroptera: Polymitarcyidae). Zootaxa 2481: 1–36.

Molineri C, Emmerich D (2010) New species and new stage descriptions of *Campsurus major* species group (Polymitarcyidae: Campsurinae), with first report of silk-case construction in mayfly nymphs. Aquatic Insects 32: 265–280. doi: 10.1080/01650424.2010.533131

Molineri C, Salles FF (2013) Phylogeny and biogeography of the ephemeral Campsurus Eaton (Ephemeroptera, Polymitarcyidae). Systematic Entomology 38: 265–277. doi: 10.1111/j.1365-3113.2012.00656.x

Molineri C, Cruz PV, Emmerich D (2011) A new species of *Asthenopus* (Ephemeroptera: Polymitarcyidae: Asthenopodinae) from Brazil and Colombia. Zootaxa 2750: 33–38.

Morrone JJ (2001) Biogeografía de América Latina y el Caribe. M&T-Manuales & Tesis SEA, Zaragoza 3, 148 pp.

Navás L (1912) Notes sur quelques Névroptères d'Afrique II. Revue de Zoologie africaine 1: 401–410.

Navás L (1915) Neuropteros sudamericanos. Segunda Serie. Broteria, Zoologica 13: 5–13.

Navás L (1916) Neuropteros sudamericanos Tercera Serie. Neuropteros del Brasil recogidos por el R.P. Joaquin da Silva Tavares S.J. Broteria, Zoologica 14: 14–35.

Navás L (1920) Insectos Sudamericanos. Tercera Serie. Anales de la Sociedad Científica Argentina 90: 52–72.

Navás L (1926) Insectos de la Argentina y Chile. Segunda Serie. Estudios 31: 103–111.

Navás L (1924) Insectos de al Argentina y Chile. Estudios 1922: 358–368.

Needham JG, Murphy HE (1924) Neotropical mayflies. Bulletin of the Lloyd Library 22, Entomol ser 4: 1–79.

Ogden TH, Gattolliat JL, Sartori M, Staniczek AH, Soldán T, Whiting MF (2009) Towards a new paradigm in mayfly phylogeny (Ephemeroptera): combined analysis of morphological and molecular data. Systematic Entomology 34: 616–634. doi:10.1111/j.1365-3113.2009.00488.x

Ortiz-Jaureguizar E, Cladera GA (2006) Paleoenvironmental evolution of southern South America during the Cenozoic. Journal of Arid Environments 66: 498–532. doi: 10.1016/j.jaridenv.2006.01.007

Pictet F-J (1843–1845) Histoire naturelle des Insectes Névroptères. Famille des Ephémérines, 300 pp. + 347 pl.

Sattler W (1967) Über die Lebensweise, insbesondere das Bauverhalten, neotropischer Eintagsfliegen-Larven (Ephemeroptera, Polymitarcidae). Beiträge zur Neotropischen Fauna 5: 89–110. doi: 10.1080/01650526709360399

Thenius E (1979) Lebensspuren von aquatischen Insektenlarven aus dem JungTertiär Niederösterreichs. Beitrage zur Paläontologie von Österreish, Wien 14: 1–17.

Thenius E (1979) Lebensspuren von Ephemeropteren-Larven aus dem Jung-Tertiär des Wiener Beckens. Annalen des Naturhistorischen Museums in Wien 82: 177–188.

Traver JR (1947) Notes on Neotropical Mayflies. Part III. Family Ephemeridae. Revista de Entomologia 18: 370–395.

Traver JR (1950) Notes on Neotropical Mayflies. Part IV. Family Ephemeridae (continued). Revista de Entomologia 21: 593–614.

Traver JR (1956) The genus *Asthenopodes* (Ephemeroptera). Comunicaciones zoologicas del Museo de Historia Natural de Montevideo 4: 1–10.

Ulmer G (1920) Übersicht über die Gattungen der Ephemeropteren, nebst Bemerkungen über einzelne Arten. Stettiner Entomologische Zeitung 81: 97–144.

Ulmer G (1921) Über einige Ephemeropteren-Typen älterer Autoren. Archiv für Naturgeschichte, Abteilung A 87: 229–267.

Ulmer G (1924) Einige alte und neue Ephemeropteren. Konowia 3: 23–37.

Ulmer G (1942) Alte und neue Eintagsfliegen (Ephemeropteren) aus Süd- und Mittelamerika. Stettiner Entomologische Zeitung 103: 98–128.

Vejhabongse NF (1937) The habit of a mayfly and the damage caused by the nymph. Journal of the Siam Society. Natural History Supplement 2: 53–56.

Walker F (1853) Ephemeridae. List of the specimens of neuropterous insects in the collection of the British Museum. The Trustees, London, 533–585.

Appendix 1

List of continuous characters and their definitions. Characters were scored from male imagos unless otherwise indicated.

0} Ratio subapical width of foretibia/subbasal width of tarsal segment 2. The width of the tibia was measured before the first tarsal segment if fused, as in *Asthenopodes* species (Figure 20).

1} Ratio length foretarsal segment 2/foretibia. Length of foretibia includes the reduced first tarsal segment if fused (in *Asthenopodes* species).

2} Ratio FW/foreleg length. Fore and hind wings length was taken from the base of the costal brace to the apex. The length of male foreleg does not include the coxa; it was taken from the base of the trochanter to the apex of the claws.

3} Ratio FW/cercus length. Cerci were measured only when complete (i.e., with a thinner and setose short portion in the apex).

4} FW ratio length/width. Width of FW refers to the maximum width (located near the Cu sector).

5} Ratio length FW/HW

6} FW, number of imv (intercalary marginal veinlets) from $ICuA_1$ to R_1. The variation in wing venation (number, length and degree of anastomosis) shown by these veinlets is difficult to formalize. For the "number of imv" (intercalary marginal veinlets), only those reaching the hind margin (attached and dettached) were counted, from $ICuA_1$ to R_1.

7} FW, marginal connectivity (n°of connections among imv/n°of imv). The anastomosis or "marginal connectivity" of these veinlets was calculated as a ratio between the total number of connections among the imv and the total number of imv counted for previous character.

8} Number of crossveins between R and M (e.g., arrows in Figure 8H), basal to R fork

9} Ratio marginal length between main longitudinal veins/imv length (mean of all values in a wing). The length of the imv in relation to the distance between the apices of main longitudinal veins is represented as the mean value of all the ratios measurable in the FW (i.e., the number of marginal interspaces between main veins, from $ICuA_1$ to R_1, frequently about 14 interspaces).

10} FW male, Rs stem length/Rs from fork to margin. The measures were taken as straight lines; in the case of the distal measure, from fork of Rs to apex of IRs.

11} Prothorax width/length. Prothorax width and length were taken in dorsal view, and are maximum values (i.e., widest and longest parts were measured respectively, including membranes).

12} Ratio median remnant of styliger plate, maximum width/length at middle

13} Ratio A (total length forceps)/E (basal width). A = total length of forceps, also as a straight line (e.g., line "g" in Figure 7A). E = basal width of forceps, taken as indicated by line "e" in Figure 7A.

14} Ratio L (length of penile lobe)/B (length of inner thumb). L = total length of penes, taken as a straight line from the base to the apex of the lobe (e.g., line "a" in Figs 7A, 8A, 12B). B = length of thumb of penes, measured as a straight line in the medial margin (line "b" in the same figures)

15} Ratio L /C. L as defined above; C = basal width of penis lobe (line "d" in Figs 7A, 8A, 12B and others)

16} Ratio L /Z (curvature in v.v.). L as defined before; Z = a measure intended to quantify the curvature of the penis lobe, it was taken in v.v. as the distance between two parallel lines as indicated by line "z" in Figure 12B.

17} Penes, ratio C (basal width)/D (subapical width). C as defined before; D = subapical width of penis lobe (line "c" in Figs 7A, 8A, 12B)

18} Prothorax width/length (female adult)

19} Cercus/FW length (female adult)

20} Egg, ratio maximum length (including polar caps)/maximum width

21} Egg, ratio maximum with/maximum width of polar cap (uncoiled)

22} Egg, polar cap, ratio maximum width/maximum length

23} Egg, polar cap, number of threads forming each cap

24} Nymph, total length of mandible/mandibular tusk length. Asthenopodinae is defined by stout tusks, and Campsurinae by slender ones, as this is subjective and difficult to score in a matrix we use continuous variation in the length of the tusk (T in Figure 5B) with respect to the total length of the mandible (L in Figure 5B).

25} Nymph, position of the large inner tubercle along the longitudinal axis of the mandible. This is formalized as the ratio: total length of mandible (L in Figure 14A) / length from base of the mandible to the transverse line bisecting the tubercle (t1 in Figure 14A).

26} Nymph, position of the small and subdistal inner tubercle along the longitudinal axis of the mandible. This is formalized as above, ratio: total length of mandible (L in Figure 14A) / length from base of the mandible to the transverse line bisecting the tubercle (t2 in Figure 14A).

27} Nymph, width of tusk as ratio between length of tusk (T) / width of tusk at the base (W). In those cases where a large tubercle is present, the width does not include it (see Figure 14A).

Discrete characters

28} Male foretarsal segment 1: 0 = distinct (Fig 20E–K); 1 = fused with tibia (Fig. 20A–C, L); 2 = fused with second tarsal segment (Fig. 20D). Most species present a distinct tarsal segment 1 in male foreleg, a strong articulation is located between the apex of the tibia and this first tarsal segment (Fig. 20E–K). In *Asthenopodes* the first tarsal segment is completely fused with the tibia, and thus the articulation is located between the fused tibiotarsus and the second tarsal segment (Fig. 20A–C). In the unique *Hubbardipes crenulatus* the first tarsal segment, while distinct, shows an incipient fusion with the second tarsal segment (Fig. 20D).

29} Male foretarsal segment 1, form: 0 = subquadrate; 1 = subrectangular; 2 = subovate.
30} Foretarsal segment 5, apex 0 = blunt or with a transverse ridge; 1 = trilobed.
31} Apex of male foretarsal claws: 0 = not or slightly expanded (Figure 7C); 1 = strongly expanded (apex 3 times wider than stalk, Fig. 13E–F).
32} Legs II and III (male): 0 = complete, functional at least in subimago; 1 = complete but weaker, non functional; 2 = tarsal segments not discernible, distorted; 3 = last segment present is trochanter.
33} FW veins: 0 = IMP connected to MP_1 (e.g., Fig. 16E, G); 1 = free (e.g., Figs 8D–E, 16A, C).
34} FW veins: 0 = MP_2 much shorter than IMP; 1 = subequal to slightly shorter.
35} FW Cu sector, ICus join hind margin on: 0 = both near or anteriad to tornus; 1 = ICu1 close to tornus, ICu2 on basitornal margin.
36} FW, max number of cells closed by imv (intercalaries marginal veins): 0 = 3 or more cells; 1 = one or two; 2 = none.
37} HW, imv: 0 = absent; 1 = 1 to 4 short; 2 = along the entire margin (or almost), long.
38} HW, anal area: 0 = with any or few crossveins; 1 = with many crossveins forming a network.
39} Short distal segment on forceps: 0 = present; 1 = absent.
40} Pedestal, form: 0 = similar width along its length; 1 = much narrower basally.
41} Median remnant of styliger plate: 0 = present; 1 = absent.
42} Median remnant of styliger plate, shape of hind margin: 0 = straight or convex; 1 = markedly concave (lateral margins projecting posteriorly, Fig. 12A–D).
43} Penial arm articulation 0 = tergite IX; 1 = sternite IX and base of pedestal.
44} Penes form: 0 = apices diverging or straight, blade-like; 1 = apices converging medially or curved ventrally.
45} Penes, apical spine: 0 = absent or slightly marked as a continuation of the penes; 1 = present, distinctly protruding from the penes (Figure 17).
46} Additional penis lobe (thumb): 0 = absent; 1 = present.
47} Cleft between large and small penile lobes: 0 = absent; 1 = short, closed (Figure 17D); 2 = long, opened (Fig. 17B, C, F).
48} Female sternum VIII, anteromedian keel: 0 = absent; 1 = present.
49} Female sternum VIII, anteromedian keel: 0 = short and blunt (Figure 13D); 1 = long and slender (Figs 18F–H, 19E–F).
50} Female sternum VIII, sockets: 0 = absent; 1 = present.
51} Female sternum VIII, position of sockets: 0 = anterior; 1 = submedian.
52} Female sternum VIII, position of sockets: 0 = contiguous; 1 = separated.
53} Female sternum VIII, anteromedian sockets: 0 = fused; 1 = small almost indistinct at each side of the keel; 2 = larger extending somewhat posteriorly from keel's base.
54} Eggs, chorionic plates (large disk-like structures, LD in Figure 7E): 0 = absent; 1 = present.
55} Eggs, chorionic plates (if present): 0 = seems aggregated small disks (Figure 13A); 1 = entire (e.g., Figure 7E).

56} Eggs, chorionic plates (if present and entire): 0 = one piece (Figs 13B–C, 18C); 1 = 2 or more pieces (Fig 18A–B, D–E).
57} Eggs, chorionic plates (small disk-like structures, SD in Figure 7E): 0 = absent; 1 = present.
58} Eggs, chorionic plates, location of small disks: 0 = among large disks (e.g., Figure 7E); 1 = below large disks (Figure 18C).
59} Eggs, polar caps: 0 = none; 1 = one; 2 = two.
60} Clypeus, median proyection: 0 = absent; 1 = present.
61} Nymphal left mandibular tusk, number of apical denticles: 0 = four; 1 = three; 2 = one.
62} Nymphal right mandibular tusk, number of apical denticles: 0 = two; 1 = one.
63} Nymphal mandibular tusks, large basal tubercle on inner margin: 0 = absent; 1 = present. Double-pointed in *Povilla* and *Asthenopus*, but less marked in the last genus (pair of black arrows in Fig. 14H, G, respectively).
64} Nymphal mandibular tusks, smaller submedian tubercle on inner margin (e.g., white arrow in Figure 14H): 0 = absent; 1 = present.
65} Nymphal mandibular tusks, inner margin distally to smaller submedian tubercle (mentioned above): 0 = smooth; 1 = with many (>5) small tubercles: 2 = with 1 pointed tubercle.
66} Nymphal mandibular tusks, small basal tubercle on outer dorsal surface: 0 = absent; 1 = present (Figure 14H).
67} Gill on abdominal segment I: 0 = bilamellate 1 = single.
68} Nymph, dorsum of head with pilose area on frons: 0 = absent; 1 = present.
69} Nymph, occipital region: 0 = strongly expanded, convex; 1 = not strongly developed, flat.
70} Nymphs, denticles on foretarsal claws: 0 = absent; 1 = present. When present generally ther is a single row of many marginal denticles, except in *Asthenopodes* where a double row is present.
71} Posterolateral spine on tergum X: 0 = absent (Figure 10E); 1 = present (Figure 15E). A small spine may be present, sometimes seeming to arise from paraproct but it actually belongs to the tergum. In *Hubbardipes crenulatus* is very short and blunt. In *Povilla* and *Asthenopus* it is acute, strong and visible dorsally. In Campsurinae it is shorter, blunt and only distinguishable when seen from below. Differing from these groups, in the nymphs of *Asthenopodes* and *Ephoron* it is not expressed.

Appendix 2

List of apomorphies from terminals and nodes. Arrows separate plesiomorphic from apomorphic states.

Ephoron:
No autapomorphies
Campsurus violaceus:
Char. 1: 0.395 → 0.357–0.360
Char. 13: 15.000–16.667 → 19.000–23.000
Char. 15: 5.417–5.769 → 2.727–2.846
Char. 17: 1.077–1.083 → 2.600
Char. 21: 1.833 → 2.625–3.333
Cleft between large and small penile lobes (47): absent → long, opened
Female sternum VIII, anteromedian sockets (53): larger extending somewhat posteriorly from keel`s base → fused
Povilla:
Char. 3: 0.339–0.347 → 0.316
FW vein IMP (33): free → IMP connected to MP1
Languidipes:
Char. 2: 1.661–1.736 → 3.174
Char. 3: 0.339–0.347 → 0.375–0.464
Char. 4: 2.000–2.214 → 2.447
Char. 5: 2.302–2.447 → 3.382
Char. 7: 0.700–1.167 → 1.667
Char. 15: 5.417–6.800 → 9.333
FW Cu sector, ICus join hind margin on (35): both near or anteriad to tornus → ICu1 close to tornus, ICu2 on basitornal margin
Styliger plate, median plate (41): present → absent
Gill on abdominal segment I (67): bilamellate → single
picteti:
Char. 0: 1.133–1.188 → 0.838–0.840
Char. 7: 1.400–1.950 → 2.000–3.353
Char. 14: 2.600–2.667 → 2.737–2.895
Char. 15: 5.818–5.909 → 8.000–8.696
Char. 16: 2.065–2.321 → 3.056–3.059
Char. 21: 1.625–2.364 → 1.222–1.516
Eggs, chorionic plates(large disk-like present) (55): entire → seems aggregated small disks
traverae:
Char. 12: 8.100 → 11.800
Char. 13: 6.714–7.400 → 4.667–4.900
Char. 17: 1.077–1.083 → 1.000
Char. 22: 3.750–3.778 → 2.143–3.667

chumuco:

Char. 9: 0.733–0.838 → 0.560–0.710
Char. 10: 0.337–0.366 → 0.389
Char. 15: 5.417–5.769 → 2.625–3.143
Char. 17: 1.077–1.083 → 2.333–2.667
Char. 19: 0.169–0.184 → 0.089–0.093
Char. 21: 1.625–2.364 → 2.688–3.067
Char. 23: 7.000–13.000 → 14.000–16.000

crenulatus:

Char. 0: 1.909–1.923 → 3.250–4.000
Char. 1: 0.645–0.667 → 0.741–0.825
Char. 5: 2.302–2.308 → 2.419–2.654
Char. 12: 4.500–5.200 → 4.286
Char. 14: 2.308–2.500 → 5.909–6.500
Char. 16: 2.000–2.174 → 3.250
Char. 17: 1.077–1.083 → 0.600–0.684
FW vein IMP (33): free → IMP connected to MP1
Nymphal mandibular tusks, smaller submedian tubercle (64): present → absent

gilliesi:

Char. 14: 2.077–2.500 → 1.905–2.067
Char. 15: 5.417–5.769 → 3.647–4.706
Char. 16: 2.000–2.174 → 1.177–1.905
Char. 21: 1.231 → 0.892–1.071
Char. 23: 7.000–13.000 → 14.000–16.000
Cleft between large and small penile lobes (47): absent → short, closed

magnus:

Char. 0: 1.833–1.923 → 1.968–2.341
Char. 3: 0.286–0.298 → 0.248–0.253
Char. 15: 3.846–4.000 → 2.857–2.933
Char. 16: 2.118–2.174 → 1.905–2.000
Char. 18: 2.222–2.714 → 1.964–2.200
Char. 24: 1.511–1.555 → 1.429–1.489

angelae:

Char. 13: 6.154–6.231 → 6.500–7.100

hubbardi:

Char. 10: 0.235–0.241 → 0.262–0.283

guarani:

Char. 0: 1.909–1.923 → 1.926–1.974
Char. 1: 0.584–0.587 → 0.429–0.579
Char. 7: 0.222–0.300 → 0.000
Char. 18: 2.714–2.913 → 3.125
Char. 24: 1.511–1.555 → 1.408
Char. 25: 1.787–1.811 → 1.818
Char. 27: 2.286–2.303 → 2.630

curtus:

Char. 0: 1.833–1.923 → 1.550–1.751
Char. 6: 10.000–11.000 → 18.000–25.000
Char. 10: 0.218–0.241 → 0.171
Char. 12: 3.545–4.400 → 3.222
Char. 14: 1.955–2.000 → 1.786
Char. 16: 2.118–2.174 → 2.273
Char. 17: 1.600–1.667 → 2.167
Char. 19: 0.323–0.353 → 0.378–0.500
Char. 24: 1.511–1.555 → 1.573–1.729

Campsurus vulturorum:

Char. 0: 1.765 → 1.864
Char. 10: 0.205–0.222 → 0.168
Char. 11: 1.273–1.333 → 1.000
Char. 14: 2.308–2.500 → 1.415
Char. 17: 1.077–1.083 → 1.071
Char. 24: 1.712 → 1.825
Char. 25: 1.494–1.542 → 1.369
Char. 27: 3.688 → 3.214

Tortopus:

Char. 0: 1.300–1.765 → 1.786
Char. 1: 0.533 → 0.536–0.600
Char. 3: 0.370–0.371 → 0.352
Char. 10: 0.205–0.222 → 0.194
Char. 17: 1.077 → 1.000
Char. 19: 0.287–0.319 → 0.277
Char. 26: 1.239–1.258 → 1.283

Tortopsis:

Char. 2: 2.044–2.268 → 2.714
Char. 3: 0.370–0.371 → 0.375–0.417
Char. 5: 2.271–2.514 → 2.568
Char. 13: 16.667 → 18.700
Char. 15: 6.364 → 11.923
Char. 19: 0.287–0.319 → 0.321–0.350
Char. 20: 1.226–1.294 → 1.147–1.171
Char. 24: 1.625–1.639 → 1.562
Char. 27: 4.000 → 4.771
Penes, apical spine (45): absent or slightly marked as a continuation of the penes → present, distinctly protruding from the penes
Female sternum VIII, sockets position (52): contiguous → separated
Nymphal mandibular tusks, smaller submedian tubercle (64): present → absent

Node 18 (*Campsurus*):

Char. 1: 0.400–0.533 → 0.395
Char. 9: 0.926–1.500 → 1.580–1.825

Char. 24: 1.625–1.639 → 1.712
Additional penis lobe (46): absent → present
Clypeus, median proyection (60): present → absent
Gill on abdominal segment I (67): single → bilamellate

Node 19 (Campsurinae):
Char. 2: 1.150–1.393 → 1.987
Char. 6: 10.000–12.000 → 6.000–9.000
Char. 7: 1.400–1.950 → 1.000
Char. 10: 0.241–0.250 → 0.205–0.222
Char. 13: 11.667 → 15.000–16.667
Char. 20: 1.322–1.476 → 1.226–1.294
Male foretarsite 1(form) (29): subquadrate → subovate
FW vein IMP (33): free → IMP connected to MP1
FW Cu sector, ICus join hind margin on (35): both near or anteriad to tornus → ICu1 close to tornus, ICu2 on basitornal margin
FW, max number of cells closed by imv (36): >3 → 0
Styliger plate, median plate (41): present → absent
Penial arm articulation (43): tergite IX → S IX and base of pedestal
Nymph, dorsum of head with velvet zone (68): absent → present

Node 20 (Campsurinae + Asthenopodinae):
No synapomorphies in the present analysis but if the root is duplicated, then the following changes define this grouping:
Char. 2: 1.081 → 1.150–1.393
Char. 3: 1.008 → 0.370–0.371
Char. 4: 1.912 → 1.983–2.027
Char. 6: 16.000 → 10.000–12.000
Char. 7: 4.188 → 1.400–1.950
Char. 9: 0.650 → 0.733–1.164
Char. 19: 0.778 → 0.287–0.319
Char. 27: 4.145 → 3.688–4.000
Short distal segments on forceps (39): present → absent
Penes form (44): fused basal 2/3 diverging → apices converging medially or curved ventrally
Female sternum VIII, sockets (50): absent → present
Nymphal mandibular tusks, smaller submedian tubercle (64): absent → present

Node 21 (*Povilla* + *Languidipes*):
Char. 2: 1.529–1.556 → 1.661–1.736
Char. 16: 2.118–2.174 → 4.300–7.000
FW veins MP2 and IMP (34): subequal → MP2 shorter than IMP
Pedestal, form (40): similar width along its length → much narrower basally
Penes form (44): apices converging medially or curved ventrally → apices diverging or straight, blade-like
Nymphal left mandibular tusk, apical denticles (61): 3 → 4

Node 22 (*Asthenopus* + *Povilla* + *Lanquidipes*):
Char. 9: 1.098–1.164 → 1.369–1.653
Char. 13: 6.333–7.692 → 5.385–5.789
Char. 18: 2.647 → 2.714–2.913
Female sternum VIII, anteromedian keel (49): short and blunt → long and slender
Female sternum VIII, anteromedian sockets (53): larger extending somewhat posteriorly from keel's base → small almost indistinct at each side of the keel
Node 23 (gilliesi + node 22)
Char. 2: 1.150–1.393 → 1.529–1.556
Char. 7: 1.400–1.429 → 0.700–1.167
Char. 13: 7.833–8.889 → 6.333–7.692
Char. 18: 2.188 → 2.647
FW, max number of cells closed by imv (36): >3 → 1–2
Node 24 (Asthenopodinae except *Asthenopodes*):
Char. 0: 1.211–1.765 → 1.909–1.923
Char. 3: 0.364–0.371 → 0.339–0.347
Char. 5: 2.167–2.271 → 2.302–2.308
Char. 12: 5.455 → 4.500–5.200
Char. 18: 2.000–2.071 → 2.188
Char. 21: 1.625–1.833 → 1.231–1.375
Char. 22: 3.750–4.000 → 4.083–4.333
Char. 24: 1.625–1.639 → 1.577
Gill on abdominal segment I (67): single → bilamellate
Node 25 (Asthenopodinae):
Char. 1: 0.400–0.533 → 0.645–0.667
Char. 13: 11.667 → 7.833–8.889
Char. 19: 0.287–0.319 → 0.169–0.184
Char. 27: 3.688–4.000 → 2.196–2.412
Female sternum VIII, anteromedian keel (48): absent → present
Eggs, chorionic plates(large disk-like) (54): absent → present
Eggs, chorionic plates(small disk-like) (57): absent → present
Nymphal left mandibular tusk, apical denticles (61): 1 → 3
Nymphal right mandibular tusk, apical denticles (62): 1 → 2
Nymphal mandibular tusks, small basal tubercle on outer dorsal surface (66): absent → present
Nymph, occipital region (69): not strongly developed, flat → strongly expanded, convex
Nymphs, denticles on fore tarsal claws (70): absent → present
Node 26 (*Asthenopodes traverae* + *A. picteti*):
Char. 1: 0.645–0.667 → 1.205–1.320
Char. 6: 10.000–12.000 → 14.000–16.000
Char. 12: 6.333–6.667 → 8.100
Char. 13: 7.833–8.889 → 6.714–7.400

Char. 14: 2.380–2.500 → 2.600–2.667
Char. 15: 5.417–5.769 → 5.818–5.909
Char. 23: 7.000–13.000 → 6.000
Styliger plate, median plate, shape of hind margin (42): straight or convex → markedly concave (lateral margins projected posteriorly)

Node 27 (*Asthenopodes*):
Char. 0: 1.211–1.765 → 1.133–1.188
Char. 5: 2.167–2.271 → 1.983–2.047
Char. 10: 0.241–0.250 → 0.337–0.366
Char. 12: 5.455 → 6.333–6.667
Apex of male foretarsal claw (31): not or slightly expanded → strongly expanded (apex 3 times wider than stalk)
Pedestal, form (40): similar width along its length → much narrower basally

Node 28 (*A. angelae* + *A. magnus*):
Char. 13: 5.385–5.789 → 6.154–6.231
Cleft between large and small penile lobes (47): long, opened → short, closed

Node 29 (*A. curtus* + *A. angelae* + *A. magnus*):
Char. 2: 1.529–1.556 → 1.456–1.457
Char. 3: 0.339–0.347 → 0.286–0.298
Char. 19: 0.292 → 0.323–0.353

Node 30 (*A. hubbardi* + *A. curtus* + *A. angelae* + *A. magnus*):
Char. 9: 1.369–1.653 → 1.730–1.850
Char. 14: 2.077–2.476 → 1.955–2.000
Char. 15: 5.417–5.778 → 3.846–4.500
Char. 17: 1.125–1.300 → 1.600–1.667

Node 31 (*Asthenopus* s.s.):
Char. 1: 0.645–0.652 → 0.584–0.587
Char. 7: 0.700–1.167 → 0.222–0.300
Male foretarsite 1(form) (29): subquadrate → subrectangular
Penes, apical spine (45): absent or slightly marked as a continuation of the penes → present, distinctly protruding from the penes
Cleft between large and small penile lobes (47): absent → long, opened
Clypeus, median proyection (60): present → absent

Node 32 (*Tortopsis* + *Tortopus*):
Char. 2: 1.987 → 2.044–2.268
Char. 6: 6.000–9.000 → 1.000
Char. 7: 1.000 → 0.000
Char. 15: 5.417–5.769 → 6.364
Fore tarsite 5 apex (30): blunt or transv ridge → trilobed
HW, anal area (38): with any or few crossveins → with many crossveins forming a network
Female sternum VIII, sockets position (51): anterior → submedian

Appendix 3

Matrix of characters and states. Ready to use in TNT.

nstates cont ;
xread
'Asthenopodinae'
72 17
&[continuous]
Ephoron 1.211 0.400 0.932-1.081 1.008-1.123 1.857-1.912 1.846-2.167 16.000 4.188 3.000 0.650 0.250 1.273 5.455 11.667 ? ? ? ? ? 0.778-0.992 1.322-1.551 0.727-1.625 2.000-5.000 ? 1.625 ? ? 4.145
Camp_violaceus 1.765 0.357-0.360 1.758-2.179 0.371-0.436 2.082-2.273 2.236-2.346 2.000-6.000 1.000-1.667 1.000-3.000 1.580-1.830 0.205-0.261 1.333-1.440 ? 19.000-23.000 2.308-2.552 2.727-2.846 1.304-1.500 2.600 1.118-1.410 0.287-0.375 1.091-1.300 2.625-3.333 3.000-4.000 ? 1.712 1.542 1.148-1.443 3.688
Povilla 1.571-2.000 0.645-0.755 1.661-1.736 0.316 1.831-2.214 2.095-2.447 1.000-15.000 0.467-0.700 1.000-2.000 1.324-1.801 0.100-0.235 3.333-3.928 3.375-5.429 4.333-7.428 4.400-6.800 4.667-6.800 4.300-7.000 1.300 2.857-4.167 0.068-0.260 1.457-1.750 ? ? 13.000 1.555 1.787 1.439 2.015
Languidipes ? ? 3.174 0.375-0.464 2.447 3.382 5.000 1.667 1.000 1.653 ? ? ? 4.545 ? 9.333 7.000 ? 2.913 0.100 ? ? ? ? ? ? ? ?
picteti 0.838-0.840 1.205-1.350 1.118-1.150 0.355-0.382 1.828-1.983 1.828-1.983 14.000-17.000 2.000-3.353 4.000-6.000 0.595-0.733 0.337-0.373 1.550-1.875 8.100 6.714-7.400 2.737-2.895 8.000-8.696 3.056-3.059 1.083-1.182 1.500-2.250 0.184-0.206 1.383-1.591 1.222-1.516 3.778-5.167 6.000 ? ? ? ?
traverae 1.133-1.192 1.320-1.478 1.022-1.183 0.364-0.406 1.895-1.986 1.957-2.059 16.000-22.000 0.750-1.950 4.000-5.000 0.838-0.890 0.223-0.366 1.310-1.880 11.800 4.667-4.900 2.600-2.667 5.818-5.909 2.065-2.321 1.000 2.000-2.071 0.180-0.203 1.476-1.605 2.364-3.000 2.143-3.667 5.000-6.000 ? ? ? ?
chumuco 1.097-1.188 0.619-0.667 1.393-1.600 0.318-0.440 1.870-2.000 1.892-2.047 9.000-12.000 1.111-2.833 3.000-4.000 0.560-0.710 0.389 1.243-1.286 6.333-6.667 7.833-9.500 2.380-2.500 2.625-3.143 1.833-2.000 2.333-2.667 2.000-2.133 0.089-0.093 1.313-1.413 2.688-3.067 2.500-3.750 14.000-16.000 1.829-2.055 ? 1.258-1.226 1.978-2.412
crenulatus 3.250-4.000 0.741-0.825 1.087-1.150 0.329-0.347 2.027-2.091 2.419-2.654 10.000-14.000 1.400-1.429 2.000-4.000 1.164-1.795 0.241 1.550-2.462 4.286 8.889-9.000 5.909-6.500 5.000-5.417 3.250 0.600-0.684 2.188 ? 1.462-1.677 1.192-1.375 4.083-6.750 4.000-7.000 1.577 ? ? 2.196
gilliesi 1.411-1.909 0.523-0.652 1.556-1.975 0.300-0.350 1.781-2.079 2.054-2.308 4.000-10.000 0.250-1.167 1.000-2.000 0.780-1.098 0.191-0.308 2.143-2.500 4.500-6.143 6.333-7.692 1.905-2.067 3.647-4.706 1.177-1.905 0.944-1.5 2.647 0.169 1.455-1.833 0.892-1.071 2.800-6.167 14.000-16.000 ? ? ? ?

magnus 1.968-2.341 0.554-0.655 1.365-1.456 0.248-0.253 1.870-2.022 2.104-2.302 10.000-22.000 0.091-0.318 0.000-2.000 1.690-3.370 0.207-0.257 1.719-2.400 3.545-6.167 6.154-6.231 2.000-2.222 2.857-2.933 1.905-2.000 1.556-1.667 1.964-2.200 0.323-0.389 1.594-1.781 1.176-1.261 3.286-4.333 4.000-5.000 1.429-1.489 1.714-1.811 1.319-1.396 2.286-2.500
angelae 1.491-1.833 0.592-0.596 1.359-1.635 0.298-0.309 1.889-2.201 2.122-2.560 5.000-11.000 0.000-0.300 1.000-4.000 1.375-2.890 0.218-0.275 2.083-2.190 3.000-4.400 6.500-7.100 1.958-2.282 4.000-4.909 2.174-3.067 1.429-2.000 2.222-2.889 0.250-0.353 1.533-1.667 1.111-1.320 3.125-4.500 3.000-5.000 1.511-1.624 1.741-1.950 1.389-1.427 2.171-2.303
hubbardi 1.923-2.133 0.530-0.587 1.529-1.769 0.339-0.355 2.000-2.091 2.300-2.600 4.000-14.000 0.143-0.500 2.000-3.000 1.730-1.850 0.262-0.283 2.100 3.571-5.125 4.692-6.000 1.714-1.955 3.583-4.500 1.870-2.118 1.600-1.800 2.714 0.292 1.448-1.741 1.111-1.318 3.143-4.500 3.000-8.000 ? ? ? ?
guarani 1.926-1.974 0.429-0.579 1.381-1.765 0.268-0.354 1.744-2.000 1.829-2.500 4.000-6.000 0.000 1.000-2.000 1.170-1.369 ? 2.150 5.200 4.833-5.789 2.077-2.476 5.778-6.000 2.080-2.600 1.125 3.125 ? 1.250-1.600 1.231 4.333 3.000-8.000 1.408 1.818 1.351 2.630
curtus 1.550-1.751 0.584 1.365-1.457 0.248-0.286 1.870-2.022 2.104-2.341 18.000-25.000 0.222-0.316 0.000-1.000 2.100-2.950 0.171 1.964-2.320 3.222 5.385 1.786 3.846 2.273 2.167 2.706-3.059 0.378-0.500 1.419-1.545 1.128-1.341 4.000-6.286 3.000-5.000 1.573-1.729 1.714-2.371 1.395-1.618 2.182-2.419
Camp_vulturorum 1.864 0.395 1.987 0.370 1.983 2.271 9.000 1.000 1.000 1.825 0.168 1.000 ? 15.000 1.415 5.769 ? 1.071 1.146 0.257-0.319 1.224-1.294 1.833 ? ? 1.825 1.369 1.117-1.237 3.214
Tortopus 1.786 0.536-0.600 2.044-2.268 0.352 ? 2.190-2.514 1.000 0.000 2.000 1.500 0.194 ? ? 16.667 ? 6.364 ? 1.000 ? 0.277 1.226-1.333 ? ? ? 1.639 1.494 1.283 4.000
Tortopsis 1.300 0.533 2.714 0.375-0.417 2.169 2.568 0.000-1.000 0.000 1.000-3.000 0.926 0.222 ? ? 18.700 ? 11.923 ? 1.077 1.407 0.321-0.350 1.147-1.171 ? ? ? 1.562 ? 1.239 4.771

```
&[numeric]
Ephoron          1000012002000000020000-0---0--0-1121000010100
Camp_violaceus   0200300120020 1?110120-10000--0-0021011001101
Povilla          0000100011011000000011100110-0-0100110100011
Languidipes      00-01000110111?-0000-----------?10011011001-
picteti          1-011110020210101000101002 10-102------------
traverae         1-011110020210101000101002110102------------
chumuco          1-011110020210001000101002110102010010110010
crenulatus       2000101002020000100010100211110211000010 0011
gilliesi         0000111010020000101110100210-102------------
magnus           0100111011020000111111110011110-2010110100011
angelae          0100111011020000111111110011110-2010110100011
hubbardi         0100111011020000111211100111 10-2------------
guarani          0100111011020000111211100111011201011010 0011
curtus           0100111011020000111211100111 10-2010110100011
Camp_vulturorum  02003001200201-1-0100-10020--0-0021011001101
Tortopus         02102001211101-110000-11020--0-0121012011101
Tortopsis        02102001211101-111000-11120--0-0121002011101
; cc - . ;
proc/;
```

ZooKeys 478: 129–137 (2015)
doi: 10.3897/zookeys.478.8995
http://zookeys.pensoft.net

RESEARCH ARTICLE

A peer-reviewed open-access journal
ZooKeys
Launched to accelerate biodiversity research

First record of the genus *Gratia* Thomas (Ephemeroptera, Baetidae) from China with the description of a new species

Weifang Shi[1], Xiaoli Tong[1]

1 *Department of Entomology, College of Natural Resources & Environment, South China Agricultural University, Guangzhou 510642, China*

Corresponding author: *Xiaoli Tong* (xtong@scau.edu.cn)

Academic editor: *E. Dominguez* | Received 9 November 2014 | Accepted 8 January 2015 | Published 28 January 2015

http://zoobank.org/BC768349-31E1-4F60-A853-0203B076E309

Citation: Shi W, Tong X (2015) First record of the genus *Gratia* Thomas (Ephemeroptera, Baetidae) from China with the description of a new species. ZooKeys 478: 129–137. doi: 10.3897/zookeys.478.8995

Abstract

A new species of Baetidae, *Gratia baibungensis* **sp. n.**, is described and illustrated based on nymphal stage collected from the southeastern Tibet (Xizang) and the genus is reported for the first time from China. This new species can be readily differentiated from its congeners by the absence of a protuberance on the posterior margin of the abdominal tergum X, glabrate simple submarginal setae on the labrum, and the posterior margin of sterna VI–IX having much longer spatulate setae.

Keywords

Mayfly, *Gratia*, new species, Oriental Region, Eastern Himalayas, Tibet

Introduction

The Eastern Himalayas is situated between the west of central Nepal and east of Myanmar, through southeastern Tibet in China to northeastern India. The area has been declared as a biodiversity hotspot (Myers et al 2000, CFPF 2005). Historically, reports of freshwater macroinvertebrate fauna from this region are abundant (Allen et al 2010). However, in southeastern Tibet, as a part of the Eastern Himalayas, the aquatic insect

fauna (mayfly in particular) remains rarely studied. You (1987) reported 13 mayfly species in Tibet, of which only 4 species were collected from the southeastern Tibet. Since then, the mayfly fauna of this region has received little attention.

In 2010, we conducted an exploration on the aquatic insect fauna in southeastern Tibet. The preliminary results revealed that mayflies have high species diversity, especially in Baetidae. Except for some species which are probably endemic to this region, most of mayfly fauna elements belong to the Indo-Malayan ecozone.

The genus *Gratia* was originally erected by Thomas (1992) based on the nymphal stage from Chiang Mai, Thailand, with *G. sororculaenadinae* Thomas as the type species. Later, Boonsoong et al (2004) found a second species of the genus, *G. narumonae* Boonsoong & Thomas, from Thailand and revised the generic concept. The present study deals with an undescribed species of the genus *Gratia* collected from southeastern Tibet.

Materials and methods

Nymphs were collected by kick-net from the riffles with cobble and gravel substrates in a 2nd-order shallow stream (approximately 1 m wide) at the Baibung Town, Medog County, southeastern Tibet. The specimens were directly placed into vials with 95% ethanol in the field and transferred into glass vials with 85% ethanol in the laboratory for preservation. Some were dissected under the stereomicroscope and were mounted on slides in Hoyer's solution for examination and illustration. Mounted structures were examined and photographed under the microscope with a digital camera attached, and the images subsequently processed with Adobe Photoshop CS6. Type specimens are housed in the Collection of Aquatic Insects and Soil Animals, Department of Entomology, College of Natural Resources and Environment, South China Agricultural University, Guangzhou, China. The comparative specimens of *G. sororculaenadinae* and *G. narumonae* were provided by Dr Boonsoong of Kasetsart University, Thailand.

Taxonomy

Key to mature nymphs of *Gratia* species

1 Posteromedial dorsal protrusion presents on abdominal terga I to IX, submarginal setae on labrum simple and glabrate [China] ..... ***G. baibungensis* sp. n.**

– Posteromedial dorsal protrusion presents on abdominal terga I to X..... **2**

2 All but the innermost two submarginal setae on labrum branched, second segment of labial palp with an inner-apical lobe [Thailand]..... ..... ***G. narumonae* Boonsoong & Thomas**

– All but the innermost two submarginal setae on labrum feathered, second segment of labial palp without an inner-apical lobe [Thailand] .... ***G. sororculaenadinae* Thomas**

***Gratia baibungensis* sp. n.**
http://zoobank.org/B4B9E4BB-FD13-47BB-8315-D96F4196B0EA

Material examined. Holotype. 1 mature nymph in ethanol, China, Tibet, Medog County, Baibung Town (29°14.65'N, 95°10.59'E, alt. 860m), 29.ix.2010, coll. Xianfu Li.

Paratypes. 2 nymphs on slides and 2 nymphs in ethanol, same data as holotype.

Other material examined. *Gratia sororculaenadinae* Thomas: 3 mature nymphs, Thailand, Chiang Mai, Mae Hlang Stream, 16.i.2007; *G. narumonae* Boonsoong & Thomas: 3 mature nymphs, Thailand, Loei Province, Tarn Sawan waterfall, 12.ii.1999.

Description. Mature nymph (Fig. 2a). Body length 4–4.5 mm, cerci slightly longer than body length, terminal filament only one segment.

Head. Capsule yellowish-brown with transverse irregular markings on vertex and frons. Antennae approximately 1.5 times the width of head; dorsal surface of scape and pedicel scatter with fine setae, and with 3–4 and 2–3 scale-like setae respectively (Fig. 1a). Labrum (Fig. 1b) rectangular, approximately 2.0 times wider than long; anteromedial notch deep with a small rounded lobe at the base, and each side with one medial long seta and a row of 7–8 robust, simple and glabrate submarginal setae sublaterally, fine and simple setae scattered posteriorly; ventrally bordered with feathered setae along the anterior margin and a distomedial arc of very fine setae. Left mandible (Fig. 1d): incisors fused with 7 denticles, prostheca robust with 5 blunt and 3–4 acute denticles apically. Right mandible (Fig. 1e): incisors fused with 6 or 7 denticles, inner incisor margin smooth without fine setae, prostheca with denticles apically and distinctly slender than the one on the left mandible, edge between prostheca and molar smooth with no serration, molar plated-like. Hypopharynx with lingua rounded and superlinguae broadly truncate, covered with abundant fine setae (Fig. 1c). Maxillae (Fig. 1f) with one canina and three dentisetae on crown of galealacinia, a row of 4 long basal setae and one short bristle-like hump seta on basis of galealacinia; maxillary palpus 2-segmented and subequal in length, terminal segment with a small tip at apex and slender than basal segment. Labium (Fig. 1g): glossae slightly shorter than paraglossae, with a row of 9 stout setae along the inner margin dorsally and 2 long robust blunt setae at the apex; paraglossae approximately 2.0 times wider than glossae, with two rows of setae ventrally and 2 stout acute setae along the inner margin dorsally; labial palpus 3-segmented, terminal segment conical with a distinctive tip at apex (Fig. 1h); the 2nd segment with an inner-apical lobe and an oblique row of 2–3 setae dorsally, the articulation between the 2nd and terminal segments obscure; dorsal surface with numerous pores on the 1st segment.

Thorax. Coloration pale brown with indistinct darker patterns. Surface of pronotum with four blunt tubercles. Metanotum with a finger-like protuberance medially (Fig. 1j). Hind wing pads reduced, approximately 2 times longer than wide (Fig. 1j). Legs (Fig. 1i) yellow brown with darker markings. Femora of all legs with a regular row of multilaterally ciliate bristles along dorsal margin, approximately 1/2 as long as femur width (Fig. 1l); stout short submarginal scale-like setae present; villopore present. Tibi-

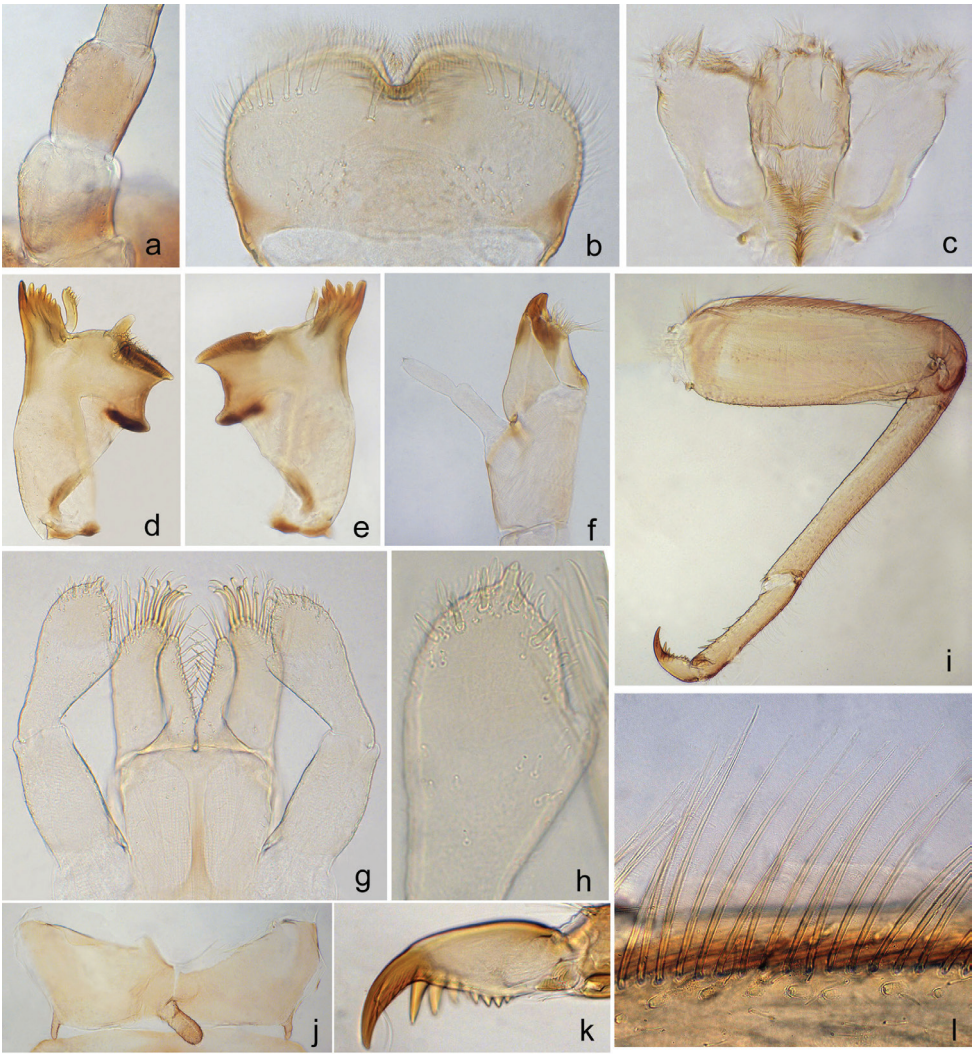

Figure 1. *Gratia baibungensis* sp. n. **a** antennal scape and pedicel **b** dorsal view of labrum **c** hypopharynx **d** left mandible **e** right mandible **f** left maxilla **g** labium **h** ventral view of labial palpus **i** foreleg **j** hindwing pad **k** hind claw **l** ciliate bristles on dorsal margin of femur.

ae subequal to femur in length; irregular rows of simple fine setae present on the dorsal margin, with length subequal to the width of tibia, submarginal stout setae present. Tarsi half the length of tibia, with irregular row of sparse fine simple setae on dorsal margin and 5–6 robust point setae on ventral margin increasing in length towards the apex, tarsus of all leg without long ventral subapical bristle. Claw with one row of 8–9 denticles and a pair of bowed subapical bristles (Fig. 1k). All legs lack coxal gills.

Abdomen. Generally yellowish-brown. Mediodorsal posterior margin of terga I–IX each with a finger-like protuberance, successively decreasing in length backwardly (Figs 2a, d): length of protuberance subequal to the tergum length on segments I–IV,

Figure 2. *G. baibungensis* sp. n. (**a–e, g, h**), *G. narumonae* (**f**) and *G. sororculaenadinae* (**i**). **a** habitus of lateral view **b** protrusion on abdominal terga VI–VII **c** paraproct **d** abdominal terga I–X **e** inner marginal bristles on cerci **f** inner marginal bristles on cerci **g** terminal filament **h** posterior margin of abdominal sterna VIII **i** sterna VII–VIII.

and approximately one third of tergum length on segment IX; surface of protuberance scattered with scale-like setae (Fig. 2b). Terga surface with scattered scale-like and fine setae, posterior margin with blunt denticles. Surface of sterna scattered with round

Table 1. Comparison of morphological characters of the three *Gratia* species.

Character	*G. baibungensis* sp. n.	*G. narumonae*	*G. sororculaenadinae*
Body length	4–4.5 mm	6.4 mm	4.7–5.8 mm
Number of scale-like setae on scape and pedicel	5–7	7–9	Approx. 30
Number of submarginal setae on labrum	1+(7–8)	1+(10–12)	1+(15–16)
Shape of submarginal setae on labrum	Simple and glabrate	Branched	Feathered
Width/length ratio of labrum	1.96	1.92	1.93
Inner-apical lobe on 2nd segment of labial palp	Present		Absent
Number of denticles on claw	8–9	8–10	7–9
Finger-like protuberance on terga	I–IX	I–X	
Ratio of scale-like setae length/ width on posterior sterna VI–IX.	2.0–4.0	1.0–2.0	
Number of scale-like setae on the inner margin of paraproct	9–14	11–16	20–25
Bristles on inner margin of cerci	Each segment with 1–4 bristles (increasing in number towards terminal)*		

* Boonsoong et al (2004) stated that cerci are devoid of bristles in both *Gratia* species, but according to our examination of the specimens of the two Thai *Gratia* species provided by Dr Boonsoong, bristles on cerci could be observed under the microscope (Fig. 2f).

scale-like setae and each sternum with a pair of friction pads on anterolateral area; posterior margin on sterna VI–IX each with a row of continuous long spatulate setae which length approximately 3–4 times the width in female nymphs (Fig. 2h) and 2–3 times the width in male nymphs. Paraproct (Fig. 2c) with numerous pores and fine bristles on the surface and 9–14 scale-like setae along the inner margin. Gills on segments I–VII, oval and untracheated, surface scattered with numerous pores, margin smooth with blunt and fine simple setae. Median caudal filament reduced to one segment (Fig. 2g), each segment of cerci on inner margin with 1–4 (increasing in number towards terminal) swimming bristles (Fig. 2e).

Adult. Unknown.

Etymology. This new species is named after Baibung, the small town near the type locality.

Distribution. China (southeastern Tibet).

Remarks. Comparison with Thai specimens of two *Gratia* species (Table 1) shows that this new species can be readily distinguished from other members of the genus by the absence of a protuberance on tergum X. In appearance, the new species is most similar to *G. narumonae* Boonsoong & Thomas, but it can be readily distinguished from the latter by the following characters:

1) all dorsal submarginal setae on labrum are glabrate and simple (vs. all but two innermost setae are branched and fimbriate in *G. narumonae*);

2) posterior margin on sterna VI–IX each with a row of continuous long spatulate setae approximately 2–4 times longer than wide (Fig. 2h), but only 1.5–2 times in *G. narumonae* (cf. Fig. 2i);
3) gill margin with blunt setae, absent in *G. narumonae*.

Habitat. Nymphs of *G. baibungensis* sp. n. inhabit the riffles area with cobble and gravel substrates in a 2nd-order shallow subtropical stream (approximately 1 m wide). However, both Thai species are found clinging to rock surfaces of tropical cascades: *G. sororculaenadinae* lives in limimadicolous zones and *G. narumonae* is more abundant in petrimadicolous zones.

Discussion

The genus *Gratia* resembles *Jubabaetis* Müller-Liebenau in appearance by the presence a regular row of ciliate bristles on the dorsal margin of the femur, the protuberance on the posterior margin of abdominal terga, and the terminal filament reduced to one segment (Müller-Liebenau 1980). However, the shield-like prolongation on the frontal margin of head and the unique mouthpart characters in *Jubabaetis* can be easily distinguished from those of *Gratia.* Similar ciliate bristles on the dorsal margin of the femur are also found in the genus *Acentrella* Bengtsson, but it can be easily separated from *Gratia* by the terminal segment of the labial palpus, which is widely rounded and slightly truncate, devoid of subapical bristles on claw, and the abdominal terga without mediodorsal protrusions.

In comparison with the related genera, the genus *Gratia* is most closely related to the genus *Baetiella* in nymphal stages by sharing many similar morphological characters (Table 2), but the peculiarity of *Gratia* is that the femur on the dorsal margin has a regular row of multilaterally ciliate bristles (unlike *Baetiella* whose femur on the dorsal margin bears a densely irregular row of glabrate bristles, especially in the basal area of femur). Boonsoong et al (2004) summarized the generic diagnosis of *Gratia*; in the present study, the nymphal generic diagnostic is modified for *Gratia* as follows:

(1) submarginal setae on labrum branched and fimbriate or simple and glabrate;
(2) hind wing pads reduced or vestigial;
(3) terminal segment of labial palpus conical with a tip on apex;
(4) femora on dorsal margin with a regular row of ciliate (feathered) bristles, tibiae and tarsi with irregular row of fine glabrate setae;
(5) femoral villopore present;
(6) claws with a pair of subapical setae;
(7) abdominal terga I–X (sometimes on I–IX) each with a finger-like protrusion on posterior margin, sterna and paraproct with conspicuous scale-like setae;
(8) terminal filament reduced to one segment, inner margin of cerci with sparse bristles.

Table 2. Summary of diagnostic characters of the genera *Gratia* and *Baetiella.*

Character	*Gratia*	*Baetiella*
Antennae length	Approx. 1.5 times width of head	
Scale-like setae on scape and pedicel	Present	Absent or present
Submarginal setae on labrum	Branched and fimbriate or simple and glabrate	Simple and glabrate
Shape of terminal segment of labial palpus	Conical with a tip on apex	Conical with or without a tip on apex
Hind wing pads	Vestigial	Vestigial or well developed
Metanotum with a protrusion medially	Present	Present or absent
Bristles on dorsal margin of femur	In a regular row with ciliate (feathered) bristles	In a dense and irregular row with glabrate bristles
Femoral villopore	Present	
Ventral subapical bristle on tarsus	Absent	
Claw with a pair of bowed subapical bristles	Present	
Posteromedial dorsal protrusion on terga	Single, on I–X (or I–IX)	Single or double or absent, at most on I–IX
Median caudal filament	One segment (conical)	One to multi-segment

Acknowledgements

This work was supported by the National Natural Sciences Foundation of China (No. 30170121). Special thanks are due to Dr Boonsatien Boonsoong for providing the specimens of two *Gratia* species. The authors are grateful to Xianfu Li for collecting the specimens and to anonymous referees for their constructive comments.

References

Allen DJ, Molur S, Daniel BA (2010) The Status and Distribution of Freshwater Biodiversity in the Eastern Himalaya. IUCN, Cambridge, UK and Gland, Switzerland, and Zoo Outreach Organisation, Coimbatore, India. https://portals.iucn.org/library/efiles/documents/RL-2010-001.pdf

Boonsoong B, Thomas A, Sangpradub N (2004) *Gratia narumonae* sp. n., a new mayfly from Thailand [Ephemeroptera, Baetidae]. Ephemera 4(1): 1–9. doi: 10.1051/limn/2012012

Critical Ecosystem Partnership Fund (2005) Ecosystem Profile: Eastern Himalayas Region, 100 pp. http://www.cepf.net/Documents/final.ehimalayas.ep.pdf

Müller-Liebenau I (1980) *Jubabaetis* gen. n. and *Platybaetis* gen. n., two new genera of the family Baetidae from the Oriental region. In: Flannagan JF, Marshall KE (Eds) Advances in Ephemeroptera Biology. Plenum Press, New York, 103–114.

Myers N, Mittermier RA, Mittermier CG, da Fonseca GAB, Kent J (2000) Biodiversity hotspots for conservation priorities. Nature 403: 853–858. doi: 10.1038/35002501

Thomas A (1992) *Gratia sororculaenadinae* n. gen., sp. n., Ephéméroptère nouveau de Thaïlande (Ephemeroptera, Baetidae). Bulletin de la Société d'Histoire naturelle de Toulouse 128: 47–51.

You DS (1987) A preliminary study of Xizang Ephemeroptera. In: Zhang SM (Ed.) Agricultural insects, spiders, plant diseases and weeds of Xizang (I). The Tibet People's Publishing House, Lhasa, 29–36.

ZooKeys 478: 139–146 (2015)
doi: 10.3897/zookeys.478.9048
http://zookeys.pensoft.net

RESEARCH ARTICLE

A peer-reviewed open-access journal
ZooKeys
Launched to accelerate biodiversity research

A new species of the genus *Seticornuta* Morley (Hymenoptera, Ichneumonidae, Metopiinae) from South Korea

Jin-Kyung Choi[1], Janko Kolarov[2], Jong-Wook Lee[1]

1 *Department of Life Sciences, Yeungnam University, Gyeongsan, 712-749, Korea* **2** *Faculty of Pedagogy, University of Plovdiv, 24 Tsar Assen Str., 4000 Plovdiv, Bulgaria*

Corresponding author: *Jong-Wook Lee* (jwlee1@ynu.ac.kr)

Academic editor: *G. Broad* | Received 1 December 2014 | Accepted 12 January 2015 | Published 28 January 2015

http://zoobank.org/0274C600-73A0-4970-BC30-C031315CAC6F

Citation: Choi J-K, Kolarov J, Lee J-W (2015) A new species of the genus *Seticornuta* Morley (Hymenoptera, Ichneumonidae, Metopiinae) from South Korea. ZooKeys 478: 139–146. doi: 10.3897/zookeys.478.9048

Abstract

Old World species of the genus *Seticornuta* Morley are reviewed. Seven species of this genus were recorded worldwide, but only one species, *S. albopilosa* (Cameron), was known from the Old World. Here, we report one new species, *S. koreana* **sp. n.**, from South Korea, and redescribe the other known Old World species, *S. albopilosa*, with photographs.

Keywords

Eastern Palaearctic, Oriental, *Seticornuta koreana*, South Korea, taxonomy, key

Introduction

Seticornuta Morley is a rarely collected genus belonging to the subfamily Metopiinae. It is a small group, consisting of seven known extant species worldwide. Until now only one species, *S. albopilosa* (Cameron, 1907), has been recorded from the Oriental and Eastern Palaearctic regions. *Seticornuta apicalis* (Cresson, 1864) and *S. terminalis*

(Ashmead, 1896) are only known to occur in North America, *S. altamirae* Gauld & Sithole, 2002 and *S. cryptica* Gauld & Sithole, 2002 in Costa Rica, *S. cortesi* Porter, 1998 in Chile, and *S. jacutinga* Araujo & Penteado-Dias, 2012 from Brazil. In this study, we describe a new species, *S. koreana* Lee & Choi, sp. n., from South Korea. We also provide a redescription and photos of *S. albopilosa*, and a key to the Old World *Seticornuta* species.

Materials and methods

Materials used in this study were collected by sweeping and Malaise trapping, after which they were deposited in the animal systematic laboratory of Yeungnam University, Gyeongsan, South Korea (YNU). Specimens were examined using an AxioCam MRc5 camera attached to a stereo microscope (Zeiss SteREO Discovery. V20; Carl Zeiss, Göttingen, Germany), processed using AxioVision SE64 software (Carl Zeiss), and optimized with a Delta imaging system (i-solution, IMT i-Solution Inc. Vancouver, Canada) Measurements are reported for the holotype followed by variation in other specimens in brackets.

Abbreviations are as follows: **NHM**, The Natural History Museum, London, United Kingdom; **ZSI**, Zoological Survey of India, Calcutta, India; **GG**, Gyeonggi-do; **CN**, Chungcheongnam-do; **GB**, Gyeongsangbuk-do; **GN**, Gyeongsangnam-do.

Results

Genus *Seticornuta* Morley, 1913

Megatrema Cameron 1907: 468. Type species: *Megatrema albopilosa* Cameron, by monotypy. Junior homonym of *Megatrema* Leach

Seticornuta Morley 1913: 310. Type species: *Seticornuta albicalcar* Morley (= *albopilosa* Cameron), by original designation.

Diagnosis. *Seticornuta* species are moderate sized about 5–12 mm and generally blackish or black and yellow. Mandibles not twisted; labrum exposed when mandibles closed (Fig. 3A). Lower face moderately convex; upper face produced upwards into a small tooth between bases of antennae, but projection does not reach frons. Posterior part of head moderately to steeply declivous behind posterior ocelli (Fig. 3C, F). Propodeum moderately short, rather flat and more abruptly declivous posteriorly, with very strong median longitudinal carinae. Tergite I short with strong lateral and median longitudinal carinae. The New World genus *Leurus* is similar but the mandibles of *Seticornuta* species are slenderer and flanged (Gauld et al. 2002). New World species differ from Old World in their smaller size, lower number of antennal flagellomeres and the weakly concave apical margin of the clypeus.

Key to Old World species of the genus *Seticornuta*

1 Antennal scape and basal flagellomeres reddish brown (Figs 2, 3D–F). Line of combined face and mandible almost square (Fig. 3D). Mesoscutum rounded in lateral view (Fig. 3F). Areola and basal area not separated by carina (Fig. 3J). Spiracles of propodeum linear. Median longitudinal carinae convergent apically (Fig. 3J). Areolet of fore wing with short stalk (stalk shorter than vein 2rs-m; Fig. 3H) ..... ***S. albopilosa*** **(Cameron, 1907)**

– Antennal scape and flagellomeres black (Figs 1, 3A–C). Line of combined face and mandible rounded (Fig. 3A). Mesoscutum steeply sloping (Fig. 3C). Areola and basal area separated by carina (Fig. 3I). Spiracles of propodeum oval. Median longitudinal carinae parallel (Fig. 3I). Fore wing with long stalked areolet (length of stalk as long as vein 2rs-m; Fig. 3G) .... ***S. koreana*** **Lee & Choi, sp. n.**

Seticornuta koreana **Lee & Choi, sp. n.**
http://zoobank.org/86CB4DCD-65BE-4E28-98F1-137AF4848425

Holotype. Female. Fore wing 9.1 mm (8.3–9.5 mm), body 11.3 mm (10.5–12.0 mm), ovipositor sheath 1.0 mm (1.0–1.1 mm) long.

Color. Black. Wings dark brown; front surfaces of fore tibia and tarsus as well as partial apical lower part of fore femur reddish brown.

Morphology. ***Head.*** Face swollen, 1.3 times as long as wide in front view; head strongly narrowed behind eye in dorsal view. Occipital carina strong dorsally and laterally, obsolescent ventrally. Frons smooth with moderately coarse and dense punctures. Inner margin of eye indented a little above antennal socket. Diameter of lateral ocellus equal to shortest distance between ocellus and eye. Flagellum thickened in basal half, tapered to apex, with 47–50 flagellomeres. First flagellomere 1.4 times as long as wide, next flagellomere transverse, and last 6–7 flagellomeres square. Clypeus not separated from face. Combined face and clypeus almost square and lower part of gena below the eye rounded in frontal view (Fig. 3A, dotted line and arrow). Face very coarsely and densely punctate, with distance between punctures 0.3 times as long as their diameter, clypeus with more sparse punctures. Upper half of face strongly protruding in profile (Fig. 3C). Mandible except teeth with moderately dense and coarse punctures. Lower tooth of mandible shorter than upper tooth. Malar space 0.33 times as long as basal width of mandible.

Mesosoma. Flattened, 1.7 times as long as high in lateral view. Pronotum smooth, impunctate, protruding into an acute tooth laterally, in dorsal view (Fig. 3B, dotted line and arrow). Epomia weak. Mesoscutum elongate, with sparse punctures, anteriorly narrowly rounded in lateral view (Fig. 3C, dotted line and arrow), notaulus weak. Scutellum flat, without lateral carinae. Epicnemial carina strong, reaching subtegular ridge. Mesopleuron strongly swollen, with sparse punctures in front half. Submeta-

Figure 1. (Holotype) Habitus of *Seticornuta koreana* Lee & Choi, sp. n. Scale bar = 2.0 mm.

pleural carina lobed. Metapleuron glabrous, impunctate, its lower front ridge strongly projecting as a tooth above mid coxa. Fore wing with petiolate areolet, length of stalk as long as 2rs-m. Hind outer angle of second discoidal cell sharp. Fore wing vein cu-a curved (Fig. 3G). Hind wing with 11 distal hamuli. Nervellus inclivous, intercepted distinctly below middle. Legs very stout. Hind femur coarsely punctate, 2.5 times as long as wide. Ratio between lengths of hind tarsomeres 63:21:18:11:20. Spurs of mid tibia of equal length. Tarsomeres 2–4 of fore leg shorter than wide. Longer spur of hind tibia 0.5 times as long as basitarsus. Propodeum with very strong median longitudinal and apical transverse carinae (Fig. 3I). Combined basal area and area superomedia with parallel sides. Basal area separated from area superomedia by weak carina in some specimens (Fig. 3I). Costula absent. Lateral area punctate except in anterior inner part. Propodeal spiracle 3.0 times as long as wide, joining pleural carina.

***Metasoma*.** Strongly punctate on second to fourth tergites, more weakly on successive following tergites. Median dorsal carinae of first tergite very strong, extending to 2/3 its length. Second tergite 0.7 times as long as wide. Epipleurum of second tergite 1.5 times as long as wide. Ovipositor sheath with long hairs. Metasoma covered with rather long hairs.

Male. Flagellum with 45 flagellomeres. Other characters as in female.

Material examined. Holotype: female, South Korea CN, Daejeon-si, Dong-gu, Daejeon University, 16 May–5 June 2006, J.W. Lee (YNU).

Paratypes. 1 male (YNU), South Korea, Seoul, Achasan, 24 August 1980, K.S. Jang; 1 female (YNU), GG, Yongmunsa, 1 September 1980, K.S. Jang; 1 male (YNU), GG, Sudong, Chukryeongsan, 28 September 1980, J.I. Kim; 1 female (YNU), South Korea CN, Buyeo-gun, Gyuam-myeon, Sumok-ri, 1-15 June 2005, J.W. Lee; 1 female (YNU), CN, Daejeon-si, Dong-gu, Daejeon University, 16 May-5 June 2006, J.W. Lee; 1 male (YNU), GB, Cheongdo-gun Unmun-myeon, Sinwon-ri, Unmunsan, Unmunsa, 17 July 1989, J.W. Lee; 1 male (YNU), GN, Jinju-si, Gajoa-dong, 19-23 June 1989, J.G. Kim

Distribution. South Korea.

Host. Unknown.

Etymology. The specific name is derived from South Korea, the country of the type specimens.

Remarks. The new species is distinguished from *S. albopilosa* by the following characters: antenna entirely black (reddish brown in basal half in *S. albopilosa*) and propodeum with areola separated from area basalis (areola merged with area basalis in *S. albopilosa*).

Seticornuta albopilosa (Cameron, 1907)

Megatrema albopilosa Cameron 1907: 468. Type: male; Type depository: NHM.
Seticornuta albicalcar Morley 1913: 310. Type: female; Type depository: ZSI.

Redescription based on holotype. Male. Fore wing 10 mm, body 13.0 mm.

Color. Black. Antennal scape and basal 1–14 flagellomeres reddish brown; wings dark brown; fore leg reddish brown, mid and hind legs blackish brown; tegula dark brown.

Morphology. *Head*. Face swollen, 1.2 times as long as wide in frontal view. Occipital carina strong from above and laterally. Frons with moderately coarse and dense punctures. Diameter of lateral ocellus equal to distance between ocellus and eye. Flagellum thickened in basal half, tapered to apex, with 42 + (antenna broken) flagellomeres. First flagellomere as long as wide, next flagellomere transverse and last several flagellomeres square. Clypeus not separated from face. Face moderately punctate, distance between punctures equal to their diameter. Malar space 0.6 times as long as basal width of mandible. Gena acuminate in frontal view (Fig. 3D, dotted line and arrow).

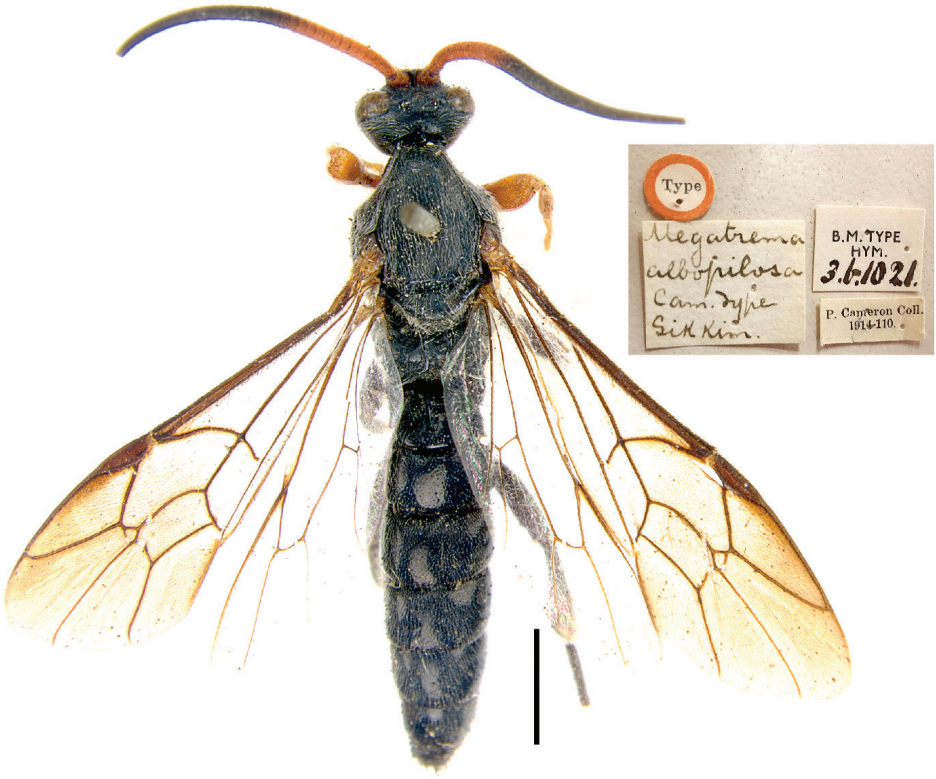

Figure 2. (Holotype) Habitus of *Seticornuta albopilosa*. Scale bar = 2.0 mm.

Mesosoma. Flattened, 2.0 times as long as high in lateral view. Lower part of pronotum smooth, impunctate, epomia weak. Pronotum rounded in dorsal view (Fig. 3E, dotted line and arrow). Mesoscutum elongate with sparse punctures, rounded in lateral view (Fig. 3F, dotted line and arrow), notaulus weak. Scutellum flat with lateral carinae. Epicnemial carina strong, reaching subtegular ridge. Areolet of fore wing present, with stalk shorter than vein 2rs-m; fore wing vein cu-a curved (Fig. 3H). Hind wing with 11 distal hamuli. Nervellus inclivous, intercepted distinctly below middle. Legs very stout. Hind femur coarsely punctate, 3.0 times as long as wide. Spurs of mid leg with of equal length. Tarsomeres 2–4 of fore leg shorter than wide. Propodeum with very strong median longitudinal and apical transverse carinae. Combined basal area and area superomedia convergent apically. Basal area not separated from carina. Costula absent. Propodeal spiracle 3.7 times as long as wide, joining pleural carina.

Metasoma. Median dorsal carinae of first tergite very strong, extending to 2/3 its length. Second tergite 0.7 times as long as wide. Metasoma covered with rather long hairs.

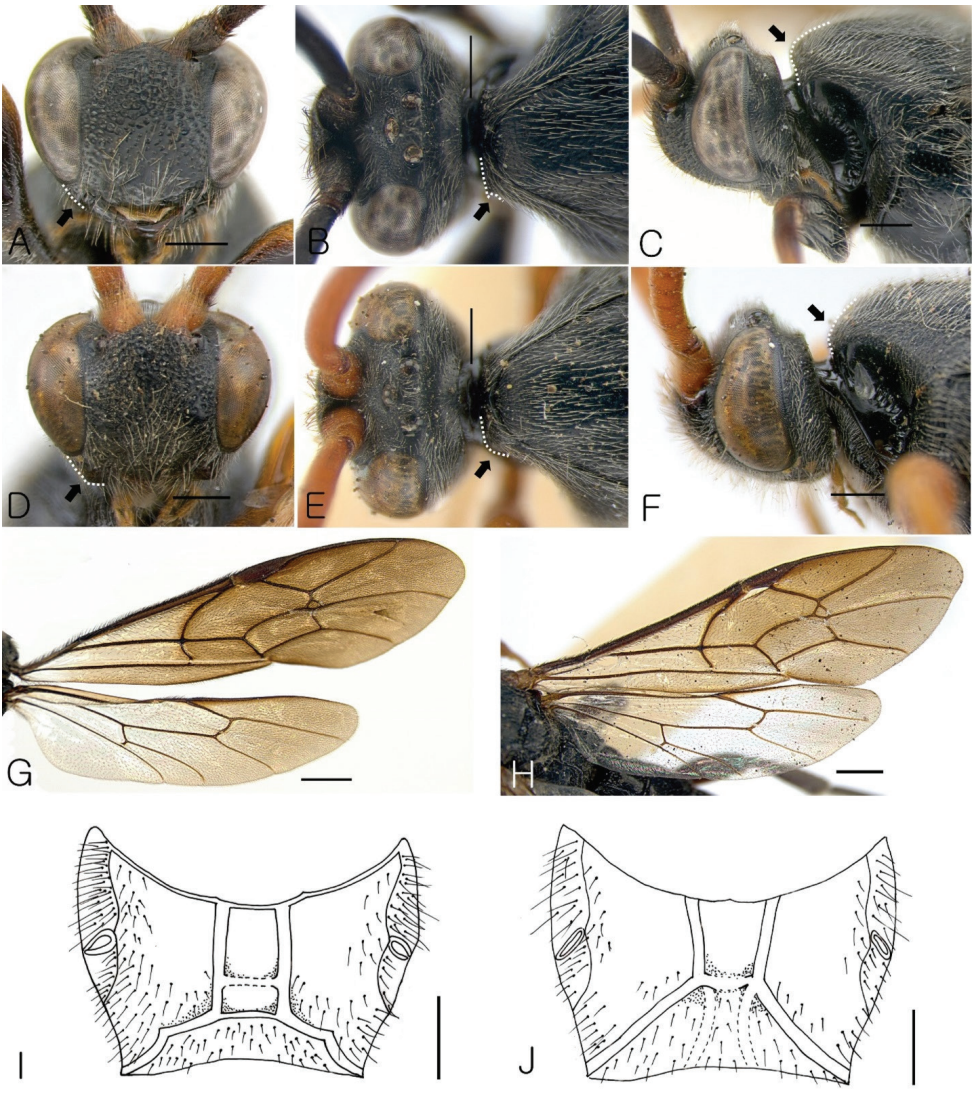

Figure 3. (**A–C, G, I**) *Seticornuta koreana* Lee & Choi, sp. n.; **A** Head in frontal view **B** Head in dorsal view **C** Head in lateral view **G** Wings **I** Propodeum (**D–F, H, J**) *Seticornuta albopilosa* **D** Head in frontal view **E** Head in dorsal view **F** Head in lateral view **H** Wings **J** Propodeum. Scale bars: **G, H** = 1.0 mm; **A–F, I, J** = 0.5 mm.

Material examined. Holotype: male of *Megatrema albopilosa* (NHM) (Fig. 2).

Distribution. Eastern Palaearctic and Oriental regions: China (Henan), India, Myanmar, Sri Lanka.

Host. Unknown.

Acknowledgements

We are deeply grateful to Dr. Gavin Broad and anonymous reviewers for reviewing this manuscript. We thank Dr. Robert R. Kula and David G. Furth of the Smithsonian Institution National Museum of Natural History, U.S.A., Dr. Kevin A. Williams of the Florida State Collection of Arthropods, Florida Department of Agriculture and Consumer Services, U.S.A., for loaning type specimens from their museums. This work was supported by the 2014 Yeungnam University Research Grant and a grant from the National Institute of Biological Resources (NIBR), funded by the Ministry of Environment (MOE) of the Republic of Korea (NIBR No. 2014-02-004).

References

Araujo CR, Penteado-Dias AM (2012) First record of *Seticornuta* Morley (Hymenoptera, Ichneumonidae, Metopiinae) from Brazil and description of a new species. Brazilian Journal of Biology 72(2): 415–418. doi: 10.1590/S1519-69842012000200025

Ashmead WH (1896) Descriptions of new parasitic Hymenoptera. Transactions of the American Entomological Society 23: 179–234.

Cameron P (1907) On some new genera and species of Ichneumonidae from the Himalayas (Hym.). Zeitschrift für Systematische Hymenopterologie und Dipterologie 7: 466–469.

Cresson ET (1864) Descriptions of North American Hymenoptera in the collection of the Entomological Society of Philadelphia. *Proceedings of the Entomological Society of Philadelphia* 3: 257–321.

Gauld ID, Sithole R, Gómez JU, Godoy C (2002) The Ichneumonidae of Costa Rica. 4. Memoirs of the American Entomological Institute, No. 66, 768 pp.

Morley C (1913) The fauna of British India including Ceylon and Burma, Hymenoptera, Vol.3. Ichneumonidae. London, British Museum, 531 pp.

Porter CC (1998) [Guide to the genera of Ichneumonidae of the Neantarctic region of southern South America.] Guía de los géneros de Ichneumonidae en la región neantártica del sur de Sudamérica. Opera Lilloana 42: 1–234.

Yu DS, Van Achterberg C, Horstmann K (2012) Taxapad 2012, Ichneumonoidea 2011. Database on flash-drive. www.taxapad.com, Ottawa, Ontario, Canada.

ZooKeys 478: 147–148 (2015)
doi: 10.3897/zookeys.478.9063
http://zookeys.pensoft.net

SHORT COMMUNICATION

A peer-reviewed open-access journal
ZooKeys
Launched to accelerate biodiversity research

New substitute name for the genus *Poliocoris* Slater, 1994 (Hemiptera, Heteroptera, Rhyparochromidae)

Dao-Wei Zhang[1], Jing Chen[2]

1 *Key Laboratory of Regional Characteristic for Conservation and Utilization of Zoology Resource in Chishui River Basin; School of life sciences, Zunyi Normal College, Zunyi, Guizhou, P. R. China, 563002* **2** *Zunyi Medical College, Zunyi, Guizhou, P. R. China, 563009*

Corresponding author: *Dao-Wei Zhang* (zhangdaowei2014@sina.com)

Academic editor: *T. Henry* | Received 4 December 2014 | Accepted 15 January 2015 | Published 28 January 2015

http://zoobank.org/40A80A09-7C50-4C47-A360-D1DFA3DA0599

Citation: Zhang D-W, Chen J (2015) New substitute name for the genus *Poliocoris* Slater, 1994 (Hemiptera, Heteroptera, Rhyparochromidae). ZooKeys 478: 147–148. doi: 10.3897/zookeys.478.9063

Abstract

Neopoliocoris **nom. n.**, a new substitute name is proposed for *Poliocoris* Slater, 1994 (Hemiptera: Heteroptera: Rhyparochromidae), preoccupied by *Poliocoris* Kirkaldy, 1910 (Hemiptera: Heteroptera: Pentatomidae). A new combination, *Neopoliocoris umbrosus* (Slater, 1994), **comb. n.** is proposed for *Poliocoris umbrosus* Slater, 1994.

Keywords

Hemiptera, Heteroptera, bugs, homonym, replacement name

Introduction

The purpose of the present paper is to provide a new substitute name for a preoccupied Rhyparochromid name in accordance with the International Code of Zoological Nomenclature (1999). The bug genus *Poliocoris* of the family Rhyparochromidae (Hemiptera: Heteroptera) was established by Slater (1994) for the species *Poliocoris umbrosus* Slater, 1994 from South Africa. We have discovered that the genus name *Poliocoris* is preoccupied and was initially introduced by Kirkaldy (1910) for a stink bug genus of the family Pentatomidae (Hemiptera: Heteroptera), with *Poliocoris amnesis*

Kirkaldy, 1910 as its type species from the USA (Florissant). According to Article 60 of the International Code of Zoological Nomenclature, we propose the new substitute name *Neopoliocoris* **nom. n.** for *Poliocoris* Slater, 1994. The resulting nomenclatural changes are summarized below.

Nomenclatural changes

Genus *Neopoliocoris* nom. n.

Poliocoris Slater 1994: 120 (Hemiptera: Heteroptera: Rhyparochromidae). Preoccupied by *Poliocoris* Kirkaldy 1910: 130 (Hemiptera: Heteroptera: Pentatomidae).

Type species. *Poliocoris umbrosus* Slater, 1994.

Distribution. South Africa.

Etymology. From the preexisting name *Poliocoris* and the prefix "Neo-" from the Greek "*neos*", meaning new; gender masculine.

***Neopoliocoris umbrosus* (Slater, 1994), comb. n.**

Poliocoris umbrosus Slater 1994: 120.

Acknowledgments

We thank Dr Thomas Henry (Systematic Entomology Laboratory, ARS, USDA, Washington DC, USA) and an anonymous referee for reading the manuscript and making some suggestions. This work was supported by the Guizhou Province Natural Science Foundation ([2014]2014, [2013]2307).

References

ICZN (1999) International Code of Zoological Nomenclature, fourth Edition. The International Trust for Zoological Nomenclature, London, 306 pp.

Kirkaldy GW (1910) Three new Hemiptera-Heteroptera from the Miocene of Colorado. Entomological News 21: 129–131.

Slater JA (1994) A new genus and three new species of Lygaeidae (Hemiptera) from South Africa, with additional records for the region. African Entomology 2: 117–122.